Exhibit 90

Br. J. exp. Path. (1984) **65**, 101–106

Effects of talc on the rat ovary

T.C. Hamilton[1]*, H. Fox[2], C.H. Buckley[2], W.J. Henderson[1] and K. Griffiths[1]
[1]*Tenovus Institute for Cancer Research, The Welsh National School of Medicine, The Heath, Cardiff CF4 4XX, Wales and* [2]*Department of Pathology, University of Manchester, Manchester M13 9PT, UK*

Received for publication 26 July 1983

Summary. Exposure of rat ovaries to talc was accomplished by intrabursal injection. As early as 1 and up to 18 months after treatment, the ovaries and associated tissue were cystic in appearance; these changes were the result of bursal distention. Histologically the ovarian tissue was decreased in amount and spread as a remnant on the inner wall of the bursa. In four of 10 treated animals but in no controls, focal areas of papillary change were noted in the surface epithelium of the ovary. Polarized light and electron microscope microanalysis confirmed the presence of talc in the surface epithelium, ovarian cortex, and connective tissue matrix of the bursa. Although the changes in the ovarian surface may be related to direct effects of talc exposure, it is postulated that these changes might also be related to constant exposure to the high concentrations of steroid hormones which have undoubtedly accumulated in the intrabursal space.

Keywords: talc, ovary, mineral dust, steroid hormones

Several factors have been suggested to be of importance in the aetiology of ovarian cancer (Fathalla 1972; Lingeman 1974, 1983; Henderson *et al.* 1979; Longo & Young 1979; Hamilton & Davies 1983). The possibility that an ascending carcinogen is implicated in the aetiology of ovarian epithelial cancer is one that has been widely canvassed (Fathalla 1972; Lingeman 1974; Henderson *et al.* 1979; Longo & Young 1979), and suspicion in this respect has fallen particularly on talc (Anonymous 1977; Henderson *et al.* 1979; Longo & Young 1979; Roe 1979). Until recently the only evidence to support this suspicion has been the finding of talc particles deeply embedded within ovarian carcinomatous tissue (Henderson *et al.* 1971), but Cramer *et al.* (1982) have now reported an epidemiological study which showed that women using dusting powders which contained talc, either on their perineum or on sanitary towels, had substantially higher risk of developing ovarian carcinoma than did those not using talc-containing preparations. An epidemiological study which describes a non-specified increased cancer risk amongst workers in talc-associated Russian industries (Katsnelson & Mokronosava 1979) also may implicate talc in the malignant process.

Cramer *et al.* (1982) have reviewed the evidence linking talc and ovarian carcinoma and concluded that there is an urgent need for animal studies to help determine the relationship between this ubiquitous environmental agent and ovarian neoplasia. We report here the preliminary results of an in-vivo study of the effects of intrabursal talc injection on the rat ovaries.

Material and methods

Female Sprague–Dawley rats bred in the

* Present address: Medicine Branch, Division of Cancer Treatment, National Cancer Institute, Building 10, Room 12N226, 9000 Rockville Pike, Bethesda, Maryland 20205, USA.

animal husbandry unit of the Tenovus Institute were used at 10–15 weeks of age. Animals were fed a standard Laboratory diet (Pilsbury Ltd, Birmingham, UK) and were provided with tap water *ad libitum*. Animals were housed in rooms maintained at 23–24°C in 12 h of artificial light and 12 h darkness. After procedures described below, animals were kept in close proximity to male rats.

The talc preparation used in the procedures to be described was Italian 00000 (100 mg/ml) in phosphate-buffered saline, sterilized by autoclave before use. This preparation was composed of a heterogeneously sized population of platey crystals (size range: 0.3–14 μm) and contained no asbestos as judged by electron microscope microanalysis (observation by W.J.H.).

The procedure for surgical implantation of talc was as follows. Ovaries were located by blunt forceps used as probes via incisions through the skin and abdominal musculature and were pulled through the opening still attached to the fallopian tube and uterus. The bursa was immobilized with fine forceps and pulled sufficiently away from the ovarian surface to allow a 25 gauge needle, attached to a 1-ml syringe, to pierce the bursa without damage to the underlying ovarian tissue. The talc suspension (100 μl) was then infused and the needle removed. The ovary was returned to the peritoneum and the muscular wall of the abdomen sutured as was the overlying skin. The procedure was bilateral and accomplished while animals were under ether anaesthesia. Age-matched controls, sham-operated, and sham-treated (vehicle only) animals were included in the experiment. A total of 95 animals were involved in the experiment; at each time point, 10 treated animals, three age-matched controls, three sham-operated, and three sham-treated animals were examined. At intervals of 1, 3, 6, 12, and 18 months after treatment, animals were killed by cervical dislocation and the peritoneum opened by midline incision. Gross changes were noted; the ovaries and adherent tissue were then fixed for light (buffered formalin) or electron (3% glutaraldehyde in phosphate buffer) microscopy. Histological examination of ovaries and associated tissue was performed on talc-treated and control animals 12 months after treatment.

To demonstrate the presence of talc in material stained (haematoxylin and eosin) for light microscopy, the sections were subjected to the Henderson replication technique (Henderson & Griffiths 1972) followed by evaluation of replicates by electron microscope microanalysis (Henderson *et al.* 1975). Identification of particulate material seen by electron microscopy in thin sections was also accomplished with electron microscope microanalysis.

Results

Autopsy revealed that one or both ovaries from rats treated with talc by intrabursal injection were macroscopically cystic in appearance (Fig. 1); no gross changes were seen in any of the control animals. Gross

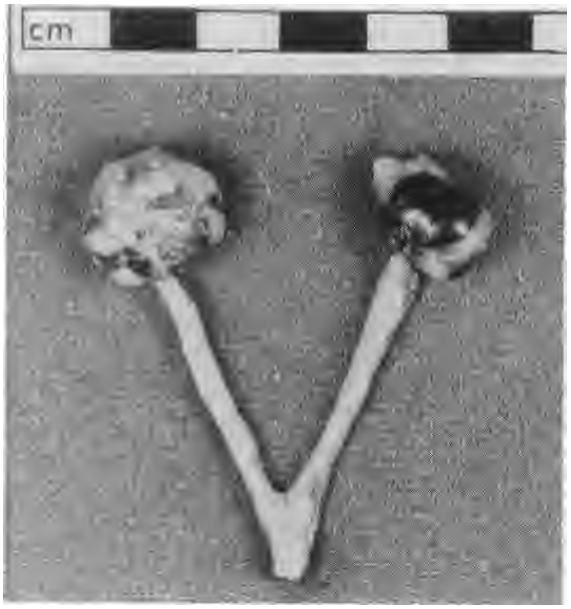

Fig. 1. Ovaries and associated gential tissue of the rat after talc treatment by intrabursal injection (see materials and methods). Animal was killed and autopsy performed 6 months after treatment. Note the apparent cyst formation and ovarian remnant just visible through the left bursa.

changes did not appear to be time-dependent as animals examined at 1, 3, 6, 12, and 18 months after treatment (10 treated animals and three each from the various control groups per time point) had similar numbers (> 50%) of grossly altered ovaries. Although oestrous cycles, as assessed by vaginal smears on sequential days, were irregular in talc-treated as well as control animals (especially apparent in older animals) day-to-day changes in the smears of individual animals indicated, however, the ovaries were still producing physiological concentrations of steroid hormones.

Histological examination showed that the cystic structures were not derived from the ovary but were due to distension of the bursal sac. The ovarian tissue was relatively decreased in amount and often spread as a thin remnant along the inner surface of a portion of the distended bursa.

The ovarian surface epithelium was, for the most part, formed by a single layer of low cuboidal cells in both injected and control cases. Focal multilayering of the ovarian surface epithelial cells, often in association with small inclusion cysts, was seen with some frequency in the injected cases but was noted with an equal frequency in the control ovaries. In four of the injected ovaries, but in none of the control cases, small, focal areas of papillary change were seen in the surface epithelium (Fig. 2). The papillae were small and usually had a connective-tissue stromal support: some papillae appeared to be purely cellular but this was almost certainly due to cross-sectioning. The epithelium covering the papillae was regular with no evidence of cytoplasmic or nuclear atypia; mitotic figures were not seen. There was no correlation between the presence of intra-ovarian foreign body granulomas (*vide infra*) and the presence of these papillary areas and where both abnormalities were present in the same ovary they bore no topographical relationship to each other.

No evidence of cellular atypia or of mitotic activity was seen in the nonpapillary areas of the surface epithelium of the injected ovaries and in no ovary was there any evidence of frank neoplasia.

Foreign body granulomas, without any

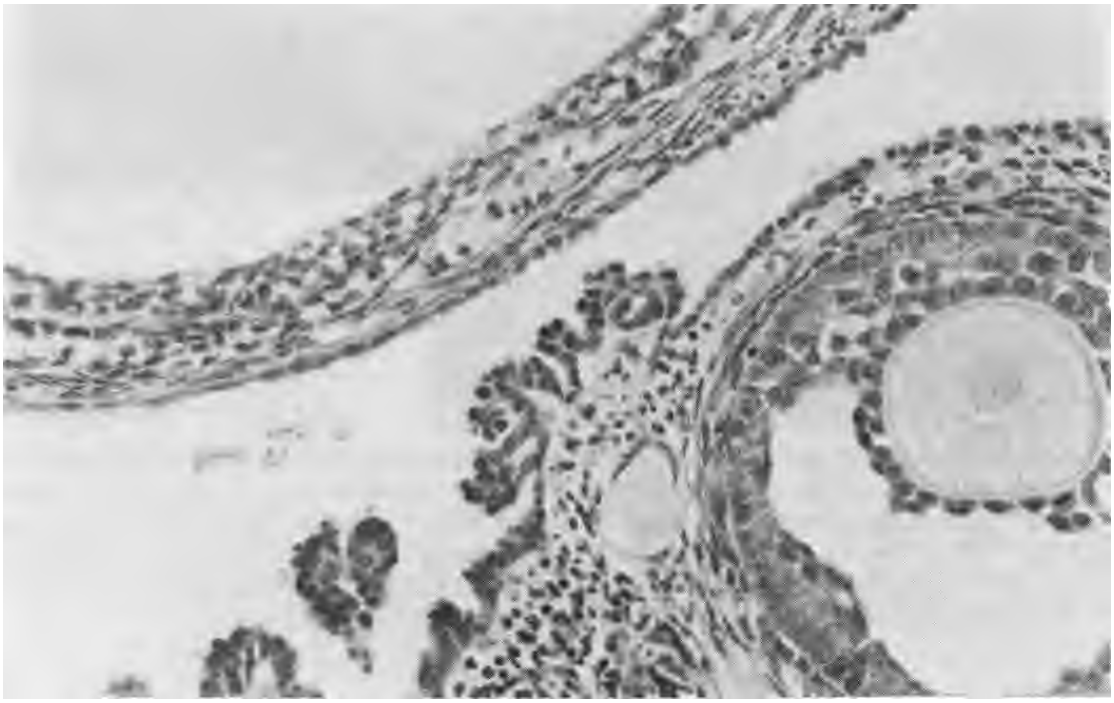

Fig. 2. An area of papillary change in the surface epithelium of a rat ovary exposed to talc by intrabursal injection. H & E × 45.

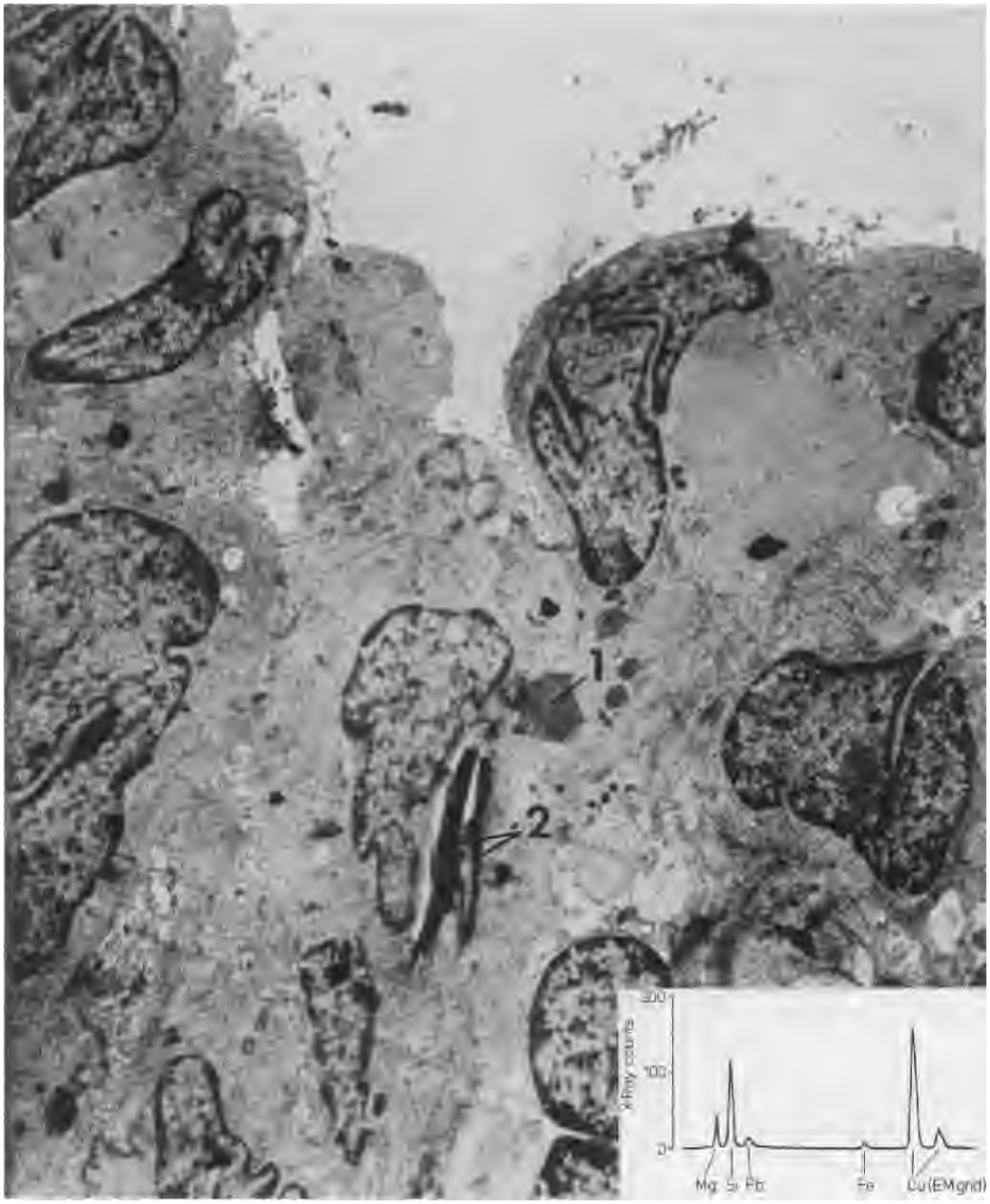

Fig. 3. Surface epithelium of a rat ovary 6 months after talc administration. A number of talc particles can be seen in one epithelial cell, demonstrating their sheet-like (1) and fibre-like (2) forms; the X-ray analysis confirms their elemental composition (inset). In order to retain the talc particles during sectioning, the tissue is cut thicker than for normal morphological assessment, which accounts for a certain loss of definition (× 6000). Analytical spectrum from sheet crystal (inset) shows the 3 : 1 silicon to magnesium ratio characteristic of talc. KV 80, Beam current 0.03 μA, 20-s count.

surrounding inflammation, were seen in five of the injected ovaries, usually in the cortical areas, and similar lesions were not uncommonly noted in the supracapsular fat and in the connective tissue matrix of the capsule. Birefringent crystals within these granulomas were judged to be talc by polarized light microscopy and this identification was readily confirmed by the Henderson replication technique (Henderson & Griffiths 1972) coupled with electron microscopic microanalysis (Henderson *et al.* 1975).

Electron microscopy revealed a heterogenously sized population of particles deeply embedded in the ovarian tissue, and on rare occasions small particles were seen within individual surface germinal epithelial cells (Fig. 3).

Discussion

In rats, intrabursal talc injection was followed by changes in the ovary and its associated tissues. Rats were chosen for this study because it was hoped that the near inclusion of the ovaries within a bursa in this species offered an opportunity for long-term exposure of the ovary to the mineral dust, once the dust was injected intrabursally. Unfortunately, bursal distention occurred as an unforeseen complication, this probably resulting from talc-induced fibrosis and obliteration of the small channel which normally allows communication between the cavity where the ovary lies and the peritoneum; the subsequent distension was almost certainly due to an accumulation of folicular fluid within the confined and enclosed space thus artificially created.

Despite the complexities introduced by the bursal distension it is of particular interest that papillary changes were seen in the surface epithelium of a proportion of the injected ovaries, for it is from this epithelium that most ovarian epithelial neoplasms, both benign and malignant, are thought to arise (Scully 1977). The papillary changes seen in this epithelium did not appear to be a reaction to an inflammatory process and were somewhat reminiscent of those noted by Graham & Graham (1967) in the ovaries of asbestos-treated guinea pig. Whether these papillae represent the first stage in the development of a surface papillary epithelial neoplasm is, of course, a moot point but such lesions are, in the human ovary, certainly regarded as precursors of surface papillomas (Fox & Langley 1976).

It is clearly tempting to attribute the papillary change in the surface epithelium of injected ovaries to the direct effects of exposure to talc but an alternative explanation has to be considered. Ovarian epithelial neoplasms in humans contain steroid hormone receptors which are probably due to retention of a control system present in the normal cells from which such tumours arise (Holt *et al.* 1981; Hamilton *et al.* 1981). Steroid hormone receptors have recently also been reported as being present in the rat ovarian surface epithelium grown *in vitro* (Hamilton *et al.* 1982, 1983) and it is therefore possible that the changes seen in the surface epithelium of the injected rat ovaries were the result of long term (rather than intermittent) exposure to the high concentration of steroid hormones present in the entrapped follicular fluid within the distended bursa.

Hopefully future studies will clarify whether one or both of these possibilities has relevance to the malignant process in the ovarian surface epithelium.

Acknowledgments

The authors wish to thank the secretaries of the Medicine Branch, NCI, for careful typing of this manuscript. One of us (T.C.H.) was supported by the Medical Research Council, UK (grant no. G977/505) during a portion of the time this work was in progress.

References

Anonymous (1977) Cosmetic talc powder. *Lancet* i, 1348–1349.

Cramer D.W., Welch W.R., Scully R.E. & Woj-

CIECHOWSKI C.A. (1982) Ovarian cancer and talc—a case-control study. *Cancer* **50**, 372–376.

FATHALLA M.F. (1972) Factors in the causation and incidence of ovarian cancer. *Obstet. Gynec. Survey* **27**, 751–768.

FOX H. & LANGLEY F.A. (1976) *Tumours of the Ovary*. London: Heinemann.

GRAHAM J. & GRAHAM R. (1967) Ovarian cancer and asbestos. *Environ. Res.* **1**, 115–128.

HAMILTON T.C. & DAVIES P. (1983) Hormone relationships in ovarian cancer. *Reviews on Endocrine Related Cancer* **14**, 19–22.

HAMILTON T.C., DAVIES P. & GRIFFITHS K. (1981) Androgen and oestrogen binding in cytosols of human ovarian tumours. *J. Endocr.* **90**, 421–431.

HAMILTON T.C., DAVIES P. & GRIFFITHS K. (1982) Oestrogen receptor-like binding in the surface germinal epithelium of the rat ovary. *J. Endocr.* **95**, 377–385.

HAMILTON T.C., DAVIES P. & GRIFFITHS K. (1983) Steroid-hormone receptor status of the normal and neoplastic ovarian surface germinal epithelium. In *Factors Regulating Ovarian Function*. Eds G.S. Greenwald & P.F. Terranova. New York: Raven. pp. 81–85.

HENDERSON W.J., JOSLIN C.A.F., TURNBULL A.C. & GRIFFITHS K. (1971) Talc and carcinoma of the ovary and cervix *J. Obstet. Gynaec. Br. Commonw.* **78**, 266–272.

HENDERSON W.J. & GRIFFITHS K. (1972) Shadow casting and replication. In *Principles and Techniques in Electron Microscopy: Biological Applications*. Ed. M.A. Hayat. New York: Van Nostrand Reinhold.

HENDERSON W.J., EVANS P.M.D., DAVIES D.J. & GRIFFITHS K. (1975) Analysis of particles in stomach tumours from Japanese males. *Environ. Res.* **9**, 240–249.

HENDERSON W.J., HAMILTON T.C. & GRIFFITHS K. (1979) Talc in normal and malignant ovarian tissue. *Lancet* **i**, 499.

HOLT J.A., LYTTLE R., LORINCZ M.A., STERN S.D. PRESS M.F. & HERBST A.L. (1981) Estrogen receptor and peroxidase activity in epithelial ovarian carcinomas *J. natn. Cancer Inst.* **67**, 307–317.

KATSNELSON B.A. & MOKRONOSAVA K.A. (1979) Non-fibrous mineral dusts and malignant tumors *J. occup. Med.* **21**, 15–20.

LINGEMAN C.H. (1974) Etiology of cancer of the human ovary: a review. *J. natn. Cancer Inst.* **53**, 1603–1618.

LINGEMAN C.H. (1983) Environmental factors in the etiology of carcinoma of the human ovary: a review. *Am. J. ind. Med.* **4**, 365–379.

LONGO D.L. & YOUNG R.C. (1979) Cosmetic talc and ovarian cancer. *Lancet* **ii**, 349–351.

ROE F.J.C. (1979) Controversy: cosmetic talc and ovarian cancer. *Lancet* **ii**, 744.

SCULLY R.E. (1977) Ovarian tumours—a review. *Am. J. Path.* **87**, 686–720.

Exhibit 91

Arch Gynecol Obstet
DOI 10.1007/s00404-009-1030-3

ORIGINAL ARTICLE

Does long-term talc exposure have a carcinogenic effect on the female genital system of rats? An experimental pilot study

Nadi Keskın · Yasemin Aktan Teksen · Esra Gürlek Ongun · Yusuf Özay · Halil Saygılı

Received: 16 December 2008 / Accepted: 2 March 2009

Abstract
Objective In several studies, the prolonged exposure to talc has been associated with development of ovarian cancer. However, some studies have advocated contrary views. The present study aims to investigate histopathological changes and whether long-term talc exposure is associated with potential carcinogenic effects on the female genital organs of rats.
Materials and methods The present study was conducted at Dumlupinar University Medical Faculty and a total of 28 Sprague–Dawley rats were included. The experimental animals were allocated into four groups having seven rats each. Groups 1 and 2 served as controls, where the rats in Group 1 did not receive any intervention and Group 2 received intravaginal saline. Groups 3 and 4 received intravaginal or perineal talc application, respectively. Talc was applied for 3 months on a daily basis. Histopathological changes in the peritoneum and female genital system were evaluated. For statistical analyses, Fisher's exact test was carried out using SPSS.
Findings In both the groups exposed to talc (Groups 3 and 4), evidence of foreign body reaction and infection, along with an increase in inflammatory cells, were found in all the genital tissues. Genital infection was observed in 12 rats in the study group and 2 rats in the control group. Neoplastic change was not found. However, there was an increase in the number of follicles in animals exposed to talc. No peritoneal change was observed. In the groups not exposed to talc, similar infectious findings were found, but there was a statistically significant difference between the groups (Groups 1 and 2 vs. Groups 3 and 4, $P > 0.05$). Neoplastic change was also not observed in these groups. Four groups were compared in terms of neoplastic effects and infections. In Groups 1, 5 rats were normal, two developed vulvovaginitis and endometritis with overinfection (in both ovaries), and one developed salpingitis (in both fallopian tubes), that is, infection was found in a total of two rats. In Group 2, only one experimental animal had endometritis. All the animals in Groups 3 and 4 developed infections.
Conclusions Talc has unfavorable effects on the female genital system. However, this effect is in the form of foreign body reaction and infection, rather than being neoplastic.

Keywords Talc · Ovary · Endometrium · Vulva

N. Keskın
Department of Obstetrics and Gynecology,
Dumlupınar University Medical Faculty, Kütahya, Turkey

Y. A. Teksen
Department of Pharmacology,
Dumlupınar University Medical Faculty, Kütahya, Turkey

E. G. Ongun
Department of Pathology,
Dumlupınar University Medical Faculty, Kütahya, Turkey

Y. Özay
College of Health Science, Ahi Evran University, Kirsehir, Turkey

H. Saygılı
Department of Obstetrics and Gynecology,
İstanbul Medical Faculty, İstanbul University, Istanbul, Turkey

N. Keskın (✉)
Dumlupınar Üniversitesi Tıp Fakültesi Hastanesi
Kadın Hastalıkları ve Doğum Anabilim Dalı Kütahya,
Tavşanlı yolu 10. km merkez kampusu, Kuhtiya, Turkey
e-mail: nadikeskin@superonline.com

Published online: 20 March 2009

Introduction

Various factors have been cited in the development of genital cancers. Many studies have been conducted regarding the potential role of talc in ovarian cancer and previously it had been widely accepted as an important etiological factor [1–4]. In recent years, some studies (meta-analysis) have been averse toward this concept [5, 6]. Asbestos is a well-known carcinogen, and described as having a particular role in the development of pleural and peritoneal mesothelioma [7]. Its association with ovarian cancer has also been demonstrated in several studies [8–10].

Talc and asbestos are both silicate minerals. Minerals are classified according to their anionic structure, and its subclasses are defined by chemical composition or structure. Classes and subclasses can be further divided into mineral groups on the basis of atomic structure and chemical similarities. Talc is a magnesium silicate hydroxide, characterized by water molecules trapped between silicate sheets, which belongs to the silicate subclass phyllosilicate and the clay group montmorillonite/smectite. The three other major phyllosilicate clay groups are kaolinite/serpentine, illite, and chlorite [5].

Asbestos is the generic or commercial name for six naturally occurring fibrous minerals including amosite, chrysotile, and crocidolite, which are used in industrial applications, and the fibrous varieties of tremolite, actinolite, and anthophyllite. Asbestos is morphologically distinct from talc and belongs to different silicate mineral groups and subgroups. The carcinogenic effects of asbestos have been extensively studied and documented in medical literature [10, 11]. It is clear that the morphologic structure of serpentine asbestos and the fibrous form of amphiboles is responsible for their carcinogenic properties, much more than its atomic constituents [12]. In contrast, talc, which is a member of the montmorillonite/smectite group, rarely occurs in the asbestiform habit (a mineral's fibrous pattern of growth). Even asbestiform talc is not as carcinogenic as asbestos owing to its chemical and physical properties [5].

Although a number of studies have examined the relation between talc and ovarian cancer, its effect on other female genital system tissues have not been investigated. In addition, the carcinogenic effect of talc has not been ascertained. The present experimental study aimed to examine carcinogenic effects of long-term talc exposure on genital system of female Sprague–Dawley rats.

Materials and methods

Experimental animals

The experimental study was conducted at Dumlupınar University Medical Faculty and approved by the institutional ethics committee for animal experiments. A total of 28 Sprague–Dawley female rats weighing 200–250 g were used as experimental animals. Animals were kept in standard cages at room temperature under normal diurnal conditions (12 h day and 12 h night). Sufficient water and food intake was provided.

Groups

The experimental animals were assigned into four different groups having seven rats each. Group 1 served as control and did not receive any intervention. Group 2 also served as control and 0.5 ml of saline was intravaginally administered to these animals. Groups 3 and 4 were study groups and received intravaginal and perineal talc application (100 mg in 0.5 ml of saline), respectively. Talc with saline was given in aerosol form to the animals; dust form was not applied. However, this application can be optimally intravaginal. Talc application was done daily for 3 months. At the beginning of the study, cervicovaginal smear samples were obtained from each animal between 08:00 and 09:00 a.m.

Histopathological examination

At the end of the experiment, the animals were sacrificed under ether anesthesia by drawing blood from their hearts thus inducing hypovolemic shock. All the internal and external genital organs (vulva, vagina, uterus, fallopian tubes, and ovaries) were surgically removed and placed in 10% formaldehyde solution. The samples were examined for the changes in the peritoneum and female genital system. Hematoxylin and eosin (H&E) staining and light microscopy was used in the histopathological examination. For statistical analysis, Fisher's exact test was performed using the SPSS software. A P value <0.05 was considered significant.

Findings

Baseline smears revealed the presence of vaginitis in only two experimental animals, whereas findings were normal for the remaining 26 rats. One of the rats detected with vaginitis belonged to the study group and one of them belonged to the control group. At baseline, the mean weight of all rats was 226 ± 24 g (average weight of study groups was 228 ± 18 g, control groups was 224 ± 30 g) and the corresponding figure at the end of 3 months was 240 ± 20 g (229 ± 17 g study groups, 251 ± 23 g were found in the control groups) showing no significant change.

Foreign body reaction, findings of infection, and increased number of inflammatory cells were found in all groups exposed to talc (Groups 3 and 4). No neoplastic

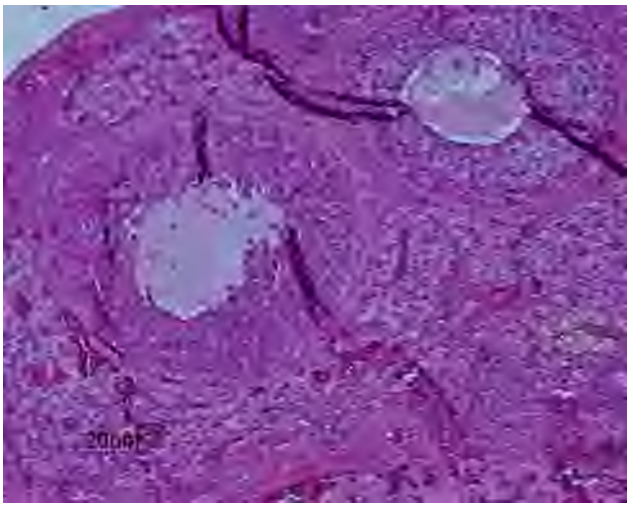

Fig. 1 An increase in the number of follicles was observed in the ovaries

change or peritoneal change was detected. Moreover, an increase in the number of follicles was observed in the ovaries of all animals in the control and study groups. (Fig. 1)

The four groups were compared in terms of neoplastic effects and infections. In Groups 1, 5 rats were normal, two developed vulvovaginitis and endometritis with over infection (in both ovaries), and one developed salpingitis (in both fallopian tubes). Infection was found in two rats. In Group 2, only one experimental animal had endometritis. In Groups 3 and 4, all the animals developed infection. Animals in Group 3 developed the following pathologies: vulvovaginitis ($n = 5$), endometritis ($n = 6$), pelvic infection ($n = 4$), ovarian infection (a total of 7 ovaries in 3 animals), and salpingitis and tubal occlusion ($n = 8$). In Group 4, all seven rats developed vulvovaginitis; furthermore, four developed endometritis, five developed pelvic infection, four developed ovarian infection (in eight ovaries), and two developed salpingitis and tubal occlusion (one unilateral and one bilateral). The analysis using Fisher's exact test showed positive correlations between following groups: Group 3 and Group 1, Group 3 and Group 2, Group 4 and Group 1, and Group 4 and Group 2 ($P < 0.05$). Other pairwise comparisons did not reveal significant results ($P > 0.05$) (Table 1).

Conclusions

The preliminary results show that in 28 rats from the 4 groups, talc had unfavorable effects on the female genital system. However, this effect seems to be in the form of foreign body reaction or infection rather than a neoplastic change. The results of previous studies are in favor of a neoplastic effect, particularly on the ovaries. However, more experimental and clinical studies are warranted to reach firm conclusions. In the study and control groups used in this research, an increase in follicle number was also observed. It should be emphasized that other environmental factors may have role in these effects. Therefore, the effect of different study conditions should also be investigated in detail.

Declaration

The present study was designed and conducted by Nadi Keskin MD, with the contributions and approval of Prof. Halil Saygili MD, an academic member of the Istanbul Medical Faculty, Istanbul University, as an extended study of 'Histopathological Changes Induced by talc Exposure in Rats' [9] previously published in 'Endokrinolojide Yönelisler Dergisi' (2005; volume 14, number 4). The language of this manuscript was edited by SPi Professional Editing Services (http://www.prof-editing.com/index.php).

Table 1 Groups of histopathological changes observed in the genital system of experimental animals

	Normal	Vulvovaginitis	Endometritis	P ID	Findings of ovarian infection ($n = 2 \times 7 = 14$)	Salpingitis and tubal occlusion ($n = 2 \times 7 = 14$)	Neoplastic changes	Preneoplastic changes
Group 1 ($n = 7$)	5	2	0	1	1 (2 ovaries)	1 (2 fallopian tubes)	0	0
Group 2 ($n = 7$)	6	0	1	0	0	0	0	0
Group 3 ($n = 7$)	0	5	6	4	7 ($2 \times 3 + 1$)*	8 (2×4)	0	0
Group 4 ($n = 7$)	0	7	4	5	8 (2×4)	5 ($2 \times 2 + 1$)**	0	0

Statistical comparisons of the groups were done by using Fischer exact test. Following positive correlations were found between groups: Group 3 and Group 1, $P = 0.021$, $P < 0.05$; Group 3 and Group 2, $P = 0.005$, $P < 0.05$; Group 4 and Group 1, $P = 0.021$, $P < 0.05$, Group 4 and Group 2, $P = 0.005$, $P < 0.05$. Other comparisons did not reveal statistically significant results ($P > 0.05$)

Group 1: control group with no intervention, Group 2: control group receiving intravaginal saline administration, Group 3: study group receiving intravaginal talc application, Group 4: study group receiving perineal talc application

* In this group, one rat had infection findings in only one ovary. For the remaining, both ovaries were involved, ** In this group, one rat had infection findings in only one fallopian tube

Discussion

Various etiological factors have been cited for genital cancers. A number of studies on talc have been conducted to investigate its effect on the development of ovarian cancer, the most fatal among these malignancies; it is commonly accepted as an important etiological factor for this cancer [1–4]. In recent years, some studies (meta-analysis) have been averse to defend this concept [5, 6]. Asbestos is a well-known carcinogen that has a particular role in the development of pleural or peritoneal mesothelioma. It has also been associated with ovarian cancer [8–10]. However, because of differences in the structure of talc and asbestos, the carcinogenic effect of asbestos has also been examined.

Talc is an important industrial material, because of its resistance to electricity, heat, and acid. Therefore, it is widely used in plastic surfaces, especially in surgical gloves, various plastic apparatus, and gynecologic services, and women are commonly known to use it for sanitation purposes. Other applications for talc include contraceptive diaphragms and condoms [5], and the treatment of pleural effusions and pleurodynia [13–15].

Surveys on the hygienic practices of women and talc application on the perineum, animal experiments, and clinical trials are among the studies that investigate the carcinogenic effects of talc [16, 17]. Since the first study showing an almost twofold increase in the risk of ovarian cancer with any perineal talc use [3], most case-control studies have demonstrated positive associations with talc use [4, 18]. Not all of them have been statistically significant [19–21]. Several studies [21–23] did not find an overall association between any genital talc use and ovarian cancer. Some studies [21, 22, 24] have demonstrated statistically insignificant trends in risk with increased frequency of talc use, duration of use, and measures of "total lifetime applications," whereas other studies [19, 20] have not observed a statistically significant dose response. With regard to histologic subtypes, a recent study by Cramer et al. [24] observed the greatest risk of talc use in invasive serous cancer; however, other studies have found increased risks for endometrioid cancers [4, 21], serous cancers [25], and invasive cancers of all subtypes [4]. Because serous cancers which account for over half of all invasive ovarian cancers, most resemble mesotheliomas, it could be hypothesized that this subtype may be most likely associated with talc use.

There have been few studies [26, 27] of talc exposure in animals and these studies have not demonstrated an increase in ovarian cancer among animals subjected to continuous talc exposure. These data should be interpreted cautiously because there are important anatomic and physiologic differences between rodents and humans. In animals, talc is often administered at high dose via aerosol exposure [26].

Some studies found a positive relation between ovarian cancer and perineal talc application. Cramer et al. [3], Rosenblatt et al. [28], and Chang et al. [4] have reported relative risks of 1.92 (%95 CI 1.3–2.9), 2.4 (%95 CI 1.1–5.3), and 1.42 (%95 CI 1.08–1.86), respectively. This shows an increased risk correlation between the use of talc as a cosmetic and ovarian cancer, but this increased risk is not significant. Studies by Cramer et al. describe the relationship between talc and ovarian cancer; thus, "Our studies have suggested an increased risk for ovarian cancer associated with the use of talcum powder in genital hygiene, but the biologic credibility of the association has been questioned."

In a meta-analysis, Huncharek implied that earlier epidemiological studies suggest an association between perineal cosmetic talc use and increased risk of epithelial ovarian cancer. This meta-analysis was performed to evaluate such an association. Available observational data do not support the existence of a causal relationship between perineal talc exposure and an increased risk of epithelial ovarian cancer [5]. Selection bias and uncontrolled confounding may account for positive associations observed in prior epidemiological studies. In addition, in a review, Muscat implied that talc is not genotoxic. Mechanistic, pathology, and animal model studies have not found evidence of a carcinogenic effect. In summary, these data collectively do not indicate that cosmetic talc causes ovarian cancer [6].

Talc has been used routinely in humans in the treatment of pleural effusions, where talc is directly applied to the human pleura. Long-term follow-up studies of humans undergoing this procedure have not shown a single case of malignancy induced by talc [13–15].

Animal data in relation to talc toxicity are important: Wagner et al. [29] used Italian talc in experimental animal study; Italian talc has been tested on rats using three routes, intra-pleural inoculation, inhalation, and ingestion. Groups exposed to superfine chrysotile asbestos and untreated controls were included for comparison. In all the experiments, animals were allowed to live out their lives. The intra-pleural inoculation of talc produced no mesotheliomas in contrast to 18 produced by the chrysotile asbestos. After ingestion, one leiomyosarcoma occurred with Italian talc and one with chrysotile asbestos. Whether these tumors are a consequence of the feeding is uncertain. The inhalation studies demonstrated that with equal dosage, talc can produce a similar amount of fibrosis as asbestos. However, the chrysotile-exposed rats developed lung adenomas, adenomatosis, and an adenocarcinoma, whereas the only lung tumor seen in animals exposed to talc was a small adenoma, which may have been an incidental finding. In another experimental animal study [30], 256 Wistar rats received a single injection of crocidolite into the right pleural cavity to induce mesotheliomas. Subsequently, they

were given right intra-pleural injections of BCG, crystalline silica, talc, carrageenan, or saline (as a control). There was no significant change in the mesothelioma rate in the rats exposed to BCG, silica or talc, but there was a threefold increase in mesothelioma incidence in the group injected with carrageenan.

Wagner, Huncharek, Hill, Muscat, and others hold that talc is not carcinogenic. Also in this study, carcinogenic effect of talc has not been determined either in any female rat genital system tissue or in ovary tissue.

In an experimental study on rats, Henderson et al. [31] demonstrated the presence of talc in the ovaries following vaginal talc application. Similarly, in the study of Egli et al. [32], carbon particles reached the fallopian tubes in 30–35 min. Therefore, talc disseminates to vulvovaginal region, endometrium, fallopian tubes, ovaries, and peritoneum after vaginal examination, raising the possibility of changes—even preneoplastic or neoplastic—due to talc exposure following perineal or vaginal talc application. Langseth et al. [33] are skeptical about the association between perineal talc application and ovarian cancer. In their article, Langseth et al. expressed that the origin of ovarian cancer is multifactorial, especially breast cancer patients who are BRCA 1 and BRCA 2 gene carriers, who have increased the risk of ovarian cancer. Therefore, the role of environmental factors such as talc and asbestos in cancer formation is suspected of being over stressed.

Salazar et al. examined histological changes in BRCA 1 gene positive women who underwent prophylactic oophorectomy because of their high inherited risk of ovarian cancer, and reported the following findings: increased follicular activity, hyperplasia of corpus luteum, hilar cell hyperplasia, pseudostratification of superficial epithelium, superficial papillomatosis, cortical stromal hyperplasia, and hyperkeratosis. These investigators defined increased follicular activity, hyperplasia of corpus luteum, and other findings as preneoplastic phenotypes in ovaries with high risk [34]. If talc application has a carcinogenic effect on ovaries, this study would also obtain similar findings. In the present study, experimental animals exposed to talc both via vaginal and perineal application for 3 months did not show the abovementioned changes except for an increased number of follicles. Although both the control and study groups showed an increase in follicle number, thus it was not attributed to talc application; however, the increase in follicle number could not be explained as well. Therefore, this study did not demonstrate an association between talc application and peritoneal/ovarian cancer.

In both groups exposed to talc (Groups 3 and 4), evidence of foreign body reaction and infection along with an increase in inflammatory cells were found in all the genital tissues. Muscat comments on this [6]: "Given the dissimilarities between talc and asbestos with regard to their fibrous shapes, the weak but increased associations in the epidemiologic studies could be attributed to other mechanisms assuming that the statistical associations are unbiased and not due to confounding. Asbestos fibers in the lung initiate an inflammatory and scarring process, and it has been proposed that ground talc, as a foreign body, might initiate an inflammatory response [35]. Pelvic inflammatory diseases, however, such as endometritis, peritonitis, tubo-ovarian access formation, and salpingo-oophoritis have in general not been associated with an increased risk of ovarian cancer."

Similar to Muscat's comments, this study also demonstrated unfavorable effects of talc on female genital system; however, it was in the form of foreign body reaction, infection, or increased adhesions, rather than neoplastic. In addition, the authors of this study believe that talc may have caused foreign body reaction, infection, or increased adhesions, which should be important for infertile patients.

Endometrial cancer is the most common genital malignancy among women. Unbalanced estrogen levels are being blamed for its etiology [36]. Various physical and chemical factors have also the potential to initiate preneoplastic and neoplastic stimulus [37]. A literature search did not reveal any study examining such an effect of talc on the endometrium. However, this study could not demonstrate any preneoplastic or neoplastic effect of talc on endometrial tissue.

Etiological factors for vulvar, vaginal, and cervical cancers have been largely discovered; in particular, HPV (Human Papilloma Virus) has been identified as an etiological factor [38]. In addition, physical and chemical factors have also been held responsible. However, talc is not counted among these factors and a clinical study examining such an effect does not exist. None of the rats in this study showed an evidence of such an effect.

Talc application has unfavorable effects on female genital system, particularly on ovaries and fallopian tubes. This usually manifests itself in the form of tissue injury, macrophage infiltration, and an increased rate of infections and development of adhesions [8, 39–41]. Holmdahl [42] emphasized the important role of talc in the development of adhesions after intraperitoneal surgery. Merritt et al. [8] reported an increase in chronic pelvic infections following perineal talc application. Ellis et al. [43] also emphasized the unfavorable effects of talc spilling from surgical gloves. In the present study, compared to the controls, a significantly increased rate of infection was found among the rats exposed to talc, which was particularly prominent for endometrial tissue, uterine tubes, and pelvic peritoneum. These tissues exhibited epithelial tissue injury, macrophage infiltration, and adhesions. Tubal adhesions are important in the context of infertility. In addition, the high rate of vulvovaginitis may have important implications for patients undergoing frequent gynecological examinations and for

immunocompromised patients attending outpatient gynecological oncology clinics.

In conclusion, the present study demonstrated unfavorable effects of talc on female genital system in the form of foreign body reaction, infection, or increased adhesions, rather than neoplastic. Moreover, the authors believe that talc may have a stimulating effect on ovaries, which should be further investigated particularly in infertile patients. However, the authors of this study highlight the fact that other environmental factors may have role in the increased follicle number presented by the control group. Therefore, separate intensive studies in the series, to demonstrate the effect of talc on the ovary should be considered.

Conflict of interest statement None.

References

1. Longo DL, Young RC (1979) Cosmetic talc and ovarian cancer. Lancet 2:1011–1012. doi:10.1016/S0140-6736(79)92576-5
2. Graham J, Graham R (1967) Ovarian cancer and asbestos. Environ Res 1:115–128. doi:10.1016/0013-9351(67)90008-4
3. Cramer DW, Welch WR, Scully Re, Wojciechoski CA (1982) Ovarian cancer and talc: a case control study. Cancer 50:37–60. doi:10.1002/1097-0142(19820715)50:2<372::AID-CNCR2820500235>3.0.CO;2-S
4. Chang S, Risch HA (1997) Perineal talc exposure and risk of ovarian carcinoma. Cancer 79:2396–2401. doi:10.1002/(SICI)1097-0142(19970615)79:12<2396::AID-CNCR15>3.0.CO;2-M
5. Huncharek MS, Muscat J, Ontilio A, Kupelnick B (2007) Use of cosmetic talc on contraceptive diaphragms and risk of ovarian cancer: a meta-analysis of nine observational studies. Eur J Cancer Prev 16(5):422–429. doi:10.1097/01.cej.0000236257.03394.4a
6. Muscat JE, Huncharek MS (2008) Perineal talc use and ovarian cancer: a critical review. Eur J Cancer Prev 17(2):139–146
7. Dunnigan J (1988) Linking chrysotile asbestos with mesothelioma. Am J Ind Med 14(2):205–209. doi:10.1002/ajim.4700140211
8. Merritt MA, Green AC, Nagle CM, Webb PM, Study Australian Cancer (2008) Ovarian Cancer: Australian Ovarian Cancer Study Group Talcum powder, chronic pelvic inflammation and NSAIDs in relation to risk of epithelial ovarian cancerInt. J Cancer 122(1):170–176
9. Saygılı H, Citil I, Bilir A (2005) Farelerde talk maruziyetinin overde neden olduğu histopatolojik değişiklikler. Endorinolojide Yönelişler Dergisi 14:4
10. Huncharek M (1986) The biomedical and epidemiological characteristics of asbestos-related diseases: a review. Yale J Biol Med 59(4):435–451
11. Mossman BT, Gee JB (1989) Asbestos-related diseases. N Engl J Med 320(26):1721–1730
12. Stanton MF, Layard M, Tegeris A et al (1981) Relation of particle dimension to carcinogenicity in amphibole asbestoses and other fibrous minerals. J Natl Cancer Inst 67(5):965–975
13. Genofre EH, Marchi E, Vargas FS (2007) Inflammation and clinical repercussions of pleurodesis induced by intrapleural talc administration. Clinics 62(5):627–634. doi:10.1590/S1807-59322007000500015
14. Kolschmann S, Ballin A, Juergens UR, Rohde G, Gessner C, Hammerschmidt S, Wirtz H, Gillissen A (2006) Talc pleurodesis in malignant pleural effusions. Pneumologie 60(2):89–95. doi:10.1055/s-2005-919139
15. Marchi E, Vargas FS, Acencio MM, Antonangelo L, Teixeira LR, Genofre EH, Light RW (2004) Talc and silver nitrate induce systemic inflammatory effects during the acute phase of experimental pleurodesis in rabbits. Chest 125(6):2268–2277. doi:10.1378/chest.125.6.2268
16. Tzonou A, Polychronopoulou A, Hsieh CC, Rebelakos A, Karakatsani A, Trichopoulos D (1993) Hair dyes, analgesics, tranquilizers and perineal talc application as risk factors for ovarian cancer. Int J Cancer 55:408–410. doi:10.1002/ijc.2910550313
17. Mills PK, Riordan DG, Cress RD, Young HA (2004) Perineal talc exposure and epithelial ovarian cancer risk in the Central Valley of California. Int J Cancer 112(3):458–464. doi:10.1002/ijc.20434
18. Chen Y, Wu PC, Lang JH, Ge WY, Hartge P, Brinton LA (1992) Risk factors for epithelial ovarian cancer in Beijing, China. Int J Epidemiol 21:23–29. doi:10.1093/ije/21.1.23
19. Whittemore AS, Wu ML, Paffenbarger RS Jr et al (1988) Personal and environmental characteristics related to epithelial ovarian cancer. II. Exposures to talcum powder, tobacco, alcohol, and coffee. Am J Epidemiol 128:1228–1240
20. Booth M, Beral V, Smith P (1989) Risk factors for ovarian cancer: a case-control study. Br J Cancer 60:592–598
21. Harlow BL, Cramer DW, Bell DA, Welch WR (1992) Perineal exposure to talc and ovarian cancer risk. Obstet Gynecol 80:19–26
22. Hartge P, Hoover R, Lesher LP, McGowan L (1983) Talc and ovarian cancer. JAMA 250:1844 (letter). doi:10.1001/jama.250.14.1844
23. Wong C, Hempling RE, Piver MS, Natarajan N, Mettlin CJ (1999) Perineal talc exposure and subsequent epithelial ovarian cancer: a case-control study. Obstet Gynecol 93:372–376. doi:10.1016/S0029-7844(98)00439-6
24. Cramer DW, Liberman RE, Titus-Ernstoff L et al (1999) Genital talc exposure and risk of ovarian cancer. Int J Cancer 81:351–356. doi:10.1002/(SICI)1097-0215(19990505)81:3<351::AID-IJC7>3.0.CO;2-M
25. Cook LS, Kamb ML, Weiss NS (1997) Perineal powder exposure and the risk of ovarian cancer. Am J Epidemiol 145:459–465
26. Boorman GA, Seely JC (1995) The lack of an ovarian effect of lifetime talc exposure in F344/N rats and B6C3F1 mice. Regul Toxicol Pharmacol 21:242–243. doi:10.1006/rtph.1995.1035
27. Hamilton TC, Fox H, Buckley CH, Henderson WJ, Griffiths K (1984) Effects of talc on the rat ovary. Br J Exp Pathol 65:101–106
28. Rosenblatt KA, Szklo M, Rosenshein NB (1992) Mineral fiber exposure and the development of ovarian cancer. Gynecol Oncol 45:20–25. doi:10.1016/0090-8258(92)90485-2
29. Wagner JC, Hill RJ, Berry G, Wagner MM (1980) Treatments affecting the rate of asbestos-induced mesotheliomas. Br J Cancer 41(6):918–922
30. Wagner JC, Berry G, Cooke TJ, Hill RJ, Pooley FD, Skidmore JW (1980) Animal experiments with talc. Br J Cancer 41(6):918–922
31. Henderson WJ, Hamilton RC, Griffiths K (1979) Talc in normal and malignant ovarian tissue. Lancet 1:499. doi:10.1016/S0140-6736(79)90860-2
32. Egli GE, Newton M (1961) The transport of carbon particles in the human female reproductive tract. Fertil Steril 12:151–155
33. Langseth H, Hankinson SE, Siemiatycki J, Weiderpass E (2008) Perineal use of talc and risk of ovarian cancer. J Epidemiol Community Health 62(4):358–360. doi:10.1136/jech.2006.047894
34. Salazar H, Godwin AK, Daly MB, Laub PB (1996) Microscopic benign and invasive malignant neoplasm and a cancer-prone phenotype in prophylactic oophorectomies. J Natl Cancer Inst 88(24):1810–1820. doi:10.1093/jnci/88.24.1810
35. Ness RB, Cottreau C (1999) Possible role of ovarian epithelial inflammation in ovarian cancer. J Natl Cancer Inst 91(17):1459–1467. doi:10.1093/jnci/91.17.1459
36. Balmer NN, Richer JK, Spoelstra NS, Torkko KC, Lyle PL, Singh M (2006) Steroid receptor coactivator AIB1 in endometrial

carcinoma, hyperplasia and normal endometrium: correlation with clinicopathologic parameters and biomarkers. Mod Pathol 19(12):1593–1605. doi:10.1038/modpathol.3800696
37. Schumacher (1956) Talc granuloma of the endometrium. Geburtshilfe Frauenheilkd 16(12):1082–1098
38. Riethmuller D, Guerrini JS, Aubin F (2007) Intraepithelial lesions and neoplasia associated with human papillomavirus infection. Bull Acad Natl Med 191(3):601–609 (discussion pp 609)
39. Scully RE, Young RH, Clement PB (1998) Tumors of the ovary, maldeveloped gonads, fallopian tube and broad ligament. In: Atlas of tumor pathology, fascicle 23, 3rd series. Armed Forces Institute of Pathology, Washington
40. Kyzer S, Gelber E, Koren R, Chaimoff C (1994) Peritoneal band containing talc: rare cause of small bowel obstruction in a previously unoperated child. J Pediatr Surg 29(12):1616–1617. doi:10.1016/0022-3468(94)90239-9
41. Regodón Vizcaino J, Fernández Yuste J, Rodríguez Sánchez E, Carbajo Vicente M (1982) Peritoneal lesions caused by powder from surgical gloves (talc and starch. Rev Esp Enferm Apar Dig 62(5):424–430
42. Holmdahl L, Risberg B, Beck DE, Burns JW, Chegini N, di Zerega GS, Ellis H (1997) Adhesions: Pathogenesis and prevention-panel discussion and summary. Eur J Surg Suppl (577):56–62
43. Ellis H (1990) The hazards of surgical glove dusting powders. Surg Gynecol Obstet 171(6):521–527

Exhibit 92

Critical Reviews in Toxicology

ISSN: 1040-8444 (Print) 1547-6898 (Online) Journal homepage: http://www.tandfonline.com/loi/itxc20

Oxidatively damaged DNA in animals exposed to particles

Peter Møller, Pernille Høgh Danielsen, Kim Jantzen, Martin Roursgaard & Steffen Loft

To cite this article: Peter Møller, Pernille Høgh Danielsen, Kim Jantzen, Martin Roursgaard & Steffen Loft (2013) Oxidatively damaged DNA in animals exposed to particles, Critical Reviews in Toxicology, 43:2, 96-118, DOI: 10.3109/10408444.2012.756456

To link to this article: http://dx.doi.org/10.3109/10408444.2012.756456

http://informahealthcare.com/txc
ISSN: 1040-8444 (print), 1547-6898 (electronic)

Critical Reviews in Toxicology

Crit Rev Toxicol, 2013; 43(2): 96–118
© 2013 Informa Healthcare USA, Inc. DOI: 10.3109/10408444.2012.756456

informa healthcare

REVIEW ARTICLE

Oxidatively damaged DNA in animals exposed to particles

Peter Møller, Pernille Høgh Danielsen, Kim Jantzen, Martin Roursgaard, and Steffen Loft

Section of Environmental Health, Department of Public Health, University of Copenhagen, Copenhagen, Denmark

Abstract

Exposure to combustion-derived particles, quartz and asbestos is associated with increased levels of oxidized and mutagenic DNA lesions. The aim of this survey was to critically assess the measurements of oxidatively damaged DNA as marker of particle-induced genotoxicity in animal tissues. Publications based on non-optimal assays of 8-oxo-7,8-dihydroguanine by antibodies and/or unrealistically high levels of 8-oxo-7,8-dihydroguanine (suggesting experimental problems due to spurious oxidation of DNA) reported more induction of DNA damage after exposure to particles than did the publications based on optimal methods. The majority of studies have used single intracavitary administration or inhalation with dose rates exceeding the pulmonary overload threshold, resulting in cytotoxicity and inflammation. It is unclear whether this is relevant for the much lower human exposure levels. Still, there was linear dose–response relationship for 8-oxo-7,8-dihydroguanine in lung tissue without obvious signs of a threshold. The dose–response function was also dependent on chemical composition and other characteristics of the administered particles, whereas dependence on species and strain could not be equivocally determined. Roles of cytotoxicity or inflammation for oxidatively induced DNA damage could not be documented or refuted. Studies on exposure to particles in the gastrointestinal tract showed consistently increased levels of 8-oxo-7,8-dihydroguanine in the liver. Collectively, there is evidence from animal experimental models that both pulmonary and gastrointestinal tract exposure to particles are associated with elevated levels of oxidatively damaged DNA in the lung and internal organs. However, there is a paucity of studies on pulmonary exposure to low doses of particles that are relevant for hazard/risk assessment.

Keywords

8-Oxo-7,8-dihydro-2′-deoxyguanosine, carbon nanotubes, nanoparticles, oxidative DNA damage, oxidative stress

History

Received 23 August 2012
Revised 30 November 2012
Accepted 4 December 2012

Table of Contents

Address for correspondence: Peter Møller, Section of Environmental Health, Department of Public Health, University of Copenhagen, Øster Farimagsgade 5A, Building 5B, 2nd Floor, DK-1014 Copenhagen, Denmark. Tel: +45 35327654. Fax: +45 35327686. E-mail: pemo@sund.ku.dk

Introduction

Oxidative stress is an important mechanism of action of adverse health effects of particles in air pollution as well as many different engineered nanoparticles. This can occur through direct generation of reactive oxygen species (ROS) by physico-chemical surface properties, by soluble compounds such as transition metals or organic compounds, altered function of mitochondria, NADPH-oxidases, cellular calcium homeostasis or through activation of inflammatory cells (Li et al., 2008a). Oxidative stress can cause damage to DNA and other cellular target molecules as well as induce inflammation through activation of redox-sensitive signaling pathways, including AP-1, MAP kinases and NF- B activation with subsequent changes in pro-inflammatory gene expression (Li et al., 2008a). This sequence of events has received some acceptance as tiered process with particle--generated ROS giving rise to oxidative stress, which promotes inflammation reactions and subsequently development of pulmonary diseases (Ayres et al., 2008). However, studies on particle toxicology sometimes use very high doses of particulate matter, which may overwhelm any biological defense mechanism. This is best described for airway exposure to particles where overload of the pulmonary clearance mechanisms lead to inflammation reactions and

DOI: 10.3109/10408444.2012.756456

associated generation of oxidative stress (Oberdörster, 1995). The level of oxidatively damaged bases in DNA in animal tissues can be considered an important general indicator of intracellular oxidative stress capable of reaching the nucleus as well as reflecting a specific carcinogenic mechanism (Møller et al., 2010a). It is possible to assess the level of oxidatively damaged DNA in tissues at the portal of entry of the body, such as the lungs or gastrointestinal tract and in remote target organs in animal experimental models, with possibly different susceptibility (Loft et al., 1998; Møller et al., 2012). Oxidatively damaged DNA is efficiently repaired in most circumstances, although some repair kinetics and mechanisms of action are likely to be dependent on the deposited dose, characteristics of the material and elapsed time. The most widely studied lesion in oxidatively damaged DNA is 8-oxo-7,8-dihydroguanine (8-oxoGua), which is most commonly measured as the 2′-deoxynucleoside 8-oxo-7,8-dihydro-2′-deoxyguanosine (8-oxodG). This lesion is mutagenic, resulting in GT-transversion if left unrepaired in DNA upon replication and such lesions are frequently found in lung cancer (Hainaut & Pfeifer, 2001). The main repair pathway for 8-oxoGua in DNA is base excision mediated by oxoguanine DNA glycosylase 1 (OGG1), as shown in Figure 1, with the lesion induced by oxidative stress resulting from exposure to particles. 8-OxoGua in DNA can also result from insertion of 8-oxodGTP after oxidation of the nucleotide pool, although this is partly prevented by nudix hydrolase 1, which cleaves phosphates of 8-oxodGTP with 8-oxodG as the final product for urinary excretion. The timing of exposure and collection of tissues as well as dose–response associations are thus likely important determinants for the level of DNA damage. The levels of 8-oxoGua in tissues can be detected by mass spectrometry (MS)-based chromatographic methods after acid hydrolysis of DNA, although this is associated with spurious oxidation of the DNA. In contrast, 8-oxodG has been widely studied by electrochemical detection (ECD) after enzymatic digestion of DNA and high-performance liquid chromatography (HPLC). It would be foolish to claim that methods belong to certain fields of research such as genetic toxicology. However, it seems that many assays of genotoxicity have spilled over from the classic field of genetic toxicology and oxidative stress research to nanotoxicology. A good example is the measurement of DNA damage by the comet assay that has been used in genetic toxicology and biomonitoring of exposure to particles for years (Møller et al., 2008) and it is now being used in nanotoxicology (Karlsson, 2010; Landsiedel et al., 2009). In addition, there also seems to be a drive toward using relatively easy assays for the detection of oxidatively damaged nucleobase lesions. This encompasses mainly antibody-based detection of 8-oxodG, although also the detection of formamidopyrimidine DNA glycosylase (FPG)-sensitive sites by the comet assay can be purchased as a commercial kit. Still, the detection of oxidatively damaged DNA nucleobases requires expertise and there is a risk that the scientific literature on nanotoxicology might be polluted by positive results because of publication bias and/or adventitious associations that are detected by unspecific methods.

The types of particles that have been investigated in studies of oxidatively damaged DNA seem to follow the same path as the historical particle exposures in inhalation toxicology (Donaldson & Seaton, 2012). The pre-2000s' publications focused on the relationship between pulmonary exposure to silica, asbestos and diesel exhaust particles (DEP) and oxidatively damaged DNA in lung tissue (Nagashima et al., 1995; Yamaguchi et al., 1999; Yamano et al., 1995). The exposure to at least quartz and asbestos has been linked to pulmonary diseases in humans in studies that date back more than a century (Donaldson & Seaton, 2012). The pulmonary health effects by exposure to diesel exhaust (DE) received increased attention in the early 1990s (Hesterberg et al., 2012), which resulted in a number of studies on chronic inhalation exposures containing poorly soluble particles such as carbon black, TiO_2 and DEP (Heinrich et al., 1995; Mauderly et al., 1994; Nikula et al., 1995). These studies

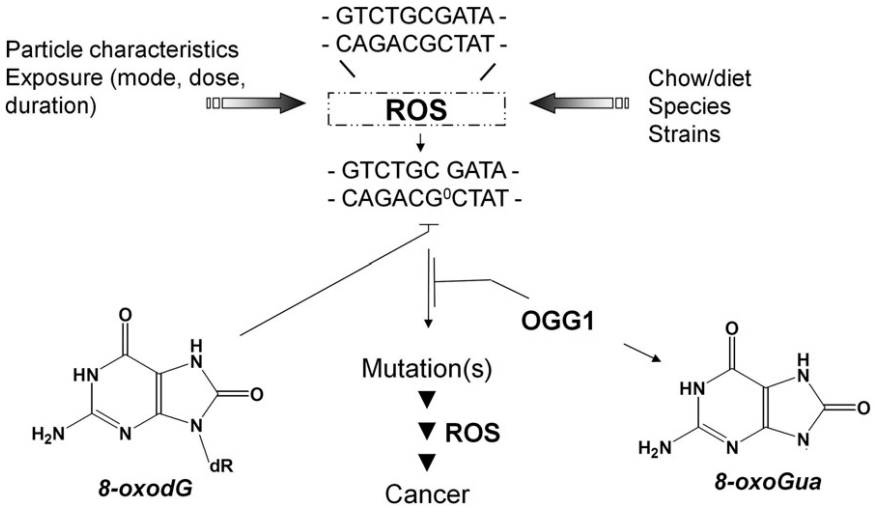

Figure 1. Guanine nucleobases in DNA can be damaged by ROS to 8-oxoGua, which can be assessed by MS after isolation by chromatographic methods. However, it is more common to measure the 2′-deoxyguanosine analog 8-oxodG by ECD after isolation by chromatographic methods. Alternative methods for the detection of the same lesions in nuclear DNA encompass enzymic detection by hOGG1 or FPG, or antibody-based methods. The 8-oxoGua in plasma, serum and urine is considered to originate from mainly OGG1-mediated repair of the nucleotide in DNA. The origin of 8-oxodG lesion in plasma, serum and urine is still being debated, although it is considered to mainly reflect sanitation of oxidation products of dGTP in the nucleotide pool as well as cell death.

indicated that it required a relatively high level of chronic exposure to observe histopathological findings and the increased tumor rate coincided with doses that caused pulmonary overload in rats (Hesterberg et al., 2012). The studies on the relationship between pulmonary exposure to poorly soluble particles (carbon black and TiO_2) and oxidative damage to DNA emerged in the early 2000s (Gallagher et al., 2003; Rehn et al., 2003). It was probably promoted by the increased awareness about the toxicological effects of particles, which previously had been considered as ''nuisance dust'', as well as a transition toward the development of the broader field of nanotoxicology as compared to inhalation studies on combustion-derived particles (Borm et al., 2006). The first studies on pulmonary exposure to carbon nanotubes showed that a single intratracheal (i.t.) instillation of single-walled carbon nanotubes (SWCNTs) in mice (0.1 or 0.5 mg/mouse) or rats (1 or 5 mg/rat) was associated with a transient inflammation response and development of granulomas in the lungs (Lam et al., 2004; Warheit et al., 2004). A later study showed that a single injection of multi-walled carbon nanotubes (MWCNTs) into the peritoneal cavity of mice (50 μg/mouse) was associated with inflammation and development of granulomas (Poland et al., 2008). Increased number of mesotheliomas in cancer-susceptible mice with a heterozygous genotype for p53 was observed after one intraperitoneal (i.p.) injection of MWCNTs at a dose of 3 mg/mouse (Takagi et al., 2008). However, i.p. injection of MWCNTs (2 or 20 mg/rat) in wild-type rats was not associated with an increased level of mesotheliomas, although the exposure elicited inflammatory reactions in the peritoneal cavity early after the exposure (Muller et al., 2009). In keeping with these observations, it has been shown that pulmonary exposure to SWCNTs by pharyngeal aspiration in mice (10–40 μg/mouse) was associated with inflammation, oxidative stress (assessed for instance by increased levels of lipid peroxidation products and depletion of glutathione in the lungs), fibrosis and development of granulomas (Shvedova et al., 2005). A later study showed that inhalation of SWCNTs (5 mg/m^3, 5 h/d for 4 d) was associated with pulmonary inflammation, oxidative stress and histopathological findings (collagen deposition and fibrosis), and these effects were stronger than the effects that were elicited by the same dose (5–20 μg/mouse) administered by a single pharyngeal aspiration (Shvedova et al., 2008). It should be noted that these effects on histopathological examinations in tissues of animals have mainly been observed in studies where the particles have been injected in the peritoneal cavity or trachea. These exposure routes have been considered acceptable for assessing the relative toxicity of test materials (Oberdörster et al., 2005). However, it has to be stressed that the doses and exposure route should be reasonable in the studies of particle-induced damage to DNA. The studies on injection of particles into the peritoneal cavity cannot be used for risk assessment of particles and the i.t. instillation of particles in the airways is a non-physiological procedure.

The purpose of this review was to assess the weight of evidence for the associations between oxidatively generated damage to nucleobases in animals after exposure to particles. We have assessed this by testing seven important hypotheses in regard to the relationship between dose of exposure to particles and oxidatively damaged nucleobases in samples from animals: (i) the apparent induction of 8-oxodG depends on the type of assay employed, (ii) the response to airway exposure depends on the mode of administration, (iii) the response depends on timing of exposure and tissue collection, (iv) the response shows species and strain differences, (v) the target organ and response depend on the route of exposure, (vi) the response depends on the particle characteristics and (vii) the response is influenced by concomitant inflammatory reactions.

Methodology

We searched the PubMed, EMBASE and Web of Science databases for publications on the association between exposure to particles and oxidatively damaged DNA in the tissues of animals. The search terms and approach are available as Supplementary Information Table S1. We identified 64 publications with results on oxidatively damaged DNA. The Supplementary Information Tables S2 (pulmonary exposure) and S3 (non-pulmonary exposure) contain data that we have abstracted from the publications and used for the meta-analysis. We have included three studies on i.p. exposure to asbestos fibers in the group of pulmonary exposure because this route of exposure has been used as surrogate for pleural exposure in studies of asbestos-generated mesothelioma (Jiang et al., 2008; Schürkes et al., 2004; Unfried et al., 2002). The i.p. exposure route for fibers has been used for half a century (Bernstein, 2007). However, it is not a physiological route of exposure and administration of high doses may have limited relevance in risk assessment.

We have analyzed the results in different strata of studies because of the variability of the studies in regard to the exposure time, quality of the assays and route of exposure. The highest weight has been attributed to data from studies with assays that we have been deemed valid by standards that were developed by the European Standards Committee on Oxidative DNA damage (ESCODD). This group of researchers from several laboratories in Europe recommended that studies, which had reported more than 5 lesions/10^6 dG of 8-oxodG in cells from young and healthy subjects should be interpreted with caution (ESCODD, 2003a,b). However, several studies on particle exposure have used extended exposure time and the animals are therefore not young by the time of sacrifice. It has been shown that there is an age-dependent accumulation of 8-oxodG in tissues of animals (Møller et al., 2010b). In addition, the exposure to some vehicles may be associated with a slightly increased level of oxidatively damaged DNA, as shown for instance for corn oil in the gastrointestinal tract (Folkmann et al., 2009). Therefore, we have regarded studies with levels of 8-oxodG in unexposed animals between 5 and 10 lesions/10^6 dG as having sufficiently validity for inclusion in the analysis. This is also in keeping with the notion that ESCODD observed that most laboratories, which used an ESCODD approved protocol for the chromatographic detection of 8-oxodG in pig liver tissue, the obtained values that were approximately 10 lesions/10^6 dG of 8-oxodG (ESCODD, 2003a). We have judged that the studies on 8-oxodG by antibody-based methods have insufficient validity if the results have been reported as ''score'' or ''arbitrary units'' because it is not

DOI: 10.3109/10408444.2012.756456

possible to obtain values on the number of lesions. In addition, the European Standards Committee on Urinary DNA Lesion Analysis has shown that the antibody-based methods generate high levels of 8-oxodG in urine (Evans et al., 2010), which presumably is because the antibodies are unspecific. A number of studies have detected the level of FPG-sensitive sites by the comet assay. The FPG-sensitive sites encompass 8-oxodG and ring-opened formamidopyrimidine lesions that are generated by oxidation reactions (Loft et al., 2008). This assessment has been validated in multi-laboratory trials by the European Comet Assay Validation Group, which generally has shown high concordance in results from different laboratories that have analyzed coded samples from the same batch of cells (Johansson et al., 2010; Møller et al., 2010c). The FPG-based detection of oxidatively damaged DNA does not have the same problems of spurious oxidation as some of the chromatographic assays and indirect calibration of for instance the comet assay with ionizing radiation-generated DNA damage indicates that the number of FPG-sensitive sites does not exceed the threshold level of 10 lesions/10^6 dG (Møller et al., 2004). Therefore, we have regarded the studies on FPG-based detection of oxidatively damaged DNA as valid in the meta-analysis. In this review, we refer to the studies as being ''optimal'' for the determination of oxidatively damaged DNA if the number of oxidized guanine nucleobase lesions were below a threshold of 10 lesions/10^6dG or the level of oxidatively damaged DNA had been obtained as FPG-sensitive sites. Otherwise, the assays have been considered ''non-optimal'' for the determination of oxidatively damaged DNA because the actual number of lesions was not reported.

We have evaluated the strength of the evidence for the test of the hypothesis as score from A (highest score) to D (lowest score). Score A was obtained if the evidence was based on studies from at least two different laboratories with optimal assays and dose–response relationship. Scores B and C were based on evidence from studies with dose–response relationships on optimal or non-optimal assays, respectively. Score D was based on evidence from studies with non-optimal assays and lack of design to detect dose–response relationships. We assessed each of the studies that are included in the review according to this score (shown in Supplementary Information Tables S2 and S3). Supplemental Figure S1 shows the historic trend in the publications according to these scores; it shows that a number of the studies on pulmonary exposure to particles obtain low scores (C or D), whereas most of the studies on non-pulmonary exposure to particles obtain high scores (A or B).

The dose–response relationships were assessed by differences in the regression coefficients. We have calculated the weighted correlation coefficient (r_w) for the studies with optimal and non-optimal determination of oxidatively damaged DNA. This analysis has been based on the mass doses (mg/kg body weight) because the older literature has mainly used this metric and it is still difficult to obtain and compare data on the number concentration, specific surface area or other exposure metrics of particles in biological media. The analysis of the difference between r_w values has been corrected for bias in z values due to multiple testing. In addition, the effect size was also calculated as the standardized mean difference (SMD) with 95% confidence interval (CI) as categorized data in Review Manager version 5.0 (The Nordic Cochrane Centre, The Cochrane Collaboration, Copenhagen, Denmark, 2008). We have analyzed the effect size as the SMD because this can be used for comparison of studies that have reported the same end points with different scales or units. The SMD is calculated as the difference in the mean outcome between the groups of exposure divided by the common standard deviation of the groups. It expresses the size of the effect in each study relative to the variability in the study. The effect size is outlined in a forest plot with a weighted effect size according to the size of the studies. In the forest plot, ''Favors control'' corresponds to increased level of oxidized DNA lesions in the group of exposed animals, whereas ''Favors experimental'' corresponds to the opposite. The forest plot has a corresponding funnel plot that shows the standard error (SE) as a function of the SMD. Ideally, it should look like a funnel or a mirror image across the central estimate of the effect size (represented with a vertical line). Deviations from the funnel shape are related to heterogeneity between the studies in the meta-analysis. We have typically observed that the funnel plots have an over-representation of publications with both large effect and SE (Møller et al., 2010b, 2011). These publications appear in the lower right-hand quadrant of the funnel plot. It is typically an indication of publication bias where among small studies those with high effect size have been published, whereas null effect studies have not.

Hypothesis 1: The effect size of oxidatively damaged DNA depends on the type of assay

The studies differ substantially in the type of assays that have been used for the detection of oxidatively damaged DNA, although the predominant assays have been chromatographic techniques and antibody-based assays. So far, these studies have focused on 8-oxodG although a large variety of direct and indirect oxidatively related modifications of DNA components exist (Cadet et al., 2012). For instance, lipid peroxidation-mediated etheno adducts have been demonstrated by HPLC-MS/MS in the liver after oral exposure to nanosized carbon black in rats (Danielsen et al., 2010); however, such studies are few and not possible to review systematically. An investigation of the effect of the assays on the outcome in terms of 8-oxodG levels as result of particle exposure can best be carried out in lung tissue because the largest number of studies has investigated airway exposure. Table 1 shows the results from an assessment in this stratum of studies that have investigated the effect of pulmonary exposure to particles. For the assessment of the effect size, we have used the results from the time point closest to 24 h after the exposure because the majority of the studies on particle-induced oxidatively damaged DNA have used this post-exposure period. This should not be viewed as 24 h is the optimal time point for detection of genotoxicity after exposure to particles. The DNA damaging potential of particles with low biopersistence could be over-estimated in a screen test with a rigorous adherence to a fixed time point shortly after a bolus exposure such as i.t. instillation. In addition, we have used the results from the lowest dose that provided a

Table 1. Stratification of studies on oxidatively damaged DNA in lung tissue according to the measurement of oxidized DNA nucleobases.

	Assays for determination of oxidized nucleobases			
Parameter	Optimal*	Non-optimal†	Not relevant‡	*p* value¶
Effect (Positive/null)§	7/8	15/1	10/1	<0.01
Exposure mode i.t. (i.p.)/inhalation	10/5	12/4	9/2	0.61
Species (rat/mouse)||	7/6	9/7	6/5	0.90
Number of animals#	36 (18–49)	33 (24–71)	43 (33–55)	NA
Daily dose (mg/kg)	3.3 (2.3–11.7)	5.6 (1.9–10.3)	5.0 (1.4–11.0)	NA
Effect size∫	0.87 (0.31–1.43)	1.14 (0.61–1.67)	NA	NA

*The studies with optimal assays for the determination of oxidatively damaged DNA have reported levels of oxidatively damaged DNA that are less than 10 lesions per unaltered nucleobases (Albrecht et al., 2005; Bourdon et al., 2012; Danielsen et al., 2010; Møller et al., 2003; Morimoto et al., 2005, 2009; Risom et al., 2003a, 2007a; Takata et al., 2009; Tokiwa et al., 1999, 2005; Tsurudome et al., 1999; van Berlo et al., 2010; Wessels et al., 2011; Yamaguchi et al., 1999). †The studies with non-optimal assays that have had high baseline level of oxidatively damage DNA (more than 10 lesions per unaltered nucleobases) or DNA damage reported as fluorescence units (Gallagher et al., 2003; Hwang et al., 2010; Ichinose et al., 1997a,b; Inoue et al., 2005, 2010; Iwai et al., 2000; Kato et al., 2012; Nagashima et al., 1995; Nehls et al., 1997; Pauluhn & Wiemann, 2011; Sato et al., 2000; Seiler et al., 2001c; Takata et al., 2011; Yamano et al., 1995). ‡The studies are considered ''not relevant'' because they have reported levels of oxidatively damaged DNA on a qualitative scale or measured the genotoxicity in tissues at time points that are weeks apart from the last exposure to particles (Aoki et al., 2001; Jiang et al., 2008; Kaewamatawong et al., 2006; Li et al., 2008b; Rehn et al., 2003; Sanbongi et al., 2003; Schürkes et al., 2004; Seiler et al., 2001a, 2004; Unfried et al., 2002; Yamanushi et al., 2001). ¶The *p* values are obtained from 2 2 contingency tables with studies grouped as having used optimal or non-optimal assays for determination of oxidatively damaged DNA. §The number of effects in this row does not match the number of studies because some studies have used more than one type of particles. ||One study used guinea pigs. #Reported as median (25–75% quartile) of the total number of animals in the study. ∫The effect size is the SMD; the 95% CI is shown within parentheses. The forest plots for the assessment of the SMD by optimal and non-optimal assays are shown in Figures S2 and S4, respectively.

statistically significant effect or the largest dose in the studies that reported statistically non-significant effects. We have grouped the studies into those that have reported levels of oxidatively damaged DNA in lung tissue (or omentum tissue) of unexposed animals with optimal (Albrecht et al., 2005; Bourdon et al., 2012; Danielsen et al., 2010; Møller et al., 2003; Morimoto et al., 2005, 2009; Risom et al., 2003a, 2007a; Takata et al., 2009; Tokiwa et al., 1999, 2005; Tsurudome et al., 1999; van Berlo et al., 2010; Wessels et al., 2011; Yamaguchi et al., 1999) or non-optimal assays for determination of low baseline levels of oxidatively damaged DNA (Gallagher et al., 2003; Hwang et al., 2010; Ichinose et al., 1997a,b; Inoue et al., 2005, 2010; Iwai et al., 2000; Kato et al., 2012; Nagashima et al., 1995; Nehls et al., 1997; Pauluhn & Wiemann, 2011; Sato et al., 2000; Seiler et al., 2001c; Takata et al., 2011; Yamano et al., 1995). A number of studies have not reported the absolute values of 8-oxodG (Aoki et al., 2001; Jiang et al., 2008; Kaewamatawong et al., 2006; Li et al., 2008b; Sanbongi et al., 2003) or have reported values of 8-oxodG in tissues at later time points (10 weeks or 90 d) after a single exposure by i.t. instillation or i.p. injection of asbestos fibers or quartz (Rehn et al., 2003; Schürkes et al., 2004; Seiler et al., 2001a, 2004; Unfried et al., 2002; Yamanushi et al., 2001). The type of investigated particles did not differ between these groups of studies; for instance, the studies on quartz and asbestos are represented in the group of studies with optimal determination of oxidized DNA (Albrecht et al., 2005; Takata et al., 2009; Yamaguchi et al., 1999) as well as the group of studies with non-optimal assays that have assessed the level of 8-oxodG at a time point close to the last exposure (Nehls et al., 1997; Seiler et al., 2001c; Takata et al., 2011) and at time points that are months apart from the last exposure (Rehn et al., 2003; Schürkes et al., 2004; Seiler et al., 2001b, 2004; Unfried et al., 2002).

Table 1 shows that there is a tendency to publications showing statistically significant effect on genotoxicity when the results have been obtained by assays with non-optimal determination of oxidatively damaged DNA ($^2 = 8.3$ and $p < 0.01$). The doses, exposure modes (inhalation versus i.t. instillation or i.p. injection) or species (mice or rats), were not associated with different statistical outcome of the levels of oxidatively damaged DNA in this stratum of publications. The SMD and 95% CI was 0.87 (95% CI: 0.31–1.43) and 1.14 (95% CI: 0.61–1.67) for the studies that had measured levels of oxidatively damaged DNA in lung tissue by optimal and non-optimal assays, respectively (see Figures S2–S5 for the forest and funnel plots of this analysis). The effect size cannot be assessed in the studies that did not report data on 8-oxodG, which included studies that measured 8-oxodG by immunohistochemistry (Aoki et al., 2001; Jiang et al., 2008; Kaewamatawong et al., 2006; Sanbongi et al., 2003). There was no difference in the reported effect size between the studies with optimal or non-optimal assays for the determination of oxidatively damaged DNA as indicated by the overlapping 95% CIs for the SMD. However, each of the groups of studies with optimal and non-optimal assays for the determination of oxidatively damaged DNA had statistically significant effects because the 95% CI of the SMD does not include zero.

We have assessed the dose–response relationship in studies with optimal and non-optimal assays that applied more than two doses of particles. The actual *r* values from the studies have not been reported, which is probably because the results have not been assessed by linear regression analysis. For the analysis of the dose–response relationship, we have therefore used the mean values of oxidatively damaged DNA in each group of exposure. In addition, it is only possible to assess the dose–response relationship in the studies of pulmonary exposure to particles because there is an insufficient number of studies on other routes of exposure that have assessed dose dependently the association between particle exposure and oxidatively damaged DNA. Other studies have not been included in this analysis of the dose–response relationship because they did not detect a dose–response relationship (Morimoto et al., 2005, 2009; Pauluhn & Wiemann, 2011). Figure 2 shows the regression coefficients

DOI: 10.3109/10408444.2012.756456

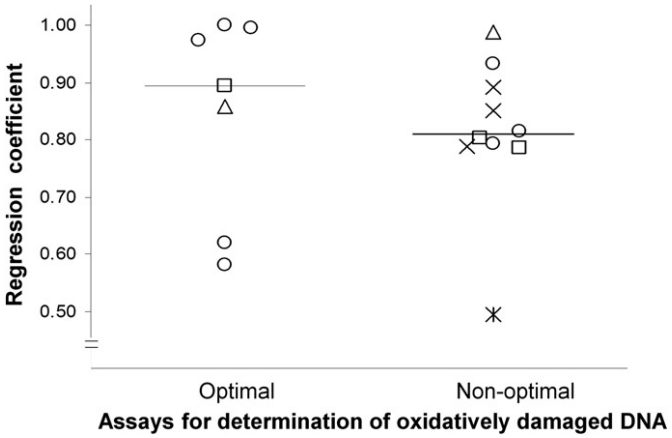

Figure 2. Regression coefficients (r) of the relationship between the applied dose of particles and the level of oxidatively damaged DNA in lung tissue of animals. Each symbol represents the results from one study. The symbols represent exposures to DEP or traffic-related particles (circles; Ichinose et al., 1997a; Møller et al., 2003; Nagashima et al., 1995; Risom et al., 2003a; Sato et al., 2000; Tokiwa et al., 1999, 2005; Tsurudome et al., 1999), asbestos (squares; Schürkes et al., 2004; Unfried et al., 2002; Yamaguchi et al., 1999), nanosized carbon black (triangles; Bourdon et al., 2012; Gallagher et al., 2003), quartz (cross; Seiler et al., 2001b,c, 2004) and TiO_2 (double cross; Rehn et al., 2003). The horizontal lines represent the weighted regression coefficient (r_w) of the studies.

from the studies that have been included in this analysis, stratified into studies that have used optimal or non-optimal assays for the detection of oxidatively damaged DNA. All the studies with optimal assays for the detection of oxidatively damaged DNA had positive r values and there was statistically significant difference between the magnitude of the r values ($p < 0.001$ and $^2 = 227.0$). The dose–response relationship of the genotoxic effect of pulmonary exposure to DEP has been investigated in four different studies (Møller et al., 2003; Risom et al., 2003a; Tokiwa et al., 1999; Tsurudome et al., 1999), whereas there is only one study that has investigated the relationship between oxidatively damaged DNA in the lung tissue and the dose of exposure to each of air pollution particles (Tokiwa et al., 2005), asbestos fibers (Yamaguchi et al., 1999) and nanosized carbon black (Bourdon et al., 2012). There was also positive r values of the studies that had used non-optimal assays for the measurement of oxidatively damaged DNA and the magnitude of r values differed between the studies ($p < 0.001$ and $^2 = 50.0$). The dose-dependent genotoxic effects of pulmonary exposure to quartz and DEP have each been investigated in three different studies (Ichinose et al., 1997a; Nagashima et al., 1995; Sato et al., 2000; Seiler et al., 2001b,c, 2004), and asbestos fibers have been investigated in two studies (Schürkes et al., 2004; Unfried et al., 2002). The relationship between the dose of nanosized carbon black (Gallagher et al., 2003) and TiO_2 (Rehn et al., 2003) and levels of oxidatively damaged DNA in lung tissue have each been investigated in one study with non-optimal assay for the detection of oxidatively damaged DNA. Overall, the r_w value for the studies with optimal assays for the detection of oxidatively damaged DNA was slightly higher ($r_w = 0.96$) than the value from the studies with non-optimal assays ($r_w = 0.86$). This difference in r_w values was statistically significant ($p < 0.001$ and $^2 = 47.0$).

A number of studies have assessed the level of 8-oxodG in serum/plasma or urine of animals that have been exposed to particles by either pulmonary or non-pulmonary route. These studies are interesting because they offer the perfect benchmark to human exposure studies that have shown increased urinary excretion of 8-oxodG in groups of particle-exposed subjects (Møller & Loft, 2010). Moreover, this marker as well as the 8-oxoGua analog has been shown to possess predictive value in regard to development of lung cancer in non-smoking humans in a prospective cohort study (Loft et al., 2006, 2012b). This is supported by several case–control studies of cancer patients, although this type of design is not as strong as the prospective studies because the increased levels of oxidatively damage DNA might be a consequence of the disease rather than a causal factor (Loft & Møller, 2006; Olinski et al., 2003). Urine, serum and plasma contain large amounts of antioxidants (e.g. uric and ascorbic acid) and there are low concentrations of 2′-deoxyguanosine. It means that there is only a low risk of spurious oxidation, whereas the complex mixture of urine with numerous waste products is a challenge to measuring 8-oxoGua by chromatographic assays (Loft et al., 2012a). The measurement of 8-oxodG in plasma/serum is also challenging because of very low concentrations and the results are therefore difficult to interpret. The effect of particle exposure on 8-oxodG concentrations in serum/plasma or urine have mainly been investigated with ELISA assays (Bai et al., 2011; Han et al., 2010; Niwa et al., 2008; Sato et al., 2006). One study showed an increased concentration of 8-oxodG in plasma after a single i.t. instillation of Min-U-Sil quartz (100 mg/kg; Sato et al., 2006), whereas another study showed increased 8-oxodG in serum after inhalation of carbon black (15.6 mg/m^3, 6 h/d and 5 d/week) for four weeks (Niwa et al., 2008). The detection of urinary excretion of 8-oxodG by antibody-based assays has shown increased effects after oropharyngeal aspiration of 40 μg/mouse of MWCNTs (Han et al., 2010) and DE inhalation (200 μg/m^3, 6 h/d, 5 d/week) for seven weeks (Bai et al., 2011). On the contrary, there is a lack of studies showing statistically significant differences in the 8-oxodG concentration between exposed and control animals in studies that have assessed this by chromatographic assays. One study found a statistically non-significantly increased level of 8-oxodG in urine by LC-MS/MS in mice exposed to nanosized carbon black (14.5 1.5 pmol/ml after an exposure dose of 500 μg/mouse on two different days by i.t. instillation) compared to controls (12.1 2.0 pmol/ml; Tellabati et al., 2010). Another study also showed statistically non-significantly higher urinary excretion of 8-oxodG, measured by HPLC-ECD, after i.t. instillation of DEP at doses of 2.7 (160.1 49.9 lesions/10^6 dG) and 0.7 mg/kg (184.4 41.1 lesions/10^6 dG) as compared to controls (156.2 74.6 lesions/10^6 dG; Møller et al., 2003). It is not possible to carry out only a meta-analysis on publications that have used optimal assays for the determination of oxidatively generated nucleobases in serum/plasma and urine. However, a meta-analysis of all studies on pulmonary particle exposure showed that the SMD was 0.99 (95% CI: 0.38–1.60) for the studies that have measured 8-oxodG in serum/plasma and urine (the forest and funnel plots are shown in Figures S6 and S7, respectively). One study on gastrointestinal tract exposure to DEP also showed statistically non-significantly increases in

the urinary excretion of 8-oxodG of exposed rats (155 30 pmol/24 h at 80 mg_{DEP}/kg_{feed}) as compared to controls (134 31 pmol/24 h) employing chromatography with tandem MS (Dybdahl et al., 2003). Although these observations indicate an effect of particle exposure on systemic markers of 8-oxodG, it should be emphasized that it is mainly based on studies with non-optimal assays for the detection of 8-oxodG.

Collectively, the observations suggest that the higher proportion of statistically significant effects for the studies with non-optimal assays for the determination of oxidatively damaged DNA could be related to publication bias, exaggerating the effects detected by optimal assays. However, there is heterogeneity for both the studies with optimal and non-optimal assays as indicated in the funnel plots in Figures S3 and S5. The analysis indicates a score A for the association between using non-optimal assays for the determination of oxidatively damaged nucleobases and reporting statistically significantly increased levels of oxidized nucleobase lesions in tissues, blood and urine after exposure to particles in the airways, peritoneal cavity or gastrointestinal tract. It can be speculated that researchers who detect 8-oxodG by antibody-based assays or ''ready to use'' kits (e.g. the Flare assay for the detection of oxidatively damaged DNA by the comet assay) are more apt to let statistically non-significant effects stay unpublished. On the contrary, it requires commitment to assess 8-oxodG by chromatographic assays or sufficiently validate the comet assay for similar purposes and those researchers might try harder to publish results that are not statistically significant.

Hypothesis 2: The generation of oxidatively damaged DNA depends on the mode of exposure

The most relevant mode of pulmonary exposure to particles is inhalation, although other modes such as i.t. instillation or intrapharyngeal aspiration are used more frequently than inhalation. The advantages and disadvantages of instillations and inhalation have been discussed for more than a decade (Driscoll et al., 2000). Exposure by i.t. instillation is sometimes justified because the material can be limited, such as small samples of authentic air pollution particles or special types of nanoparticles. However, the same dose applied by bolus exposure and inhalation may not elicit the same level of effect because of differences in the dose rate, particle distribution and clearance mechanisms. It has been shown that rats that received 500 (fine) or 750 (ultrafine) μg of TiO_2 particles by inhalation had less pulmonary inflammation as compared with i.t. instillation (Osier & Oberdörster, 1997). The same effect toward higher level of pulmonary inflammation was observed in a study on nanosized carbon black where i.t. instillation of 18 μg/mouse elicited a stronger effect than the presumed same dose administered by 30 min inhalation of 60 mg/m^3 of particles (Jacobsen et al., 2009). These findings fit well with the tumor load after inhalation and i.t. instillation (Borm et al., 2004; Oberdörster, 2002). A comparison of the doses of particles that is associated with increased lung tumor risk indicates that it could be the effect (i.e. the number of animals with lung tumors) that is increased by i.t. instillation as compared to inhalation, whereas the dose

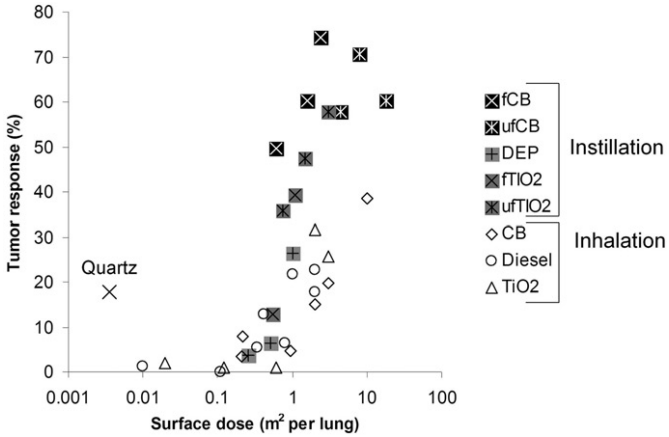

Figure 3. Relationship between the dose of particles (reported as surface/lung) and risk of lung cancer (tumor response) in rats after exposure by inhalation or i.t. instillation (results redrawn from Borm et al., 2004; Oberdörster, 2002).

that elicits the effect is similar for inhalation and i.t. instillation (Figure 3). Assuming the induction of oxidatively damaged DNA follows the same pattern, which seems reasonable because genotoxicity is considered to be an important intermediate event in carcinogenicity, one would be able to obtain the same information about the genotoxic potential with the use of fewer animals that were exposed to particles by i.t. instillation as compared to inhalation.

There are more studies that have investigated the induction of oxidatively damaged DNA after i.t. instillation of particles as compared to inhalation (Table 1). Of the 31 studies with exposures by i.t. instillation (or i.p. injection) in Table 1, 26 studies show statistically significant effects on the level of oxidatively damaged DNA. For the inhalation exposure, there seems to be an equal distribution of studies that have reported statistically significant outcome (six studies) or null effect (five studies). Overall, there is a tendency that studies on i.t. instillation (or i.p. injection) of particles show statistically significant effects ($^2 = 3.85$ and $p < 0.05$). Still, it might be more important to notice that among the studies with optimal assays for the determination of oxidatively damaged DNA, there seems to be more studies on inhalation exposure that show statistically non-significant effects (Morimoto et al., 2005, 2009; Risom et al., 2007a; Wessels et al., 2011) than statistically significant effects (Risom et al., 2003a). The opposite was observed for studies on i.t. instillation (or pharyngeal aspiration) where six studies showed statistically significant effect (Bourdon et al., 2012; Møller et al., 2003; Takata et al., 2009; Tokiwa et al., 1999, 2005; Yamaguchi et al., 1999), whereas four studies reported null effects on oxidatively damaged DNA at the time point of 24 h after the last exposure (Albrecht et al., 2005; Danielsen et al., 2010; Tsurudome et al., 1999; van Berlo et al., 2010). This distribution is not statistically significantly different ($^2 = 2.14$ and $p = 0.14$), which could be due to insufficient number of studies to obtain sufficient statistical power. There is clearly a paucity of studies on inhalation exposure in regard to generation of oxidized DNA in lung tissue.

DOI: 10.3109/10408444.2012.756456

The overall evaluation of the relationship between the mode of exposure and the effect size indicates a score A for the support of the hypothesis that inhalation exposure is associated with lower induction of oxidized DNA lesions as compared with instillations.

Hypothesis 3: The level of oxidatively damaged DNA depends on timing of exposure and tissue collection

The duration of exposure and post-exposure period varies substantially between the studies, although a majority of the studies have assessed the level of oxidatively damaged DNA at 24 h after the last exposure to particles. The observations from studies with optimal assays for the determination of oxidatively damaged DNA in lung tissue suggest that the level of genotoxicity was highest closest to the exposure. This has been documented for a single i.t. instillation of 2 or 4 mg/rat of DEP that had peak levels of 8-oxodG at 2 h (2.5-fold) and lower fold-induction at 8 (1.9-fold) and 24 h (1.4-fold) in measurements with high reliability because of low baseline levels of 8-oxodG in the controls (Tsurudome et al., 1999). The elevated levels of 8-oxodG occurred concomitantly with decreased OGG1 repair activity and there was transcriptional upregulation of *Ogg1* at days 5 and 7 after the exposure (Tsurudome et al., 1999). The same effect of OGG1-mediated DNA repair was observed in mice after inhalation of DEP where a single 90 min inhalation exposure to 80 mg/m^3 increased the level of 8-oxodG in lung tissue; the same dose administered on four consecutive days by 90-min inhalation exposures to 20 mg/m^3 had no effect on the level of 8-oxodG, whereas there was increased transcription of *Ogg1*, which repairs the lesion efficiently (Risom et al., 2003a). In keeping with this, the same 4 20 mg/m^3 inhalation exposure regimen caused increased levels of 8-oxodG in the lungs of *Ogg1* knockout mice, indicating that this effective repair system was able to remove DEP-generated oxidation damage to DNA (Risom et al., 2007a). The decline in oxidatively damaged DNA after a single exposure was also observed after an i.t. instillation of nanosized carbon black; there was a dose-dependent increase in the level of FPG-sensitive sites in lung tissue at day 1 after the exposure (lowest dose was 18 µg/mouse), whereas there was a gradual decline in the level of FPG-sensitive sites with only effect at the highest dose at day 3 (162 µg/mouse) and no effect at day 28 after the exposure (Bourdon et al., 2012). Similar results were observed after exposure to DEP (0.05–5 mg/kg), which was associated with increased levels of FPG-sensitive sites in the liver 24 h after a single i.p. injection, whereas there were no effect after 6 h (Folkmann et al., 2007).

The studies on non-optimal assays for the determination of 8-oxodG by HPLC-ECD also support a bell-shaped time-curve response to particle exposure in the airways. Mice that had been exposed to DEP as a single i.t. instillation (0.3 mg/mouse) had a peak response of 8-oxodG in the lungs at day 2 after the exposure (Nagashima et al., 1995). Similar observations were done in a study with a single i.t. instillation of chrysotile asbestos fibers (2 mg/rat), where the highest level of 8-oxodG in lung tissue was obtained one day after the exposure (Takata et al., 2011), whereas a lower dose (1 mg/rat) was associated with a bell-shaped time-curve with a peak at 14 d after the exposure (Takata et al., 2009). Other studies on i.p. injection of crocidolite asbestos fibers also indicated larger effects at week 10, as compared to week 20, after the exposure (Schürkes et al., 2004; Unfried et al., 2002). Studies on colloidal silica particles indicated less staining of 8-oxodG by immunohistochemistry at day 30 as compared to day 1 after a single i.t. instillation of 30 µg/mouse (Kaewamatawong et al., 2006). In addition, a single i.t. exposure to quartz (2.5 mg/rat of DQ12) showed a bell-shaped effect of immunostaining of 8-oxoGua with a peak at day 21 after the exposure (Nehls et al., 1997), although later studies by the same group indicated a tendency toward even higher levels of 8-oxoGua at day 90 after the exposure (Seiler et al., 2001a,c). The elevated levels of 8-oxodG at these late time points may be related to the development of neoplastic diseases or dysfunction of the organ, whereas it may not be relevant in regard to the intrinsic oxidizing ability of particles in organs of animals. In general, it seems that the largest effect on the generation of oxidatively damaged DNA is obtained within hours to days after a single exposure. In regard to inhalation exposure, it is more difficult to assess the best time window of effect; one study showed a larger difference in the level of 8-oxodG between exposed and controls after three months inhalation of DE (3.5 mg/m^3, 17 h/d and 3 d/week) than after one month of exposure in rats (Iwai et al., 2000), whereas two studies in rats exposed to printer toner of relatively large size (mass median size 3–4.5 µm) for either 1 or 2 years had no effect (Morimoto et al., 2005, 2009).

The time window of effect on 8-oxodG in the studies on non-pulmonary exposure to particles is not well investigated. Some studies on DEP exposure in rats indicate that an effect is observed at 24 h after an oral or i.p. exposure, whereas the effect is smaller at 6 h after the exposure (Danielsen et al., 2008b; Folkmann et al., 2007). This collaborates well with the null effects that have been observed after continuous exposure by the chow feed for 21 d, which has been attributed to increased expression of the OGG1 repair enzyme (Dybdahl et al., 2003; Risom et al., 2003b, 2007b). In another study, there was increased hepatic 8-oxodG at 16 weeks, but not 12 weeks after a single intravenous injection of quantum dots (40 or 160 pmol in 100 µl/mouse); this increase in genotoxicity coincided with a hepatic inflammatory response (TNF and IL-6) and elevated serum levels of alanine and aspartate aminotransferases (Lin et al., 2011).

The relatively swift repair of oxidatively damaged DNA in animal tissue indicates that the detection of increased levels of 8-oxodG at a single time point, is mainly useful for the assessment of genotoxic potential. An examination of DNA damage level at a single time point, such as 24 h after the last exposure, provides little information about the steady-state levels. Still, it has been reported that tandem lesions of 8-oxodG in the genome are refractory to excision by DNA glycosylases (Bergeron et al., 2010). This means that even a single exposure might generate lesions that are difficult to repair and consequently such lesions may give rise to mutations. Still, for risk assessment it is important to use repeated exposures and express time-weighted doses (e.g. mg h/m^3 in inhalation studies), which is in keeping with the exposure assessment in studies on for instance tobacco smoke (pack years) and radon (working level months).

The overall evaluation of the time window of the measurements of oxidatively damaged DNA to determine effects of particles indicates a score A for support of the hypothesis that the timing of pulmonary and non-pulmonary exposure and tissue collection influence the response. Elevated levels of oxidatively damaged DNA appear to be observed mainly within days after a single high-dose exposure and the lesions vanish within weeks after the exposure.

Hypothesis 4: The induction of oxidatively damaged DNA depends on species or strain differences

The studies on species differences in regard to particle toxicology seem to have focused on pulmonary inflammation as a possible mechanistic reason for the fact that rats develop lung tumors after exposure to poorly soluble particles, whereas mice, hamsters, guinea pigs and non-human primates are less susceptible. It has been shown that rats developed more severe inflammation than mice, whereas hamsters did not develop inflammation following inhalation of TiO_2 (1–50 mg/m^3, 6 h/d, 5 d/week) for 13 weeks (Bermudez et al., 2002, 2004). A direct comparisons of the same dose of nanosized carbon black (1–50 mg/m^3, 6 h/d, 5 d/week for 13 weeks) showed that hamsters developed less pulmonary inflammation as compared to mice and rats (Elder et al., 2005). An assessment of oxidative stress biomarkers in the bronchoalveolar lavage fluid (BALF) showed that cells from rats produced more superoxide anion radicals as compared to cells from mice and hamsters, whereas there seemed to be a similar response in regard to the activity of antioxidant enzymes such as glutathione peroxidase, superoxide dismutase and glutathione reductase in BALF (Carter et al., 2006). However, other authors have reported that Syrian golden hamsters as compared to Sprague–Dawley rats had less glutathione concentration in the lung; the hamsters had also lower glutathione peroxidase and γ-glutamyl-cysteine synthase activity, whereas the glutathione reductase activity was higher in rats as compared to hamsters (Borzone et al., 2009). An assessment of the antioxidant activity in alveolar macrophages indicated that hamsters had higher levels of catalase activity, whereas the glutathione concentration as well as superoxide dismutase activity and resistance toward oxidation of glutathione was the same in rats and hamsters (Dörger et al., 1997). Lower levels of glutathione in alveolar macrophages of C57BL/6 J as compared to ICR mice has been associated with higher level of cigarette smoke-induced oxidative stress and susceptibility of ICR mice to develop emphysema (Vecchio et al., 2010). There is also evidence for differences in the tissue iron levels between different strains of mice; e.g. it has been shown that C57BL/6 and BALB/c mice in the lung tissue had 66 and 210 μg/g of iron, respectively (Hahn et al., 2009). These observations suggest inter-species and strain differences in the basal levels of components of the antioxidant defense system, which could be related to different evolutionary adaptation to oxidative stress. This may also transpire to differences between tissues in the same species or strain as it was shown in a study on oral exposure to the oxidizing agent sodium dichromate, where differences in tumor development in the alimentary canal was related to oxidative stress as mode of action (Thompson et al., 2011, 2012).

The majority of studies on particle-generated oxidative damage to DNA have been carried out on mice and rats. It is therefore easier to highlight the notable exceptions that constitute one study on pulmonary DEP exposure in guinea pigs (Møller et al., 2003) and two studies on asbestos fibers, glass fibers and quartz in hamsters (Seiler et al., 2001a,b; Yamaguchi et al., 1999). The exposure to crocidolite asbestos (0.5–2 mg/rat by i.t. instillation) increased the level of 8-oxodG in both Wistar rats and Syrian hamsters, whereas the dose of glass fibers had no effect in a study of 8-oxodG measured by HPLC-ECD with low baseline levels in controls (Yamaguchi et al., 1999). The other study showed higher pulmonary levels of 8-oxodG in Wistar rats as compared to Chinese hamsters at day 90 after i.t. instillation of DQ12 (0.75–12 mg/kg by i.t. instillation), although it should be emphasized that the authors used the same antibody for the detection for 8-oxodG in the two species and it was measured by immunohistochemistry (Seiler et al., 2001a,b). The aforementioned studies do not clearly indicate differences between rats and other species in regard to particle-mediated generation of oxidatively damaged DNA in animal tissues.

There are approximately equal numbers of studies that have reported results on oxidatively damaged DNA in mice and rats after pulmonary exposure, whereas it is a limitation for the analysis of strain or species differences that the same researchers use the same combination of animals and methods for measuring oxidatively damaged DNA. It has been shown that outbred C57BL/6 mice had higher levels of 8-oxodG than inbred BALB/c mice after six months inhalation of DEP (100 μg/m^3, 7 h/d and 5 d/week), although it should be emphasized that the 8-oxodG was detected by ELISA in lung tissue (Li et al., 2008b). Another study showed that outbred ICR mice had larger induction of 8-oxodG in lung tissue as compared to inbred BALB/c mice after i.t. instillation of 0.25–2 mg of carbonaceous particles from pulmonary tissue of non-smoking lung cancer patients (Tokiwa et al., 2005). This may indicate that BALB/c mice are relatively resistant to particle-induced oxidatively damaged DNA in lung tissue. However, it has been shown that topical exposure to ionizing radiation on the lungs of BALB/c mice generated a dose-dependent induction of 8-oxodG (Risom et al., 2003c). The same group of authors also showed that a 90 min inhalation exposure to 80 μg/m^3 of DEP was associated with increased levels of 8-oxodG in lung tissue of BALB/c mice (Dybdahl et al., 2004; Risom et al., 2003a). We have not found studies that have investigated strain differences between rats in regard to exposure to particles. Still, one study exposed either inbred Fischer 344 rats or outbred C57BL/6 J mice to carbon nanoparticles by inhalation (Wessels et al., 2011). However, this study is not particularly useful for the assessment of strain species in particle-mediated oxidative damaged to DNA because the low dose did not generate DNA damage.

Besides species and strain, experimental conditions such as diet, in particular related to fat or nutrient antioxidants might influence the susceptibility to particle-induced oxidatively damaged DNA, although the available data are scarce. Guinea pigs, which like humans are dependent on dietary vitamin C did not appear particularly susceptible to DEP exposure by

DOI: 10.3109/10408444.2012.756456

instillation (Møller et al., 2003). In rats, high-fat diets appeared to increase the genotoxicity of DEP by i.t. instillation, whereas carotenoids reduced the response although the baseline level of 8-oxodG was above the realistic levels (Nagashima et al., 1995; Yamanushi et al., 2001). In humans, carotenoid supplementation is not likely to influence responses to particles as shown by no effect of beta-carotene on 8-oxodG excretion in smokers (van Poppel et al., 1995).

Collectively, the studies, which are included in our review, cannot be used to firmly determine whether or not some types of species or strains are particularly susceptible to generation of oxidized nucleobases. The support for the test of this hypothesis would achieve a score C because it is mainly based on non-optimal assays for the determination of oxidatively damaged DNA, albeit with assessment of dose–response relationships.

Hypothesis 5: The target organ and response depend on the route of exposure and non-pulmonary exposure to particles is associated with increased levels of oxidatively damaged DNA

The majority of studies have investigated the effect of pulmonary exposure to particles, although the list of publications with results on oxidatively damaged DNA after non-pulmonary exposure is slowly increasing (Supplementary Table S3). This is paralleled with an increased focus on toxicological aspects of oral exposure to particles (Card et al., 2011; Møller et al., 2011) and detection, characterization and risk assessment of nanoparticles in foods (Dekkers et al., 2011; Tiede et al., 2008). There is also attention on modulation of tight junction proteins in regard to reduced barrier function in lung cell (Lehmann et al., 2009) and gut mucosa tissue (Folkmann et al., 2012; Mutlu et al., 2011). Especially, the development of nanomaterials could increase the exposure to particles by other routes than the airways. However, even the airway exposure to particles is associated with gastrointestinal tract exposure by clearance mechanisms. It has been shown that 18% of the deposited dose of 15 nm particles in lungs after inhalation was cleared into the gastrointestinal tract after 6 h (Semmler et al., 2004). Recent observations by SPECT/CT imaging has demonstrated 8.3–18.7% and 23.3–50.6% of the deposited dose of particles after short-term inhalation was cleared to the stomach in rats and mice, respectively (Kuehl et al., 2012). Similar observations have been obtained in humans (Leach et al., 2012), indicating that the clearance of particles to the gut is also important in humans. In addition, computer models indicate that 20% and 60% of the inhaled mass of particles are cleared to the stomach after 5 and 200 h, respectively (Sturm, 2007). There is also evidence from a study using endotracheal inhalation and forced respiration that the clearance of particles to the gastrointestinal tract during the first three days after cessation of the exposure was 37% and 38% for 1.7 and 0.8 µm particles, respectively (Kreyling et al., 1993). Although it cannot be ascertained for sure, it seems that especially inhalation toxicologists have considered that the clearance of particles to the gastrointestinal tract corresponded to the particles being removed from the target tissue. This may be true in regard to inflammatory reactions in the lungs, whereas some results suggest that it may not apply to oxidatively damaged DNA where gastrointestinal exposure to 0.64 mg/kg of nanosized carbon black induced the 8-oxodG level in the liver, whereas the equivalent dose did not increase the level of 8-oxodG in the lungs by i.t. instillation (Danielsen et al., 2010).

The studies on non-pulmonary exposure to particles can be grouped into single and repeated exposures. There are studies showing increased levels of oxidatively damaged DNA in the liver after a single injection of 0.05–5 mg/kg of DEP in the peritoneal cavity (Folkmann et al., 2007) or 40–160 pmol of quantum dots injected intravenously (Lin et al., 2011). One study investigated the effect of subcutaneous injection of TiO_2 that were either uncoated or coated with stearic acid; increased staining of 8-oxodG by immunohistochemistry was reported, yet it is difficult to determine the significance of this result because there were no assessment of 8-oxodG in unexposed mice (Onuma et al., 2009). The level of FPG-sensitive sites in the liver was unaltered in the offspring of dams that had been exposed to nanosized carbon black by inhalation (42 mg/m^3 for 1 h/d) on gestation day 8–18 (Jackson et al., 2012). A few recent studies have also emerged with very high baseline levels of 8-oxodG in liver tissue or embryos, which there is no need to discuss in detail because of the risk of spurious oxidation in those results (Girgis et al., 2012; Khalil et al., 2011; Reliene et al., 2005). Most of the studies have investigated the level of oxidatively damaged DNA in organs after gastrointestinal tract exposure. Single exposures have been associated with increased levels of 8-oxodG in the liver after exposure to DEP, SWCNT and fullerenes C_{60} (Danielsen et al., 2008b, 2010; Folkmann et al., 2009). However, there has been mixed results in regard to repeated exposures where ingestion of chow with DEP for 21 d was not associated with statistically non-significantly increased 8-oxodG in the liver (Dybdahl et al., 2003; Risom et al., 2003b, 2007b), whereas oral exposure to TiO_2 (500 mg/kg) and ZnO (50 or 300 mg/kg) increased levels of 8-oxodG in the liver (Sharma et al., 2012; Trouiller et al., 2009). It has also been reported that rats after a 21-day feeding period on chow with DEP had elevated levels of FPG-sensitive sites in the lungs (Müller et al., 2004). The difference between the statistically significant effect on 8-oxodG in the liver after single and repeated DEP exposure is striking. It has been hypothesized that the lack of genotoxicity in the repeated exposure studies was due to increased removal of 8-oxodG by, especially the OGG1-mediated base excision repair pathway (Dybdahl et al., 2003). However, a study on *Ogg1*$^{-/-}$ mice, which were exposed to 0.8 or 8 mg/kg of DEP, was not associated with increased levels of 8-oxodG or FPG-sensitive sites in the liver and lungs (Risom et al., 2007b). It has also been speculated that the differences could be due to different types of DEP – standard reference material 1650 (SRM1650) and SRM2975 – that has been used for these experiments (Risom et al., 2007a). The National Institute of Standards and Technology issued first SRM1650, which had been collected from the heat exchanger of a dilution type facility after 200 engine hours, representing combustion particles from a heavy-duty diesel engine. The SRM2975 sample consisted of particles that had been collected from a filtering system of

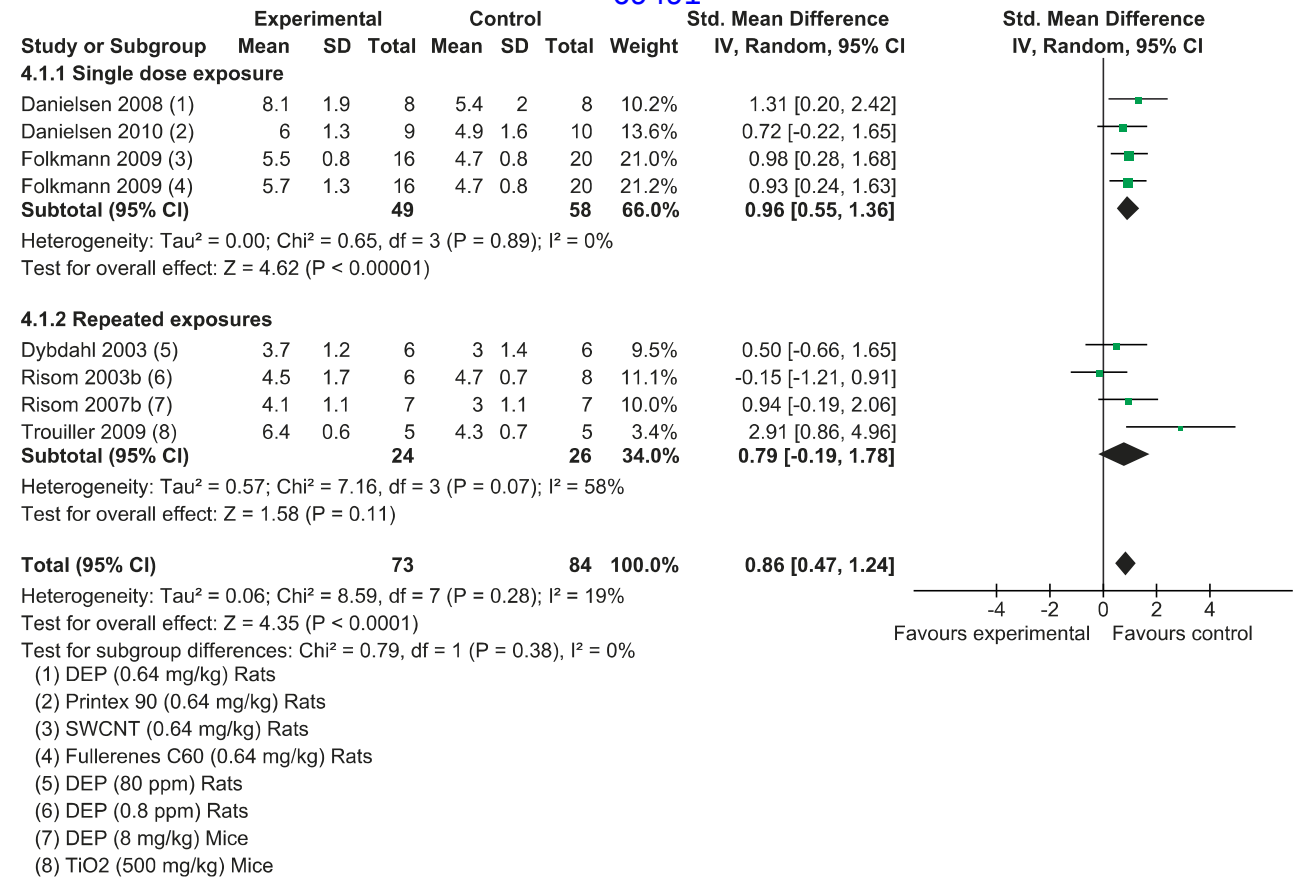

Figure 4. Forest plot of the effect size of oxidatively damaged DNA in the liver after oral exposure to particles. The corresponding funnel plot is shown in Supplementary Information Figure S5.

an industrial diesel-powered forklift. SRM2975 contains less extractable organic compounds, polycyclic aromatic hydrocarbons (PAHs) and Fenton-type transition metals (iron and copper) than SRM1650. Still, direct comparisons of genotoxic effect indicated that SRM1650 and SRM2975 generate similar levels of FPG-sensitive sites in A549 lung epithelial cells (Danielsen et al., 2008a). A later study with A549 cells with or without co-culture with monocytic THP-1 cells indicated that SRM2975 had higher potency toward ROS generation and increased the level of FPG- and hOGG1-sensitive sites as compared to SRM1650 (Jantzen et al., 2012).

A collective analysis of the studies indicates that all the studies on single gastrointestinal exposures have shown increased levels of 8-oxodG in the liver of rats exposed to 0.64 mg/kg of DEP (Danielsen et al., 2008b), fullerenes C_{60} or SWCNT (Folkmann et al., 2009) or nanosized carbon black (Danielsen et al., 2010). A study of single exposure to 2000 mg/kg of quantum dots also showed increased levels of 8-oxodG in the liver, although it should be emphasized that the baseline levels of 8-oxodG was more than 35 lesions/10^6 dG (Khalil et al., 2011). The studies on repeated exposures to DEP have shown statistically non-significant effects in the liver of mice and rats (Dybdahl et al., 2003; Risom et al., 2003b, 2007b), whereas one study showed increased levels of 8-oxodG in mice that had been exposed to 500 mg/kg of TiO_2 in the drinking water (Trouiller et al., 2009). There is also one study on oral administration of ZnO, showing increased levels of 8-oxodG in the liver, yet the baseline level of 8-oxodG (13 lesions/10^6 dG) was high (Sharma et al., 2012). Another study administered nanogold or gold–cobalt nanoalloy (80–320 mg/kg/d for 7 or 14 d) to mice, yet the baseline levels of 8-oxodG in the liver was unrealistically high (Girgis et al., 2012). Figure 4 shows a forest plot of the studies that have reported levels of 8-oxodG in the liver after oral exposure to particles (the corresponding funnel plot is shown in Figure S8). Interestingly, it can be seen that all the studies have shown increased 8-oxodG in the liver of particle exposed animals. The SMD for the single exposure studies was 0.96 (95% CI: 0.55–1.36), which was not different from the repeated exposure studies that had an SMD of 0.79 (95% CI: 0.19–1.78). As such the overall estimate of the effect size is statistically significant, indicating higher levels in exposed animals compared with the unexposed controls.

The overall evaluation of the association between non-pulmonary exposure to particles and oxidatively damaged DNA with liver as the primary target of gastrointestinal exposure is supported with evidence achieving a score B because there are several studies showing effect with optimal assays, whereas there are few studies that have investigated or reported dose–response relationship.

Hypothesis 6: Characteristics of particles and fibers determine the levels of oxidatively damaged DNA

It is well recognized that biological effects can be influenced by many particle characteristics including size, agglomeration

DOI: 10.3109/10408444.2012.756456

state, hygroscopicity, biodurability, shape, surface area, charge, soluble compounds and chemical composition (Oberdörster et al., 2005), although few of these have been directly assessed in relation to oxidative damage to DNA. Over the years, the research has somehow changed from studies of oxidatively damaged DNA in tissue of animals by hazardous agents such as asbestos fibers, quartz or combustion particles to hazard identification of new types of engineered nanomaterials such as carbon nanotubes. This has to some extent evoked the search for benchmark particles for positive responses as well as putatively inert particles that do not generate oxidative damage to DNA at the same dose level as the test particles. An assessment of relevant benchmark particles should in principle build on studies from an array of nanomaterials that are investigated under the same experimental conditions with validated biomarkers. However, it has been more common to compare the level of oxidatively damaged DNA in tissues after exposure to well-established carcinogenic particles and non-carcinogenic counterparts. This is obviously based on the notion that the generation of oxidatively damaged DNA is an important step in the mechanism of carcinogenesis.

Using HPLC-ECD for the detection of low baseline levels of 8-oxodG, it was shown that chrysotile asbestos markedly increased the level of 8-oxodG, whereas the same dose of forsterite (1 mg/rat by i.t. instillation) had no effect on oxidative damage to DNA in the lungs (Takata et al., 2009). Another study based on chromatographic detection of 8-oxodG showed increased genotoxicity in the lungs after i.t. instillation of crocidolite asbestos (0.5–2 mg/animal) and unaltered levels of 8-oxodG after exposure to glass fibers (negative control, 2 mg/animal) in Syrian hamsters and rats (Yamaguchi et al., 1999). The i.p. injection of asbestos fibers has often been used as a surrogate for pleural exposure in studies of asbestos-mediated development of mesothelioma. Using this exposure, it was shown that crocidolite asbestos (1–2 mg/rat) and man-made vitreous fibers (14.7–100 mg/rat) generated similar levels of 8-oxodG in omental tissue, although it should be emphasized that the analysis was based on an antibody-based method (Schürkes et al., 2004). The man-made vitreous fibers had an intermediate length with a 25% fraction of carcinogenic fibers. The toxicity of synthetic vitreous fibers depends on the biopersistence and especially the longer fibers are not efficiently cleared from the lungs (Bernstein, 2007). Another study using antibody-based detection of 8-oxodG showed that a standard type of quartz (DQ12) generated oxidized DNA lesions at day 90 after i.t. instillation of a single dose (1.2 mg/rat), whereas the genotoxicity by four different commercially available types of quartz ranged from being as genotoxic as DQ12 to being non-genotoxic (Seiler et al., 2004). A similar report by the same authors also showed that DQ12 generated 8-oxodG at day 90 after a single i.t. instillation (0.6 mg/rat), whereas the exposure to 0.15–2 mg/rat of two different types of TiO_2 had no effect on the level of antibody-based detection of 8-oxodG (Rehn et al., 2003). The studies on the induction of 8-oxodG by asbestos fibers or quartz have mainly been assessed at relatively late time points after the exposure, which suggests that the effect could be related to inflammation-mediated oxidative stress rather than direct particle-mediated oxidation of DNA nucleobases.

A direct comparison between nanosized carbon black and air pollution particles was carried out in an instillation study that had low baseline levels of 8-oxodG measured by HPLC-MS/MS, although this showed unaltered levels of genotoxicity that could be due to the relatively low dose (0.64 mg/kg; Danielsen et al., 2010). A well-designed study, which unfortunately had a high baseline level of 8-oxodG in the lung tissue of controls (23.5 lesions/10^6 dG), showed that inhalation of 50 mg/m^3 of Sterling V (70 nm and 37 m^2/g) for 13 weeks was not associated with increased level of 8-oxodG in the lung, whereas there was increased level of 8-oxodG by inhalation exposure to Printex 90 (16 nm and 300 m^2/g; Gallagher et al., 2003). Another study with even higher baseline level of 8-oxodG in the lung tissue (40.1 lesions/10^6 dG) showed that a putatively non-toxic TiO_2 sample did not generate 8-oxodG in the lungs after i.t. instillation (0.1 mg/mouse once a week for 10 weeks), whereas the same dose of DEP or washed DEP (particles with organics removed) generated 8-oxodG in the lungs (Ichinose et al., 1997b). A direct comparison of PM_{10} (referred to as ''Asian dust'') and nanosized TiO_2 showed the same level of induction of 8-oxodG, measured by ELISA in lung tissue, after i.t. instillation of 20 mg/kg twice a week for 12 weeks (Hwang et al., 2010). One study has also investigated the level of 8-oxodG in BALF by LC-MS/MS, which showed that fine ZnO (250 nm, 7.2–45.2 mg/m^3) elicited a higher effect than did nanosized ZnO (35 nm, 2.1–12.1 mg/m^3) after 6 h inhalation exposure (Ho et al., 2011). However, it is difficult to compare the genotoxicity in BALF of exposed and non-exposed animals because the particle-induced inflammation alters the content of cells.

Figure 5 shows an analysis of the dose–response relationship between pulmonary exposure to particles and generation of 8-oxodG in the lungs of animals. The graph encompasses only studies that have measured 8-oxodG by optimal assays with low levels of oxidatively damaged DNA in the control group. It can be seen that a range of particles from combustion of DE (Møller et al., 2003; Risom et al., 2003a, 2007a; Tsurudome et al., 1999), traffic-generated particles (Tokiwa et al., 1999, 2005), nanosized carbon black or air pollution particles (Danielsen et al., 2010) and quartz (Albrecht et al., 2005) can be fitted well to a linear relationship between the mass dose and induction of 8-oxodG without obvious signs of a threshold. By exception, the exposure to asbestos fibers seems to generate a higher induction of 8-oxodG (Takata et al., 2009), although it is only based on one publication. A possible particular ability to cause DNA damage by asbestos fibers could be due to generation of oxidative stress through multiple mechanisms including surface reactivity, mitochondrial dysfunction and inflammation with frustrated phagocytosis (Huang et al., 2011).

There are few publications containing results on oxidatively damaged DNA in tissues after non-pulmonary exposure to particles and only one group has made an effort to compare the potency of particles after gastrointestinal exposure. This group showed that 0.64 mg/kg of SWCNT or fullerenes C_{60} elicited the same effect in lung tissue and liver of rats after intragastric exposure (Folkmann et al., 2009). The same dose of nanosized carbon black (0.64 mg/kg of Printex 90)

increased the level of 8-oxodG in the liver after intragastric exposure, whereas particles collected from the ambient air in a village with many wood stoves or particles collected from combustion of wood had no effect on the generation of 8-oxodG in the liver (Danielsen et al., 2010). Moreover, these authors have compared the effect of these particles with DEP on the same dose and exposure duration in rats and showed that the highest induction of 8-oxodG was produced by DEP and nanosized carbon black (Møller et al., 2012).

Collectively, the results indicate that particles with different composition at the same mass dose can generate quite different levels of oxidatively damaged DNA in the lungs and liver after pulmonary and gastrointestinal exposure. The overall evaluation of the ability of measurements of oxidatively damaged DNA to discriminate between different types of particles indicates a score C for the evidence regarding pulmonary exposure because the evaluation is mainly based on non-optimal assays with high baseline level of 8-oxodG and antibody-based techniques. For the gastrointestinal exposure, the evidence score is B, although there are presently relatively few studies and the observations need to be reproduced by other laboratories. Bearing these limitations in mind, there is supporting evidence that the induction of oxidatively damaged DNA in animal tissues after pulmonary and gastrointestinal exposure depends on particle characteristics.

Hypothesis 7: Particle-mediated inflammation is associated with oxidative damage to nucleobases

The association between pulmonary inflammation and development of lung disease is a hallmark in inhalation toxicology. It has been concluded that experimental studies on inhalation exposure to crystalline silica strongly suggest that inflammation can be the driving force of genotoxicity (Borm et al., 2011). Crystalline silica is a coarse size type of particle that typically falls outside the poorly soluble particles in regard to tumorigenic potency, as shown in Figure 3, where quartz on mass basis is carcinogenic at a lower dose than other particles. Still, the surface area of particles, which increases dramatically for nanosized particles, correlates with the level of pulmonary inflammation (Duffin et al., 2007; Stoeger et al., 2006). However, it is less clear whether or not airway exposure to particles generates oxidative damage to DNA at doses that do not elicit inflammatory reactions. It has been highlighted that particle-mediated genotoxicity may be due to either a direct (primary) or an indirect (secondary) pathway leading to DNA damage (Donaldson et al., 2010). In principle, this means that it might be possible to observe genotoxicity after exposure to particles that are not inflammogenic. However, the particles that have been tested so far seem to be both genotoxic and inflammogenic, which might be because researchers have focused on the most hazardous types of particles in attempt to unravel the mechanisms of action by exposure to particles. One solution, therefore, is to assess the threshold doses where statistically significant effects in terms of pulmonary inflammation and genotoxicity occur by exposure to particles. A previous assessment of the studies on pulmonary exposure to combustion-derived particles indicated that the majority of studies had used doses of particles that typically would generate pulmonary overload in rats (Møller et al., 2008). The lung overload phenomenon in rats exposed to high levels of poorly soluble particles such as carbon black, titanium dioxide, talc and coal dust has been reviewed extensively (Hesterberg et al., 2012; ILSI, 2000; Oberdörster, 1995; US EPA, 2002; Valberg & Crouch, 1999). The current paradigm whereby inhalation of very high levels of poorly soluble particle leads to lung tumors in rats, encompasses successively: (1) deposition of particles in the lungs, (2) impairment of macrophage-mediated lung clearance, (3) accumulation of excessive lung burdens of particles and (4) initiation of inflammatory response to which rats are particularly vulnerable. In situations of chronic inflammation, the ongoing release of ROS from pulmonary macrophages and neutrophils damages the lung tissue and stimulates tissue repair, increasing the chances of DNA transcription errors as well as directly causes DNA lesions and mutations. This paradigm dogmatically places the generation of pulmonary inflammation as the culprit by which DNA damage occurs in tissues of animals. However, as pointed by other authors, this can be regarded as a secondary pathway of genotoxicity; the primary way encompasses a direct-acting insult of the particles by generation of ROS (Donaldson et al., 2010). The pulmonary overload phenomenon has been reported to occur in a dose range of 0.5–2 $mg_{particle}/g_{lung\ weight}$ (Borm et al., 2004). The results in Figure 5 show that relatively few studies with optimal assays for the detection of 8-oxodG have exposed animals to doses below the threshold of pulmonary overload in rats. However, there is no obvious sign of a threshold for 8-oxodG formation. In a study of DEP exposure in guinea pigs

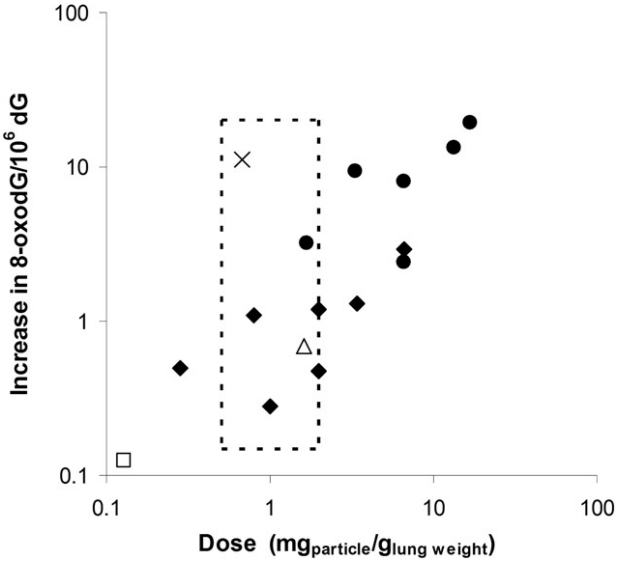

Figure 5. Relationship between the dose of particles and induction of 8-oxodG in lung tissue. The symbols represent various types of DEP (diamonds; Møller et al., 2003; Risom et al., 2003a, 2007a; Tsurudome et al., 1999), carbonaceous air pollution particles (circles; Tokiwa et al., 1999, 2005), nanosized carbon black and ambient air particles (open square; Danielsen et al., 2010), quartz (open triangle; Albrecht et al., 2005) and asbestos fibers (single cross; Takata et al., 2009). The square, marked by dotted lines, represents the dose level where pulmonary overload typically occurs.

DOI: 10.3109/10408444.2012.756456

the lowest dose (0.7 mg/animal) was associated with a small and not statistically significant increase in levels of 8-oxodG (3.0 0.7 lesions/10^6 dG) compared with controls (2.6 0.8 lesions/10^6 dG; Møller et al., 2003). Another study also showed low level of 8-oxodG induction in lungs of rats that were exposed by i.t. instillation to 0.64 mg/kg of nanosized carbon black or particles collected from ambient air or wood combustion (Danielsen et al., 2010). A few studies have measured the induction of FPG-sensitive sites at low doses; Wessels et al. (2011) observed no difference in BALF content and FPG-sensitive sites in the lungs of mice after nose-only inhalation exposure to 142 μg/m^3 of carbon nanoparticles at 3 4 h duration, corresponding to about 18 $\mu g_{particles}$/mouse assuming total deposition. The same researchers also showed that pharyngeal aspiration of a very large dose (100 mg/kg) of DQ12 quartz was associated with pulmonary inflammation, whereas there were unaltered levels of FPG-sensitive sites in lung tissue (van Berlo et al., 2010).

Collectively, the data suggest that there is both little inflammation and genotoxicity in the ''low dose'' area, whereas the ''high dose'' area is associated with genotoxicity and inflammation. This evaluation is based on score A because the studies have used optimal assays for the detection of oxidatively damaged DNA. There is at present no direct experimental evidence for the notion that inflammation is a prerequisite for the generation of oxidatively damaged DNA in the lung. In fact, this is difficult to ascertain because it requires finding a type of particle that specifically target oxidative stress to nuclear DNA without inducing cytoplasmic oxidative stress triggering inflammation pathways (Li et al., 2008a) and the use of particles that cause inflammation without any oxidative stress. Otherwise, it might be feasible to block the inflammatory response pharmacologically and investigate genotoxic effects at doses that would otherwise elicit inflammation.

Discussion

A substantial number of studies – 64 publications – have shown that exposure to particles by pulmonary and gastro-intestinal route is associated with elevated levels of oxidatively damaged DNA in tissues of animals. Moreover, the dose–response relationship appears linear without a clear threshold for airway exposure. We have focused on the generation of 8-oxodG because it is a mutagenic DNA lesion and there is evidence for its relationship with development of cancer in humans. Unfortunately, the literature on 8-oxodG is haunted by publications with results that should be interpreted with caution because the DNA most likely has been oxidized during the isolation procedure. It is a problem that apparently persist today in particle toxicology as evidenced by recently published publications with unrealistically high baseline levels of 8-oxodG. This methodological problem was recognized already in the 1990s where it generated a heated debate about the true level of 8-oxodG in nuclear DNA and it promoted the establishment of ESCODD. Nonetheless, there are ongoing efforts to promote the same nomenclature of 8-oxodG and attention to use valid methods (Cadet & Poulsen, 2010; Cadet et al., 2012; Cooke et al., 2010). It is our impression that results with very high levels of 8-oxodG are rarely published in journals with specific scopes on oxidative stress, DNA damage or mutagenesis, which might be because of the stronger awareness on this problem among reviewers in such journals. It might be a coincidence that the recent publications with unrealistically high levels of 8-oxodG have been published in toxicology journals, whereas such journals are obviously in the forefront in regard to the requirements on particle characteristics. We suggest that stringency is also considered in regard to the validity of biomarkers such as oxidation products of DNA. ESCODD suggested a threshold for 8-oxodG of 5 lesions/10^6 dG, although it was noted that the true level was probably lower (approximately 1 lesion/10^6 dG) in tissues of young and healthy animals (Collins et al., 2004). A different problem is the popularity of unspecific assays such as the antibody-based detection of 8-oxodG by ELISA or immunohisto-chemistry. Our assessment shows that the publications on antibody-based assays and unrealistically high levels of 8-oxodG (suggesting experimental problems due to spurious oxidation of DNA) more frequently reported increased levels of genotoxicity as compared to the publications that have reported results from optimal assays with low baseline levels of 8-oxodG. The detection of oxidatively damaged DNA in tissues of animals as FPG or hOGG1-sensitive sites by the comet assay, alkaline elution or alkaline unwinding are good alternative methods to the chromatographic assays. These assays should be regarded as unspecific measurements of 8-oxodG; still, the increased levels of FPG- or hOGG1-sensitive sites can be regarded as an indication of oxidative stress-generated DNA lesions. The vague statement relates mainly to the fact that some studies have shown that cultured cells exposed to direct-acting alkylating agents have elevated levels of FPG-sensitive sites (Smith et al., 2006; Speit et al., 2004). It is possible that the elevated levels of genotoxicity are related to some alkylated ring-opened formamidopyrimidine lesions, although it remains to be determined whether or not these lesions are relevant in animals without exposure to alkylating agents. Recent observations in cultured A549 or BEAS-2B cells also suggest a risk of false-negative results on FPG-sensitive sites because of reduced glycosylase activity after exposure to: (1) silver nanoparticles because of dissolution of ions and (2) exposure to CeO_2 and Co_3O_4 by mechanisms that are not yet elucidated (Kain et al., 2012). A number of materials, including stainless steel, subway, MnO_2, Fe_3O_4, NiO and SiO_2 particles did not interact with the FPG enzyme.

We have used 8-oxodG as measurement of oxidatively DNA damage, which is principally because we think that it is one of the best validated oxidative stress biomarkers in regard to development of cancer. It is a mutagenic lesion in the relevant biomolecule (DNA), which places it directly in the center of the mechanism of cancer development. In addition, the increased excretion of 8-oxoGua (originating from the repair of DNA) and 8-oxodG (originating putatively from degradation of 8-oxodGTP in the nucleotide pool) is associated with lung cancer in non-smoking humans in a prospective cohort study (Loft et al., 2006, 2012b). This is strong evidence for a causal association between oxidatively

damaged DNA and risk of lung cancer in humans because reverse causality is not a problem in cohort studies as compared to case-control studies (Loft & Møller, 2006; Olinski et al., 2003). Moreover, the urinary excretion of 8-oxoGua or 8-oxodG in the samples from the cohort study was measured with HPLC-ECD. In comparison, it is becoming increasingly popular to measure these oxidatively damaged nucleobases by ELISA techniques, which lack specificity and consequently give rise to high levels of 8-oxodG in samples of urine (Evans et al., 2010). There is, to the best of our knowledge, no publication from biobank-based cohort studies that have assessed the predictive value of 8-oxodG or 8-oxoGua in plasma or serum with validated techniques, which could be because the concentrations of these oxidation products are about two orders of magnitude lower than the concentration in urine (Lam et al., 2012). Still, the levels of 8-oxoGua (or similar lesions such as FPG-sensitive sites) are probably best characterized as proxy measure of oxidative stress. In perspective, this is rarely a major concern in epidemiology where for instance the measurement of ambient concentrations of toxicants is considered to be a proxy measure of the true exposure. Other relevant oxidative stress biomarkers include lipid peroxidation products and their derived adducts on DNA. These lipid peroxidation-derived exocyclic DNA adducts are interesting in regard to particle toxicology because they are pre-mutagenic lesions (Møller & Wallin, 1998). The National Institute of Environmental Health Sciences has organized the Biomarkers of Oxidative Stress Study that is a multi-laboratory initiative with the aim to identify specific and sensitive biomarkers for non-invasive measurements of oxidative stress. The first trials used acute CCl_4 poisoning in rats as model for oxidative stress, which showed that the classic spectrophotometric measurement of thiobarbituric reactive substances was relatively insensitive as compared to more specific measurements of malondialdehyde and isoprostanes (Kadiiska et al., 2005a,b). The same study also reported that the measurement of 8-oxodG in urine with an ELISA kit was not a particularly good biomarker for CCl_4-induced oxidative stress, which is not surprising considering that the antibody-based detection of 8-oxodG in urine is an unreliable assay. The measurement of plasma antioxidants in the same model of acute CCl_4 poisoning indicated that α-tocopherol, coenzyme Q, ascorbic acid, uric acid, glutathione and total antioxidant capacity (Trolox assay) in plasma did not generate unambiguous results in regard to the level of oxidative stress (Kadiiska et al., 2000). A later study on ozone inhalation in rats (2 or 5 ppm for 2 h) led to the conclusion that plasma levels of glutathione, tocopherols, uric acid and ascorbic acid were not sensitive biomarkers of oxidative damage by ozone *in vivo* (Kadiiska et al., 2011).

The measurement of oxidatively damaged DNA is only one type of genotoxic endpoint and the hazard identification could include other measures of DNA damage. A recent systematic review on genotoxicity endpoints in molecular epidemiology of ambient air pollution has assessed the evidence of association between exposure and effect on the basis of the Venice criteria (Demetriou et al., 2012). The highest score in the Venice criteria is obtained for an exposure–effect association that is based on a large number of subjects, replication in independent investigations (preferably evidence from meta-analyses) and protection from bias. This showed that PAH adducts in DNA and oxidatively damaged DNA received higher scores than chromosome aberrations, micronuclei and DNA methylation patterns. The PAH-DNA adducts are relevant biomarkers for exposures to combustion-derived particles, whereas the measurements of oxidative damage, chromosome changes and DNA methylations (affecting gene expression and associated with genomic instability) are markers of three different and possibly independent mechanisms of DNA damage that could have widespread relevance in particle toxicology. However, the measurement of chromosome damage requires collection and *ex vivo* culture of cells, which typically means that these endpoints are measured in bone marrow cells rather than target tissues. In addition, the detection of mutants and mutation spectra are possible, although it is time-consuming and the sensitivity is relatively low in repair-competent cells from wild-type animals. The exposure to DEP or nanosized carbon black generated only a modest increase in the mutant frequency in lung cells (Jacobsen et al., 2008a, 2011), although the mutation spectrum in the carbon black exposed cells was in keeping with the mutation spectrum of ROS-generating agents (Jacobsen et al., 2011). Increased mutagenicity was also observed in type II alveolar cells of rats exposed to carbon black by i.t. instillation (Driscoll et al., 1997). Despite an increased generation of 8-oxodG after inhalation of 80 mg/m^3 of DEP for 1.5 h (corresponding to 1 mg h/m^3, assuming that rats inhale 0.2 m^3/d), there was only a modest and statistically non-significant effect of 1.2-fold (95% CI: 0.98–1.4-fold) increased mutation frequency in the lungs of mice (Dybdahl et al., 2004). However, the limited mutagenic effect could be due to lack of time for fixation of mutations after exposure, which is usually applied for optimum mutation detection. Inhalation of DE for 4 weeks (12 h/d, 7 d/weeks) was associated with a statistically significantly increased level of 1.2-fold (1 mg/m^3, corresponding to 2.8 mg h/m^3) or 4.8-fold (6 mg/m^3, corresponding to 16.8 mg h/m^3) increased mutation frequency in lung cells (Sato et al., 2000).

Our critical assessment of the association between pulmonary exposure to particles and levels of oxidatively damaged DNA in lung tissues from animals shows that asbestos, DEP, quartz and nanosized carbon black can generate genotoxicity in a dose-dependent manner and without a clear threshold although the low-dose level has not been well studied (Figures 2 and 5). It should be emphasized that the type of particles differs; for instance, the effect of quartz has only been investigated dose-dependently with antibody-based methods. In addition, the studies on DEP differ in regard to the type of materials being generated from different engines, which has been shown to play a role in cultured cells (Hemmingsen et al., 2011; Jantzen et al., 2012). Still, the overall interpretation of the studies is that the pulmonary exposure (and for asbestos also i.p. exposure as surrogate for pleural exposure) to a relative large array of particles is associated with a dose-dependent increase in the levels of oxidatively damaged DNA. The overall r_w value for the studies with optimal or non-optimal assays for the determination of oxidatively damaged DNA was 0.92, which indicates that 84% of the variation in the levels of oxidatively damaged DNA is explained by dose of particles on

DOI: 10.3109/10408444.2012.756456

group level. However, it should be emphasized that the r_w values are obtained from the group means and it does not take the residual variation of the individual studies into account. Therefore, the r_w values should be interpreted as ''best case'' rather than a ''worst case'' scenario in regard to the true relationship between the exposure to particles and generation of oxidatively damaged DNA.

There is a paucity of studies on pulmonary exposure of engineered nanomaterials such as carbon nanotubes and fullerenes C_{60}, although it has been shown that gastrointestinal tract exposure is associated with elevated levels of 8-oxodG in the liver and lungs (Folkmann et al., 2009). Cell culture studies in lung epithelial cells also have indicated increased levels of oxidatively damaged DNA after exposure to SWCNT and fullerenes C_{60} (Jacobsen et al., 2008b). The highest effect on oxidatively damaged DNA was observed within a few days after i.t. instillation of particles and this exposure route may generate higher level of genotoxicity as compared with inhalation exposure. Inhalation should be the mode of choice for pulmonary exposure, although i.t. instillation can be used in studies designed to test differences in potency between particles or situations where there is limited amount of material (Oberdörster et al., 2005). However, studies on i.t. instillation of particles have less relevance than inhalation studies in risk assessment because the particles are suspended in a delivery vehicle rather than air. Thus, the particles may be chemically and physically different from the fresh, whole and airborne particles, to which people are exposed. In addition, particles that are administered by intracavitary injection in the lungs may bypass or inhibit (e.g. overload of clearance) the normal respiratory defense mechanisms, resulting in a response that would not occur with inhalation of particles at the lower levels to which humans are exposed. Furthermore, it may deliver clusters of particles that would not normally become airborne or would not be able to deposit in the lower lung via the inspired air stream. Direct injection of particles into the cavity also results in an instantaneous deposition of very high concentrations of particles, which are unevenly distributed in the body cavity, resulting in extremely high doses and dose rates. The situation is even worse when airborne particles are administered by i.p. injection because many of the clearance mechanisms operative in the lung airways and alveoli are not present in this cavity. Bolus exposures are more common in the gastrointestinal tract; for instance, after meals in humans. However, it should be acknowledged that rodents typically have a more continuous ingestion pattern than humans. Still, the meta-analysis in our study showed similar effect size of 8-oxodG in the liver of animals after a single dose and repeated exposures (Figure 4).

The inhalation route of exposure is clearly superior to the non-physiological routes such as injections in the trachea or peritoneal cavity. However, the few inhalation studies in our meta-analysis, for the most part, have exposed animals to high concentrations compared to actual human ambient or even workplace exposures to particles, where exposures are generally low and the resulting dose and dose rate to the deep lung is much lower. At the extremely high exposure levels used in the particle inhalation studies, the tissue doses have probably been so high that the inflammatory and other effects, including oxidative damage to DNA, might be secondary events occurring because of tissue overload. Thus, most of the inhalation studies may not be relevant for understanding the mechanisms in the low-dose area, which does not entail pulmonary overload. The dose range in Figure 5 is 0.125–19.5 $mg/g_{lung\ weight}$. It corresponds to one-day exposure situations where humans would inhale air with 10–1625 mg/m^3 of particles, assuming that humans inhale 12 m^3/d and lung mass is 1000 g. These exposure levels are much higher than human ambient exposures (0.002–0.01 mg/m^3) or even occupational exposures (0.07–0.8 mg/m^3) to DEP (US EPA, 2002).

The assessment of studies on pulmonary exposure to particles shows that the studies using direct injection of particles into the cavity predominates, suggesting that few of the studies are useful for risk assessment. As an illustration, Supplementary Table S2 lists 48 studies on pulmonary exposure to particles; removal of studies with non-optimal assays reduces the list of relevant studies to 15 publications on various inhalation and intracavity exposures to particles. Among these, nine studies used direct injection of high doses into the cavity, whereas two studies have used single administration by i.t. instillation of doses that would be below the lung pulmonary overload threshold in rats (Danielsen et al., 2010; Møller et al., 2003). Four of the five studies on inhalation exposure have used concentrations that could be associated with pulmonary overload. The remaining one study on inhalation exposure with a dose that was not likely to be associated with pulmonary overload probably has low statistical power because of relatively few animals per exposure group (Wessels et al., 2011). There is need for future studies to focus more on exposure–effect relationships in the low-dose area. It also implies that the statistical power could be an important issue in future studies because it will be more difficult to detect true biological effects in the low-dose area. For instance, a statistically non-significant effect was observed at the dose of 20 mg/m^3 in the study by Risom et al. (2003a); the exposed animals had approximately 800 extra lesions of 8-oxodG per diploid cell as compared to the controls. This would have required a group size of more than 100 mice to achieve a statistically significant effect at this dose. The focus on effects in the low-dose area comes with the price of substantially larger group sizes, which possibly reach the numbers that are used in epidemiological studies. For instance, the adjusted relative risk was 1.14 (95% CI: 1.04–1.23) for lung cancer per 10 $\mu g/m^3$ for fine particles in the Cancer Prevention Study II cohort, which included approximately 500 000 subjects (Pope III et al., 2002).

There has been debate about the association between exposure to high concentrations of particles and risk of lung cancer. For instance, it has been anticipated that a major issue in the IARC classification of DE would be the relevance of pulmonary overload in regard to cancer risk in rats (McClellan et al., 2012). However, the IARC working group has concluded that there was sufficient evidence in experimental animals for the carcinogenicity of DEP (Benbrahim-Tallaa et al., 2012). On the same note as the debate about the classification of DEP, the IARC group 3 classification in 1997 for coal dust has been taken as an illustrative example of a

worker population (i.e. coal miners) without excessive risk of lung tumors, although they are subject to lung overload with evidence of impaired lung clearance and non-cancer pulmonary diseases, including chronic pulmonary inflammation, pulmonary fibrosis and localized emphysema (Hesterberg et al., 2012). Although it is futile to speculate on the outcome of a reclassification by IARC on coal dust, it is worth mentioning that the deficiency of lung cancer mortality in the coal miners might be related to a particularly strong example of the healthy worker effect (Stayner & Graber, 2011).

The results from our meta-analysis have not indicated that a particular type of material should be particularly suitable as bench-mark particle. Bench-mark control particles have rarely been incorporated in the design of studies on oxidatively damaged DNA, although there are studies that have used DQ12 quartz or asbestos as reference samples for studies on commercially types of quartz and fibers, respectively (Seiler et al., 2004; Shürkes et al., 2004; Yamaguchi et al., 1999). In addition, DQ12 quartz or nanosized carbon black have been used as reference particles for studies on DNA damage in the lung after exposure to TiO_2 and combustion-derived particles (Danielsen et al., 2010; Rehn et al., 2003). Above all, these studies illustrate the limitations of selection of bench-mark particles for *in vivo* studies on oxidatively damaged DNA because the exposure to quartz mainly generated elevated levels of oxidized DNA nucleobases at time points several weeks after the exposure and nanosized carbon black generated the same level of 8-oxodG as the combustion-derived particles. In addition, SRM2975 can be used as bench-mark particles for combustion-derived or ambient air particles, yet the particles were generated 30 years ago and they do not represent the types of DEP from modern diesel engines. In fact, there is evidence that the modern technology in recent diesel engines generates exhaust that is different from the traditional DE (Hesterberg et al., 2012; McClellan et al., 2012).

The current concept indicates that pulmonary exposure to particles can be associated with cytotoxicity, inflammation and oxidative stress if the dose is sufficiently high. It is clear that particle-generated inflammation is associated with oxidative stress (Hesterberg et al., 2012) and there seems to be consensus among a number of researchers that particle-generated oxidative stress is associated with inflammation reactions (Ayres et al., 2008). In fact, the principles for characterization of the potential human health effects from exposure to nanomaterials list BAL damage markers, oxidative stress, histopathology (with focus on inflammatory processes and development of fibrosis) and cell proliferation as tier 1 in the testing strategy (Oberdörster et al., 2005). This seems to be a wise testing strategy considering that it is difficult to know for sure which mechanism comes first. Among the 15 studies with optimal assays for oxidatively damaged DNA (Supplementary Table S2), only a few studies have assessed cytotoxicity or histopathologic changes in the lungs. One of these studies showed that a single i.t. instillation (1 mg/rat) of chrysotile asbestos had peak inflammation responses and cytotoxicity (assessed by lactate dehydrogenase (LDH) activity in BALF) at day 3 after the exposure, whereas the peak level of 8-oxodG occurred at day 14 after the exposure (Takata et al., 2009). The studies on inhalation of toner revealed unaltered 8-oxodG levels in lung tissue, whereas there were small foci of collagen and particle-laden macrophages; these findings were dose-dependent (1.6–16.3 mg/m^3 for 6 h/d and 5 d/week) and the effect was more pronounced after two years of exposure as compared to one year (Morimoto et al., 2005, 2009). There is a paucity of studies that assess the relationship between cytotoxicity, inflammation, histopathological findings and oxidatively damaged DNA in animal tissues after exposure to particles. Cell culture experiments on DEP indicate that the concentrations that generated cytotoxicity (assessed by increased LDH activity or WST-1 formation) and oxidatively damaged DNA are relatively close (Danielsen et al., 2008a, 2009; Forchhammer et al., 2012; Hemmingsen et al., 2011; Jantzen et al., 2012). Other authors have reported that a size fraction of ambient air particles below 0.5 μm showed no association between LDH activity and generation of oxidatively damaged DNA in human A549 lung epithelial cells, whereas there was a positive correlation for the particle size fraction that was above 0.5 μm (Wessels et al., 2010). Results on ambient air particles indicated increased levels of 8-oxodG in A549 cells after 3 h of exposure, whereas neither the LDH activity in the cell culture medium nor the cellular WST-1 formation changed (Danielsen et al., 2011). The levels of 8-oxodG or FPG-sensitive sites were increased in A549 cells at 4 h, without signs of cytotoxicity (assessed as trypan blue staining), after exposure to airborne particles from a subway station (Karlsson et al., 2005, 2008a,b). The exposure of mouse or human lung epithelial cells to quartz increased the level of FPG-sensitive sites at concentrations that were not associated with increased LDH activity in the cell culture medium (Fanizza et al., 2007; Jacobsen et al., 2007). The LDH assay has been a standard test in respiratory toxicology for cytotoxicity, whereas it is now being regarded as an assay with inherent limitations in cell cultures because of interactions between particles and the enzyme in the cell culture medium (Han et al., 2011). However, there is little interference between nanosized carbon black particles and the LDH enzyme in cell culture media, although it is a clearly black suspension (Vesterdal et al., 2012). Nevertheless, it has been suggested to use at least two different cytotoxicity assays in cell culture studies on particles (Stone et al., 2009). The concentrations of particles in cultured cells are typically much higher than the concentrations in the lung lining fluid after inhalation of realistic concentrations of airborne particles. Thus, it suggests that the pulmonary exposure to particles can generate oxidative damage to DNA without concomitant cytotoxicity, although it should be clear that high concentrations may cause direct cytotoxicity with secondary damage to the DNA.

The analysis of oxidatively damaged DNA in tissues is a gross estimate of the genotoxicity across several cell types that may have different sensitivity to particle-generated oxidative stress and DNA damage. The immunostaining of 8-oxodG in tissue sections should in principle be the optimal technique for detection of cell-specific susceptibility to oxidative damage after exposure to particles. However, caution should be exercised in interpretation of the results by immunostaining of 8-oxodG in lung tissue because the antibodies are unspecific and, at least in urine, gives rise to

DOI: 10.3109/10408444.2012.756456

measurements of rather high levels of oxidatively damaged nucleobases (Cooke et al., 2008). The unspecific antibody binding to 8-oxodG is also suggested by observations that immunostaining occurred in the cytoplasma as well as the nucleus in lung tissue sections from mice after exposure to silica by i.t. instillation (Kaewatawong et al., 2006). Nevertheless, it has been described that pulmonary exposure to particles was associated with immunostaining of 8-oxodG in alveolar cells (Nehls et al., 1997), macrophages and polymorphonuclear leukocytes (Inoue et al., 2005) and bronchial epithelial cells (Aoki et al., 2001; Hwang et al., 2010). In addition, Kaewamatawong et al. (2006) reported that a single i.t. instillation of ultrafine silica generated pulmonary inflammation and increased the level of 8-oxodG staining in bronchial and alveolar epithelial cells as well as macrophages at post-exposure day 1, whereas the 8-oxodG immunostaining day 3 and 7 was mainly observed in macrophages. Overall, the data suggest that the induction of 8-oxodG can occur in several cell types in the lung, although it depends on the post-exposure time point. There is still little information about the exposure to particles in the gastrointestinal tract. We have measured the levels of 8-oxodG in colon mucosa cells because of the assumption that the epithelium would be the main exposure site as the particles pass through the intestine (Daniselsen et al., 2008a; Dybdahl et al., 2003; Folkmann et al., 2009; Risom et al., 2003b, 2007b). However, it is also possible that uptake of particles by transcytosis in microfold cells in the vicinity of Peyer's patches as well as paracellular transport because of leaky tight junctions may expose cells in lamina propria directly to particles (Hoet et al., 2004; Møller et al., 2012).

We have assumed that the genotoxic potential of the different types of particles across studies can be compared by the mass dose (reported in mg/kg). This might introduce a limitation in the assumption, which should be acknowledged, although it does not impede the general picture that the exposure to particles is associated with higher levels of oxidatively damaged DNA. The heterogeneity in the forest plots (Figures S2 and S4) may originate from differences in doses between particles, although it is also possible that it arises from publication bias of studies that showed statistically significant effects by chance. It is interesting that the highest effect sizes were obtained by asbestos fibers and quartz in the forest plot of studies that have used optimal assays for the detection of oxidatively damaged DNA in lung tissue (Figure S2). The biological effects can be influenced by many particle characteristics including size, agglomeration state, hygroscopicity, biodurability, shape, surface area, charge, soluble compounds and chemical composition. This is illustrated in animal studies on pulmonary inflammation after exposure to carbon-based and TiO_2-based particles (Duffin et al., 2007; Saber et al., 2012; Stoeger et al., 2006).

It has been shown that surface coating of DQ12 quartz reduced the extent of pulmonary inflammation and DNA strand breaks measured by the comet assay in lung epithelial cells at day 3 after a single i.t. instillation of 2 mg/rat (Knaapen et al., 2002). There is a paucity of studies that assess these characteristics in relation to induction of oxidatively damaged DNA damage. In addition, a recent study showed a correlation between the mass dose of carbon nanotubes (120 μg/mouse), SWCNT (40 μg/mouse) and asbestos (120 μg/mouse) and inflammation after pharyngeal aspiration, whereas the specific surface area or particle number showed less consistency in the correlation with toxicological responses in the lungs (Murray et al., 2012). We looked for information on particle characteristics in the original publications that are included in this review. This was somewhat unsuccessful because the old publications contain relatively little information on particle characteristics that are considered important by the present standards. The suspensions for i.t. instillations or i.p. injections have used different types of solvents (saline or phosphate buffer saline) with or without addition of agents that stabilizes the dispersion (Tween 80, lecithin or BALF). It has been shown by dynamic light scattering analysis that both the sonication procedure and the type of stabilizer affects agglomeration, and hence, the particle size and stability of the dispersions of TiO_2, ZnO, silicates, SWCNT and DEP (Bihari et al., 2008). It is clear that suspension of particles in saline, water or culture medium with serum generates differences in the particle size determined by Nanosight Tracking Analysis (Frikke-Schmidt et al., 2011; Hemmingsen et al., 2011). The protein coating on particles, which occur in biological fluids, might affect the toxicologically effect in target tissue cells although the impact on genotoxicity is still unresolved (Donaldson et al., 2010).

Conclusion

In summary, the results of this analysis show that there is compelling evidence from animal experimental models showing that both pulmonary and gastrointestinal tract exposure to particles are associated with elevated levels of oxidatively damaged DNA in the lungs and internal organs. There is substantial evidence that exposure to particles are associated dose-dependently with the generation of oxidatively damaged DNA in lung tissue after airway exposure, whereas dose-dependent relationships have not been thoroughly assessed for other routes of exposures with optimal assays for DNA damage. Most studies on pulmonary exposure to particles have used doses that are associated with pulmonary overload in rats. However, it seems that the induction of 8-oxodG occurs dose-dependently below this threshold. Administration of particles by high-dose bolus exposure seems to generate higher levels of oxidatively damaged DNA in animal organs and the genotoxicity was typically highest at time points close to the last exposure. It has not been possible to obtain information about the sensitivity of species and strains in regard to oxidatively damaged DNA after exposure to particles. In addition, there is only limited evidence indicating differences in the genotoxic potency of particles. This is mainly because the available studies have used non-optimal assays for the determination of differences between hazardous and non-hazardous particles. It has not been common practice to include bench-mark control particles in the studies on oxidatively damaged DNA, although there are studies that have used quartz or nanosized carbon black as reference particles (Danielsen et al., 2010; Rehn et al., 2003). Our meta-analysis has not uncovered the existence of particles with high genotoxic potential, which

could be used reliable positive bench-mark control samples in studies of particle-generated oxidative damage to DNA in animal tissues. In addition, there is a paucity of studies with both realistic exposures in the low-dose area and sufficient number of animals; such studies should be started only after careful statistical power analysis and the number of animals per group should possibly be counted in hundreds rather than tens. It should, however, be emphasized that this demand might collide with the focus on reducing the number of animals used for toxicology. Unfortunately, this might cause researchers to use high doses related to a dogmatic reasoning that a p value below 0.05 equals a real biological effect. A further way forward in particle toxicology is the meta-analysis, which allows joint quantitative assessment of multiple studies each possible showing insignificant effect and was used by Valberg & Crouch (1999) to assess the tumor response in rats. The strength of the meta-analysis is governed by the quality of the available studies. As studies on low-dose exposures run the risk of being under-powered statistically, it will be important to collect these in meta-analysis and this requires equal publication success of studies with statistically significant and null effect findings. Beyond these critical notes about the quality of the available studies and suggestions for more focus on assay validity, realistic doses and physiologically relevant exposure routes in the future particle toxicology, the publications in our review collectively show compelling evidence that the detection of oxidatively damaged DNA in animal organs is a valuable research tool for the investigation of mechanisms of action in regard to particle-generated cancers.

Declaration of interest

The authors have sole responsibility for the writing and content of this article. No personal relationships with other people or organizations within the last five years have influenced the author's work. The authors have not served as expert witnesses in any litigation related to the subject of the review.

The study was funded by grants from the Danish Research Councils, The Center for Pharmaceutical Nanomedicine and Nanotoxicology and the Lundbeck Foundation ''Center for Biomembranes in Nanomedicine''.

References

Albrecht C, Knaapen AM, Becker A, et al. (2005). The crucial role of particle surface reactivity in respirable quartz-induced reactive oxygen/nitrogen species formation and APE/Ref-1 induction in rat lung. Respir Res, 6, 129.

Aoki Y, Sato H, Nishimura N, et al. (2001). Accelerated DNA adduct formation in the lung of the Nrf2 knockout mouse exposed to diesel exhaust. Toxicol Appl Pharmacol, 173, 154–60.

Ayres JG, Borm P, Cassee FR, et al. (2008). Evaluating the toxicity of airborne particulate matter and nanoparticles by measuring oxidative stress potential – a workshop report and consensus statement. Inhal Toxicol, 20, 75–99.

Bai N, Kido T, Suzuki H, et al. (2011). Changes in atherosclerotic plaques induced by inhalation of diesel exhaust. Atherosclerosis, 216, 299–306.

Benbrahim-Tallaa L, Baan RA, Grosse Y, et al. (2012). Carcinogenecity of diesel-engine and gasoline-engine exhausts and some nitroarenes. Lancet Oncol, 13, 663–4.

Bergeron F, Auvre F, Radicella JP, et al. (2010). HO* radicals induce an unexpected high proportion of tandem base lesions refractory to repair by DNA glycosylases. Proc Natl Acad Sci USA, 107, 5528–33.

Bermudez E, Mangum JB, Asgharian B, et al. (2002). Long-term pulmonary responses of three laboratory rodent species to subchronic inhalation of pigmentary titanium dioxide particles. Toxicol Sci, 70, 86–97.

Bermudez E, Mangum JB, Wong BA, et al. (2004). Pulmonary responses of mice, rats, hamsters to subchronic inhalation of ultrafine titanium dioxide particles. Toxicol Sci, 77, 347–57.

Bernstein DM. (2007). Synthetic vitreous fibers: a review toxicology, epidemiology and regulations. Crit Rev Toxicol, 37, 839–86.

Bihari P, Vippola M, Schultes S, et al. (2008). Optimized dispersion of nanoparticles for biological in vitro and in vivo studies. Part Fibre Toxicol, 5, 14.

Borm PJ, Robbins D, Haubold S, et al. (2006). The potential risks of nanomaterials: a review carried out for ECETOC. Part Fibre Toxicol, 3, 11.

Borm PJ, Schins RP, Albrecht C. (2004). Inhaled particles and lung cancer, part B: paradigms and risk assessment. Int J Cancer, 110, 3–14.

Borm PJ, Tran L, Donaldson K. (2011). The carcinogenic action of crystalline silica: a review of the evidence supporting secondary inflammation-driven genotoxicity as a principal mechanism. Crit Rev Toxicol, 41, 756–70.

Borzone GR, Liberona LF, Bustamante AP, et al. (2009). Differences in lung glutathione metabolism may account for rodent susceptibility in elastase-induced emphysema development. Am J Physiol Regul Integr Comp Physiol, 296, R1113–23.

Bourdon JA, Saber AT, Jacobsen NR, et al. (2012). Carbon black nanoparticle instillation induces sustained inflammation and genotoxicity in mouse lung and liver. Part Fibre Toxicol, 9, 5.

Cadet J, Loft S, Olinski R, et al. (2012). Biologically relevant oxidants and terminology, classification and nomenclature of oxidatively generated damage to nucleobases and 2-deoxyribose in nucleic acids. Free Radic Res, 46, 367–81.

Cadet J, Poulsen H. (2010). Measurement of oxidatively generated base damage in cellular DNA and urine. Free Radic Biol Med, 48, 1457–9.

Card JW, Jonaitis TS, Tafazoli S, et al. (2011). An appraisal of the published literature on the safety and toxicity of food-related nanomaterials. Crit Rev Toxicol, 41, 22–49.

Carter JM, Corson N, Driscoll KE, et al. (2006). A comparative dose-related response of several key pro- and antiinflammatory mediators in the lungs of rats, mice, hamsters after subchronic inhalation of carbon black. J Occup Environ Med, 48, 1265–78.

Collins AR, Cadet J, Möller L, et al. (2004). Are we sure we know how to measure 8-oxo-7,8-dihydroguanine in DNA from human cells? Arch Biochem Biophys, 423, 57–65

Cooke MS, Loft S, Olinski R, et al. (2010). Recommendations for standardized description of and nomenclature concerning oxidatively damaged nucleobases in DNA. Chem Res Toxicol, 23, 705–7.

Cooke MS, Olinski R, Loft S, et al. (2008). Measurement and meaning of oxidatively modified DNA lesions in urine. Cancer Epidemiol Biomarkers Prev, 17, 3–14.

Danielsen PH, Loft S, Jacobsen NR, et al. (2010). Oxidative stress, inflammation and DNA damage in rats after intratracheal instillation or oral exposure to ambient air and wood smoke particulate matter. Toxicol Sci, 118, 574–85.

Danielsen PH, Loft S, Kocbach A, et al. (2009). Oxidative damage to DNA and repair induced by Norwegian wood smoke particles in human A549 and THP-1 cell lines. Mutat Res, 674, 116–22.

Danielsen PH, Loft S, Møller P. (2008a). DNA damage and cytotoxicity in type II lung epithelial (A549) cell cultures after exposure to diesel exhaust and urban street particles. Part Fibre Toxicol, 5, 6.

Danielsen PH, Møller P, Jensen KA, et al. (2011). Oxidative stress, DNA damage, and inflammation induced by ambient air and wood smoke particulate matter in human A549 and THP-1 cell lines. Chem Res Toxicol, 24, 168–84.

Danielsen PH, Risom L, Wallin H, et al. (2008b). DNA damage in rats after a single oral exposure to diesel exhaust particles. Mutat Res, 637, 49–55.

Dekkers S, Krystek P, Peters RJ, et al. (2011). Presence and risks of nanosilica in food products. Nanotoxicology, 5, 393–405.

Demetriou CA, Raaschou-Nielsen O, Loft S, et al. (2012). Biomarkers of ambient air pollution and lung cancer: a systematic review. Occup Environ Med, 69, 619–27.

DOI: 10.3109/10408444.2012.756456

Donaldson K, Poland CA, Schins RP. (2010). Possible genotoxic mechanisms of nanoparticles: criteria for improved test strategies. Nanotoxicology, 4, 414–20.

Donaldson K, Seaton A. (2012). A short history of the toxicology of inhaled particles. Part Fibre Toxicol, 9, 13.

Dörger M, Allmeling AM, Neuber A, et al. (1997). Interspecies comparison of rat and hamster alveolar macrophage antioxidative and oxidative capacity. Environ Health Perspect, 105, 1309–12.

Driscoll KE, Costa DL, Hatch G, et al. (2000). Intratracheal instillation as an exposure technique for the evaluation of respiratory tract toxicity: uses and limitations. Toxicol Sci, 55, 24–35.

Driscoll KE, Deyo LC, Carter JM, et al. (1997). Effects of particle exposure and particle-elicited inflammatory cells on mutation in rat alveolar epithelial cells. Carcinogenesis, 18, 423–30.

Duffin R, Tran L, Brown D, et al. (2007). Proinflammogenic effects of low-toxicity and metal nanoparticles in vivo and in vitro: highlighting the role of particle surface area and surface reactivity. Inhal Toxicol, 19, 849–56.

Dybdahl M, Risom L, Bornholdt J, et al. (2004). Inflammatory and genotoxic effects of diesel particles in vitro and in vivo. Mutat Res, 562, 119–31.

Dybdahl M, Risom L, Møller P, et al. (2003). DNA adduct formation and oxidative stress in colon and liver of Big Blue rats after dietary exposure to diesel particles. Carcinogenesis, 24, 1759–66.

Elder A, Gelein R, Finkelstein JN, et al. (2005). Effects of subchronically inhaled carbon black in three species. I. Retention kinetics, lung inflammation, histopathology. Toxicol Sci, 88, 614–29.

ESCODD (2003a). Comparative analysis of baseline 8-oxo-7,8-dihydroguanine in mammalian cell DNA, by different methods in different laboratories: an approach to consensus. Carcinogenesis, 23, 2129–33.

ESCODD (2003b). Measurement of DNA oxidation in human cells by chromatographic and enzymic methods. Free Radic Biol Med, 34, 1089–99.

Evans MD, Olinski R, Loft S, et al. (2010). Toward consensus in the analysis of urinary 8-oxo-7,8-dihydro-2′-deoxyguanosine as a noninvasive biomarker of oxidative stress. FASEB J, 24, 1249–60.

Fanizza C, Ursini CL, Paba E, et al. (2007). Cytotoxicity and DNA-damage in human lung epithelial cells exposed to respirable a-quartz. Toxicol in Vitro, 21, 586–94.

Folkmann JK, Risom L, Hansen CS, et al. (2007). Oxidatively damaged DNA and inflammation in the liver of dyslipidemic ApoE $^{-/-}$ mice exposed to diesel exhaust particles. Toxicology, 237, 134–44.

Folkmann JK, Risom L, Jacobsen NR, et al. (2009). Oxidatively damaged DNA in rats exposed by oral gavage to C60 fullerenes and single-walled carbon nanotubes. Environ Health Perspect, 117, 703–8.

Folkmann JK, Vesterdal L, Sheykhzade M, et al. (2012). Endothelial dysfunction in normal and prediabetic rats with metabolic syndrome exposed by oral gavage to carbon black nanoparticles. Toxicol Sci, 129, 98–107.

Forchhammer L, Loft S, Roursgaard M, et al. (2012). Expression of adhesion molecules, monocytes interactions and oxidative stress in human endothelial cells exposed to wood smoke and diesel exhaust particles. Toxicol Lett, 209, 121–8.

Frikke-Schmidt H, Roursgaard M, Lykkesfeldt J, et al. (2011). Effect of vitamin C and iron chelation on diesel exhaust particle and carbon black induced oxidative damage and cell adhesion molecule expression in human endothelial cells. Toxicol Lett, 203, 181–9.

Gallagher J, Sams II R, Inmon J, et al. (2003). Formation of, 8-oxo-7,8-dihydro-2′-deoxyguanosine in rat lung DNA following subchronic inhalation of carbon black. Toxicol Appl Pharmacol, 190, 224–31.

Girgis E, Khalil WK, Emam AN, et al. (2012). Nanotoxicity of gold and gold-cobalt nanoalloy. Chem Res Toxicol, 25, 1086–98.

Hahn P, Song Y, Ying GS, et al. (2009). Age-dependent and gender-specific changes in mouse tissue iron by strain. Exp Gerontol, 44, 594–600.

Hainaut P, Pfeifer GP. (2001). Patterns of p53 G →T transversions in lung cancers reflect the primary mutagenic signature of DNA-damage by tobacco smoke. Carcinogenesis, 22, 367–74.

Han SG, Andrews R, Gairola CG. (2010). Acute pulmonary response of mice to multi-wall carbon nanotubes. Inhal Toxicol, 22, 340–7.

Han X, Gelein R, Corson N, et al. (2011). Validation of an LDH assay for assessing nanoparticle toxicity. Toxicology, 287, 99–104.

Heinrich U, Fuhst R, Rittinghausen S, et al. (1995). Chronic inhalation exposure of Wistar rats and two different strains of mice to diesel engine exhaust, carbon black, and titanium dioxide. Inhal Toxicol, 7, 533–56.

Hemmingsen JG, Møller P, Nøjgaard JK, et al. (2011). Oxidative stress, genotoxicity, vascular cell adhesion molecule expression in cells exposed to particulate matter from combustion of conventional diesel and methyl ester biodiesel blends. Environ Sci Technol, 45, 8545–51.

Hesterberg TW, Long CM, Bunn WB, et al. (2012). Health effects research and regulation of diesel exhaust: an historical overview focused on lung cancer risk. Inhal Toxicol, 24, 1–45.

Ho M, Wu KY, Chein HM, et al. (2011). Pulmonary toxicity of inhaled nanoscale and fine zinc oxide particles: mass and surface area as an exposure metric. Inhal Toxicol, 23, 947–56.

Hoet PHM, Brüske-Hohlfelt I, Salata OV. (2004). Nanoparticles – known and unknown health risks. J Nanobiotechnol, 2, 12.

Huang SX, Jaurand MC, Kamp DW, et al. (2011). Role of mutagenicity in asbestos fiber-induced carcinogenicity and other diseases. J Toxicol Environ Health Part B, 14, 179–245.

Hwang YJ, Jeung YS, Seo MH, et al. (2010). Asian dust and titanium dioxide particles-induced inflammation and oxidative DNA damage in C57BL/6 mice. Inhal Toxicol, 22, 1127–33.

Ichinose T, Yajima Y, Nagashima M, et al. (1997a). Lung carcinogenesis and formation of 8-hydroxy-deoxyguanosine in mice by diesel exhaust particles. Carcinogenesis, 18, 185–92.

Ichinose T, Yamanushi T, Seto H, et al. (1997b). Oxygen radicals in lung carcinogenesis accompanying phagocytosis of diesel exhaust particles. Int J Oncol, 11, 571–5.

ILSI Risk Science Institute workshop participants. (2000). The relevance of the rat lung response to particle overload for human risk assessment: a workshop consensus report. Inhal Toxicol, 12, 1–17.

Inoue K, Takano H, Yanagisawa R, et al. (2005). Effects of nano particles on antigen-related airway inflammation in mice. Respir Res, 6, 106.

Inoue K, Yanagisawa R, Koike E, et al. (2010). Repeated pulmonary exposure to single-walled carbon nanotubes exacerbates allergic inflammation of the airway: possible role of oxidative stress. Free Radic Biol Med, 48, 924–34.

Iwai K, Adachi S, Takahashi M, et al. (2000). Early oxidative DNA damages and late development of lung cancer in diesel exhaust-exposed rats. Environ Res, 84, 255–64.

Jacobsen NR, Møller P, Cohn CA, et al. (2008a). Diesel exhaust particles are mutagenic in FE1-Muta^{TM} Mouse lung epithelial cells. Mutat Res, 641, 54–7.

Jacobsen NR, Møller P, Jensen JA, et al. (2009). Lung inflammation and genotoxicity following pulmonary exposure to nanoparticles in ApoE $^{-/-}$ mice. Part Fibre Toxicol, 6, 2.

Jacobsen NR, Pojana G, White P, et al. (2008b). Genotoxicity, cytotoxicity and reactive oxygen species induced by single-walled carbon nanotubes and C_{60} fullerenes in the FE1-Muta^{TM} Mouse lung epithelial cells. Environ Mol Mutagen, 49, 476–87.

Jacobsen NR, Saber AT, White P, et al. (2007). Increased mutant frequency by carbon black, but not quartz, in the lacZ and cII transgenes of muta mouse lung epithelial cells. Environ Mol Mutagen, 48, 451–61.

Jacobsen NR, White PA, Gingerich J, et al. (2011). Mutation spectrum in FE1-Muta^{TM} Mouse lung epithelial cells exposed to nanoparticulate carbon black. Environ Mol Mutagen, 52, 331–7.

Jackson P, Hougaard KS, Boisen AM, et al. (2012). Pulmonary exposure to carbon black by inhalation or instillation in pregnant mice: effects on liver DNA strand breaks in dams and offspring. Nanotoxicology, 5, 486–500.

Jantzen K, Roursgaard M, Madsen CD, et al. (2012). Oxidative damage to DNA by diesel exhaust particle exposure in co-cultures f human lung epithelial cells and macrophages. Mutagenesis. 2012. [Epub ahead of print]. doi:10.1093/mutage/ges035.

Jiang L, Nagai H, Ohara H, et al. (2008). Characteristics and modifying factors of asbestos-induced oxidative DNA damage. Cancer Sci, 99, 2142–51.

Johansson C, Møller P, Forchhammer L, et al. (2010). An ECVAG trial on assessment of oxidative damage to DNA measured by the comet assay. Mutagenesis, 25, 125–32.

Kadiiska MB, Gladen BC, Baird DD, et al. (2000). Biomarkers of oxidative stress study: are plasma antioxidants markers of CCl_4 poisoning? Free Radic Biol Med, 28, 838–45.

Kadiiska M, Gladen BC, Baird DD, et al. (2005a). Biomarkers of oxidative stress study II: are oxidation products of lipids,

proteins, and DNA markers of CCl_4 poisoning? Free Radic Biol Med, 38, 698–710.
Kadiiska MB, Gladen BC, Baird DD, et al. (2005b). Biomarkers of oxidative stress study III. Effects of the nonsteroidal anti-inflammatory agents indomethacin and meclofenamic acid on measurements of oxidative products of lipids in CCl_4 poisoning. Free Radic Biol Med, 38, 711–8.
Kadiiska MB, Hatch GE, Nyska A, et al. (2011). Biomarkers of Oxidative Stress Study IV: ozone exposure of rats and its effect on antioxidants in plasma and bronchoalveolar lavage fluid. Free Radic Biol Med, 51, 1636–42.
Kaewamatawong T, Shimada A, Okajima M, et al. (2006). Acute and subacute pulmonary toxicity of low dose of ultrafine colloidal silica particles in mice after intratracheal instillation. Toxicol Pathol, 34, 958–65.
Kain J, Karlsson HL, Möller L. (2012). DNA damage induced by micro- and nanoparticles-interaction with FPG influences the detection of DNA oxidation in the comet assay. Mutagenesis, 27, 491–500.
Karlsson HL. (2010). The comet assay in nanotoxicology research. Anal Bioanal Chem, 398, 651–66.
Karlsson HL, Cronholm P, Gustafsson J, et al. (2008b). Copper oxide nanoparticles are highly toxic: a comparison between metal oxide nanoparticles and carbon nanotubes. Chem Res Toxicol, 21, 1726–32.
Karlsson HL, Holgersson A, Möller L. (2008a). Mechanisms related to the genotoxicity of particles in the subway and from other sources. Chem Res Toxicol, 21, 726–31.
Karlsson HL, Nilsson L, Möller L. (2005). Subway particles are more genotoxic than street particles and induce oxidative stress in cultured human lung cells. Chem Res Toxicol, 18, 19–23.
Kato T, Totsuka Y, Ishino K, et al. (2012). Genotoxicity of multi-walled carbon nanotubes in both in vitro and in vivo assay systems. Nanotoxicology. 2012. [Epub ahead of print]. doi:10.3109/17435390.2012.674571.
Khalil WK, Girgis E, Emam AN, et al. (2011). Genotoxicity evaluation of nanomaterials: DNA damage, micronuclei, 8-hydroxy-2-deoxyguanosine induced by magnetic doped CdSe quantum dots in male mice. Chem Res Toxicol, 24, 640–50.
Knaapen AM, Albrecht C, Becker A, et al. (2002). DNA damage in lung epithelial cells isolated from rats exposed to quartz: role of surface reactivity and neutrophilic inflammation. Carcinogenesis, 23, 1111–20.
Kreyling WG, Cox C, Ferron GA, et al. (1993). Lung clearance in Long-Evans rats after inhalation of porous, monodisperse cobalt oxide particles. Exp Lung Res, 19, 445–67.
Kuehl PJ, Anderson TL, Candelaria G, et al. (2012). Regional particle size dependent deposition of inhaled aerosols in rats and mice. Inhal Toxicol, 24, 27–35.
Lam CW, James JT, McCluskey R, et al. (2004). Pulmonary toxicity of single-wall carbon nanotubes in mice 7 and 90 days after intratracheal instillation. Toxicol Sci, 77, 126–34.
Lam PM, Misty V, Marczylo TH, et al. (2012). Rapid measurement of 8-oxo-7,8-dihydro-2′-deoxyguanisine in human biological matrices using ultra-high-performance liquid chromatography-tandem mass spectrometry. Free Radic Biol Med, 52, 2057–63.
Landsiedel R, Kapp MD, Schulz M, et al. (2009). Genotoxicity investigations on nanomaterials: methods, preparation and characterization of test material, potential artifacts and limitations – many questions, some answers. Mutat Res, 681, 241–58.
Leach CL, Kuehl PJ, Chand R, et al. (2012). Characterization of respiratory deposition of fluticasone-salmeterol hydrofluoroalkane-134a and hydrofluoroalkane-134a beclomethasone in asthmatic patients. Ann Allergy Asthma Immunol, 108, 195–200.
Lehmann AD, Blank F, Baum O, et al. (2009). Diesel exhaust particles modulate the tight junction protein occludin in lung cells in vitro. Part Fibre Toxicol, 6, 26.
Li YJ, Kawada T, Takizawa H, et al. (2008b). Airway inflammatory responses to oxidative stress induced by prolonged low-dose diesel exhaust particle exposure from birth differ between mouse BALB/c and C57BL/6 strains. Exp Lung Res, 34, 125–39.
Li N, Xia T, Nel AE. (2008a). The role of oxidative stress in ambient particulate matter-induced lung diseases and its implications in the toxicity of engineered nanoparticles. Free Radic Biol Med, 44, 1689–99.
Lin CH, Yang MH, Chang LW, et al. (2011). Cd/Se/Te-based quantum dot 705 modulated redox homeostasis with hepatotoxicity in mice. Nanotoxicology, 5, 650–63.
Loft S, Danielsen P, Løhr M, et al. (2012a). Urinary excretion of 8-oxo-7,8-dihydroguanine as biomarker of oxidative damage to DNA. Arch Biochem Biophys, 518, 142–50.
Loft S, Danielsen PH, Mikkelsen L, et al. (2008). Biomarkers of oxidative damage to DNA and repair. Biochem Soc Trans, 36, 1071–6.
Loft S, Deng X-S, Tuo J, et al. (1998). Experimental study of oxidative DNA damage. Free Radic Res, 29, 525–39.
Loft S, Møller P. (2006). Oxidative DNA damage and human cancer: need for cohort studies. Antioxid Redox Signal, 8, 1021–31.
Loft S, Svoboda P, Kasai H, et al. (2006). Prospective study of 8-oxo-7,8-dihydro-2′-deoxyguanosine excretion and the risk of lung cancer. Carcinogenesis, 27, 1245–50.
Loft S, Svoboda P, Kawai K, et al. (2012b). Association between 8-oxo-7,8-dihydroguanine excretion and risk of lung cancer in a prospective study. Free Radic Biol Med, 52, 167–72.
Mauderly JL, Snipes MB, Barr EB, et al. (1994). Pulmonary toxicity of inhaled diesel exhaust and carbon black in chronically exposed rats – Part I: neoplastic and nonneoplastic lung lesions. HEI Res Rep, 68, 1–75.
McClellan RO, Hesterberg TW, Wall JC. (2012). Evaluation of carcinogenic hazard of diesel engine exhaust needs to consider revolutionary changes in diesel technology. Regul Toxicol Pharmacol, 63, 225–58.
Møller P, Daneshvar B, Loft S, et al. (2003). Oxidative DNA damage in vitamin C supplemented guinea pigs after intratracheal instillation of diesel exhaust particles. Toxicol Appl Pharmacol, 189, 39–44.
Møller P, Folkmann JK, Danielsen PH, et al. (2012). Oxidative stress generated to DNA by gastrointestinal exposure to insoluble particles. Curr Mol Med, 12, 732–45.
Møller P, Folkmann JK, Forchhammer L, et al. (2008). Air pollution, oxidative damage to DNA, carcinogenesis. Cancer Lett, 266, 84–97.
Møller P, Friis G, Christensen PH, et al. (2004). Intra-laboratory comet assay sample scoring exercise for determination of formamidopyrimidine DNA glycosylase sites in human mononuclear blood cell DNA. Free Radic Res, 38, 1207–14.
Møller P, Jacobsen NR, Folkmann JK, et al. (2010a). Role of oxidative damage in toxicity of particulates. Free Radic Res, 44, 1–46.
Møller P, Loft S. (2010). Oxidative damage to DNA and lipids as biomarkers of exposure to air pollution. Environ Health Perspect, 118, 1126–36.
Møller P, Løhr M, Folkmann JK, et al. (2010b). Aging and oxidatively damaged nuclear DNA in animal organs. Free Radic Biol Med, 48, 1275–85.
Møller P, Mikkelsen L, Vesterdal LK, et al. (2011). Hazard identification of particulate matter on vasomotor dysfunction and progression of atherosclerosis. Crit Rev Toxicol, 41, 339–68.
Møller P, Möller L, Godschalk RW, et al. (2010c). Assessment and reduction of comet assay variation in relation to DNA damage: studies from the European Comet Assay Validation Group. Mutagenesis, 25, 109–11.
Møller P, Wallin H. (1998). Adduct formation, mutagenesis and nucleotide excision repair of DNA damage produced by reactive oxygen species and lipid peroxidation products. Mutat Res, 410, 271–90.
Morimoto Y, Hirohashi M, Kasai T, et al. (2009). Effect of polymerized toner on rat lung in chronic inhalation study. Inhal Toxicol, 21, 898–905.
Morimoto Y, Kim H, Oyabu T, et al. (2005). Negative effect of long-term inhalation of toner on formation of 8-hydroxydeoxyguanosine in DNA in the lungs of rats in vivo. Inhal Toxicol, 17, 749–53.
Muller J, Delos M, Panin N, et al. (2009). Absence of carcinogenic response to multiwall carbon nanotubes in a 2-year bioassay in the peritoneal cavity of the rat. Toxicol Sci, 110, 442–8.
Müller AK, Farombi EO, Møller P, et al. (2004). DNA damage in lung after oral exposure to diesel exhaust particles in Big Blue((R)) rats. Mutat Res, 550, 123–32.
Murray AR, Kisin ER, Tkach AV, et al. (2012). Factoring-in agglomeration of carbon nanotubes and nanofibers for better prediction of their toxicity versus asbestos. Part Fibre Toxicol, 9, 10.
Mutlu EA, Engen PA, Soberanes S, et al. (2011). Particulate matter air pollution causes oxidant-mediated increase in gut permeability in mice. Part Fibre Toxicol, 8, 19.
Nagashima M, Kasai H, Yokota J, et al. (1995). Formation of an oxidative DNA damage, 8-hydroxydeoxyguanosine, in mouse lung

DOI: 10.3109/10408444.2012.756456

DNA after intratracheal instillation of diesel exhaust particles and effects of high dietary fat and beta-carotene on this process. Carcinogenesis, 16, 1441–5.

Nehls P, Seiler F, Rehn B, et al. (1997). Formation and persistence of 8-oxoguanine in rat lung cells as an important determinant for tumor formation following particle exposure. Environ Health Perspect, 105, 1291–6.

Nikula KJ, Snipes MB, Barr EB, et al. (1995). Comparative pulmonary toxicities and carcinogenicities of chronically inhaled diesel exhaust and carbon black in F344 rats. Fundam Appl Toxicol, 25, 80–94.

Niwa Y, Hiura Y, Sawamura H, et al. (2008). Inhalation exposure to carbon black induces inflammatory response in rats. Circ J, 72, 144–9.

Oberdörster G. (1995). Lung particle overload: implications for occupational exposures to particles. Regul Toxicol Pharmacol, 21, 123–35.

Oberdörster G. (2002). Toxicokinetics and effects of fibrous and nonfibrous particles. Inhal Toxicol, 14, 29–56.

Oberdörster G, Maynard A, Donaldson K, et al. (2005). Principles for characterizing the potential human health effects from exposure to nanomaterials: elements of a screening strategy. Part Fibre Toxicol, 2, 8.

Olinski R, Gackowski D, Rozalski R, et al. (2003). Oxidative DNA damage in cancer patients: a cause or a consequence of the disease development? Mutat Res, 531, 177–90.

Onuma K, Sato Y, Ogawara S, et al. (2009). Nano-scaled particles of titanium dioxide convert benign mouse fibrosarcoma cells into aggressive tumor cells. Am J Pathol, 175, 2171–83.

Osier M, Oberdörster G. (1997). Intratracheal inhalation vs intratracheal instillation: differences in particle effects. Fundam Appl Toxicol, 40, 220–7.

Pauluhn J, Wiemann M. (2011). Siderite. ($FeCO_3$) and magnetite. (Fe_3O_4) overload-dependent pulmonary toxicity is determined by the poorly soluble particle not the iron content. Inhal Toxicol, 23, 763–83.

Poland CA, Duffin R, Kinloch I, et al. (2008). Carbon nanotubes introduced into the abdominal cavity of mice show asbestos-like pathogenicity in a pilot study. Nat Nanotechnol, 3, 423–8.

Pope III CA, Burnett RT, Thun MJ, et al. (2002). Lung cancer, cardiopulmonary mortality, and long-term exposure to fine particulate air pollution. JAMA, 287, 1132–41.

Rehn B, Seiler F, Rehn S, et al. (2003). Investigation on the inflammatory and genotoxic lung effects of two types of titanium dioxide: untreated and surface treated. Toxicol Appl Pharmacol, 189, 84–95.

Reliene R, Hlavacova A, Mahadevan B, et al. (2005). Diesel exhaust particles cause increased levels of DNA deletions after transplacental exposure in mice. Mutat Res, 570, 245–52.

Risom L, Dybdahl M, Bornholdt J, et al. (2003a). Oxidative DNA damage and defence gene expression in the mouse lung after short-term exposure to diesel exhaust particles by inhalation. Carcinogenesis, 24, 1847–52.

Risom L, Dybdahl M, Møller P, et al. (2007a). Repeated inhalations of diesel exhaust particles and oxidatively damaged DNA in young oxoguanine DNA glycosylase (OGG1) deficient mice. Free Radic Res, 41, 172–81.

Risom L, Møller P, Dybdahl M, et al. (2007b). Dietary exposure to diesel exhaust particles and oxidatively damaged DNA in young oxoguanine DNA glycosylase, 1 deficient mice. Toxicol Lett, 175, 16–23.

Risom L, Møller P, Hansen M, et al. (2003b). Dietary elevated sucrose modulation of diesel-induced genotoxicity in the colon and liver of Big Blue rats. Arch Toxicol, 77, 651–6.

Risom L, Møller P, Vogel U, et al. (2003c). X-ray-induced oxidative stress: DNA damage and gene expression of HO-1, ERCC1 and OGG1 in mouse lung. Free Radic Res, 37, 957–66.

Saber AT, Jensen KA, Jacobsen NR, et al. (2012). Inflammatory and genotoxic effects of nanoparticles designed for inclusion in paints and lacquers. Nanotoxicology, 6, 453–71.

Sanbongi C, Takano H, Osakabe N, et al. (2003). Rosmarinic acid inhibits lung injury induced by diesel exhaust particles. Free Radic Biol Med, 34, 1060–9.

Sato H, Sone H, Sagai M, et al. (2000). Increase in mutation frequency in lung of Big Blue rat by exposure to diesel exhaust. Carcinogenesis, 21, 653–61.

Sato T, Takeno M, Honma K, et al. (2006). Heme oxygenase-1, a potential biomarker of chronic silicosis, attenuates silica-induced lung injury. Am J Respir Crit Care Med, 174, 906–14.

Schürkes C, Brock W, Abel J, et al. (2004). Induction of 8-hydroxydeoxyguanosine by man made vitreous fibres and crocidolite asbestos administered intraperitoneally in rats. Mutat Res, 553, 59–65.

Seiler F, Rehn B, Rehn S, et al. (2001a). Evidence of a no-effect level in silica-induced rat lung mutagenicity but not in fibrogenicity. Arch Toxicol, 74, 716–9.

Seiler F, Rehn B, Rehn S, et al. (2001b). Significant differences in the cellular and molecular reactions of rat and hamster lung after quartz exposure. Toxicol Lett, 119, 11–9.

Seiler F, Rehn B, Rehn S, et al. (2001c). Quartz exposure of the rat lung leads to a linear dose response in inflammation but not in oxidative DNA damage and mutagenicity. Am J Respir Cell Mol Biol, 24, 492–8.

Seiler F, Rehn B, Rehn S, et al. (2004). Different toxic, fibrogenic and mutagenic effects of four commercial quartz flours in the rat lung. Int J Hyg Environ Health, 207, 115–24.

Semmler M, Seitz J, Erbe F, et al. (2004). Long-term clearance kinetics of inhaled ultrafine insoluble iridium particles from the rat lung, including transient translocation into secondary organs. Inhal Toxicol, 16, 453–9.

Sharma V, Singh P, Pandey AK, et al. (2012). Induction of oxidative stress, DNA damage and apoptosis in mouse liver after sub-acute oral exposure to zinc oxide nanoparticles. Mutat Res, 745, 84–91.

Shvedova AA, Kisin ER, Mercer R, et al. (2005). Unusual inflammatory and fibrogenic pulmonary responses to single-walled carbon nanotubes in mice. Am J Physiol Lung Cell Mol Physiol, 289, L698–708.

Shvedova AA, Kisin E, Murray AR, et al. (2008). Inhalation vs. aspiration of single-walled carbon nanotubes in C57BL/6 mice: inflammation, fibrosis, oxidative stress, and mutagenesis. Am J Physiol Lung Cell Mol Physiol, 295, L552–65.

Smith CC, O'Donovan MR, Martin EA. (2006). hOGG1 recognizes oxidative damage using the comet assay with greater specificity than FPG or ENDOIII. Mutagenesis, 21, 185–90.

Speit G, Schutz P, Bonzheim I, et al. (2004). Sensitivity of the FPG protein towards alkylation damage in the comet assay. Toxicol Lett, 146, 151–8.

Stayner LT, Graber JM. (2011). Does exposure to coal dust prevent or cause lung cancer? Occup Environ Med, 68, 167–8.

Stoeger T, Reinhard C, Takenaka S, et al. (2006). Instillation of six different ultrafine carbon particles indicates a surface area threshold dose for acute lung inflammation in mice. Environ Health Perspect, 114, 328–33.

Stone V, Johnston H, Schins RP. (2009). Development of in vitro systems for nanotoxicology: methodological considerations. Crit Rev Toxicol, 39, 613–26.

Sturm R. (2007). A computer model for the clearance of insoluble particles from the tracheobronchial tree of the human lung. Comput Biol Med, 37, 680–90.

Takagi A, Hirose A, Nishimura T, et al. (2008). Induction of mesothelioma in $p53^{+/}$ mouse by intraperitoneal application of multi-wall carbon nanotube. J Toxicol Sci, 33, 105–16.

Takata A, Yamauchi H, Toya T, et al. (2009). Forsterite exposure causes less oxidative DNA damage and lung injury than chrysotile exposure in rats. Inhal Toxicol, 21, 739–46.

Takata A, Yamauchi H, Toya T, et al. (2011). Effectiveness of serum megakaryocyte potentiating factor in evaluating the effects of chrysotile and its heated products on respiratory organs. Toxicol Appl Pharmacol, 252, 123–9.

Tellabati A, Fernandes VE, Teichert F, et al. (2010). Acute exposure of mice to high-dose ultrafine carbon black decreases susceptibility to pneumococcal pneumonia. Part Fibre Toxicol, 7, 30.

Thompson CM, Proctor DM, Haws LC, et al. (2011). Investigation of the mode of action underlying the tumorigenic response induced in B6C3F1 mice exposed orally to hexavalent chromium. Toxicol Sci, 123, 58–70.

Thompson CM, Proctor DM, Suh M, et al. (2012). Comparison of the effects of hexavalent chromium in the alimentary canal of F344 rats and B6C3F1 mice following exposure in drinking water: implications for carcinogenic modes of action. Toxicol Sci, 125, 79–90.

Tiede K, Boxall AB, Tear SP, et al. (2008). Detection and characterization of engineered nanoparticles in food and the environment. Food Addit Contam, 25, 795–821.

Tokiwa H, Sera N, Nakanishi Y. (2005). Involvement of alveolar macrophages in the formation of 8-oxodeoxyguanosine associated with exogenous particles in human lungs. Inhal Toxicol, 17, 577–85.

Tokiwa H, Sera N, Nakanishi Y, et al. (1999). 8-Hydroxyguanosine formed in human lung tissue and the association with diesel exhaust particles. Free Radic Biol Med, 27, 1251–8.

Trouiller B, Reliene R, Westbrook A, et al. (2009). Titanium dioxide nanoparticles induce DNA damage and genetic instability in vivo in mice. Cancer Res, 69, 8784–9.

Tsurudome Y, Hirano T, Yamato H, et al. (1999). Changes in levels of 8-hydroxyguanine in DNA, its repair and OGG1 mRNA in rat lungs after intratracheal administration of diesel exhaust particles. Carcinogenesis, 20, 1573–6.

Unfried K, Schürkes C, Abel J. (2002). Distinct spectrum of mutations induced by crocidolite asbestos: clue for 8-hydroxydeoxyguanosine-dependent mutagenesis in vivo. Cancer Res, 62, 99–104.

U.S. Environmental Protection Agency (EPA). (2002) Health assessment document for diesel engine exhaust. Prepared by the National Center for Environmental Assessment, Washington, DC, for the Office of Transportation and Air Quality; EPA/600/8-90/057F. Available from: National Technical Information Service, Springfield, VA; PB2002-107661, and <http://www.epa.gov/ncea>.

Valberg PA, Crouch EA. (1999). Meta-analysis of rat lung tumors from lifetime inhalation of diesel exhaust. Environ Health Perspect, 107, 693–9.

van Berlo D, Wessels A, Boots AW, et al. (2010). Neutrophil-derived ROS contribute to oxidative DNA damage induction by quartz particles. Free Radic Biol Med, 49, 1685–93.

van Poppel G, Poulsen H, Loft S, et al. (1995). No influence of beta carotene on oxidative DNA damage in male smokers. J Natl Cancer Inst, 87, 310–11.

Vecchio D, Arezzini B, Pecorelli A, et al. (2010). Reactivity of mouse alveolar macrophages to cigarette smoke is strain dependent. Am J Physiol Lung Cell Mol Physiol, 298, L704–13.

Vesterdal LK, Mikkelsen L, Folkmann JK, et al. (2012). Carbon black nanoparticles and vascular dysfunction in cultured endothelial cells and artery segments. Toxicol Lett, 214, 19–26.

Warheit DB, Laurence BR, Reed KL, et al. (2004). Comparative pulmonary toxicity assessment of single-wall carbon nanotubes in rats. Toxicol Sci, 77, 117–25.

Wessels A, Birmili W, Albrecht C, et al. (2010). Oxidant generation and toxicity of size-fractionated ambient particles in human lung epithelial cells. Environ Sci Technol, 44, 3539–45.

Wessels A, van Berlo D, Boots AW, et al. (2011). Oxidative stress and DNA damage responses in rat and mouse lung to inhaled carbon nanoparticles. Nanotoxicology, 5, 66–78.

Yamaguchi R, Hirano T, Ootsuyama Y, et al. (1999). Increased 8-hydroxyguanine in DNA and its repair activity in hamster and rat lung after intratracheal instillation of crocidolite asbestos. Jpn J Cancer Res, 90, 505–9.

Yamano Y, Kagawa J, Hanaoka T, et al. (1995). Oxidative DNA damage induced by silica in vivo. Environ Res, 69, 102–7.

Yamanushi TT, Ichinose T, Seto H, et al. (2001). The effect of dietary carotenoids on lung tumorigenesis induced by intratracheally instillated diesel exhaust particles. J Nutr Sci Vitaminol (Tokyo), 47, 32–9.

Exhibit 93

Alterations in Gene Expression in Human Mesothelial Cells Correlate with Mineral Pathogenicity

Arti Shukla[1]*, Maximilian B. MacPherson[1]*, Jedd Hillegass[1], Maria E. Ramos-Nino[1], Vlada Alexeeva[1], Pamela M. Vacek[2], Jeffrey P. Bond[3], Harvey I. Pass[4], Chad Steele[5], and Brooke T. Mossman[1]

Departments of [1]Pathology, [2]Medical Biostatistics, and [3]Microbiology and Molecular Genetics, University of Vermont College of Medicine, Burlington, Vermont; [4]Department of Cardiothoracic Surgery, NYU Langone Medical Center, New York, New York; and [5]Department of Medicine, University of Alabama at Birmingham School of Medicine, Birmingham, Alabama

Human mesothelial cells (LP9/TERT-1) were exposed to low and high (15 and 75 $\mu m^2/cm^2$ dish) equal surface area concentrations of crocidolite asbestos, nonfibrous talc, fine titanium dioxide (TiO_2), or glass beads for 8 or 24 hours. RNA was then isolated for Affymetrix microarrays, GeneSifter analysis and QRT-PCR. Gene changes by asbestos were concentration- and time-dependent. At low nontoxic concentrations, asbestos caused significant changes in mRNA expression of 29 genes at 8 hours and of 205 genes at 24 hours, whereas changes in mRNA levels of 236 genes occurred in cells exposed to high concentrations of asbestos for 8 hours. Human primary pleural mesothelial cells also showed the same patterns of increased gene expression by asbestos. Nonfibrous talc at low concentrations in LP9/TERT-1 mesothelial cells caused increased expression of 1 gene Activating Transcription Factor 3 (*ATF3*) at 8 hours and no changes at 24 hours, whereas expression levels of 30 genes were elevated at 8 hours at high talc concentrations. Fine TiO_2 or glass beads caused no changes in gene expression. In human ovarian epithelial (IOSE) cells, asbestos at high concentrations elevated expression of two genes (*NR4A2, MIP2*) at 8 hours and 16 genes at 24 hours that were distinct from those elevated in mesothelial cells. Since *ATF3* was the most highly expressed gene by asbestos, its functional importance in cytokine production by LP9/TERT-1 cells was assessed using siRNA approaches. Results reveal that *ATF3* modulates production of inflammatory cytokines (IL-1β, IL-13, G-CSF) and growth factors (VEGF and PDGF-BB) in human mesothelial cells.

Keywords: mesothelioma; crocidolite asbestos; talc; titanium dioxide; gene profiling

A myriad of natural and synthetic fibers and particles, including nanomaterials, are being introduced into the workplace and environment, and *in vitro* screening tests on human cell types are needed to predict their toxicity and mechanisms of action, especially in target cells of disease. Asbestos is a group of well-characterized fibrous minerals that are associated with the development of nonmalignant (asbestosis) and malignant (lung cancers, pleural, and peritoneal mesotheliomas) diseases in occupational cohorts (1–3), yet the molecular mechanisms of asbestos-related diseases are poorly understood. Although it is widely acknowledged that fibrous geometry, surface and chemical composition, and durability are important features in the development of asbestos-associated diseases, how these contribute to cell toxicity and transformation are unclear. Moreover, the early molecular events leading to injury by asbestos fibers and other pathogenic or innocuous particulates in human cells that may be targets for the development of disease remain enigmatic.

CLINICAL RELEVANCE

Results of work here suggest that transcriptional profiling can be used to reveal molecular events by mineral dusts that are predictive of their pathogenicity in mesothelioma.

The objective of work here was to compare acute toxicity and gene expression profiles of crocidolite asbestos, the type of asbestos most pathogenic in the causation of human mesothelioma (3, 4), to nonfibrous talc, fine titanium dioxide (TiO_2), and glass beads in a contact-inhibited, hTERT-immortalized human mesothelial cell line (5). In comparative studies, we also evaluated toxicity of particulates and gene expression changes in a contact-inhibited SV40 Tag-immortalized human ovarian epithelial cell line (IOSE) (6). This cell type is not implicated in asbestos-induced diseases, but is occasionally linked to inflammation and the development of ovarian cancer after use of talcum powder in the pelvic region, although such links are highly controversial (7).

Although most studies have evaluated the biological effects of particles and fibers on an equal mass or weight basis, the number, surface area, and reactivity of particulates at equal weight concentrations may be vastly different. Moreover, recent *in vitro* (8, 9) and *in vivo* (10–12), studies have confirmed that toxicity, oxidative stress, and inflammatory effects of ultrafine and other particles are related directly to surface area. For these reasons, and to avoid possible confounding alterations in gene expression or toxicity that might reflect or be masked in cells in different phases of the cell cycle, we introduced particulates at equal surface areas to confluent monolayers of human mesothelial (LP9/TERT-1) and human ovarian epithelial (IOSE) cells in a maintenance medium. Moreover, our studies included a nonfibrous talc sample and fine TiO_2 and glass particles, both traditionally used as nontoxic and nonpathogenic control particles in *in vitro* and animal experiments (reviewed in Refs. 13 and 14). Our studies provide novel insight into the early molecular events and responses occurring in human cells after exposure to asbestos and these materials.

MATERIALS AND METHODS

Human Mesothelial and Ovarian Epithelial Cell Cultures

Human mesothelial LP9/TERT-1 (LP9) cells, an hTERT-immortalized cell line phenotypically and functionally resembling normal human mesothelial cells (5), were obtained from Dr. James Rheinwald (Dana Farber Cancer Research Institute, Boston, MA). Human pleural mesothelial cells (NYU474) were isolated surgically from

(*Received in original form April 11, 2008 and in final form November 24, 2008*)

* These authors contributed equally to this research.

This work was supported by NIEHS training grant T32ES007122 to B.T.M., a contract from EUROTALC and the Industrial Minerals Association of North America, and NCI P01 CA 114,047 (H.I.P. and B.T.M.).

Correspondence and requests for reprints should be addressed to Arti Shukla, Ph.D., Department of Pathology, University of Vermont College of Medicine, 89 Beaumont Avenue, Burlington, VT 05405. E-mail: Arti.Shukla@uvm.edu

This article contains microarray data which can be found as a repository using the accession number GSE14034.

Am J Respir Cell Mol Biol Vol 41. pp 114–123, 2009
Originally Published in Press as DOI: 10.1165/rcmb.2008-0146OC on December 18, 2008
Internet address: www.atsjournals.org

cancer-free patients by Dr. Harvey Pass (New York University, New York, NY). Briefiy, tissue sample 2 × 2 cm^2 was harvested into saline solution and rinsed immediately with PBS (1×) and Dulbecco's modified Eagle's medium (DMEM) (1×). The tissue was then digested with 0.2% Collagenase type 1 (MP Biomedical Inc., Solon, OH) for 3 hours at 37°C. Finally, the digested tissue was scraped and cells collected were centrifuged for 5 minutes at 300 × *g*. The cell pellet thus obtained was resuspended in DMEM containing 10% fetal bovine serum (FBS) and 2% penicillin–streptomycin, transferred into 6-well plate, and allowed to grow at 5% CO_2 and 37°C. Mesothelial cells were characterized by staining with calretinin antibody. An SV40 Tag-immortalized, anchorage-dependent human ovarian epithelial cell line (IOSE 398) (6) was a kind gift from Dr. Nelly Auersperg (Canadian Ovarian Tissue Bank, University of British Columbia, Vancouver, BC, Canada). LP9/TERT-1 cells were maintained in 50:50 DMEM/F-12 medium containing 10% FBS, and supplemented with penicillin (50 units/ml), streptomycin (100 μg/ml), hydrocortisone (100 μg/ml), insulin (2.5 μg/ml), transferrin (2.5 μg/ml), and selenium (2.5 μg/ml). IOSE cells were maintained in 50:50 199/MCB105 medium containing 10% FBS and 50 μg/ml gentamicin. Cells at near confiuence were switched to maintenance medium containing 0.5% FBS for 24 hours before particulate exposure. NYU474 cells were grown to near confiuence in DMEM containing 10% FBS and supplemented with penicillin (50 units/ml) and streptomycin (100 μg/ml).

Characterization of Mineral Preparations

The physical and chemical characterization of the NIEHS reference sample of crocidolite asbestos has been reported previously (15). The surface area of asbestos fibers and particles was measured using nitrogen gas sorption analysis to allow computation of identical amounts of surface areas of particulates to be added to cells. Fiber and particle size dimensions were determined by scanning electron microscopy (SEM) as described previously (16). In addition, talc was examined using field emission scanning electron microscopy (FESEM) and transmission electron microscopy (TEM). The chemical composition, surface area, mean size, and source of each particulate preparation is presented in Table 1.

Introduction of Particulates to Cells

After sterilization under ultraviolet light overnight to avoid endotoxin and microbial contamination, particulates were suspended in HBSS at 1 mg/ml, sonicated for 15 minutes in a water bath sonicator, and triturated five times through a 22-gauge needle. This suspension was added to cells in medium.

SEM to Determine Particulate/Cell Interactions

Cells were grown on Thermonox plastic cover slips (Nalge Nunc International, Naperville, IL), exposed to particulates for 24 hours, and then processed for SEM as described previously (16). After samples were critical point-dried, they were mounted on aluminum specimen stubs and dried before being sputter-coated with gold and palladium in a Polaron sputter coater (Model 5100; Quorum Technologies, Guelph, ON, Canada) and examined on a JSM 6060 scanning electron microscope (JEOL USA, Inc., Peabody, MA).

Cell Viability Studies

After 24 hours, cells were collected with Accutase cell detachment reagent, and final cell suspensions in Accutase/complete medium/HBSS were mixed with 0.4% trypan blue stain, which is retained by dead cells. After 5 minutes, unstained cells were counted using a hemocytometer to determine the total number of viable cells per dish.

Based on the results of cell viability studies, asbestos and nonfibrous talc were evaluated in LP9 mesothelial cells for changes in gene expression at both low and high concentrations (15 and 75 $\mu m^2/cm^2$ dish) at 8 hours, and at low concentrations of minerals (15 $\mu m^2/cm^2$ dish) at 24 hours. These concentrations did not cause morphologic or toxic cellular changes at these time points. Negative control groups included cells exposed to fine TiO_2 (15 $\mu m^2/cm^2$ dish) at 8 and 24 hours and glass beads (75 $\mu m^2/cm^2$) at 24 hours. In IOSE cells, gene expression of all particulates was evaluated at 75 $\mu m^2/cm^2$ at 8 and 24 hours, as preliminary experiments revealed that no significant changes in mRNA levels were observed at 15 $\mu m^2/cm^2$ dish of asbestos. In NYU474 human mesothelial cells, QRT-PCR was used to validate a selected subset of gene expression changes identified by arrays in LP9/TERT-1 cells. Cells were exposed to 15 and 75 $\mu m^2/cm^2$ asbestos for 24 hours, and 8 genes highly expressed in LP9 cells were examined by QRT-PCR (*see below*).

RNA Preparation

Total RNA was prepared using an RNeasy Plus Mini Kit according to the manufacturers' protocol (Qiagen, Valencia, CA), as previously described (17).

Affymetrix Gene Profiling

Microarrays were performed on samples from three independent experiments. All cell types, time points, and mineral types and concenrations were included in all three experiments. For each experiment, $n = 3$ dishes were pooled into one sample per treatment group. Each of the pooled samples was analyzed on a separate array (i.e., $n = 3$ arrays per condition [3 independent biological replicates]). All procedures were performed by the Vermont Cancer Center DNA facility using standard Affymetrix protocol as previously described (14, 17). Each probe array, Human U133A 2.0 (Affymetrix, Santa Clara, CA) was scanned twice (Hewlett-Packard GeneArray Scanner, Palo Alto, CA), the images overlaid, and the average intensities of each probe cell compiled. Microarray data were analyzed using GeneSifter software (VizX Labs, Seattle, WA). This program used a "*t* test" for pairwise comparison and a Benjamini-Hochberg test for false discovery rate (FDR 5%) to adjust for multiple comparisons. A 2-fold cutoff limit was used for analysis.

Quantitative Real-Time PCR

Total RNA (1 μg) was reverse-transcribed with random primers using the Promega AMV Reverse Transcriptase kit (Promega, Madison, WI) according to the recommendations of the manufacturer, as described previously (17). In NYU474 mesothelial cells, eight genes (*ATF3*, *SOD2*, *PTGS2*, *FOSB*, *TFPI2*, *PDK4*, *NR4A2*, and *IL-8*) most highly expressed in LP9 cells were evaluated using the ΔΔCt method. Duplicate or triplicate assays were performed with RNA samples isolated from at least three independent experiments. The values obtained from cDNAs and hypoxanthine phosphoribosyl transferase (*hprt*) controls provided relative gene expression levels for the gene locus investigated. The primers and probes used to validate gene expression as observed in microarrays were purchased from Applied Biosystems (Foster City, CA).

TABLE 1. CHARACTERIZATION OF PARTICULATES

Name	Chemical Composition	Mean Surface Area ± SE (m^2/g)	Mean Size (μm)*	Source
Crocidolite Asbestos	$Na_2Fe_3^{2+}Fe_2^{3+}Si_8O_{22}(OH)_2$	14.97 ± 0.605	7.4 × 0.25	NIEHS Reference Sample
Talc (MP 10-52)†	$Mg_3Si_4O_{10}(OH)_2$	16.03 ± 0.654	1.1	Barrett's Minerals, Inc.
Titanium Dioxide	TiO_2	9.02 ± 0.185	0.69	Fisher Scientific
Glass Beads	SiO_2	2.78 ± 0.215	2.06	Polysciences Inc.

* Length X width for crocidolite asbestos, and diameter for nonfibrous talc, TiO_2, and glass beads.

† Although standard reference samples of asbestos and some particulates are available for use by the scientific community, reference samples of talc currently do not exist. For these reasons, the nonfibrous talc sample was also characterized for physical properties, particle size distribution (0.70 μm minimum to 1.20 μm maximum), and chemical/mineralogical (talc 95%, chlorite 4.5–5%, dolomite 0.3%) composition. For complete analysis or obtaining samples, please contact Brooke Mossman, Mark Ellis (markellis@ima-na.org), or Michelle Wyart at EUROTALC (mwyart@ima-europe.eu).

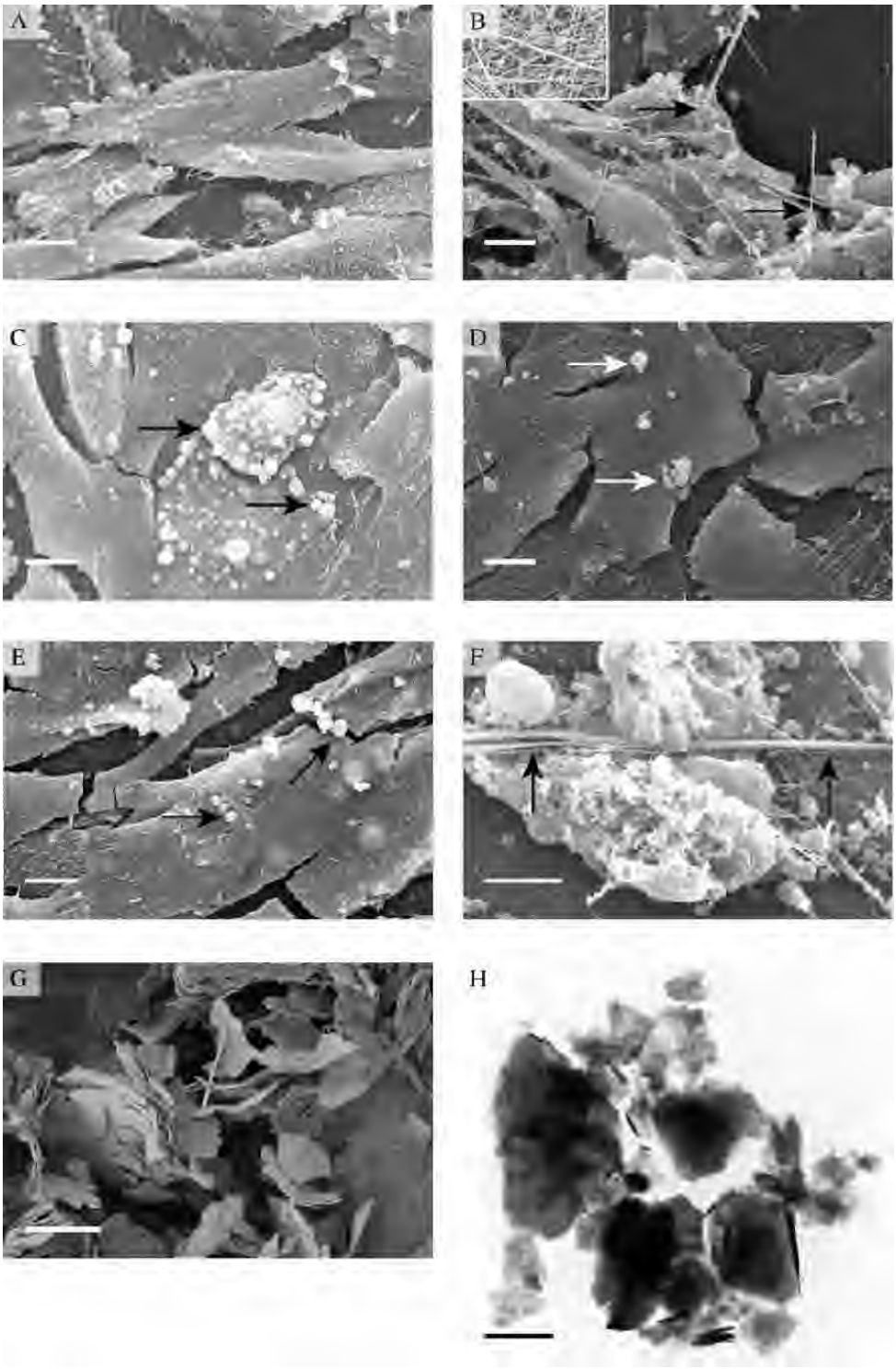

Figure 1. Interaction of fibers and particles with (*A–E*) LP9/TERT-1 human mesothelial cells and (*F*) IOSE ovarian epithelial cells after 24 hours of exposure to (*B*, *E*, *F*) high and (*C*, *D*) low concentrations of particulates. (*G*) Field emission scanning electron microscopy (FESEM) and (*H*) transmission electron microscopy (TEM) show structure of nonfibrous talc. (*A*) Morphology of unexposed near-confiuent LP9/TERT-1 cells. (*B*) Membrane blebbing and piling up of cells in response to crocidolite asbestos (*arrows*). (*C*) Nonfibrous talc and (*D*) fine TiO_2 (*arrows*) on cell surface. (*E*) Single and small clumps of glass beads on plasma membrane. (*F*) Interaction of asbestos fibers (*arrows*) with IOSE cells that exhibit an exudate and membrane ruffiing in response to fibers. *Bars* = 10 μm. (*G*) FESEM and (*H*) TEM showing morphology of platy talc bulk material. *Bars* = 2 μm.

Transfection of LP9 Cells with siRNA

On-Target plus Non-targeting siRNA #1 (scrambled control), and On-Target plus SMART pool human *ATF3* siRNA (100 nM; Dharmacon, Lafayette, CO) were transfected into LP9 cells at near confiuence using Lipofectamine 2000 (Invitrogen, Carlsbad, CA), following the manufacturer's protocol. The efficiency of *ATF3* knockdown was determined by QRT-PCR after 48 and 72 hours.

Bio-Plex Analysis of Cytokine and Chemokine Concentrations in Medium of LP9/TERT-1 Cells

To quantify cytokine and chemokine levels in conditioned medium of cells transfected with siATF3 or scrambled control and exposed to asbestos for 24 hours, a multiplex suspension protein array was performed using the Bio-Plex protein array system as described previously (17) and a Human Cytokine 27-plex panel (Bio-Rad, Hercules, CA). Three biological replicates were used for each treatment group.

Statistical Analysis

Data from QRT-PCR and cell viability assays were evaluated by ANOVA using the Student Neuman-Keul's procedure for adjustment of multiple pairwise comparisons between treatment groups or using the nonparametric Kruskal-Wallis and Mann-Whitney tests. Differences with P values ≤ 0.05 were considered statistically significant.

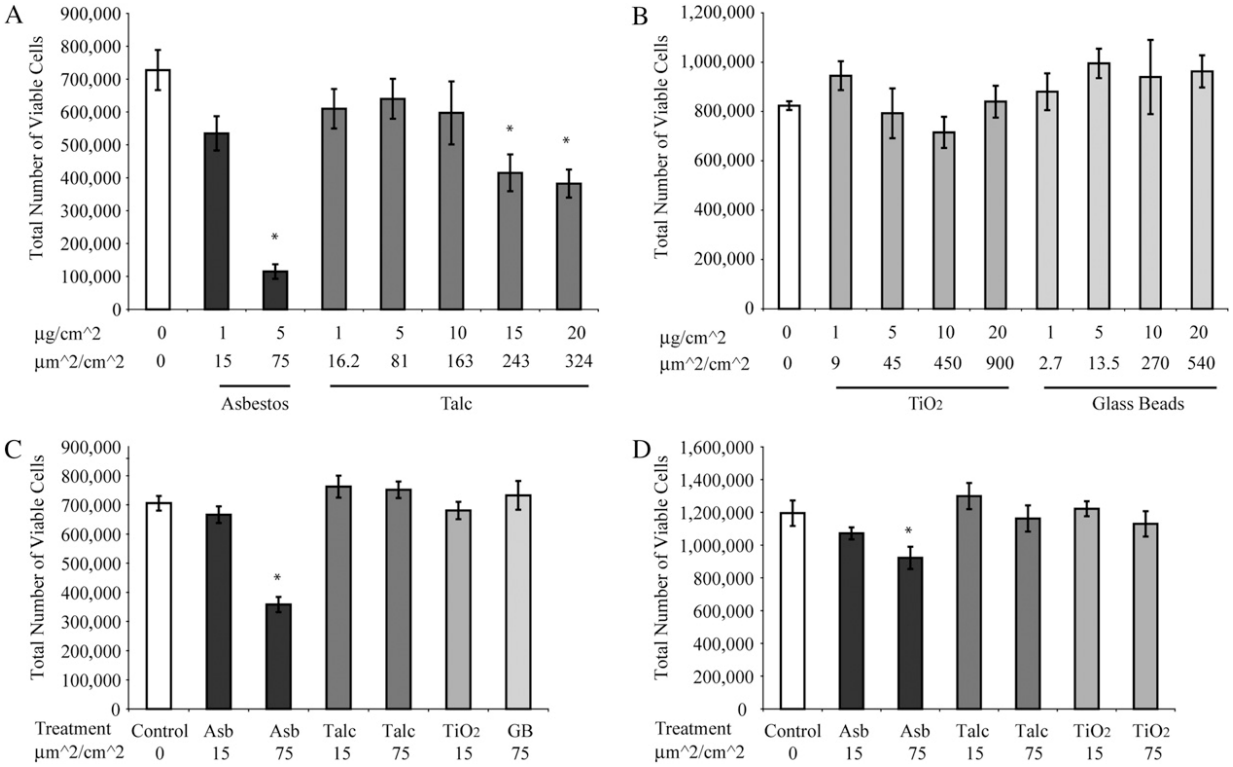

Figure 2. Cell viability after 24 hours of exposure to asbestos fibers and particles in (*A–C*) LP-9/TERT-1 and (*D*) IOSE (D). Mean +/− SE of 1 (A, B) or 3 (C, D) individual experiments where $n = 3$ per group per experiment. * $P \leq 0.05$ compared with untreated (0) groups.

RESULTS

Characterization of Particulate Preparations

Table 1 shows the major chemical formulas of crocidolite asbestos fibers (defined as having a greater than 3:1 length to width ratio) and particle samples used in experiments, although trace amounts of other elements occur in the NIEHS asbestos standards (15). In addition, we examined the morphology and cellular interactions of asbestos fibers, talc, and other particles using SEM (Figure 1). These studies revealed that only high (75 $\mu m^2/cm^2$) surface area concentrations of asbestos caused membrane blebbing and other toxic manifestations in cells (Figures 1B and 1F). In contrast, particles of nonfibrous talc (Figure 1C), fine TiO_2 (Figure 1D), and glass beads (Figure 1E) were nontoxic. Both asbestos fibers and particles were observed on the cell surface and were encompassed by cells. Nonfibrous talc occurred in platy particles that were uniform in appearance as viewed by FESEM (Figure 1G) and TEM (Figure 1H).

Asbestos Fibers at High Concentrations Are Toxic to LP9/TERT-1 Human Mesothelial Cells and Less So to Ovarian Epithelial Cells in Contrast to Particle Preparations

Figure 2 shows the results of trypan blue exclusion tests in LP9/TERT-1 and IOSE cells. In LP9/TERT-1 cells (Figures 2A–2C), asbestos at high surface area concentrations (75 $\mu m^2/cm^2$) caused significant decreases (50–80%) in cell viability that were more striking than those observed in IOSE cells (Figure 2D). Nonfibrous talc at 75 $\mu m^2/cm^2$ was nontoxic, and significant increases in toxicity were only achieved with addition of talc at $\geq$ 3-fold higher concentrations in LP9/TERT-1 cells (Figure 2A), but not in IOSE cells (data not shown). Neither TiO_2 nor glass beads were significantly toxic to either cell type over a range of concentrations (Figure 2B).

Asbestos Fibers, but Not Particle Preparations, Cause Dose- and Time-Related Changes in Gene Expression in Human LP9 Mesothelial Cells

Figure 3 shows a summary of significantly increased or decreased (> 2-fold compared with untreated controls) gene expression by asbestos (Figures 3A–3C) and nonfibrous talc (Figure 3D) in LP9/TERT-1 cells as well as the classification of genes by ontology. These studies revealed that gene expression changes by low concentrations of asbestos were less (29 increases) than at high concentrations (236 alterations including decreases) at 8 hours. Moreover, numbers of significant mRNA level alterations (205) at low concentrations of asbestos increased over time. In contrast, fewer numbers (30) of gene expression increases were observed at high concentrations of talc at 8 hours compared with identical surface areas of asbestos (236 changes), and no decreases in gene expression were observed. No significant alterations in gene expression were observed with low concentrations of talc at 24 hours or with TiO_2 or glass beads at either concentration or time point (data not shown). The major genes affected by asbestos or talc in LP9/TERT-1 cells are listed in Tables 2–4. This information reveals that the fold-increases in common genes expressed by asbestos-treated cells increase in a dose-related fashion at 8 hours. Although dose–responses were observed with talc at 8 hours, the numbers of significant gene increases as well as fold-increases were less than that observed with asbestos and decreased over time. Since mRNA expression of *ATF3* and *IL8* were increased by either asbestos or talc in LP9/TERT-1 cells, the increased expression of these genes was verified by QRT-PCR in mineral-exposed cells as compared with untreated control cells (Figure 4).

In NYU474 cells, QRT-PCR was used to validate that eight asbestos-induced genes in LP9 cells were up-regulated in

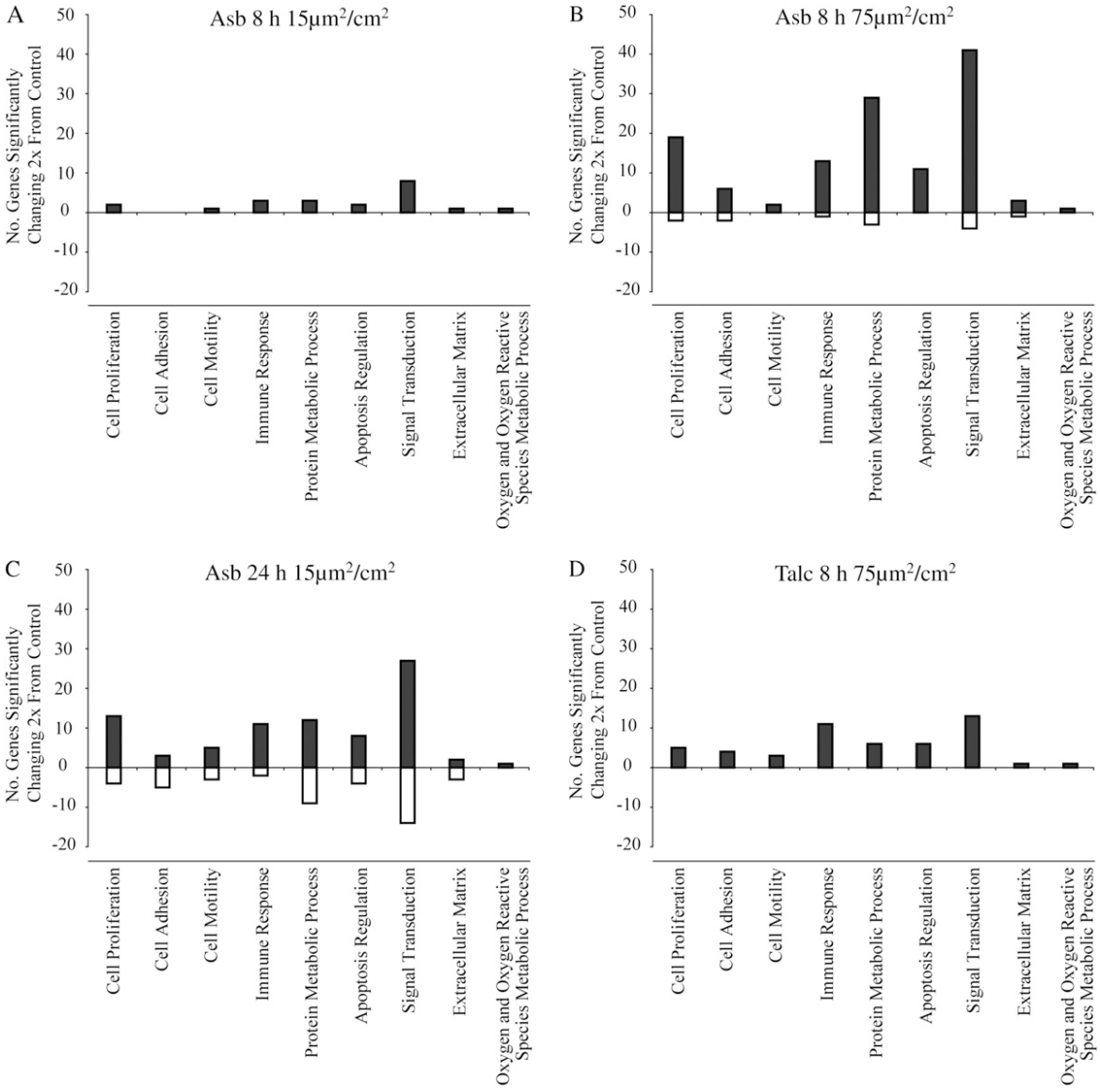

Figure 3. Numbers of changes ($P \leq 0.05$) in gene expression and classification by ontology in LP9/TERT-1 cells after exposure to (*A*–*C*) crocidolite asbestos or (*D*) nonfibrous talc.

normal human mesothelial cells (*ATF3*, *PTGS2* or *COX2*, *FOSB*, *IL8*, *NR4A2*, and *TFPI2*). Results showed that mRNA levels of six of the eight genes evaluated were increased in a dose-responsive fashion after exposure to asbestos for 24 hours (Figure 5).

IOSE Ovarian Epithelial Cells Exhibit Few Gene Expression Changes in Response to Asbestos

In contrast to LP9/TERT-1 and NYU474 mesothelial cells, IOSE cells showed no significant gene up-regulation or down-regulation in response to lower concentrations of asbestos at 8 or 24 hours (data not shown). At high concentrations of asbestos at 8 hours, mRNA levels of only two genes (*NR4A2* and *CXCL2* or *MIP2*) were increased in comparison to untreated IOSE cells (Table 4). At 24 hours, high concentrations of asbestos caused less than 4-fold increases in expression of only 16 genes, and decreased expression of 1 gene, *Profilin 1* (data not shown). No significant mRNA changes were observed with nonfibrous talc, fine TiO_2 or glass beads at either time point.

Inhibition of *ATF3* by siRNA Alters Asbestos-Induced Cytokines in LP9/TERT-1 Cells

Since *ATF3* was a common gene up-regulated by asbestos in mesothelial cells its functional role in cytokine production in LP9 cells was evaluated. As shown in Figure 6A, *ATF3* was successfully inhibited in LP9/TERT-1 cells using siATF3 as described in Materials and Methods. Cells transfected with control siRNA or siATF3 were then exposed to asbestos (75 $\mu m^2/cm^2$ $n = 3$) for 24 hours, and medium was collected and analyzed for cytokines and growth factors using Bio-Plex analyses. Inhibition of *ATF3* altered levels of asbestos-induced infiammatory cytokines (IL-1β, IL-13, G-CSF) and the growth factor (PGDF-BB) in LP9/TERT-1 cells (Figure 6B). Trends in diminishing levels of VEGF were also observed, although not statistically significant.

DISCUSSION

Gene expression analysis has been used for the classification of soluble toxicants in rodent and human cells *in vitro*. Models of

TABLE 2. TOP 10 GENES AFFECTED BY CROCIDOLITE ASBESTOS AT 8 AND 24 H IN LP9/TERT-1 HUMAN MESOTHELIAL CELLS

Concentration	Low ($15\ \mu m^2/cm^2$)		High ($75\ \mu m^2/cm^2$)
Time	8 h	24 h	8 h
	Fold Change		
Up-regulated			
Activating transcription factor 3 (*ATF3*)	9	9	27
Prostaglandin-endoperoxide synthase 2 (PTGS2)	7	8	16
Superoxide Dismutase 2 (SOD2)	6	6	2
Chemokine (C-X-C motif) ligand 3 (CXCL3)	4	NC	16
FBJ murine osteosarcoma viral oncogene homolog B (FOSB)	4	NC	NC
Tissue factor pathway inhibitor 2 (TFPI2)	4	14	11
Pyruvate dehydrogenase kinase, isozyme 4 (PDK4)	3	9	15
Chemokine (C-X-C motif) ligand 2 (CXCL2)	3	NC	NC
Angiopoietin-like 4 (ANGPLT4)	3	NC	NC
Kruppel-like factor 4 (gut) (KLF4)	3	NC	NC
Interleukin 8 C-terminal variant, 211506_s_t (IL8)	NC	8	12
Interleukin 1 receptor-like 1 (IL1R1)	NC	6	11
Nuclear receptor subfamily 4 (NR4A2)	NC	NC	11
Solute carrier family 7 (SLC7A2)	NC	6	10
Pleckstrin homology-like domain (PHLDA1)	NC	7	NC
Interleukin 8 (IL8)	NC	6	NC
Down-regulated			
Inhibitor of DNA binding 3 (ID3)	NC	NC	−5
Inhibitor of DNA binding 1 (ID1)	NC	NC	−3
Cytochrome P450, family 24 (CYP24A1)	NC	NC	−3
Basic helix-loop-helix domain (BHLHB3)	NC	NC	−3
SMAD family member 6 (SMAD6)	NC	NC	−3
S-phase kinase associated protein 2 (SKP2)	NC	NC	−3
Cadherin 10, type 2 (CDH10)	NC	NC	−3
START domain containing 5 (STARD5)	NC	NC	−3
211042_x_at	NC	NC	−2
Interferon-induced protein with tetratricopeptide (IFIT1)	NC	NC	−2
Oxytocin receptor (OXTR)	NC	−6	NC
Transcribed locus	NC	−5	NC
Chromosome 5 open reading frame (C5orf13)	NC	−5	NC
Cytochrome P450, family 24 (CYP24A1)	NC	−4	NC
Chromosome 21 open reading frame (C21orf7)	NC	−3	NC
KIAA1199	NC	−3	NC
Methyltransferase like 7A (METTL7A)	NC	−3	NC
PDZ domain containing RING finger 3 (PDZRN3)	NC	−3	NC
Periplakin (PPL)	NC	−3	NC
Phospholipase-C-like 1 (PLCL1)	NC	−3	NC

Definition of abbreviation: NC, no significant ($P \leq 0.05$) change > 2-fold from control.

transcript profiling for discrimination of toxic and nontoxic compounds in liver and other organs have also been developed in rodents (18), confirming the hypothesis that predictive modeling for classification of toxic agents and carcinogens is feasible. Here we used toxicogenomic approaches in human mesothelial cells, a cell type exquisitely sensitive to asbestos (19) and human contact-inhibited ovarian epithelial cells, a cell type not linked to carcinogenesis by asbestos, to determine whether the magnitude of altered gene expression by insoluble particulates correlated with their toxicity to cells and documented pathogenicity in humans. Although a recent study has examined gene expression profiles comparatively in crocidolite asbestos–exposed human lung adenocarcinoma (A549) and SV40-immortalized bronchial (BEAS-2B) or pleural mesothelial cell lines (MET5A) by cluster analysis (20), our studies are the first to examine gene expression changes by asbestos in comparison to other well-characterized particles in a human cell line that exhibits features of normal mesothelial cells (5). Although strict comparisons between cell types are not justified because SV40 Tag was used to immortalize the IOSE ovarian epithelial cell line (6), and SV40 infection is known to decrease sensitivity of human mesothelial cell lines to toxicity by asbestos (21), our studies suggest that the increased numbers of gene expression alterations observed in LP9/TERT-1 human mesothelial cells reflect elevated sensitivity of this cell type to asbestos. NYU474 human mesothelial cells were more resistant that LP9/TERT-1 cells to asbestos toxicity, permitting us to perform QRT-PCR studies at both concentrations of asbestos at 24 hours. These results confirmed common dose-related patterns of gene expression in mesothelial cells versus ovarian epithelial (IOSE) cells.

It is generally recognized that geometry and length and width (i.e., aspect ratio) of durable fibers such as amphibole asbestos types (crocidolite, amosite) are important properties determining toxicity, transforming potential, and carcinogeniciy in rodents and humans (13, 22, 23). Since talc can occur in various geometries (nonfibrous and fibrous) and can be contaminated with other minerals, including amphiboles, in some mining deposits (reviewed in Ref. 24), we used a well-characterized, nonfibrous talc sample here to allow evaluation of a particle not causing mesotheliomas or pleural sarcomas in rodents (23). Moreover, nonfibrous talc is regarded as noncarcinogenic in humans (25). Since talc is a magnesium silicate, and Mg^{2+} may interact with negatively charged molecules on the cell surface to

TABLE 3. GENES UP-REGULATED BY NONFIBROUS TALC IN LP9/TERT-1 HUMAN MESOTHELIAL CELLS

Gene	Fold Increase
8 h Low (15 μm²/cm²)	
Activating transcription factor 3 (*ATF3*)	3
8 h High (75 μm²/cm²)	
Activating transcription factor 3 (*ATF3*)	13
Inhibin, beta A (INHBA)	9
Chemokine (C-X-C motif) ligand 3 (CXCL3)	7
Superoxide dismutase 2 (SOD2)	7
Interleukin 8 C-terminal variant, 211506_s_t (IL8)	6
Prostaglandin-endoperoxide synthase 2 (PTGS2)	5
Interleukin 8 (IL8)	5
FBJ murine osteosarcoma viral oncogene homolog B (FOSB)	5
Tumor necrosis factor alpha-induced protein 6 (TNFAIP6)	4
Tissue factor pathway inhibitor 2 (TFPI2)	4
Chemokine (C-X-C motif) ligand 2 (CXCL2)	3
Intercellular adhesion molecule 4 (CICAM4)	3
ChaC, cation transport regulator homolog 1 (ChaC 1)	3
Nuclear receptor subfamily 4, group A, member 3 (NR4A3)	3
Pleckstrin homology-like domain, family A, member 1 (PHLDA1)	3
Interleukin 6 (IL-6)	3
Phorbol -12-myristate-13-acetate-induced protein 1 (PMA1P1)	3
Oxidized low density lipoprotein (lectin-like) receptor 1 (OLR1)	3
Chemokine (C-C motif) ligand 20 (CCL20)	3
v-maf musculoaponeurotic fibrosarcoma oncogene homolog F	3
Interleukin 1, alpha (IL-1α)	2
Tumor necrosis factor-α induced protein 3 (TNFA1P3)	2
Interleukin 1 receptor-like 1 (IL1RL1)	2
Angiopoieten-like 4 (ANGPLT4)	2
Kruppel-like factor 4 (KLF4)	2
GTP binding protein overexpressed in skeletal muscle (GEM)	2
Pentraxin-related gene, rapidly induced by IL-1 beta (PTX3)	2
Interleukin 1 beta (IL-1β)	2
HSPB (heat shock 27 kD) associated protein 1 (HSPBAP1)	2
Kynureninase (KYNU)	2

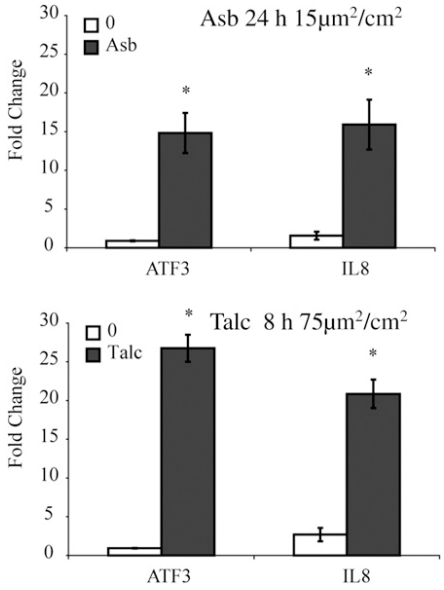

Figure 4. QRT-PCR confirms significant increases in *ATF3* and *IL8* expression by crocidolite asbestos at low concentrations and nonfibrous talc at high concentrations in LP9/TERT-1 mesothelial cells. **P* < 0.05 as compared to untreated (0) groups.

disturb cell homeostasis (reviewed in Ref. 26), this may explain the few mRNA expression increases that were observed initially with talc at 8 hours. However, these changes were not observed at 24 hours, suggesting that human mesothelial cells adapt to or undergo repair after exposure to this mineral.

Our gene profiling data here and in inhalation studies using chrysotile asbestos (14) also support the concept that fine TiO_2 is nontoxic and nonpathogenic to mesothelial or other cell types. Likewise, in the rat, inhalation of fine TiO_2 (defined as particles > 0.1 μm in diameter), in contrast to ultrafine (particles < 0.1 μm in diameter) does not give rise to predictive markers of toxicity, inflammation, pulmonary fibrosis, or oxidative stress, as indicated by elevated levels of Mn-containing superoxide dismutase (*SOD2*) in cells from bronchopulmonary lavage (27). The increased reactivity and toxicity of ultrafine particles as compared with larger fine or coarse particles have also been confirmed in a number of *in vitro* and *in vivo* experiments and is often attributed to their increased surface area and/or ability to penetrate lung cells.

TABLE 4: GENES UPREGULATED BY CROCIDOLITE ASBESTOS IN IOSE HUMAN OVARIAN CELLS

Gene	Fold increase
8 h High (75 μm²/cm²)	
Nuclear receptor subfamily 4 (NR4A2)	4
Chemokine (C-X-C motif) ligand 2 (MIP2)	2
24 h High (75 μm²/cm²)	
Nuclear receptor subfamily 4 (NR4A2)	4
DNA-damage-inducible transcript 3 (DDIT3)	3
Stromal cell-derived factor 2-like 1(SDF2L1)	3
Heat shock 70 kD protein 1A (HSPA1A)	3
DnaJ (Hsp40) homolog, subfamily C (DNAJC3)	2
Paraspeckle component 1	2
Heat shock 70 kD protein 1B (HSPA1B)	2
Homocysteine-inducible, endoplasmic reticulum stress-inducible, ubiquitin-like domain member (HERPUD1)	2
Serum/glucocorticoid regulated kinase family, member 3 (SKG3)	2
DnaJ (Hsp40) homolog, subfamily B, member 9 (DNAJB9)	2
Arginine-rich, mutated in early stage tumors (ARMET)	2
Syntaxin 1A (brain) (STX1A)	2
Heat shock 70 kD protein 5 (HSPA5)	2
ADAM metallopeptidase with thrombospondin type 1 motif	2
Heat shock protein 90kDa beta (Grp94), member 1 (HSP90B1)	2

Our studies reveal a number of novel genes induced by asbestos in LP9/TERT-1 cells. As previously described in a lung epithelial cell line (C10) or mouse lungs after inhalation of crocidolite asbestos (28), increases in expression of the early response gene, *FOSB*, that encodes a dimer of the activator protein-1 transcription factor, were seen. Increases in expression of several other genes linked to cell signaling proteins and transcription factor activation were observed in asbestos-exposed cells, including *NR4A2* and *PDK4*. A novel gene up-regulated at all time points and concentrations of asbestos or talc in human mesothelial cells was activating transcription factor 3 (*ATF3*), a member of the cAMP-responsive element–binding (CREB) transcription factor family that encodes two different isoforms leading to repression or activation of genes. Silencing of *ATF3* in the present study by siRNA significantly altered expression of a number of asbestos-induced inflammatory cytokines and growth factors documented in malignant mesotheliomas (29, 30). In support of our results here, other studies using *ATF3*-deficient mice and *in vitro* approaches have shown that *ATF3* is a negative regulator of pulmonary inflammation, eosinophilia, and airway responsiveness (31). Moreover, *ATF3* also negatively regulates IL-6 gene transcription in an NF-κB model of up-regulation using melanoma cells (32). In addition, trends in production of VEGF, a known important angiogenic peptide and independent prognostic factor in human mesotheliomas (33), were observed. We have recently shown that an extracellular signal–related

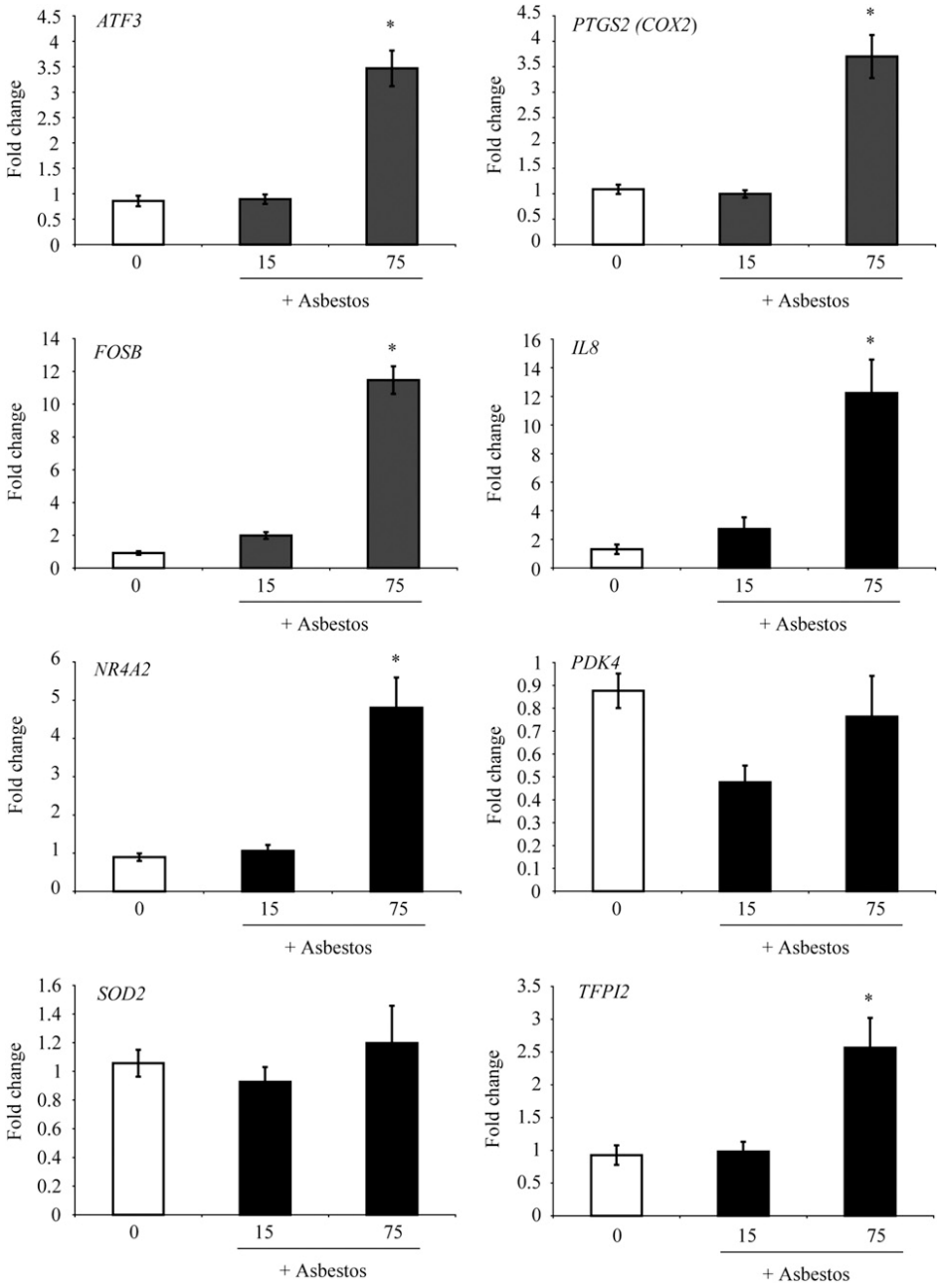

Figure 5. QRT-PCR confirms that human primary pleural mesothelial cells (NYU474) show similar patterns of asbestos-induced gene expression when compared with LP9/TERT-1 mesothelial cells. NYU474 cells were exposed to crocidolite asbestos (15 or 75 $\mu m^2/cm^2$) for 24 hours and cDNA was used for QRT-PCR. *$P \leqslant 0.05$ as compared with untreated cells (0).

CREB pathway in C10 lung epithelial cells modulates apoptosis after asbestos exposure (34), and recent studies are focusing on the effects of silencing *CREB* or *ATF3* on other functional and phenotypic changes in human mesothelial and mesothelioma cells (A. Shukla and colleagues, unpublished data).

Several other genes up-regulated by talc at 8 hours or affected by asbestos at both 8 and 24 hours may be important in repair from mineral-induced responses. For example, *SOD2*, (Mn-containing superoxide dismutase) is an antioxidant protein occurring in the mitochondria, a target cell organ of asbestos-induced apoptosis (35). *PTGS2* (prostaglandin-endoperoxide syntase or cyclooxygenase) is a key enzyme in prostenoid biosynthesis associated with modulation of mitogenesis and infiammation. More recently, this pathway has been explored after interaction of ultrafine particles with alveolar macrophages (9). *ANG PTL4* (angiopoietin-4) encodes a serum hormone directly involved in regulating glucose homeostasis and lipid metabolism and is an apoptosis survival factor for vascular endothelial cells. The up-regulation of angiopoietin-4 is also thought to play a role in inhibition of tumor cell motility and metastasis. *KLF4* (Kruppel-like factor 4) is a negative regulator of cell proliferation and can be a positive or negative modulator of DNA transcription.

Increased expression of genes encoding different cytokines/chemokines (i.e., *IL8*) and their receptors or ligands (e.g., IL-8 C-terminal variant, *IL1R1*, *CXCL2* or *MIP2*, *CXCL3*, and *TFP12*) by asbestos or talc suggests that the mesothelial cell also may play a role in chemotaxis, infiammation, and blood coagulation. A number of gene expression changes by asbestos also support the hypothesis that this fibrous mineral affects calcium-dependent processes including related protein kinase cascades, cell adhesion, and protein/lipid metabolism (Table 2). Although numbers of changes were more modest in IOSE cells, with the exception of *NR4A2* and *CXCL2*, a unique subset of genes was induced by asbestos in this cell type (Table 4).

Results of work here suggest that transcriptional profiling can be used to reveal molecular events by mineral dusts that are

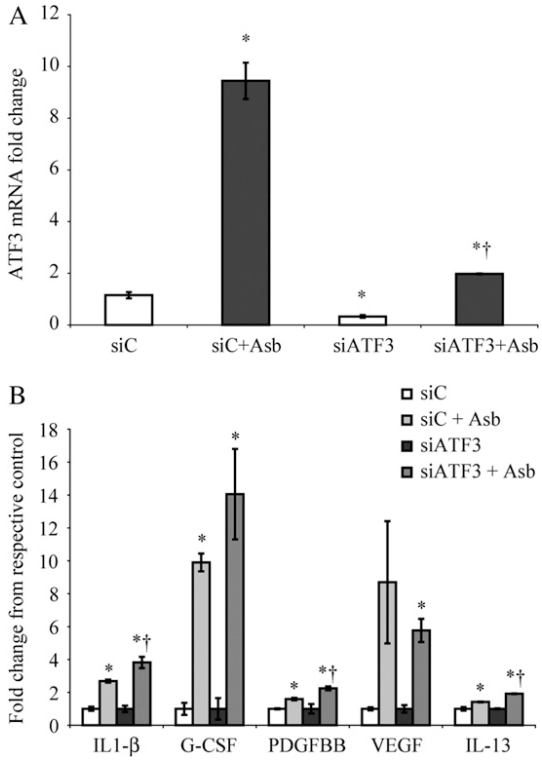

Figure 6. *ATF3* inhibition using siRNA approaches alters asbestos-induced production of infiammatory cytokines and growth factors. (*A*) LP9/TERT-1 cells transfected with siATF3 show significant inhibition of *ATF3* mRNA levels (untreated control [siC] versus siATF3 and asbestos-treated [siC Asb versus siATF3 Asb] groups). *$P \leqslant 0.05$ as compared with siC; †$P \leqslant 0.05$ as compared with siC Asb group. (*B*) siATF3 altered asbestos-induced cytokine levels as detected in medium at 24 hours using Bio-Plex analyses. *$P \leqslant 0.05$ as compared with control groups (siC and siATF3), respectively; †$P \leqslant 0.05$ as compared with asbestos-exposed scrambled control group (siC).

predictive of their pathogenicity in mesothelioma. Moreover, they reveal early and novel gene responses, including calcium-dependent transcription factors and antioxidant enzymes that may be pursued for their functional significance using RNA silencing or other approaches.

Conflict of Interest Statement: B.T.M. received support by EUROTALC and The Industrial Minerals Association (IMA) (11/1/05–10/31/06) for $90,000 for research. None of the other authors has a financial relationship with a commercial entity that has an interest in the subject of this manuscript.

Acknowledgments: The authors thank the Vermont Cancer Center DNA Analysis Facility for performing oligonucleotide microarray and real-time quantitative PCR, and Gary Tomiano (Minteg International, Inc./Specialty Minerals, Inc., Easton, PA) for talc characterization.

References

1. Mossman BT, Gee JB. Asbestos-related diseases. *N Engl J Med* 1989; 320:1721–1730.
2. Mossman BT, Churg A. Mechanisms in the pathogenesis of asbestosis and silicosis. *Am J Respir Crit Care Med* 1998;157:1666–1680.
3. Robinson BW, Lake RA. Advances in malignant mesothelioma. *N Engl J Med* 2005;353:1591–1603.
4. Mossman BT, Bignon J, Corn M, Seaton A, Gee JB. Asbestos: scientific developments and implications for public policy. *Science* 1990;247: 294–301.
5. Dickson MA, Hahn WC, Ino Y, Ronfard V, Wu JY, Weinberg RA, Louis DN, Li FP, Rheinwald JG. Human keratinocytes that express hTERT and also bypass a p16(INK4a)-enforced mechanism that limits life span become immortal yet retain normal growth and differentiation characteristics. *Mol Cell Biol* 2000;20:1436–1447.
6. Choi JH, Choi KC, Auersperg N, Leung PC. Overexpression of follicle-stimulating hormone receptor activates oncogenic pathways in pre-neoplastic ovarian surface epithelial cells. *J Clin Endocrinol Metab* 2004;89:5508–5516.
7. Merritt MA, Green AC, Nagle CM, Webb PM. Talcum powder, chronic pelvic infiammation and NSAIDs in relation to risk of epithelial ovarian cancer. *Int J Cancer* 2008;122:170–176.
8. Mossman BT, Shukla A, Fukagawa NK. Highlight Commentary on "Oxidative stress and lipid mediators induced in alveolar macrophages by ultrafine particles". *Free Radic Biol Med* 2007;43:504–505.
9. Beck-Speier I, Dayal N, Karg E, Maier KL, Schumann G, Schulz H, Semmler M, Takenaka S, Stettmaier K, Bors W, *et al.* Oxidative stress and lipid mediators induced in alveolar macrophages by ultrafine particles. *Free Radic Biol Med* 2005;38:1080–1092.
10. Oberdorster G, Ferin J, Gelein R, Soderholm SC, Finkelstein J. Role of the alveolar macrophage in lung injury: studies with ultrafine particles. *Environ Health Perspect* 1992;97:193–199.
11. Brown DM, Wilson MR, MacNee W, Stone V, Donaldson K. Size-dependent proinfiammatory effects of ultrafine polystyrene particles: a role for surface area and oxidative stress in the enhanced activity of ultrafines. *Toxicol Appl Pharmacol* 2001;175:191–199.
12. Donaldson K, Tran CL. Infiammation caused by particles and fibers. *Inhal Toxicol* 2002;14:5–27.
13. Health Effects Institute - Asbestos Research. Asbestos in public and commercial buildings: a literature review and synthesis of current knowledge. Cambridge, MA: The Health Effects Institute; 1991.
14. Sabo-Attwood T, Ramos-Nino M, Bond J, Butnor KJ, Heintz N, Gruber AD, Steele C, Taatjes DJ, Vacek P, Mossman BT. Gene expression profiles reveal increased mClca3 (Gob5) expression and mucin production in a murine model of asbestos-induced fibrogenesis. *Am J Pathol* 2005;167:1243–1256.
15. Campbell WJ, Huggins CW, Wylie AG. Chemical and physical characterization of amosite, chrysotile, crocidolite, and nonfibrous tremolite for oral ingestion studies Washington, DC: National Institute of Environmental Health Sciences; 1980. No. 8542.
16. Blumen SR, Cheng K, Ramos-Nino ME, Taatjes DJ, Weiss DJ, Landry CC, Mossman BT. Unique uptake of acid-prepared mesoporous spheres by lung epithelial and mesothelioma cells. *Am J Respir Cell Mol Biol* 2007;36:333–342.
17. Shukla A, Lounsbury KM, Barrett TF, Gell J, Rincon M, Butnor KJ, Taatjes DJ, Davis GS, Vacek P, Nakayama KI, *et al.* Asbestos-induced peribronchiolar cell proliferation and cytokine production are attenuated in lungs of protein kinase C-delta knockout mice. *Am J Pathol* 2007;170:140–151.
18. Steiner G, Suter L, Boess F, Gasser R, de Vera MC, Albertini S, Ruepp S. Discriminating different classes of toxicants by transcript profiling. *Environ Health Perspect* 2004;112:1236–1248.
19. Lechner JF, Tokiwa T, LaVeck M, Benedict WF, Banks-Schlegel S, Yeager H Jr, Banerjee A, Harris CC. Asbestos-associated chromosomal changes in human mesothelial cells. *Proc Natl Acad Sci USA* 1985;82:3884–3888.
20. Nymark P, Lindholm PM, Korpela MV, Lahti L, Ruosaari S, Kaski S, Hollmen J, Anttila S, Kinnula VL, Knuutila S. Gene expression profiles in asbestos-exposed epithelial and mesothelial lung cell lines. *BMC Genomics* 2007;8:62.
21. Cacciotti P, Barbone D, Porta C, Altomare DA, Testa JR, Mutti L, Gaudino G. SV40-dependent AKT activity drives mesothelial cell transformation after asbestos exposure. *Cancer Res* 2005;65:5256–5262.
22. Davis JM, Addison J, Bolton RE, Donaldson K, Jones AD, Smith T. The pathogenicity of long versus short fibre samples of amosite asbestos administered to rats by inhalation and intraperitoneal injection. *Br J Exp Pathol* 1986;67:415–430.
23. Stanton MF, Layard M, Tegeris A, Miller E, May M, Morgan E, Smith A. Relation of particle dimension to carcinogenicity in amphibole asbestoses and other fibrous minerals. *J Natl Cancer Inst* 1981;67:965–975.
24. Guthrie GD Jr, Mossman BT. Health effects of mineral dusts. Washington, DC: Mineralogical Society of America; 1993.
25. IARC. Silica and some silicates. *IARC Monogr Eval Carcinog Risk Chem Hum* 1987;42:185.
26. Mossman B, Light W, Wei E. Asbestos: mechanisms of toxicity and carcinogenicity in the respiratory tract. *Annu Rev Pharmacol Toxicol* 1983;23:595–615.
27. Janssen YM, Heintz NH, Mossman BT. Induction of c-fos and c-jun proto-oncogene expression by asbestos is ameliorated by N-acetyl-L-cysteine in mesothelial cells. *Cancer Res* 1995;55:2085–2089.

28. Ramos-Nino ME, Heintz N, Scappoli L, Martinelli M, Land S, Nowak N, Haegens A, Manning B, Manning N, MacPherson M, *et al.* Gene profiling and kinase screening in asbestos-exposed epithelial cells and lungs. *Am J Respir Cell Mol Biol* 2003;29:S51–S58.
29. Yoshimoto A, Kasahara K, Saito K, Fujimura M, Nakao S. Granulocyte colony-stimulating factor-producing malignant pleural mesothelioma with the expression of other cytokines. *Int J Clin Oncol* 2005;10:58–62.
30. Vogelzang NJ, Herndon JE II, Miller A, Strauss G, Clamon G, Stewart FM, Aisner J, Lyss A, Cooper MR, Suzuki Y, *et al.* High-dose paclitaxel plus G-CSF for malignant mesothelioma: CALGB phase II study 9234. *Ann Oncol* 1999;10:597–600.
31. Gilchrist M, Henderson WR Jr, Clark AE, Simmons RM, Ye X, Smith KD, Aderem A. Activating transcription factor 3 is a negative regulator of allergic pulmonary infiammation. *J Exp Med* 2008;205:2349–2357.
32. Karst AM, Gao K, Nelson CC, Li G. Nuclear factor kappa B subunit p50 promotes melanoma angiogenesis by upregulating interleukin-6 expression. *Int J Cancer* 2009;124:494–501.
33. Demirag F, Unsal E, Yilmaz A, Caglar A. Prognostic significance of vascular endothelial growth factor, tumor necrosis, and mitotic activity index in malignant pleural mesothelioma. *Chest* 2005;128: 3382–3387.
34. Barlow CA, Barrett TF, Shukla A, Mossman BT, Lounsbury KM. Asbestos-mediated CREB phosphorylation is regulated by protein kinase A and extracellular signal-regulated kinases 1/2. *Am J Physiol Lung Cell Mol Physiol* 2007;292:L1361–L1369.
35. Shukla A, Stern M, Lounsbury KM, Flanders T, Mossman BT. Asbestos-induced apoptosis is protein kinase C delta-dependent. *Am J Respir Cell Mol Biol* 2003;29:198–205.

Exhibit 94

PHYTOTHERAPY RESEARCH
Phytother. Res. **21**, 579 586 (2007)
Published online 14 March 2007 in Wiley InterScience
(www.interscience.wiley.com) **DOI**: 10.1002/ptr.2117

Pycnogenol reduces Talc-induced Neoplastic Transformation in Human Ovarian Cell Cultures

Amber R. Buz Zard* and Benjamin H. S. Lau

Department of Biochemistry and Microbiology, School of Medicine, Loma Linda University, Loma Linda, CA 92350, USA

Talc and poor diet have been suggested to increase the risk of developing ovarian cancer; which can be reduced by a diet rich in fruit and vegetables. Talc is ubiquitous despite concern about its safety, role as a possible carcinogen and known ability to cause irritation and inflammation. It was recently shown that Pycnogenol (Pyc; a proprietary mixture of water-soluble bioflavonoids extracted from French maritime pine bark) was selectively toxic to established malignant ovarian germ cells. This study investigated talc-induced carcinogenesis and Pyc-induced chemoprevention. Normal human epithelial and granulosa ovarian cell lines and polymorphonuclear neutrophils (PMN) were treated with talc, or pretreated with Pyc then talc. Cell viability, reactive oxygen species (ROS) generation and neoplastic transformation by soft agar assay were measured. Talc increased proliferation, induced neoplastic transformation and increased ROS generation time-dependently in the ovarian cells and dose-dependently in the PMN. Pretreatment with Pyc inhibited the talc-induced increase in proliferation, decreased the number of transformed colonies and decreased the ROS generation in the ovarian cells. The data suggest that talc may contribute to ovarian neoplastic transformation and Pyc reduced the talc-induced transformation. Taken together, Pyc may prove to be a potent chemopreventative agent against ovarian carcinogenesis. Copyright © 2007 John Wiley & Sons, Ltd.

Keywords: ovarian cancer; talc; Pycnogenol ; human neutrophils.

INTRODUCTION

Ovarian cancer is the sixth most commonly occurring cancer and ranks fifth in cancer deaths among women, accounting for more deaths than any other cancer of the female reproductive system. Epidemiological studies have suggested that diet, talc, industrial pollutants, smoking, asbestos and infectious agents may increase the risk of developing ovarian cancer (American Cancer Society, 2000) and may do so by causing localized inflammation (Ness and Cottreau, 1999). Specifically, talc exposure has been cited as a risk factor because of its similarity to asbestos (Cramer *et al.*, 1999).

Talc is a layered magnesium silicate [$Mg_3Si_4O_{10}(OH)_2$]. It is used in cosmetics (as the primary ingredient in talcum powder), pharmaceuticals (as an excipient in tablets) and in many other industrial applications (Bremmell and Addai-Mensah, 2005). Talc is used medically to induce pleurodesis because of its known ability to cause irritation and inflammation (Holthouse and Chleboun, 2001). Animal studies showed a systemic migration of talc particles to various organs despite route of entry (Henderson *et al.*, 1986; Werebe *et al.*, 1999). Exposure of rat ovaries to talc leads to cyst formation (Hamilton *et al.*, 1984). Talc was also shown to cause superoxide anion generation and release from murine macrophages (Van Dyke *et al.*, 2003). Thus controversy continues to surround the topic of talc, its safety (Janssen, 2004) and its role as a possible carcinogen (Cramer *et al.*, 1999; Wong *et al.*, 1999).

Lifestyle factors are important in the etiology of ovarian cancer and current evidence suggests the risk can be reduced by eating a diet rich in fruit and vegetables, among other lifestyle choices (Hanna and Adams, 2006). For the past 20 years, researchers have proposed that nutritional factors play one of the most important roles in the etiology of human cancer. It is estimated that 35% (range 10 70%) of all cancers are diet related and that consumption of certain fruits and vegetables is inversely associated with the incidence of specific forms of cancer. Past research has indicated that a large number of bioactive components, which proved to be protective on different stages of cancer formation, have been identified in nutrients that are of plant origin (Knasmuller and Verhagen, 2002).

Pycnogenol (Pyc) is a proprietary mixture of water-soluble bioflavonoids extracted from the bark of French maritime pine (*Pinus maritima* Aiton; currently known as *Pinus pinaster* Aiton). The main constituents of Pyc are phenolic compounds, broadly divided into monomers (catechin, epicatechin and taxifolin) and condensed flavonoids (classified as procyanidins and proanthocyanidins). Pyc is known to possess potent antioxidant activity, it not only scavenges the free radicals but it also enhances the endogenous antioxidant systems (Nelson *et al.*, 1998; Wei *et al.*, 1997). Pyc has also been shown to selectively induce apoptosis in breast cancer cells (Huynh and Teel, 2000) and induce differentiation and apoptosis in human promyeloid leukemia cells (Huang *et al.*, 2005). It was previously

* Correspondence to: Dr Amber R. Buz Zard, Department of Biochemistry and Microbiology, School of Medicine, Loma Linda University, Loma Linda, CA 92350, USA.
E-mail: abuzzard03b@llu.edu
Contract/grant sponsor: Horphag Research, Geneva, Switzerland.

Received 4 October 2006
Revised 1 January 2007
Accepted 8 January 2007

shown that Pyc selectively induced cell death in established malignant ovarian germ cells *in vitro* (Buz Zard and Lau, 2004). This study now reports that Pyc prevents talc-induced neoplastic transformation of normal ovarian cells, *in vitro*.

MATERIALS AND METHODS

Reagents and chemicals. Pycnogenol was supplied by Horphag Research (Geneva, Switzerland). Talc, crystal violet, Giemsa stain, RPMI-1640 medium and other miscellaneous chemicals were purchased from Sigma (St Louis, MO). Polymorphoprep™ was purchased from Greiner Bio-One, Inc. (Longwood, FL). Dulbecco s modification of Eagle's Medium (DMEM), Ham's F-12 medium and penicillin streptomycin (P-S) were purchased from Cellgro (Herndon, VA). Fetal bovine serum (FBS) was purchased from HyClone (Logan, UT). The CellTiter 96 AQueous One Solution Cell Proliferation Assay was purchased from Promega (Madison, WI). High strength analytical grade agarose was purchased from Bio-Rad (Hercules, CA). Ionagar No. 2 was purchased from Oxoid (London, UK). 5-(and-6)-Carboxy-2′,7′-dichlorodihydrofluorescein diacetate (carboxy-H_2DCFDA) was purchased from Molecular Probes (Carlsbad, CA).

Water soluble extraction of Pycnogenol . Pyc was incubated at 56 C for 5 h in double distilled water, allowed to cool to room temperature and filtered using a Steriflip Vacuum Filtration System (0.22 µm Durapore PVDF membrane; Millipore Corporation, Bedford, MA).

Cell culture and treatments. Two cell cultures of human origin were maintained at 37 °C in a humidified atmosphere containing 5% CO_2. OSE2a (immortalized normal ovarian epithelial) and GC1a (immortalized normal ovarian granulosa) cell cultures were donated by Dr Hitoshi Okamura at Kumamoto University, Japan (Okamura *et al.*, 2003). The cell lines were maintained in a 1:1 mixture of DMEM and Ham s F-12 medium supplemented with 10% FBS and 100 IU/mL P-S. In preparation for either talc or Pyc + talc treatments, each cell line was seeded (1×10^5 cells/ml) and grown to 80% confluence, unless otherwise specified. Cells were incubated with 0 500 µg/mL talc from 24 to 120 h; or 0 500 µg/mL Pyc for 24 h followed by 5 µg/mL talc for 24 or 72 h.

Neutrophil isolation and culture. Peripheral blood polymorphonuclear neutrophils (PMN) and monocytes were obtained from heparinized venous blood from healthy volunteers (protocol approved by Loma Linda University Institutional Review Board for Human Studies) and isolated by Polymorphoprep™ density gradient centrifugation followed by the hypotonic lysis of erythrocytes. The purity of PMNs was determined by Giemsa staining as greater than 95%. Purified cells were suspended at 5×10^5 cells/mL in RPMI-1640 containing 2 mM L-glutamine, 1 mM sodium pyruvate, supplemented with 10% FBS and 100 IU/mL P-S; and treated with varying concentrations of talc for 24 or 72 h. ROS generation was detected as detailed below.

Cell viability assay. The CellTiter 96 AQueous One Solution Cell Proliferation Assay was used to measure cell viability (Buz Zard and Lau, 2004). The MTS [3-(4,5-dimethylthiazolyl-2-yl)-5-(3-carboxymethoxyphenyl)-2-(4-sulfophenyl)-2H-tetrazolium, inner salt] solution was used according to manufacturer s instructions. The absorbance was read at 490 nm using a model 3550 Microplate Reader (Bio-Rad). The percent cell viability was calculated as the absorbance of the treated cells divided by the absorbance of the untreated-control cells multiplied by 100.

Neoplastic transformation assay. A characteristic of cancer cells is their ability to grow and to divide when held in suspension without attachment or with minimal attachment to a rigid surface (Leung *et al.*, 2004). Thus, growth in soft agar demonstrates *in vitro* transformation of cells to their neoplastic counterparts (Morales *et al.*, 2003). After 72 h of incubation in the presence of talc; or in the presence of 0 500 µg/mL Pyc for 24 h followed by 5 µg/mL talc for 72 h, cells were collected, washed and suspended in 0.35% agarose at 5000 cells/well and layered on top of a base of 0.5% agar. The plates were incubated at 37 °C in a humidified incubator for 14 days. The cells were stained with 0.005% crystal violet and colonies were counted using an inverted microscope (Cory *et al.*, 1987).

Reactive oxygen species (ROS) detection. Carboxy-H_2DCFDA is a non-fluorescent dye that permeates the cells where it is deacetylated by viable cells to 2′,7′-dichlorofluorescin (DCFH), which is then oxidized to fluorescent 2′,7′-dichlorofluorescein (DCF) by endogenous hydrogen peroxide (H_2O_2) (Wan *et al.*, 1993). The cells were seeded in Optilux™ 96-well plates (BD Falcon, Bedford, MA) and treated with 0 to 500 µg/mL Pyc for 24 h. H_2O_2 (100 µM) was used as a positive control. Carboxy-H_2DCFDA (5 µM) was added and incubated for 1 h. The fluorescence intensity (excitation 485 nm/emission 530 nm) was measured as arbitrary fluorescent units (AFU) using a model 7600 Microplate Fluorometer (Cambridge Technology, Inc., Watertown, MA). The percent AFU (a.k.a. % ROS generation) was calculated as the treated cell-AFU divided by the untreated cell-AFU multiplied by 100. Immediately following the fluorescence detection, the fluorescence intensity was normalized by the cell viability assay.

Statistical analysis. Data were reported as mean ± SE. Statistical analysis was performed with the Student s paired *t*-test.

RESULTS

All experiments were performed a minimum of three times with reproducible results.

Effect of talc on cell viability of normal ovarian cells

Talc caused a bell-shaped curve response in OSE2a cells, with a statistically significant increase seen at 5 µg/mL (24 h) and a statistically significant decrease at 200 µg/mL (72 h) and 500 µg/mL (24 and 72 h) (Fig. 1).

DOI: 10.1002/ptr

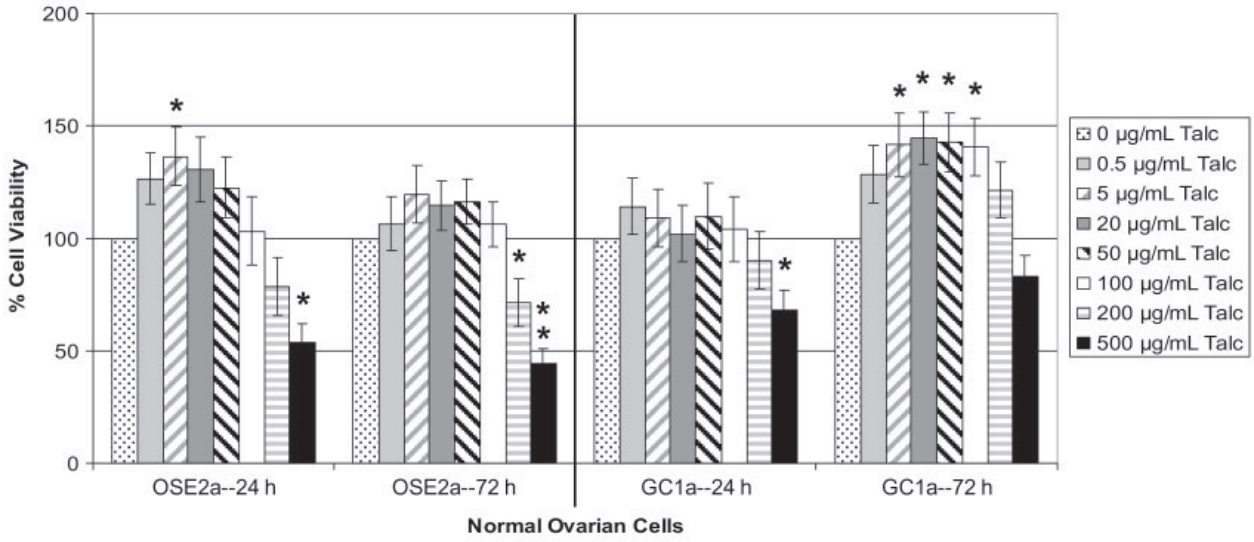

Figure 1. Effect of talc on the cell viability of ovarian cells. Normal ovarian epithelial (OSE2a) and normal ovarian stromal (GC1a) cells were treated with various concentrations of talc for 24 and 72 h. Cell viability was measured by the MTS assay and the percent cell viability was calculated as the absorbance of the treated cell divided by the absorbance of the untreated-control cells multiplied by 100. Each data point represents mean ± SE of five determinations. Statistical significance was determined by the Student's paired *t*-test. * $p < 0.05$, ** $p < 0.01$ comparing the treatment with the respective untreated control.

Also seen in Fig. 1, talc caused a bell-shaped curve response in GC1a cells, with a statistically significant increase seen at 5, 20, 50 and 100 µg/mL (72 h) and a statistically significant decrease at 500 µg/mL (24 h).

Effect of talc on neoplastic transformation of normal ovarian cells

Since the ability to grow suspended in soft agar is a characteristic of cells being transformed to their neoplastic counterparts (Leung *et al.*, 2004; Morales *et al.*, 2003), the study determined whether talc would be able to induce such a transformation. As shown in Fig. 2, talc caused a statistically significant increase in the number of transformed colonies in the OSE2a cells at 5 and 20 µg/mL talc and in the GC1a cells at 5, 20 and 100 µg/mL talc, compared with the untreated control. An exception was seen in the 100 µg/mL talc treatment in the OSE2a cells in which the number of transformed colonies was reduced significantly.

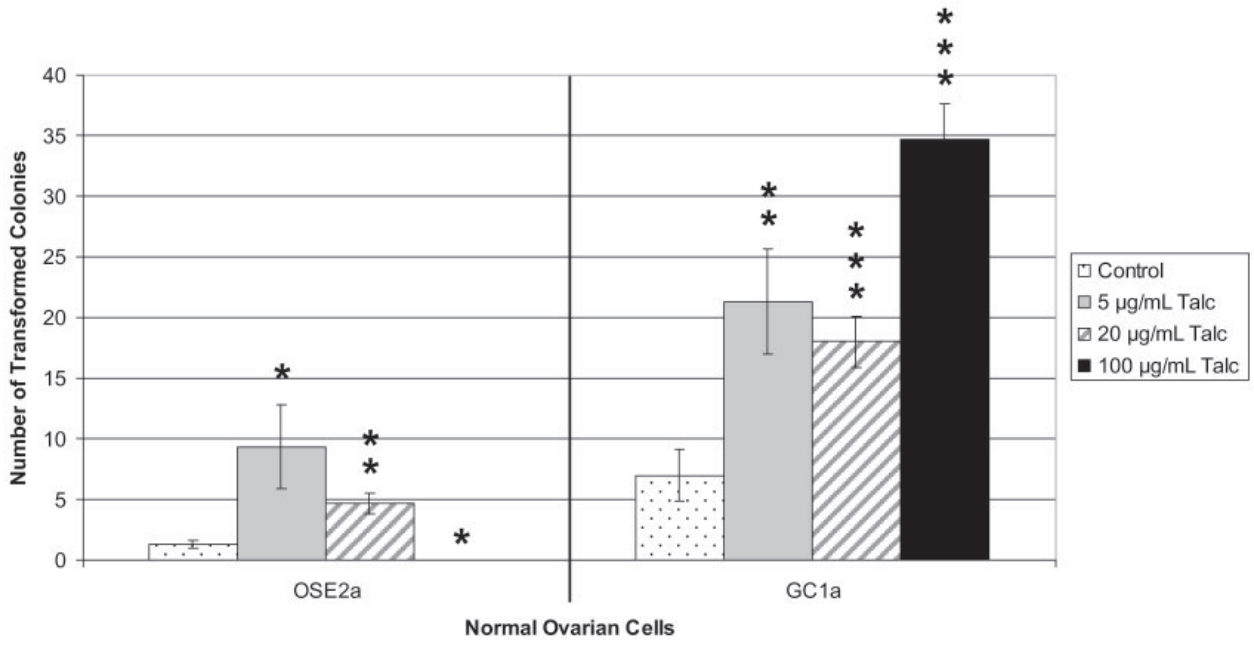

Figure 2. Neoplastic transformation of ovarian cells by talc. Normal ovarian epithelial (OSE2a) and normal ovarian stromal (GC1a) cells were incubated with various concentrations of talc for 72 h, collected, washed, seeded in soft agar suspension and grown for 14 days before colonies were counted. Each data point represents mean ± SE of three determinations. Statistical significance was determined by the Student's paired *t*-test. * $p < 0.05$, ** $p < 0.01$ and *** $p < 0.001$ comparing the treatment with the respective untreated control (0 µg/mL talc).

DOI: 10.1002/ptr

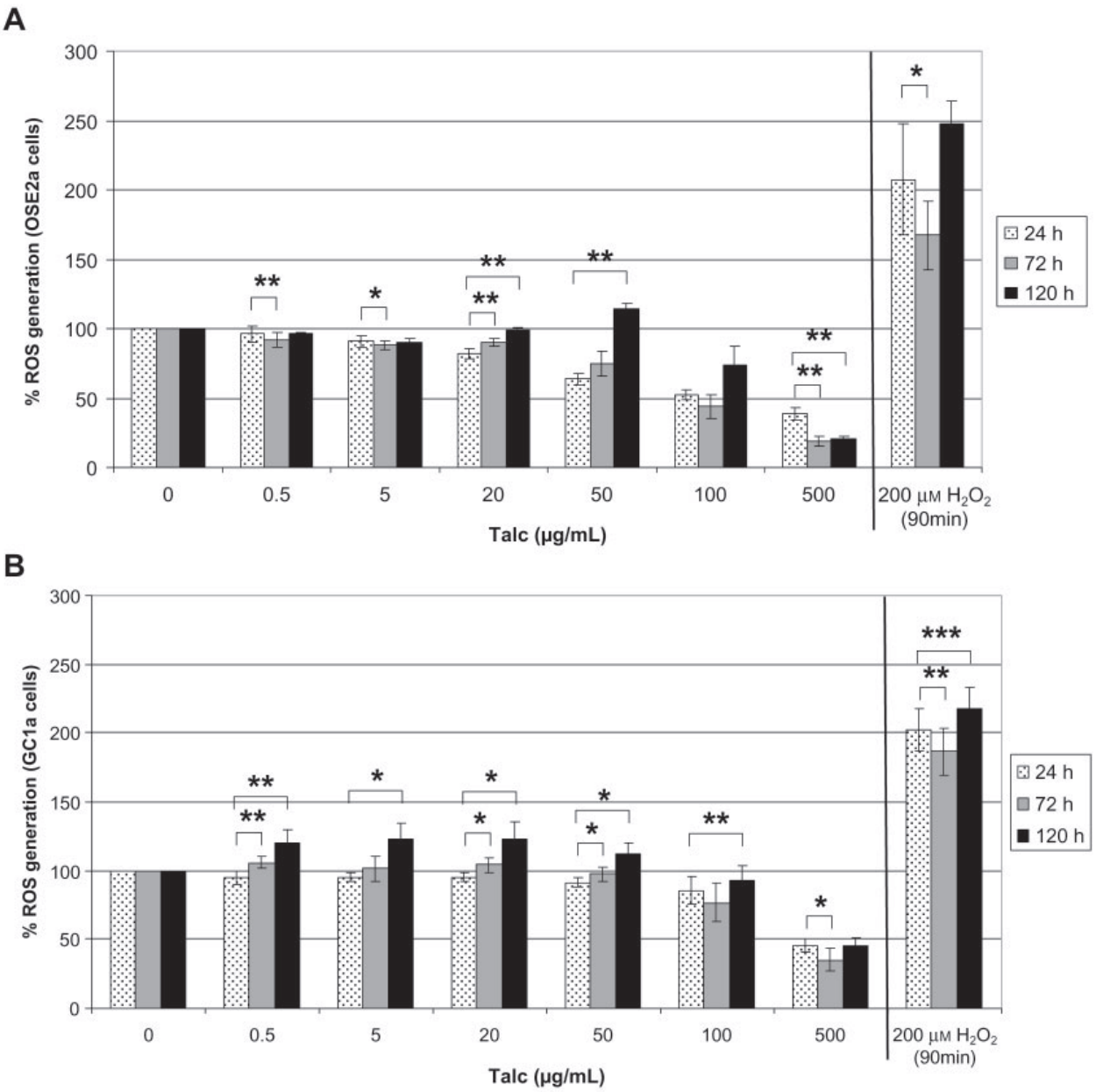

Figure 3. ROS generation of ovarian cells in response to talc treatments. Normal ovarian epithelial (OSE2a) and normal ovarian stromal (GC1a) cells were treated with various concentrations of talc for 24, 72 and 120 h and H_2O_2 during the last 90 min of each respective time point. H_2O_2 was used as a positive control for this assay. Fluorescence intensity were measured as arbitrary fluorescent units (AFU) at ex 485 nm/em 530 nm and normalized with the cell viability assay. Percent AFU (a.k.a. % ROS generation) was calculated as the average AFU of the treated cell divided by the average AFU of the untreated-control cells multiplied by 100. (A) ROS generation in OSE2a cells in response to talc treatments. (B) ROS generation in GC1a cells in response to talc treatments. Each data point represents mean ± SE of three determinations. Statistical significance was determined by the Student's paired *t*-test. * $p < 0.05$, ** $p < 0.01$ and *** $p < 0.001$ comparing the treatment with the respective untreated control (as demonstrated by the horizontal brackets).

Effect of talc on ROS generation in normal ovarian cells

Talc caused an initial dose-dependent decrease in ROS generation (24 h) which increased with time in OSE2a cells (Fig. 3A). However, as time increased, ROS generation rebounded and increased compared with the values at 24 h. A statistically significant increase was seen at 20 µg/mL (72 and 120 h) and 50 µg/mL (120 h). Talc also caused an initial dose-dependent decrease in ROS generation (24 h) in GC1a cells (Fig. 3B), but ROS generation increased with time in the talc treated cells. A statistically significant increase was seen with 0.5, 20 and 50 µg/mL (72 and 120 h), as well as 5 and 100 µg/mL (120 h) compared with the respective 24 h value.

Effect of talc on ROS generation in PMN

Since oxidative stress is often a component of the tumor microenvironment (Valko *et al.*, 2004), the study tested whether talc was capable of inducing ROS generation

DOI: 10.1002/ptr

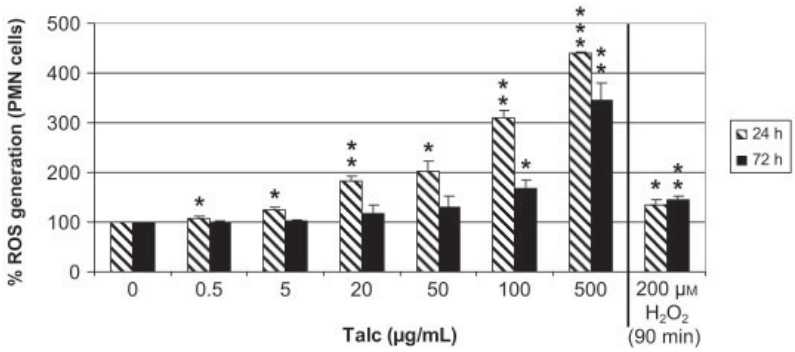

Figure 4. ROS generation of polymorphonuclear neutrophils (PMN) in response to talc treatments. PMNs were treated with various concentrations of talc for 24 and 72 h and H_2O_2 during the last 90 min of each respective time point. H_2O_2 was used as a positive control for this assay. Fluorescence intensity were measured as arbitrary fiuorescent units (AFU) at ex 485 nm/em 530 nm and normalized with the cell viability assay. Percent AFU (a.k.a. % ROS generation) was calculated as the average AFU of the treated cell divided by the average AFU of the untreated-control cells multiplied by 100. ROS generation of PMNs in response to talc treatments. Each data point represents mean ± SE of three determinations. Statistical significance was determined by the Student's paired *t*-test. * $p < 0.05$, ** $p < 0.01$ and *** $p < 0.001$ comparing the treatment with the respective untreated control.

in human PMNs. Talc caused a dose-dependent increase in ROS generation at both time points (Fig. 4). The increase was statistically significant at 0.5, 5, 20, 50 µg/mL (24 h) and 100 and 500 µg/mL (24 and 72 h). The maximum ROS generation was seen at 500 µg/mL and was increased over 4-fold at 24 h and 3.5-fold at 72 h, compared with the respective untreated cells.

Effect of pretreatment with Pyc on talc-induced cell viability changes in normal ovarian cells

Pretreatment with Pyc did not cause a statistically different change in cell viability in the OSE2a cells (Fig. 5A). Pretreatment with Pyc caused a general decrease in cell viability in the GC1a cells (Fig. 5B) compared with the respective untreated GC1a cells. One exception is that of a slight, but statistically significant, increase in cell viability at 100 µg/mL Pyc + 5 µg/mL talc (72 h) compared with the respective untreated GC1a cells (Fig. 5B).

Effect of pretreatment with Pyc on talc-induced neoplastic transformation of normal ovarian cells

Pretreatment with Pyc decreased the number of neoplastically transformed colonies induced by talc in

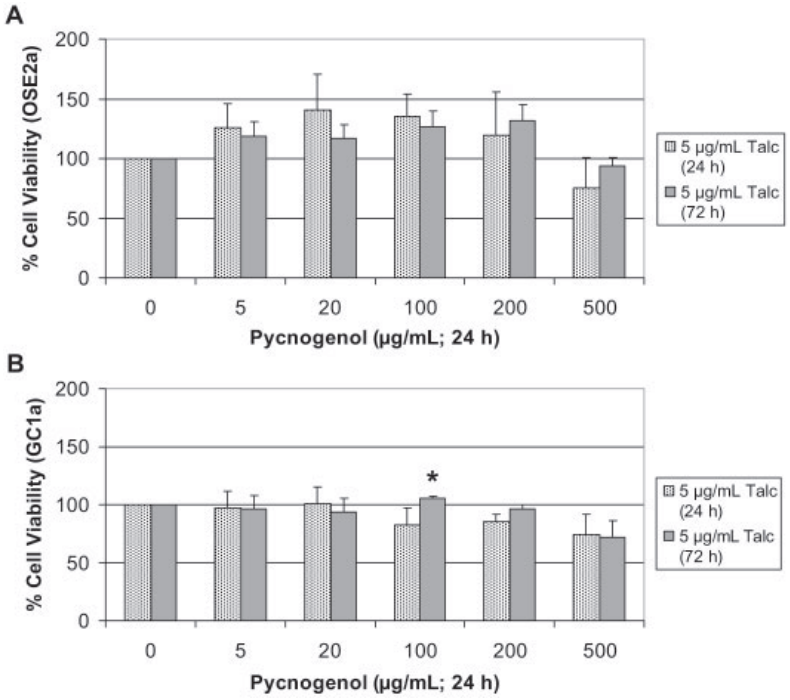

Figure 5. Effect of Pyc + talc treatments on the cell viability of ovarian cells. Normal ovarian epithelial (OSE2a) and stromal (GC1a) cells were treated with 0–500 µg/mL Pyc for 24 h followed by 5 µg/mL talc for 24 and 72 h. Cell viability was measured by the MTS assay and percent cell viability was calculated as the absorbance of the treated cell divided by the absorbance of the untreated-control cells multiplied by 100. (A) OSE2a cells. (B) GC1a cells. Each data represent mean ± SE of four determinations. Statistical significance was determined by the Student's paired *t*-test. * $p < 0.05$ comparing the treatment with the respective untreated control.

DOI: 10.1002/ptr

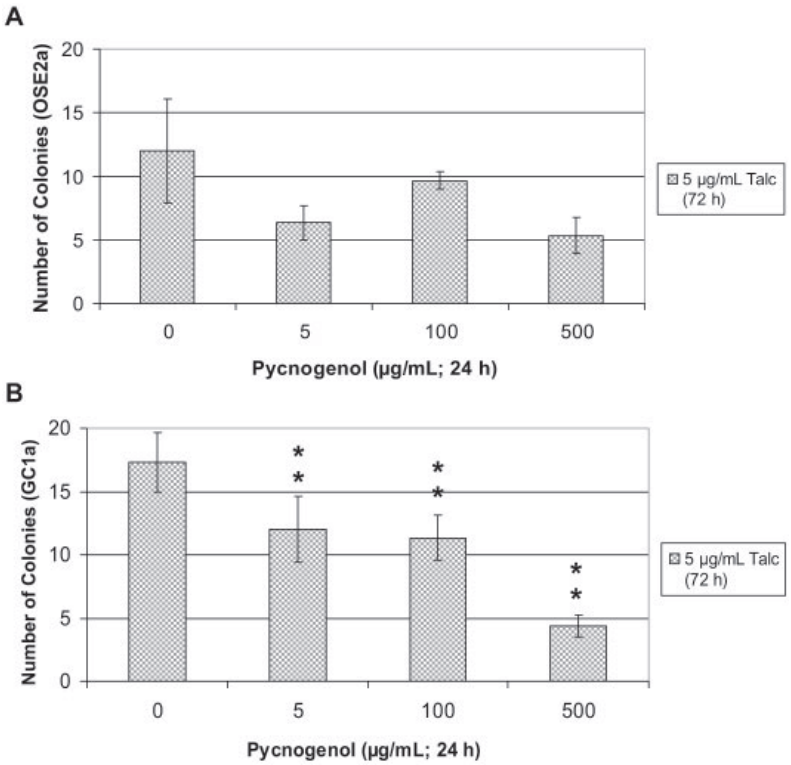

Figure 6. Pyc-induced protection against neoplastic transformation of ovarian cells by talc. Normal ovarian epithelial (OSE2a) and stromal (GC1a) cells were incubated with 0–500 µg/mL Pyc for 24 h followed by 5 µg/mL talc for 72 h, collected, washed, seeded in soft agar suspension and grown for 14 days before colonies were counted. (A) OSE2a cells. (B) GC1a cells. Each data represent mean ± SE of three determinations. Statistical significance was determined by the Student's paired *t*-test. ** $p < 0.01$ comparing the treatment with the respective control.

the OSE2a cells, but not in a statistically significant manner (Fig. 6A). Pretreatment with Pyc (5, 100 and 500 µg/mL; 24 h) caused a statistically significant decrease in the number of talc-induced neoplastically transformed colonies in the GC1a cells (Fig. 6B).

Effect of pretreatment with Pyc on talc-induced ROS generation in normal ovarian cells

Pretreatment with Pyc caused a statistically significant decrease in ROS generation at 5, 20, 50, 100 and 200 µg/mL Pyc + 5 µg/mL talc (24 h); and 500 µg/mL Pyc + 5 µg/mL talc (24 and 72 h) in the OSE2a cells (Fig. 7A). Pretreatment with Pyc caused a statistically significant decrease in ROS generation at 5, 20, 50, 200 and 500 µg/mL Pyc + 5 µg/mL talc (24 h) in the GC1a cells (Fig. 7B). Pretreatment with Pyc caused a statistically significant decrease in ROS generation at 5, 20, 50, 100, 200 and 500 µg/mL Pyc + 5 µg/mL talc (72 h) in the GC1a cells (Fig. 7B). The decrease seen at 100 µg/mL Pyc + 5 µg/mL talc (24 h) was not statistically significant (Fig. 7B).

DISCUSSION

Cancer development is a multi-step process comprising a series of cellular and molecular changes that are mediated by various endogenous and exogenous stimuli, such as aberrantly expressed ROS (Storz, 2005). Although ROS are a byproduct of endogenous biochemical processes, ROS (such as H_2O_2) at high concentrations or expressed in a chronic nature can damage cellular macromolecules and contribute to neoplastic transformation and tumor growth (Nicco *et al.*, 2005). A characteristic of neoplastically transformed cells is their ability to grow and to divide when held in suspension without attachment or with minimal attachment to a rigid surface (Leung *et al.*, 2004; Morales *et al.*, 2003). Our data show that talc not only increased cell viability (Fig. 1A), but also caused an increase in transformed cells in both the stromal and epithelial ovarian cells by their ability to grow, divide and form colonies while being suspended in soft agar (Fig. 2A).

It is known that substances that raise the intracellular level of H_2O_2 are able to trigger normal cell proliferation and abolish tumor cell proliferation (Ness and Cottreau, 1999; Nicco *et al.*, 2005). In normal cells, the basal level of H_2O_2 is low and its increase is initially associated with cell growth. H_2O_2 at high concentrations or expressed in a chronic nature in normal cells, can damage cellular macromolecules and contribute to neoplastic transformation and tumor growth (Nicco *et al.*, 2005). In this study, talc was shown to increase the ROS generation, after an initial suppression, in a time-dependent manner in the normal stromal cells (Fig. 3B) and less strongly in the normal epithelial cells (Fig. 3A).

Recent studies have expanded the concept that inflammation is a critical component of tumor progression. The neoplastic process (proliferation, survival and

DOI: 10.1002/ptr

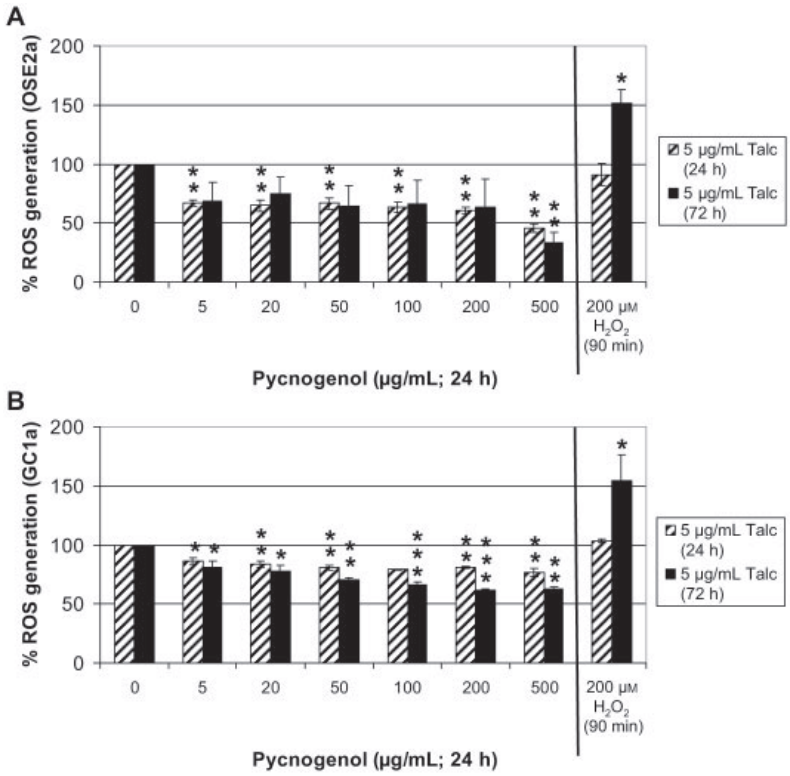

Figure 7. ROS generation of ovarian cells in response to Pyc + talc. Normal ovarian epithelial (OSE2a) and stromal (GC1a) cells were treated with 0–500 µg/mL Pyc for 24 h, followed by 5 µg/mL talc for 24 or 72 h and H_2O_2 (the last 90 min of each time point) as a positive control. Fluorescence intensity (AFU) was measured at ex 485 nm/em 530 nm and normalized by cell viability assay. The percent ROS generation was calculated as the average AFU of treated divided by AFU of untreated-control multiplied by 100. (A) OSE2a cells. (B) GC1a cells. Each data point represents mean ± SE of three determinations. Statistical significance was determined by the Student's paired *t*-test. * $p < 0.05$, ** $p < 0.01$ and *** $p < 0.001$ comparing the treatment with the respective untreated control.

migration) is linked with the tumor microenvironment and synchronized with inflammatory cells (Valko *et al.*, 2004). Polymorphonuclear neutrophils and macrophages are a main source of exogenous ROS in that they release large quantities of ROS in response to a variety of stimuli. This exogenously produced ROS is crucial in the innate immune system of the host for killing invading bacteria but may also be responsible for tissue injury, when expressed excessively or inappropriately (Lewis and Pollard, 2006). Inflammatory cells are prominent in the stromal compartment of virtually all types of malignancy. These highly versatile cells respond to the presence of stimuli in different parts of tumors (Balkwill and Mantovani, 2001). In an *in vitro* study of rat cells, both macrophages and neutrophils were found to be mutagenic in response to alpha-quartz dust, talc and diesel soot; however, neutrophils appeared to have a greater mutagenic effect (Driscoll *et al.*, 1997). This study found that talc not only increased the ROS generation in the ovarian cells (Fig. 3), but also increased the expression of ROS by the neutrophils (Fig. 4).

Talc has been shown to be ubiquitous in our modern environment (Bremmell and Addai-Mensah, 2005) despite concerns raised about its safety (Janssen, 2004), its role as a possible carcinogen (Cramer *et al.*, 1999; Wong *et al.*, 1999), and its known ability to cause irritation and inflammation (Holthouse and Chleboun, 2001). The data show that talc is capable of increasing cell proliferation, inducing neoplastic transformation of both the normal stromal and epithelial ovarian cells *in vitro*; and increasing ROS generation in these cells as well as the PMN cells.

Cancer chemoprevention is regarded as an efficient strategy to prevent cancer. The most useful cancer chemopreventive compounds will have minimal long-term toxicity, while significantly reducing tumor incidence, delaying tumor onset or preventing tumor progression (Kapadia *et al.*, 2003). It was hypothesized that Pyc, shown to induce apoptosis in various malignant cells (Huang *et al.*, 2005; Huynh and Teel, 2000), could prevent talc-induced neoplastic transformation of normal ovarian cells. It was recently shown that Pyc selectively induced cell death in established malignant ovarian germ cells *in vitro* (Buz Zard and Lau, 2004). The present study showed that Pyc was capable of inhibiting the above mentioned talc-induced changes. Pretreatment with Pyc prevented the characteristic talc-induced increase in cell viability of GC1a cells (Fig. 5B). Pretreatment with Pyc was able to decrease the ROS generation compared with the respective controls both in a dose- and time-dependent manner (Fig. 7). The data show that pretreatment with Pyc reduced the number of talc-induced transformed colonies in both cell lines (Fig. 6). In the GC1a cells, the decrease in the number of transformed colonies was statistically significant at all concentrations of Pyc (Fig. 6B).

DOI: 10.1002/ptr

In conclusion, our *in vitro* data suggest that: (1) talc may contribute to ovarian carcinogenesis in humans by way of inducing aberrant ROS generation and (2) Pyc reduces talc-induced neoplastic transformation of ovarian cells. Taken together, Pyc may prove to be a chemopreventative agent against ovarian carcinogenesis.

Acknowledgements

This study was partially supported by a grant from Horphag Research, Geneva, Switzerland (Otherwise, there is no conflict of interest). We thank Dr Hitoshi Okamura for the cell lines. We thank El Chay for his guidance. We thank Vandana Shah, Marsha Yarnell and Christina Wright for their assistance.

REFERENCES

American Cancer Society. 2000. *Ovarian Cancer*, 1–29.

Balkwill F, Mantovani A. 2001. Infiammation and cancer: back to Virchow? *Lancet* **357**: 539–545.

Bremmell KE, Addai-Mensah J. 2005. Interfacial-chemistry mediated behavior of colloidal talc dispersions. *J Colloid Interface Sci* **283**: 385–391.

Buz'Zard AR, Lau BHS. 2004. Selective toxicity of Pycnogenol for malignant ovarian germ cells *in vitro*. *Int J Cancer Prev* **1**: 207–212.

Cory S, Bernard O, Bowtell D, Schrader S, Schrader JW. 1987. Murine c-myc retroviruses alter the growth requirements of myeloid cell lines. *Oncogene Res* **1**: 61–76.

Cramer DW, Liberman RF, Titus-Ernstoff L *et al.* 1999. Genital talc exposure and risk of ovarian cancer. *Int J Cancer* **81**: 351–356.

Driscoll KE, Deyo LC, Carter JM, Howard BW, Hassenbein DG, Bertram TA. 1997. Effects of particle exposure and particle-elicited infiammatory cells on mutation in rat alveolar epithelial cells. *Carcinogenesis* **18**: 423–430.

Hamilton TC, Fox H, Buckley CH, Henderson WJ, Griffiths K. 1984. Effects of talc on the rat ovary. *Br J Exp Pathol* **65**: 101–106.

Hanna L, Adams M. 2006. Prevention of ovarian cancer. *Best Pract Res Clin Obstet Gynaecol* **20**: 339–362.

Henderson WJ, Hamilton TC, Baylis MS, Pierrepoint CG, Griffiths K. 1986. The demonstration of the migration of talc from the vagina and posterior uterus to the ovary in the rat. *Environ Res* **40**: 247–250.

Holthouse DJ, Chleboun JO. 2001. Talc serodesis – report of four cases. *J R Coll Surg Edinb* **46**: 244–245.

Huang WW, Yang JS, Lin CF, Ho WJ, Lee MR. 2005. Pycnogenol induces differentiation and apoptosis in human promyeloid leukemia HL-60 cells. *Leukemia Res* **29**: 685–692.

Huynh HT, Teel RW. 2000. Selective induction of apoptosis in human mammary cancer cells (MCF-7) by pycnogenol. *Anticancer Res* **20**: 2417–2420.

Janssen JP. 2004. Is thoracoscopic talc pleurodesis really safe? *Monaldi Arch Chest Dis* **61**: 35–38.

Kapadia GJ, Azuine MA, Sridhar R *et al.* 2003. Chemoprevention of DMBA-induced UV-B promoted, NOR-1-induced TPA promoted skin carcinogenesis, and DEN-induced phenobarbital promoted liver tumors in mice by extract of beetroot. *Pharmacol Res* **47**: 141–148.

Knasmuller S, Verhagen H. 2002. Impact of dietary factors on cancer causes and DNA integrity: new trends and aspects. *Food Chem Toxicol* **40**: 1047–1050.

Leung DW, Tompkins C, Brewer J *et al.* 2004. Phospholipase C delta-4 overexpression upregulates ErbB1/2 expression, Erk signaling pathway, and proliferation in MCF-7 cells. *Mol Cancer* **3**: 15.

Lewis CE, Pollard JW. 2006. Distinct role of macrophages in different tumor microenvironments. *Cancer Res* **66**: 605–612.

Morales CP, Gandia KG, Ramirez RD, Wright WE, Shay JW, Spechler SJ. 2003. Characterisation of telomerase immortalised normal human oesophageal squamous cells. *Gut* **52**: 327–333.

Nelson AB, Lau BHS, Ide N, Rong Y. 1998. Pycnogenol inhibits macrophage oxidative burst, lipoprotein oxidation and hydroxyl radical-induced DNA damage. *Drug Dev Indust Pharm* **24**: 139–144.

Ness RB, Cottreau C. 1999. Possible role of ovarian epithelial infiammation in ovarian cancer. *J Natl Cancer Inst* **91**: 1459–1467.

Nicco C, Laurent A, Chereau C, Weill B, Batteux F. 2005. Differential modulation of normal and tumor cell proliferation by reactive oxygen species. *Biomed Pharmacother* **59**: 169–174.

Okamura H, Katabuchi H, Ohba T. 2003. What we have learned from isolated cells from human ovary? *Mol Cell Endocrinol* **202**: 37–45.

Storz P. 2005. Reactive oxygen species in tumor progression. *Front Biosci* **10**: 1881–1896.

Valko M, Izakovic M, Mazur M, Rhodes CJ, Telser J. 2004. Role of oxygen radicals in DNA damage and cancer incidence. *Mol Cell Biochem* **266**: 37–56.

Van Dyke K, Patel S, Vallyathan V. 2003. Lucigenin chemiluminescence assay as an adjunctive tool for assessment of various stages of infiammation: a study of quiescent infiammatory cells. *J Biosci* **28**: 115–119.

Wan CP, Myung E, Lau BH. 1993. An automated microfiuorometric assay for monitoring oxidative burst activity of phagocytes. *J Immunol Methods* **159**: 131–138.

Wei ZH, Peng QL, Lau BHS. 1997. Pycnogenol enhances endothelial cell antioxidant defenses. *Redox Rep* **3**: 219–224.

Werebe EC, Pazetti R, Milanez DC, Jr *et al.* 1999. Systemic distribution of talc after intrapleural administration in rats. *Chest* **115**: 190–193.

Wong C, Hempling RE, Piver MS, Natarajan N, Mettlin CJ. 1999. Perineal talc exposure and subsequent epithelial ovarian cancer: a case-control study. *Obstet Gynecol* **93**: 372–376.

Exhibit 95

Cytotoxicity and Apoptosis Induction by Nanoscale Talc Particles from Two Different Geographical Regions in Human Lung Epithelial Cells

Mohd Javed Akhtar,[1,2] Maqusood Ahamed,[3] M. A. Majeed Khan,[3] Salman A. Alrokayan,[3] Iqbal Ahmad,[2] Sudhir Kumar[1]

[1]Fibre Toxicology Division, Indian Institute of Toxicology Research, Lucknow 226001, India

[2]Department of Zoology, University of Lucknow, Lucknow 226007, India

[3]King Abdullah Institute for Nanotechnology, King Saud University, Riyadh 11451, Saudi Arabia

Received 25 October 2012; revised 16 January 2012; accepted 21 January 2012

ABSTRACT: We have characterized the physicochemical properties of nanotalc particles from two different geographical regions and examined their toxicity mechanisms in human lung epithelial (A549) cells. Indigenous nanotalc (IN) of Indian origin and commercial nanotalc (CN) of American origin were used in this study. Physicochemical properties of nanotalc particles were characterized by X-ray diffraction (XRD), transmission electron microscopy (TEM), energy dispersive X-ray spectroscopy (EDS), Brunauer-Emmet-Teller (BET), and dynamic light scattering (DLS). Results showed that both IN and CN particles significantly induce cytotoxicity and alteration in cell cycle phases. Both IN and CN particles were found to induce oxidative stress indicated by induction of reactive oxygen species (ROS), lipid peroxidation, and depletion of antioxidant levels. DNA fragmentation and caspase-3 enzyme activation due to IN and CN particles exposure were also observed. We further showed that after iron chelation, IN and CN particles produce significantly less cytotoxicity, oxidative stress, and genotoxicity to A549 cells as compared with nonchelated particles. In conclusion, this study demonstrated that redox active iron plays significant role in the toxicity of IN and CN particles, which may be mediated through ROS generation and oxidative stress. © 2012 Wiley Periodicals, Inc. Environ Toxicol 29: 394–406, 2014.

Keywords: nanotalc particles; physicochemical characterization; iron chelation; toxicity; apoptosis

INTRODUCTION

Talc is a mineral compound [$Mg_3Si_4O_{10}$ $(OH)_2$] with unique attributes and significant commercial importance. Talc is widely used due to its intrinsic properties such as high thermal stability, low electrical conductivity, good absorption and adsorption properties, and high crystallinity (Pérez-Maqueda et al., 2005; Nkoumbou et al., 2008). Talc is utilized in various applications including paper, paint, cosmetic, plastic, ceramic, pesticide, and pharmaceuticals (Carretero, 2002; Bizi et al., 2003; Petit et al., 2004). Hence, occupational and consumer exposures to talc particles are wide and complex (Jaynes and Zartman, 2005). It has been reported that talc mine workers show higher rates of lung cancer and other respiratory diseases (National Toxicology Program, 1993). Epidemiologic evidence also suggests a possible association between genital use of talcum powder and risk of ovarian cancer (Wild,

Correspondence to: M. Ahamed; e-mail: maqusood@gmail.com or mahamed@ksu.edu.sa

Contract grant sponsor: King Abdulaziz City for Science and Technology (KACST) under the National Plan for Science and Technology (NPST).

Contract grant number: 10-NAN1201-02

Contract grant sponsor: University Grants Commission (UGC), New Delhi, India (to M.J.A.)

Published online 13 February 2012 in Wiley Online Library (wileyonlinelibrary.com). DOI 10.1002/tox.21766

2006; Buz'Zard and Lau, 2007; Gates et al., 2008; Langseth et al., 2008). Talc also appears to induce reactive oxygen species (ROS) generation, oxidative stress, and infiammation (Harlow and Hartge, 1995; Buz'Zard and Lau, 2007).

Due to enhanced intrinsic properties, nanoscale talc particles are extensively utilized in many commercial and industrial products (Akhtar et al., 2008; Balamurugan and Maiti, 2010; Sakthivel and Pitchumani, 2011). Despite the wide-spread applications, there is a serious lack of information concerning the mechanisms of toxicity of nanotalc particles. Previously, we have observed that human cells exposed to nanotalc particles induce oxidative stress-mediated cytotoxicity (Akhtar et al., 2010a). However, physicochemical characterization of nanotalc particles and their association with the toxicological response in human cells is still remains unclear.

There are numerous reports suggesting that ROS is an important mediator of the toxicity of minerals such as asbestos and silica (Aung et al., 2007; Akhtar et al., 2010b). It has been known for years that the surface iron (II) or leachable iron (II) on mineral surfaces reduces molecular oxygen to superoxide anion, which is then dismutated to hydrogen peroxide (Shukla et al., 2003). In the presence of asbestos or silica, hydrogen peroxide and superoxide react via a Fenton reaction and/or Haber–Weiss reaction driven by iron to form the potent hydroxyl radical in vitro leading to cellular oxidative damage (Persson et al., 2003).

The aim of this work was to characterize the physicochemical properties of nanotalc particles and to determine the role of iron in the toxicity mechanisms of nanotalc particles in human lung epithelial (A549) cells. We utilized two types of nanotalc particles from different geographical origins; indigenous nanotalc (IN) of Indian origin and commercial nanotalc (CN) of American origin. Cytotoxicity of IN and CN particles was examined by MTT and LDH assays. Oxidative stress response of IN and CN particles was assessed by measuring reactive oxygen species (ROS), lipid peroxidation (LPO), glutathione (GSH), superoxide dismutase (SOD), and catalase (CAT). Apoptotic response of IN and CN particles was evaluated by cell cycle analysis, DNA fragmentation, and caspase-3 enzyme activity. To explore the role of iron in the toxicity of IN and CN particles, we utilized deferoxamine mesylate (DFOM), a well-known iron chelator. The physicochemical properties of IN and CN particles were characterized by X-ray diffraction (XRD), transmission electron microscopy (TEM), energy dispersive X-ray spectroscopy (EDS), Brunauer-Emmet-Teller (BET), and dynamic light scattering (DLS). The A549 cells, derived from human lung carcinoma, have been widely utilized in toxicological studies (Zhang et al., 2010; Akhtar et al., 2010a,b; Ahamed et al., 2011a,b,c).

MATERIALS AND METHODS

Nanotalc Particles and Reagents

We have utilized the nanotalc particles from two different geographical regions. Indigenous nanotalc (IN) particles were collected from Rajasthan, India, as reported in our previous publication (Akhtar et al., 2010a). American origin commercial nanotalc (CN) particles (size 70–12 nm) were purchased from M.K. Impex (Mississauga, Canada).

Fetal bovine serum (FBS), penicillin-streptomycin, DMEM/F-12 medium, and HBSS were purchased from Invitrogen Co. (Carlsbad, CA). MTT [3-(4,5-dimethylthiazol-2-yl)-2,5 diphenyltetrazolium bromide], 2,7-dichlorofiuorescin diacetate (DCFH-DA), deferoxamine mesylate (DFOM), glutathione (GSH), thiobarbituric acid (TBA), propidium iodide (PI), RNase A, diethylenetriaminepentaacetic acid (DETAPAC), *N*-acetyl-asp-glu-val-asp-7-amido-4-trifiuoromethylcoumarin (Ac-DEVD-AFC), 7-amido-4-trifiuoromethylcoumarin (AFC) standard, Bradford reagent, and bovine serum albumin (BSA) were obtained from Sigma-Aldrich (St. Louis, MO). Apoptotic DNA Ladder Kit was bought from Roche. All other chemicals used were of the highest purity available from commercial sources.

Characterization of Nanotalc Particles

Crystalline nature of both IN and CN particles were examined by taking X-ray diffraction (XRD) pattern at room temperature with the help of PANalytical X'Pert X-ray diffractometer equipped with a Ni filtered using Cu-K_α (λ = 1.54056 Å) radiations as X-ray source. Morphology and size of IN and CN particles were examined by field emission transmission electron microscopy (FETEM) (JEM-2100F, JEOL Inc., Tokyo, Japan) at an accelerating voltage of 200 kV. To check the purity of IN and CN particles, an energy dispersive X-ray spectroscopy (EDS) analysis was performed. Brunauer-Emmet-Teller (BET) surface area measurement of IN and CN particles was determined by multipoint nitrogen adsorption at 77 K using a Beckman Coulter SA3100 device.

Dynamic light scattering (DLS) and laser Doppler velocimetry (LDV) for the characterization of hydrodynamic size and zeta potential (ζ) of IN and CN particles in distilled water and cell culture media were performed on a Malvern Instruments Zetasizer Nano-ZS instrument as described by Murdock et al. (2008).

Treatment of Nanotalc Particles with Deferoxamine Mesylate

We treated both IN and CN particles with DFOM for iron chelation. In brief, IN and CN particles were incubated with 10 mM DFOM at a concentration of 1000 μg/mL for

20 h as described by Aung et al. (2007). Then particles were washed three times with cell culture medium by centrifuging at 4000 rpm for 10 min followed by resuspension.

Cell Culture and Exposure to Nanotalc Particles

Human lung epithelial (A549) cells were obtained from National Centre for Science (NCCS), Pune, India. Cells were used between passages 10 and 20. Cells were cultured in DMEM/F-12 medium supplemented with 10% FBS and 100 U/mL penicillin-streptomycin at 5% CO_2 and 37°C. At 85% confiuence, cells were harvested using 0.25% trypsin and were subcultured into 75 cm^2 fiasks, 6-well plates, or 96-well plates according to selection of experiments. Cells were allowed to attach the surface for 24 h before treatment. IN and CN particles were suspended in cell culture medium and diluted to a appropriate concentration (200 μg/mL). Suspension of nanotalc particles were then sonicated using a sonicator bath at room temperature for 10 min at 40 W to avoid particles agglomeration before administration to the cells. The selection of the 200 μg/mL concentration of nanotalc particles was based on our previous publication (Akhtar et al., 2010a). All the data presented in this study was that of 48 h exposure. Cells not exposed to nanotalc particles served as controls in each experiment.

Cell Viability Assay

Viability of A549 cells after exposure to nanotalc particles was assessed by MTT assay as described by Mossman (1983). The MTT assay assesses the mitochondrial function by measuring ability of viable cells to reduce MTT into blue formazon product. In brief, 10,000 cells per well were seeded in 96-well plate and exposed to IN and CN particles at the concentration of 200 μg/mL for 48 h. After the exposure completed, the medium was removed from each well to avoid interference of particles and replaced with new medium containing MTT solution in an amount equal to 10% of culture volume, and incubated for 3 h at 37°C until a purple colored formazan product developed. The resulting formazan product was dissolved in acidified isopropanol. Further, the 96-well plate was centrifuged at 2500 rpm for 5 min to settle down the remaining particles present in the solution. Then, a 100 μL supernatant was transferred to other fresh wells of 96-well plate and absorbance was measured at 570 by using a microplate reader (FLUOstar-Omega).

Lactate Dehydroganase Leakage Assay

Lactate dehydrogenase (LDH) is an enzyme widely present in cytosol that converts lactate to pyruvate. When plasma membrane integrity is disrupted, LDH leaks into culture media and its extracellular level is elevated. LDH assay was carried out with the method described earlier (Wroblewski and LaDue, 1955; Welder et al., 1991). In brief, 10,000 cells per well were seeded in 96-well plate and exposed to IN and CN particles at the concentration of 200 μg/mL for 48 h. After the exposure completed, the 96-well plate was centrifuged at 2500 rpm for 10 min to get the cell culture media. Then, a 100 μL of culture media transferred to new fresh tube containing 100 μL of sodium pyruvate (2.5 mg/mL phosphate buffer) and 100 μL of reduced nicotinamide adenine dinucleotide (NADH) (2.5 mg/mL phosphate buffer) in a total volume of 3.0 mL (0.1 M potassium phosphate buffer, pH 7.4). The rate of NADH oxidation was determined by following the decrease in absorbance at 340 nm for 3 min at 30-s interval using a spectrophotometer (Thermo-Spectronic).

Cell Cycle Analysis

Cell cycle distribution was assayed by determining DNA content. Cells were treated with IN and CN particles for 48 h. After exposure, cells were fixed in 3% (w/v) paraformaldehyde for 10 min, permeabilized on ice in phosphate buffer saline-0.5% Triton X-100 for 15 min, washed and resuspended in 0.5 ml of phosphate buffer saline containing 1% FBS, 1 mg/ml RNaseA, and 50 μg/ml propidium iodide. The samples were incubated for 30 min at 37°C. The data were acquired and analyzed on FACS-Calibur fiow cytometer (Becton-Dickinson LSR II, San Jose, CA) using Cell Quest 3.3 software.

Measurement of Reactive Oxygen Species

For the measurement of ROS generation, cells were cultured in 12-well plate. The production of intracellular ROS was measured using 2,7-dichlorofiuorescin diacetate (DCFH-DA) (Wang and Joseph, 1999). The DCFH-DA passively enters the cell where it reacts with ROS to form the highly fiuorescent compound dichlorofiuorescein (DCF). Briefiy, 10 mM DCFH-DA stock solution (in methanol) was diluted in culture medium without serum or other additive to yield a 100 μM working solution. After exposure to IN and CN particles, cells were washed twice with HBSS and then incubated in 1 mL working solution of DCFH-DA at 37°C for 30 min. Cells were lysed in alkaline solution and centrifuged at 3000 rpm for 10 min. Then, a 200 μL supernatant (from 12-well plate) was transferred to the fresh well of black 96-well plates and fiuorescence was measured using at 485 nm excitation and 520 nm emission using a microplate reader (FLUOstar-Omega). The values of ROS were expressed as percent of fiuorescence intensity relative to controls.

Membrane Lipid Peroxidation Assay

The extent of membrane lipid peroxidation (LPO) was estimated by measuring the formation of thiobarbituric acid reactive species (TBARS) using the method of Ohkawa et al. (1979). Briefiy, cells were cultured in 75 cm^2 culture fiask and exposed to IN and CN particles at the concentration of 200 μg/mL for 48 h. After the treatment, a 200 μL of cell suspension was mixed with 800 μL of LPO assay cocktail containing TBA (0.4%, w/v), sodium dodecyl sulphate (0.5%, w/v), and acetic acid (5 %, v/v). Reaction mixture was then incubated at 95°C for 1 h. After cooling to room temperature the reaction mixture was centrifuged at 5000 rpm for 5 min. The absorbance of the supernatants was read at 532 nm against the standard. The amount of TBARS was expressed as nmol/mg protein.

Intracellular Glutathione Assay

Intracellular GSH was quantified using the method of Hissin and Hilf (1976). Briefiy, cells were cultured in 75 cm^2 culture fiask and exposed to IN and CN particles at the concentration of 200 μg/mL for 48 h. After the exposure completed, cells were lysed in 20 mM Tris (pH 7.0) and the centrifuged at 10,000 rpm for 10 min at 4°C. Further, protein of the supernatant was precipitated using 1% perchloric acid and again centrifuged at 10,000 rpm for 5 min at 4°C to get supernatant. Then 20 μL of supernatant was mixed with 160 μL of 0.1M potassium phosphate-5 mM EDTA buffer (pH 8.3) and 20 μL *O*-phthalaldehyde (1 mg/mL in methanol) in a black 96-well plate. After 2 h of incubation at room temperature in the dark, fiuorescence was measured at emission wavelength of 460 nm and excitation wavelength of 350 nm. The amount of GSH was expressed as nmol GSH/mg protein.

Antioxidant Enzymes Activity Assay

Cells were cultured in 75 cm^2 culture fiask and exposed to IN and CN particles at the concentration of 200 μg/mL for 48 h. After the exposure completed, cells were harvested in ice-cold phosphate buffer saline and washed twice with phosphate buffer saline at 4°C. The cell pellets were then lysed in cell lysis buffer. Following centrifugation (10,000 rpm for 10 min 4°C) the supernatant (i.e. cell lysate) was maintained on ice until assayed for activity of superoxide dismutase (SOD) and catalase (CAT) enzymes. The total SOD was determined using pyrogallol assay following the procedure described by Marklund and Marklund (1974), based on the competition between pyrogallol oxidation by superoxide radicals and superoxide dismutation by SOD, and spectrophotometrically read at 420 nm. The amount of SOD inhibiting the reaction rate by 50% in the given assay conditions was defined as one unit of SOD. The results were expressed as units/min/mg protein.

CAT activities were assayed by the method described by Claiborne (1985). One unit of CAT activity is defined as the amount of enzyme that decomposes 1 μmol H_2O_2/min. CAT activities were given as μmol H_2O_2 decomposed/min/mg protein.

DNA Ladder Assay

Cells were cultured in 6-well plate and exposed to IN and CN particles at the concentration of 200 μg/mL for 48 h. At the end of exposure DNA was extracted using an apoptotic DNA Ladder Kit (Roche, Cat# 11835246001). The extracted DNA was then evaluated on a 1% agarose gel using ethidium bromide. DNA fragmentation pattern was documented by a gel documentation system.

Assay of Caspase-3 Enzyme

Cells were cultured in 6-well plate and exposed to IN and CN particles at the concentration of 200 μg/mL for 48 h. Activity of caspase-3 enzyme was determined using a standard fiuorometric microplate assay (Walsh et al., 2008) with some modifications. A reaction mixture containing 30 μL of cell lysate, 20 μL of Ac-DEVD-AFC (caspase-3 substrate), and 150 μL of protease reaction buffer (50 mM Hepes, 1 mM EDTA, and 1 mM DTT), pH 7.2, was incubated for 15 min. Fluorescence of reaction mixture was measured at 5 min interval for 15 min at excitation/emission wavelengths of 430/535 nm using a microplate reader (FLUOstar-Omega). A standard of 7-amido-4-trifiuoromethylcoumarin (AFC) ranging from 5 to 15 μM was prepared and its fiuorescence was recorded for calculation of caspase-3 activity in terms of pmol AFC released/min/mg protein.

Estimation of Protein

The protein content was measured by the method of Bradford (1976) using Bradford reagent (Sigma-Aldrich, St. Louis, MO), along with bovine serum albumin as standard.

Statistics

All the data represented in this study are means $\pm$ SD of three identical experiments made in three replicate. Statistical significance was determined by one-way analysis of variance (ANOVA) followed by Dunnett's multiple comparison test. Significance was ascribed at $p < 0.05$. All analyses were conducted using the Prism software package (GraphPad Software).

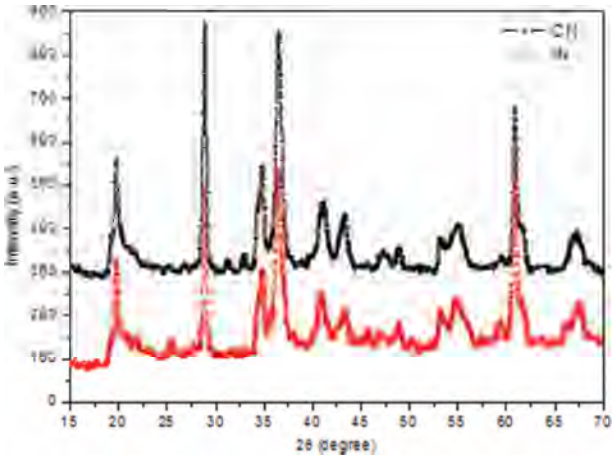

Fig. 1. XRD pattern of two types of nanotalc particles. IN; indigenous nanotalc particles, CN; commercial nanotalc particles. [Color figure can be viewed in the online issue, which is available at wileyonlinelibrary.com.]

RESULTS

Characterization of IN and CN Particles

Characterization of IN and CN particles was performed using a combination of XRD, TEM, DLS, zeta-potential, and BET in order to provide clear insight into crystalline nature, morphology, particle size, surface property, and chemical composition. These properties are necessary for a better understanding of nanotoxicology.

Figure 1 represents the XRD pattern of IN and CN particles. Image clearly exhibits that the crystalline nature of both IN and CN particles were same. The average size of nanocrystals calculated from the XRD results using Scherrer's equation (Patterson, 1939) was found to be 93 and 89 nm for IN and CN particles, respectively. Figure 2(A,B) show the typical TEM images of IN and CN particles, respectively. Images show that particles are aggregated. We never found small independent crystals in the TEM images.

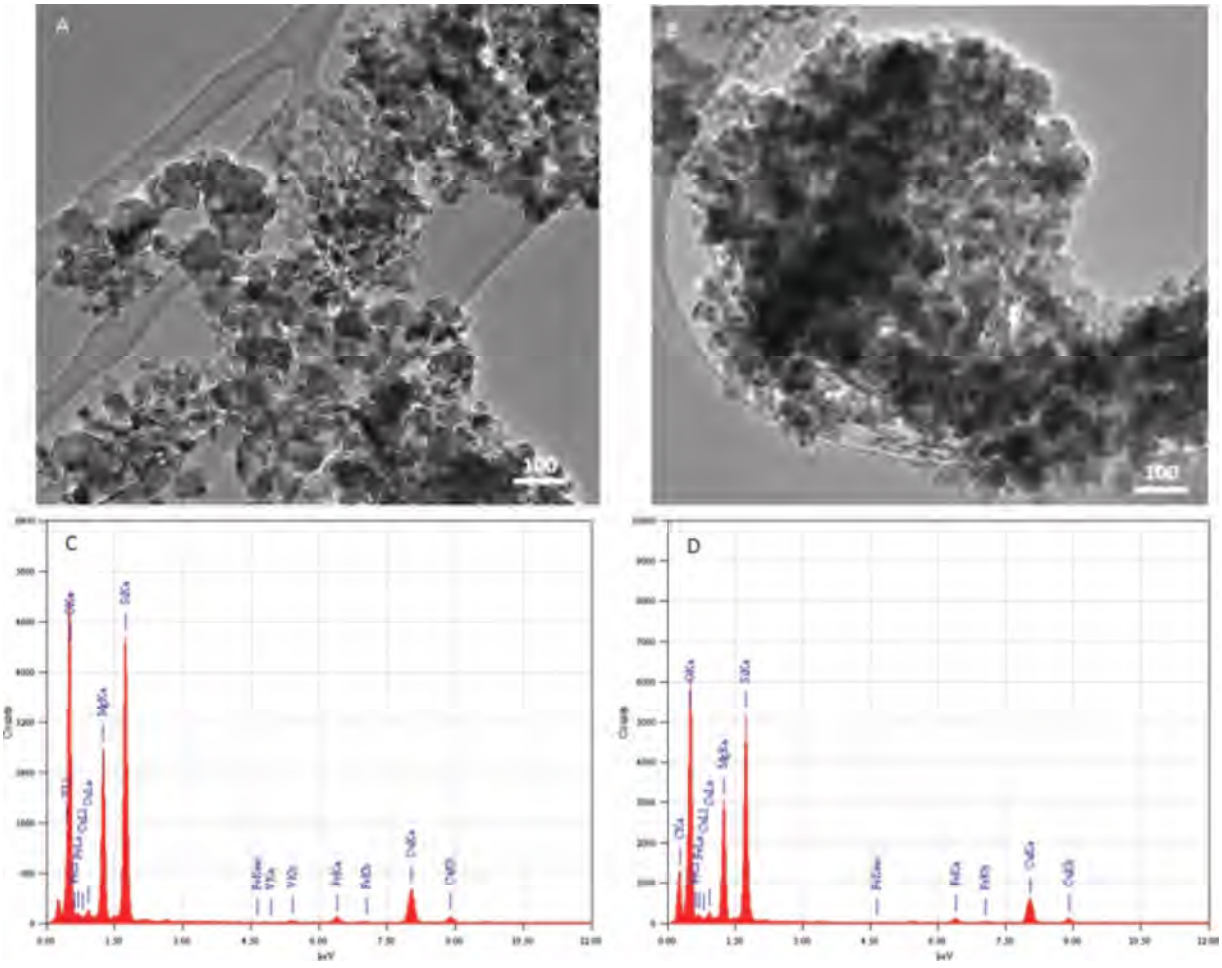

Fig. 2. TEM characterization of nanotalc particles. (A) FETEM of indigenous nanotalc particles, (B) FETEM of commercial nanotalc particles, (C) EDS spectrum of indigenous nanotalc particles, and (D) EDS spectrum of commercial nanotalc particles. [Color figure can be viewed in the online issue, which is available at wileyonlinelibrary.com.]

TABLE 1. Physicochemical properties of two types of nanotalc particles

	Indigenous Nanotalc (IN)	Commercial Nanotalc (CN)
Average XRD size (nm)	93	89
Average TEM size (nm)	94	91
Surface area (m^2/g)	15.4	15.7
Hydrodynamic size (nm)		
Distilled water	782	735
Cell culture medium	671	643
Zeta potential (−mV)	20.3	20.8
Iron content (%)[a]	0.19	0.08

[a]This information is obtained from our previous publication (Akhtar et al., 2010a).

The average TEM size of IN and CN particles were 94 and 91 nm, respectively, which were consistent with the value observed by XRD. The EDS spectra of IN and CN particles are given in Figure 2(C,D), respectively. The presence of Cu and C signals was from the carbon-coated-copper TEM-grid. Presence of iron peaks in both IN and CN particles are in agreement with our previous reports where atomic absorption spectroscopy data showed that 0.19% and 0.08% of iron present in IN and CN particles, respectively (Akhtar et al., 2010 a). The specific surface area of IN and CN particles determined by BET was 15.4 and 15.7 m^2/g respectively.

The physicochemical properties of IN and CN particles are listed in Table 1. All the data from XRD, electron microscopy, and associated techniques was obtained under high vacuum and constitutes the size, morphology, and composition analysis characteristics of nanotalc particles. However, once the nanotalc particles were introduced aqueous media, the sizes changed to approximately 5 to 10 times of the primary size. The average hydrodynamic size of IN and CN particles in distilled water was 782 nm and 735 nm while in cell culture media was 671 and 643 nm, respectively. The higher size of IN and CN particles in aqueous state as compared to XRD and TEM results was due to the tendency of particles to aggregate in the aqueous state. This finding is supported by other investigators (Murdock et al., 2008) and has been briefiy discussed in our previous publications (Ahamed et al., 2010a,b). The tendency of particles to form aggregates depends strongly on the surface charge. The particle charge, determined as zeta-potential by laser doppler velocimetry (LDV) was −20.3mV and −20.8 for IN and CN, respectively.

IN and CN Particles Induced Cytotoxicity

We examined the cell viability (MTT assay) and membrane damage (LDH leakage) as cytotoxicity end points. MTT results demonstrated that both IN and CN particles induced significant reduction in cell viability. The MTT reduction

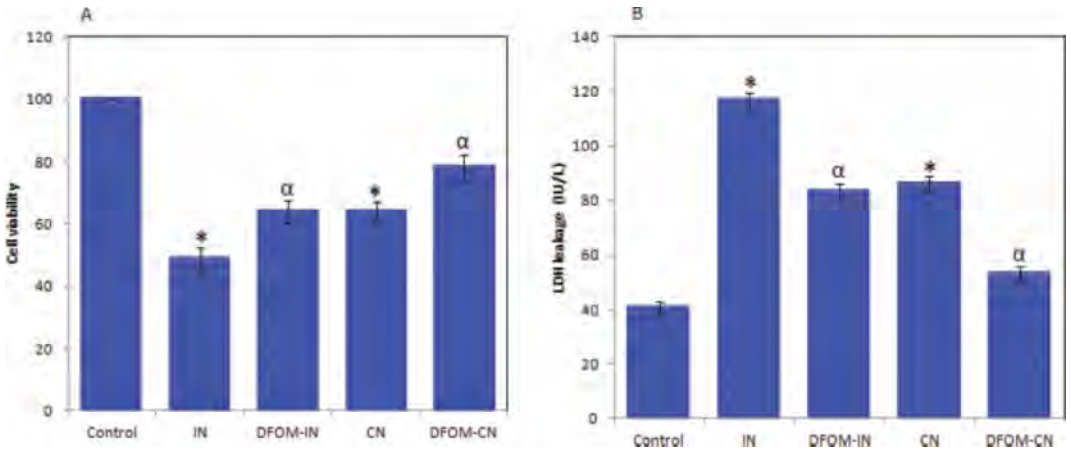

Fig. 3. Comparative effects of nanotalc particles and iron-chelated nanotalc particles on cell viability and LDH release in human lung epithelial A549 cells. Cells were treated with two types of nanotalc particles at the concentration of 200 μg/mL for 48 h. Iron chelator deferoxamine mesylate (DFOM) was co-exposed with nanotalc particles. At the end of treatment MTT and LDH assays were determined as described in materials and methods. (A) MTT assay and (B) LDH assay. Data represented are mean ± SD of three identical experiments made in three replicates. *Statistically significant difference in cell viability reduction and LDH release as compared with the controls ($p < 0.05$ for each). [z]Iron chelation by DFOM significantly reduces the cytotoxicity caused by nanotalc particles ($p < 0.05$ for each). IN; indigenous nanotalc particles, CN; commercial nanotalc particles, DFOM-IN; indigenous nanotalc particles treated with DFOM, DFOM-CN; commercial nanotalc particles treated with DFOM. [Color figure can be viewed in the online issue, which is available at wileyonlinelibrary.com.]

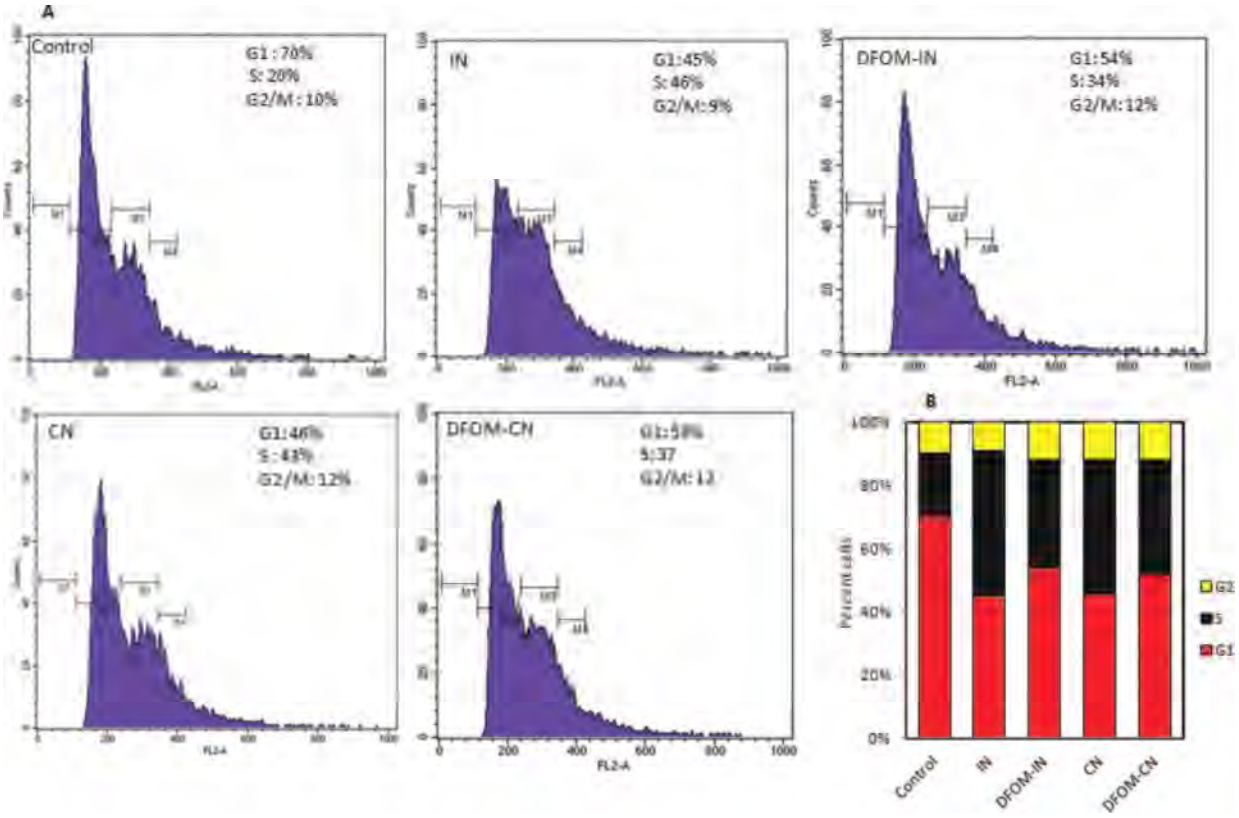

Fig. 4. Comparative effects of nanotalc particles and iron-chelated nanotalc particles on cell cycle in human lung epithelial A549 cells. Cells were treated with two types of nanotalc particles at the concentration of 200 μg/mL for 48 h. Iron chelator deferoxamine mesylate (DFOM) was coexposed with nanotalc particles. At the end of treatment cell cycle was analyzed as described in materials and methods. (A) Raw data generated by fiow cytometric analysis of selected representative samples. The *y*-axis denotes cell count and the *x*-axis represents DNA content. M1, M2, M3, and M4 represent the SubG1, G1, S, and G2/M phase, respectively. (B) Percent of the distribution of cells in the G1, S, and G2/M phase of cell cycle. IN; indigenous nanotalc particles, CN; commercial nanotalc particles, DFOM-IN; indigenous nanotalc particles treated with DFOM, DFOM-CN; commercial nanotalc particles treated with DFOM. [Color figure can be viewed in the online issue, which is available at wileyonlinelibrary.com.]

observed after 48 h at the concentration of 200 μg/mL was 49% and 64% for IN and CN particles, respectively [Fig. 3(A)]. Both IN and CN particles were also found to induce LDH leakage in A549 cells [Fig. 3(B)]. To determine whether our observed cytotoxicity was due iron content, we treated both IN and CN particles with an iron chelator DFOM and tested the cytotoxic effect of chelated nanotalc particles in A549 cells. Results showed that iron chelated IN and CN particles induce less cytotoxicity than those of non-chelated one (Fig. 3).

IN and CN Particles Induced Cell Cycle Changes

Alteration in the cell cycle phases by IN and CN particles in A549 cells are shown in Figure 4. Both IN and CN particles induced significant S phase arrest. The S phase was 20% in the control. It was changed to 46% and 43% in the cells treated with IN and CN particles respectively. However, iron chelated IN and CN particles exert less effect on cell cycle arrest than those of nonchelated IN and CN particles.

IN and CN Particles Induced Oxidative Stress

ROS generation leads to oxidative damage, which has been reported to be one of the important mechanisms of nanoparticles toxicity (Ahamed et al., 2010c; Ahamed et al., 2011a,b). The potential of IN and CN particles to induce oxidative stress was examined by measuring the ROS, LPO, GSH, SOD, and CAT in A549 cells. Results showed that both IN and CN particles induced the

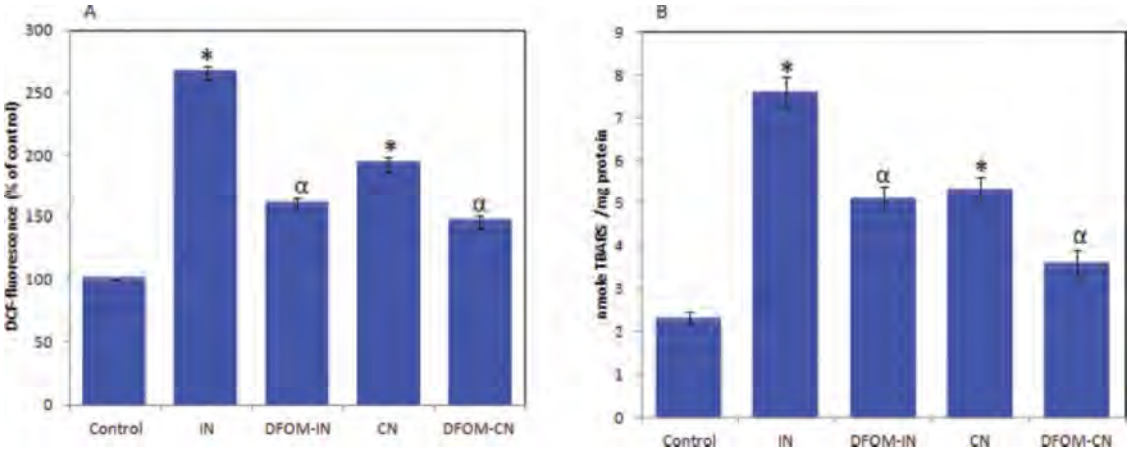

Fig. 5. Comparative effects of nanotalc particles and iron-chelated nanotalc particles on oxidant generations in human lung epithelial A549 cells. Cells were treated with two types of nanotalc particles at the concentration of 200 μg/mL for 48 h. Iron chelator deferoxamine mesylate (DFOM) was coexposed with nanotalc particles. At the end of treatment ROS and LPO levels were determined as described in materials and methods. (A) ROS and (B) LPO. Data represented are mean $\pm$ SD of three identical experiments made in three replicates. *Statistically significant difference in ROS and LPO induction as compared with the controls ($p < 0.05$ for each). $^{\alpha}$Iron chelation by DFOM significantly reduces the ROS and LPO induction caused by nanotalc particles ($p < 0.05$ for each). IN; indigenous nanotalc particles, CN; commercial nanotalc particles, DFOM-IN; indigenous nanotalc particles treated with DFOM, DFOM-CN; commercial nanotalc particles treated with DFOM. [Color figure can be viewed in the online issue, which is available at wileyonlinelibrary.com.]

intracellular ROS and LPO levels [Fig. 5(A,B)]. Nanotalc particles induced oxidative stress was further evidenced by depletion of GSH, SOD, and CAT [Fig. 6(A,B,C)]. Moreover, chelation of iron from IN and CN particles significantly reduced the oxidative stress due to these particles.

IN and CN Particles Induced Apoptosis

Apoptosis is executed by series of cysteine proteases known as caspases (Takadera and Ohyashiki, 2007; Tang et al., 2010). Caspase-9 activation is dependent on the release of cytochrome c from mitochondria to form the apoptosome which in turn activates caspase-3. In the present study, significant higher activity of caspase-3 enzyme was observed suggesting the involvement of caspase cascade in IN and CN particles induced apoptosis in A549 cells [Fig. 7(B)]. Figure 7(B) shows that in untreated cells, the DNA was intact whereas the cells treated with IN and CN particles had started apoptotic DNA fragmentation. Besides, iron chelation from IN and CN particles induced less DNA fragmentation as compared with the nonchelated particles.

Taken together, our data highlight the role of iron contaminant present in IN and CN particles in causing the cytotoxicity, oxidative stress, and apoptosis in human lung epithelial cells.

DISCUSSION

Characterization of physicochemical properties of nanoparticles has been suggested in the nanotoxicology research (Murdock et al., 2008; Li et al., 2011). Several parameters including shape, size, crystal structure, purity, hydrodynamic size, aggregation of particles, and aqueous stability have already been suggested (Nel et al., 2006; Yu et al., 2009). In this study, we employed XRD, TEM, EDS, BET, and DLS techniques to characterize the physicochemical properties of IN and CN particles. XRD and TEM results indicated that both IN and CN particles were crystalline, highly aggregated, and having the iron content as a contaminant. Aggregation and stability of nanoparticles in aqueous state are major concerns in nanotoxicity research. Both IN and CN particles were also aggregated in water and cell culture media as well. Zeta potential data also showed that the aqueous suspension of both IN and CN particles were not much stable in aqueous state. The hydrodynamic size of nanotalc particles was found to be approximately seven to eight times higher than those calculated from TEM and XRD. The higher size of nanoparticles in aqueous suspension as compared with XRD and TEM sizes might be due to the tendency of particles to aggregate in aqueous state. This finding is supported by other investigators (Bai et al., 2009) and has been briefiy discussed in our previous publication (Ahamed et al., 2010b).

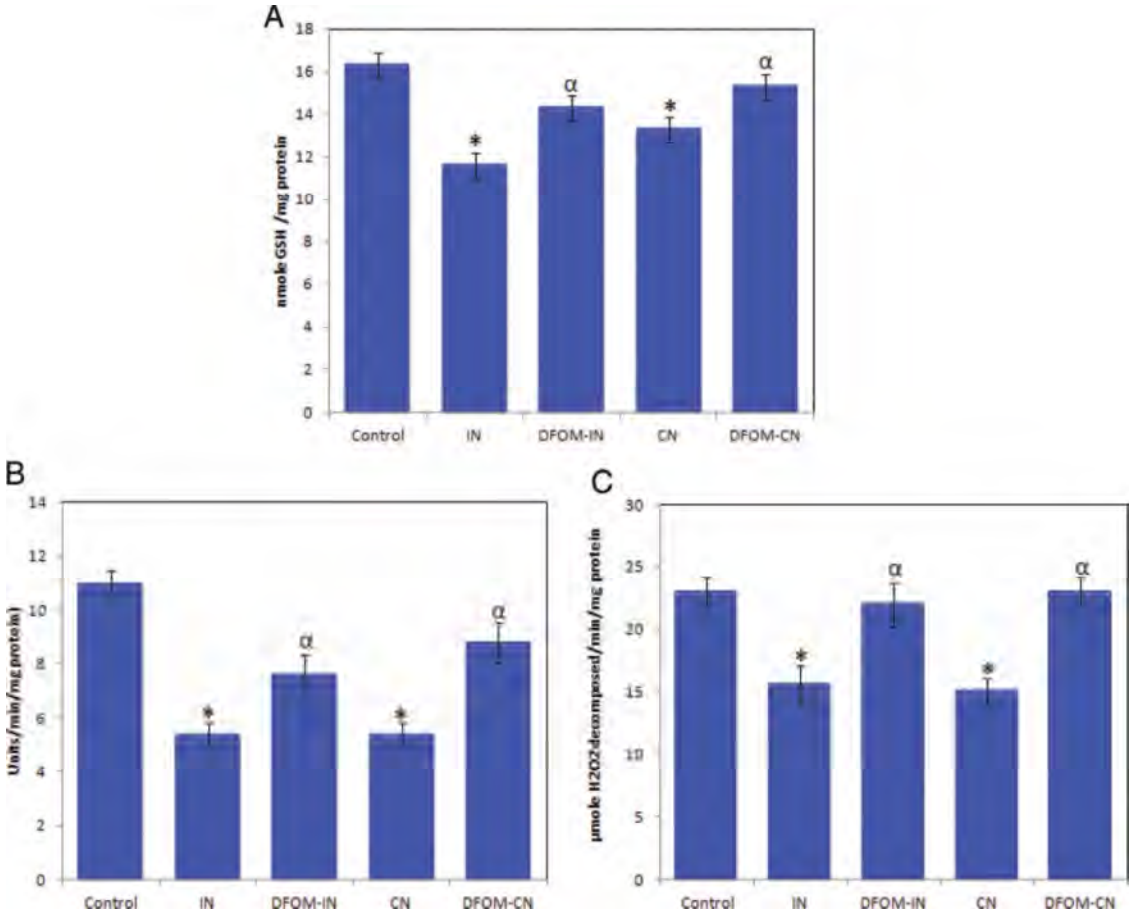

Fig. 6. Comparative effects of nanotalc particles and iron-chelated nanotalc particles on antoxidants reduction in human lung epithelial A549 cells. Cells were treated with two types of nanotalc particles at the concentration of 200 μg/mL for 48 h. Iron chelator deferoxamine mesylate (DFOM) was coexposed with nanotalc particles. At the end of treatment GSH, SOD, and CAT levels were determined as described in materials and methods. (A) GSH, (B) SOD, and (C) CAT. Data represented are mean $\pm$ SD of three identical experiments made in three replicates. *Statistically significant difference in GSH, SOD, and CAT reduction as compared to the controls ($p < 0.05$ for each). $^{\alpha}$Iron chelation by DFOM significantly induces the GSH, SOD, and CAT depletion caused by nanotalc particles ($p < 0.05$ for each). IN; indigenous nanotalc particles, CN; commercial nanotalc particles, DFOM-IN; indigenous nanotalc particles treated with DFOM, DFOM-CN; commercial nanotalc particles treated with DFOM. [Color figure can be viewed in the online issue, which is available at wileyonlinelibrary.com.]

In this study, we observed that IN and CN particles induced cell viability reduction and membrane damage in A549 cells. Both IN and CN particles also induced the cell cycle arrest in the S phase leading to apoptosis. In a previous study, S phase arrest was observed in mouse peritoneal macrophages (RAW264.7) exposed to silver nanoparticles (Park et al., 2010), and S phase arrest was also observed in human lung epithelial cells exposed to carbon black particles coated with benzo(a)pyrene (Mroz et al., 2007). Asharani et al. (2009) reported that starch-coated silver NPs induced G2/M phase arrest and DNA damage in human glioblastoma cells and fibroblasts. A perturbation of the cell cycle preceded by a reduction in cell viability associated with accumulation of cells in S phase leading to cell death is typical of compounds inhibiting DNA synthesis (Binkova et al., 2000; Park et al., 2010).

Cellular integrity is affected by oxidative stress when the production of ROS overwhelms antioxidant defense mechanism (Halliwell and Gutteridge, 1990). Our results showed that both IN and CN particles induce oxidant levels and deplete the antioxidant levels in human lung epithelial (A549) cells. LPO and ROS were significantly higher while the antioxidant GSH was significantly lower in cells treated with IN and CN particles. Antioxidant enzymes SOD and

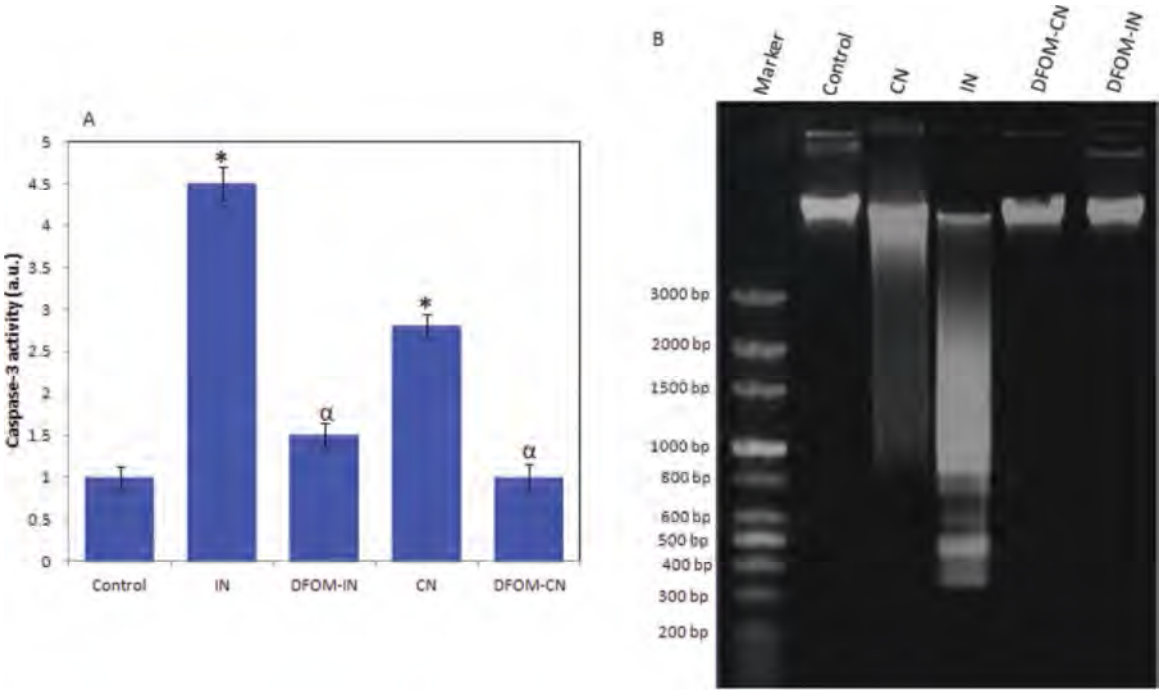

Fig. 7. Comparative effects of nanotalc particles and iron-chelated nanotalc particles on apoptotic markers in human lung epithelial A549 cells. Cells were treated with two types of nanotalc particles at the concentration of 200 μg/mL for 48 h. Iron chelator deferoxamine mesylate (DFOM) was coexposed with nanotalc particles. At the end of treatment DNA ladder and caspase-3 activity were determined as described in materials and methods. (A) Caspase-3 activity. Data represented are mean $\pm$ SD of three identical experiments made in three replicates. *Statistically significant difference in caspase-3 activation as compared with the controls ($p < 0.05$ for each). $^{\alpha}$Iron chelation by DFOM significantly reduces the activity of caspase-3 by nanotalc particles ($p < 0.05$ for each). (B) Representative image of DNA fragmentation. IN; indigenous nanotalc particles, CN; commercial nanotalc particles, DFOM-IN; indigenous nanotalc particles treated with DFOM, DFOM-CN; commercial nanotalc particles treated with DFOM. [Color figure can be viewed in the online issue, which is available at wileyonlinelibrary.com.]

CAT levels were also significantly lower in exposed cells. GSH constitutes the first line of the cellular defense mechanism against oxidative injury and is the major intracellular redox buffer in ubiquitous cell types (Meister, 1989). GSH acts as a cosubstrate in the GSH peroxidase-catalyzed reduction of hydrogen peroxide or lipid peroxides (Forman et al., 1997) leading to its depletion. Previous studies demonstrated that ROS generation following GSH depletion caused mitochondrial damage (Martensson et al., 1989), which has been implicated in apoptosis (Green and Reed, 1998). Enzymes such as SOD and CAT are meant for nullifying cellular oxidative stress. SOD catalyzes the dismutation of superoxide anion (O_2^-) to hydrogen peroxide (H_2O_2). CAT reduces hydrogen peroxide (H_2O_2) to water (H_2O) and oxygen (O_2) (Claiborne, 1985).

The activity of caspase-3 enzyme was significantly higher in cells treated with IN and CN particles. Apoptotic DNA fragmentation was observed in cells exposed to IN and CN particles. Caspases are activated in response to diverse cell death stimuli and ultimately dismantle the cell through restricted proteolysis of numerous cellular proteins that (Timmer and Salvesen, 2007). The activated caspase-3 is capable of autocatalysis as well as cleaving and activating other members of the caspase family, leading to rapid and irreversible apoptosis (Wang et al., 1996). Our previous studies also reported that different types of nanoparticles have potential to induce apoptosis in different kind of cells (Ahamed et al., 2010a; 2010b; 2010c; Ahamed et al., 2010b,c; 2011a).

In the toxicity mechanism of minerals, the iron content has been a key factor. In the present study, EDS analysis showed the presence of iron contamination in both IN and CN particles. These results are in agreement with our previous report where atomic absorption spectroscopy showed the presence of 0.19% and 0.08% of iron in IN and CN particles respectively (Akhtar et al., 2010a). Iron-dependent

ROS generation from fibers results in the generation of hydroxyl radicals through the Fenton reaction and the Haber-Weiss cycle. Iron-dependent ROS generation requires redox cycling of iron and does not necessarily require H_2O_2 or ROS (Halliwell and Gutteridge, 1990). The differential amount of iron present in the two types of nanotalc particles prompted us to investigate the role of iron by sequestering them with an iron chelator, deferoxamine mesylate (DFOM). Sequestering of redox active iron from IN and CN particles by DFOM caused significantly less cytotoxicity, oxidative stress, and genotoxicity than those of the nonchelated IN and CN particles. Similarly, incubation of crocidolite or chrysotile fibers overnight with deferoxamine (5 mM) to inactivate iron catalyzed oxygen radical production also significantly decreased asbestos-induced apoptosis (Broaddus et al., 1996). The role of iron in minerals such as asbestos or silica has been well reported in infiammation and carcinogenesis (Ghio et al., 1992; Hardy and Aust. 1995). Zastawny et al. (1995) have reported on DNA base modifications and membrane damage in cultured mammalian cells treated with iron itself. Similarly, intracellular iron was found to play a critical role in hydrogen peroxide-induced DNA damage (Barbouti et al., 2001). It is also worth to mention that IN particles caused higher toxicity to A549 cells than those of CN particles. This might be due to higher amount of iron present in IN particles (0.19%) as compared with the CN particles (0.08%).

In conclusion, both IN and CN particles significantly induced cytotoxicity, oxidative stress, and apoptosis in human lung epithelial cells. Further, chelation of iron from IN and CN particles by deferoxamine mesylate treatment caused significantly less toxicity as compared to non-chelated IN and CN particles. Therefore, iron content plays a significant role in the toxicity of IN and CN particles, which may be mediated through ROS generation and oxidative stress. This study suggests that one must be very careful regarding the metal impurities like iron present in nanotalc particles before commercial and industrial applications.

REFERENCES

Ahamed M, AlSalhi MS, Siddiqui MKJ. 2010a. Silver nanoparticle applications and human health. Clin Chim Acta 411:1841–1848.

Ahamed M, Posgai R, Gorey TJ, Nielsen M, Hussain S, Rowe J. 2010b. Silver nanoparticles induced heat shock protein 70, oxidative stress and apoptosis in *Drosophila melanogaster*. Toxicol Appl Pharmacol 242:263–269.

Ahamed M, Siddiqui MA, Akhtar MJ, Ahmad I, Pant AB, Alhadlaq HA. 2010c. Genotoxic potential of copper oxide nanoparticles in human lung epithelial cells. Biochem Biophys Res Commun 396:578–583.

Ahamed M. 2011a. Toxic response of nickel nanoparticles in human lung epithelial A549 cells. Toxicol In Vitro 25:930–936.

Ahamed M, Akhtar MJ, Raja M, Ahmad I, Siddiqui MKJ, AlSalhi MS, Alrokayan SA. 2011b. ZnO nanorod induced apoptosis via p53, survivin and bax/bcl-2 pathways mediated by oxidative stress in human alveolar adenocarcinoma cells. Nanomedcine:NBM 7:904–913.

Ahamed M, Akhtar MJ, Siddiqui MA, Ahmad J, Musarrat J, Al-Khedhairy AA, AlSalhi MS, Alrokayan SA. 2011c. Oxidative stress mediated apoptosis induced by nickel ferrite nanoparticles in cultured A549 cells. Toxicology 283:101–108.

Akhtar S, Shukla D, Kumar V. 2008. Studies on effect of nanotalc filler on nucleation, crystal morphology and crystallization behaviour of semi-crystalline plastics. Solid State Phenomena 136:161–174.

Akhtar MJ, Kumar S, Murthy RC, Ashquin M, Khan MI, Patil G, Ahmad I. 2010a. The primary role of iron-mediated lipid peroxidation in the differential cytotoxicity caused by two varieties of talc nanoparticles on A549 cells and lipid peroxidation inhibitory effect exerted by ascorbic acid. Toxicol In Vitro 24:1139–1147.

Akhtar MJ, Ahamed M, Kumar S, Siddiqui H, Patil G, Ashquin M, Ahmad I. 2010b. Nanotoxicity of pure silica mediated through oxidant generation rather than glutathione depletion in human lung epithelial cells. Toxicology 276:95–102.

AshaRani PV, Mun G, Hande MP, Valiyaveettil S. 2009. Cytotoxicity and genotoxicity of silver nanoparticles in human cells. ACS Nano 3:279–290.

Aung W, Hasegawa S, Furukawa T, Saga T. 2007. Potential role of ferritin heavy chain in oxidative stress and apoptosis in human mesothelial and mesothelioma cells: Implications for asbestos-induced oncogenesis. Carcinogenesis 28:2047–2052.

Balamurugan GP, Maiti SN. 2010. Effects of nanotalc inclusion on mechanical, microstructural, melt shear rheological, and crystallization behavior of polyamide 6-based binary and ternary nanocomposites. Polym Eng Sci 50:1978–1993.

Bai W, Zhang Z, Tian W, He X, Ma Y, Zhao Y, Chai Z. 2009. Toxicity of zinc oxide nanoparticles to zebrafish embryo: A physicochemical study of toxicity mechanism. J Nanopart Res 12:1645–1654.

Barbouti A, Doulias PT, Zhu BZ, Frei B, Galaris D. 2001. Intracellular iron, but not copper, plays a critical role in hydrogen peroxide-induced DNA damage. Free Radical Biol Med 31: 490–498.

Binkova B, Giguère Y, Rossner Jr P, Dost M, Srm RJ. 2000. The effect of dibenzo[a, 1]pyrene and benzo[a]pyrene on human diploid lung fibroblasts: The induction of DNA adducts, expression of p53 and p21(WAF1) proteins and cell cycle distribution. Mutat Res 471:57–70.

Bizi M, Flament MP, Leterne P, Baudet G, Gayot A. 2003. Relation between structural characteristics of talc and its properties as an antisticking agent in the production of tablets. Eur J Pharm Sci 19:373–379.

Bradford MM. 1976. A rapid and sensitive method for the quantitation of microgram quantities of protein utilizing the principle of protein-dye binding. Anal Biochem 72:248–254.

Broaddus VC, Yang L, Scavo LM, Ernst JD, Boylan AM. 1996. Asbestos induces apoptosis of human and rabbit pleural mesothelial cells via reactive oxygen species. J Clin Invest 98: 2050–2059.

Buz'Zard AR, Lau BH. 2007. Pycnogenol reduces talc-induced neoplastic transformation in human ovarian cell cultures. Phytother Res 21:579–286.

Carretero MI. 2002. Clay minerals and their beneficial effects upon human health. Appl Clay Sci 21:155–163.

Claiborne A. 1985. Catalase activity. In: Greenwald RA, editor. Handbook of Methods for Oxygen Radical Research. CRC Press Inc. pp283–284.

Forman HJ, Liu R, Tian L. 1997. Glutathione cycling in oxidative stress. In: Clerch LB, Massaro DJ, editors.Oxygen, Gene Expression, and Cellular Function: Lung Biology in Health and Disease, Vol. 105. New York: Marcel Dekker. pp99–112.

Gates MA, Tworoger SS, Terry KL, Titus-Ernstoff L, Rosner B, De Vivo I, Cramer DW, Hankinson SE. 2008. Talc use, variants of the GSTM1, GSTT1, and NAT2 genes, and risk of epithelial ovarian cancer. Cancer Epidemiol Biomar Prev 17: 2436–2444.

Green DG, Reed JC. 1998. Mitochodria and apoptosis. Science 281:1309–1312.

Halliwell B, Gutteridge JM. 1990. Role of free radicals and catalytic metal ions in human disease: An overview. Methods Enzymol 186:1–85.

Hardy JA, Aust AE. 1995. Iron in asbestos chemistry and carcinogenicity. Chem Rev 95:97–118.

Harlow BL, Hartge PA. 1995. A review of perineal talc exposure and risk of ovarian cancer. Regul Toxicol Pharmacol 21: 254–260.

Hissin PJ, Hilf R. 1976. A fiuorometric method for determination of oxidized and reduced glutathione in tissues. Anal Biochem 74:214–226.

Jaynes WF, Zartman RE. 2005. Origin of talc, iron phosphates, and other minerals in biosolids. Soil Sci Soc Am J 69: 1047–1056.

Langseth H, Hankinson SE, Siemiatycki J, Weiderpass E. 2008. Perineal use of talc and risk of ovarian cancer. J Epidemiol Community Health 62:358–360.

Li Y, Sun L, Jin M, Du Z, Liu X, Guo C, Li Y, Huang P, Sun Z. 2011. Size-dependent cytotoxicity of amorphous silica nanoparticles in human hepatoma HepG2 cells. Toxicol in Vitro 25:1343–1352.

Marklund S, Marklund G. 1974. Involvement of the superoxide anion radical in the autooxidation of pyrogallol and a convenient assay for superoxide dismutase. Euro J Biochem 47:469–474.

Martensson J, Jain A, Frayer ,W, Meister A. 1989. Glutathione metabolism in the lung: inhibition of its synthesis leads to lammellar body and mitochondrial defects. Proc Natl Acad Sci USA 86:5296–5300.

Meister A. 1989. Taniguchi N, Higashi T, Sakamoto Y, Meister A, eds. In: *Glutathione Centennial: Molecular Properties and Clinical Applications*. New York, NY: Academic Press.

Mroz RM, Schins RP, Li H, Drost EM, Macnee W, Donaldson K. 2007. Nanoparticle carbon black driven DNA damage induces growth arrest and AP-1 and NFkappaB DNA binding in lung epithelial A549 cell line. J Physiol Pharmacol 58(Suppl 5):461–470.

Mossman T. 1983. Rapid colorimetric assay for cellular growth and survival: Application to proliferation and cytotoxicity assays. J Immunol Methods 65:55–63.

Murdock RC, Braydich-Stolle L, Schrand AM, Schlager JJ, Hussain SM. 2008. Characterization of nanomaterial dispersion in solution prior to in vitro exposure using dynamic light scattering technique. Toxicol Sci 101:239–253.

National Toxicology Program. 1993. NTP Toxicology and Carcinogenesis Studies of Talc (Non-Asbestiform) in Rats and Mice (Inhalation Studies), Vol. 421. pp1–287.

Nel A, Xia T, Madler L, Li N. 2006. Toxic potential of materials at the nanolevel. Science 311:622–627.

Nkoumbou C, Villieras F, Njopwouo D, Ngoune CY, Barres O, Pelletier M, Razafitianamaharavo A, Yvon J. 2008. Physicochemical properties of talc ore from three deposits of Lamal Pougue area (Yaounde Pan-African Belt, Cameroon), in relation to industrial uses. Appl Clay Sci 41:113–132.

Ohkawa H, Ohisi N, Yagi Y. 1979. Assay for lipid peroxides in animal tissues by thiobarbituric acid reaction. Anal Biochem 95:351–358.

Park EJ, Yi J, Kim Y, Choi K, Park K. 2010. Silver nanoparticles induce cytotoxicity by a Trojan-horse type mechanism. Toxicol In Vitro 24:872–878.

Patterson AL, 1939. The Scherrer formula for x-ray particle size determination. Phys Rev 56:978–782.

Pérez-Maqueda LA, Duran A, Pérez-Rodriguez JL. 2005. Preparation of submicron talc particles by sonication. Appl Clay Sci 28:245–255.

Persson HL, Yu Z, Tirosh O, Eaton JW, Brunk UT. 2003. Prevention of oxidant-induced cell death by lysosomotropic iron chelators. Free Radic Biol Med 34:1295–1305.

Petit S, Martin F, Wiewora A, De Parseval P, Decarreau A. 2004. Crystal chemistry of talc: A near infrared (NIR) spectroscopy study. Am Mineral 89:319–326.

Sakthivel S, Pitchumani B. 2011. Production of nano talc material and its applicability as filler in polymeric nanocomposites. Particle Sci Technol 29:441–449.

Takadera T, Ohyashiki T. 2007. Caspase-dependent apoptosis induced by calcineurin inhibitors was prevented by glycogen synthase kinase-3 inhibitors in cultured rat cortical cells. Brain Res 1133:20–26.

Tang X, Guo Y, Nakamura K, Huang H, Hamblin M, Chang L, Villacorta L, Yin K, Ouyang ,H, Zhang J. 2010. Nitroalkenes induce rat aortic smooth muscle cell apoptosis via activation of caspase-dependent pathways. Biochem Biophys Res Commun 397:239–244.

Timmer JC, Salvesen GS. 2007. Caspase substrates. Cell Death Differ 14:66–72.

Wang H, Joseph JA. 1999. Quantifying cellular oxidative stress by dichlorofiuorescein assay using microplate reader. Free Radic Biol Med 27:612–616.

Wang X, Zelenski NG, Yang J, Sakai J, Brown MS, Goldstein JL. 1996. Cleavage of sterol regulatory element binding proteins (SREBPs) by cpp32 during apoptosis. EMBO J 15:1012–1020.

Welder AA, Grant R, Bradlaw J, Acosta D. 1991. A primary culture system of adult rat heart cells for the study of toxicologic agent. In Vitro Cell Dev Biol 27:921–926.

Wild P. 2006. Lung cancer risk and talc not containing asbestiform fibres: A review of the epidemiological evidence. Occup Environ Med 63:4–9.

Wroblewski F, LaDue JS. 1955. Lactate dehydrogenase activity in blood. Proc Soc Exp Biol Med 90:210–213.

Yu KO, Grabinski CM, Schrand AM, Murdock RC, Wang W, Gu B, Schlager JJ, Hussain SM. 2009. Toxicity of amorphous silica nanoparticles in mouse keratinocytes. J Nanopart Res 11:15–24.

Zastawny TH, Altman SA, Randers-Eichhorn L, Madurawe R, Lumpkin JA, Dizdaroglu M, Rao G. 1995. DNA base modifications and membrane damage in cultured mammalian cells treated with iron ions. Free Radic Biol Med 18: 1013–1022.

Zhang J, Zhang T, Ti X, Shi J, Wu C, Ren X, Yin X. 2010. Curcumin promotes apoptosis in A549/DDP multidrug-resistant human lung adenocarcinoma cells through an miRNA signaling pathway. Biochem Biophys Res Commun 6:1–6.

Exhibit 96

Toxicology in Vitro 24 (2010) 1139–1147

Contents lists available at ScienceDirect

Toxicology in Vitro

journal homepage: www.elsevier.com/locate/toxinvit

The primary role of iron-mediated lipid peroxidation in the differential cytotoxicity caused by two varieties of talc nanoparticles on A_{549} cells and lipid peroxidation inhibitory effect exerted by ascorbic acid

Mohd Javed Akhtar [a], Sudhir Kumar [b], Ramesh Chandra Murthy [c], Mohd Ashquin [a], Mohd Imran Khan [a], Govil Patil [a], Iqbal Ahmad [a,*]

[a] Fibre Toxicology Division, Indian Institute of Toxicology Research (CSIR), Lucknow 226 001, UP, India
[b] Department of Zoology, University of Lucknow, Lucknow 226 001, UP, India
[c] Analytical Chemistry Division, Indian Institute of Toxicology Research (CSIR), Lucknow 226 001, UP, India

ARTICLE INFO

Article history:
Received 8 October 2009
Accepted 3 March 2010
Available online 10 March 2010

Keywords:
Talc nanoparticles
Cytotoxicity
Lipid peroxidation
Reactive oxygen species
Glutathione
Oxidative stress
Iron contamination

ABSTRACT

Talc particles, the basic ingredient in different kinds of talc-based cosmetic and pharmaceutical products, pose a health risk to pulmonary and ovarian systems due to domestic and occupational exposures. Two types of talc nanoparticles depending on the source of geographical origin – indigenous- and commercial talc nanoparticles were assessed for their potential *in vitro* toxicity on A_{549} cells; along with indigenous conventionally used microtalc particles. Cell viability, determined through live/dead staining and 3-(4,5-dimethyl thiazol-2-yl)-2,5-diphenyl tetrazolium bromide (MTT) assay, decreased as a function of concentration, origin and size of particles. Both varieties of talc nanoparticles differentially induced lipid peroxidation (LPO), which was correlated with the pattern of lactate dehydrogenase (LDH) leakage, reactive oxygen species (ROS) generation, and glutathione (GSH) depletion. Relatively higher cytotoxicity of indigenous nanotalc could be attributed to its higher content of iron as compared to commercial nanotalc. The known scavenger of ROS, L-ascorbic acid significantly inhibited LPO induction due to talc particles. Data suggest that nanotalc toxicity on A_{549} cells was mediated through oxidative stress, wherein role of iron-mediated LPO was much pronounced in differential cytotoxicity.

1. Introduction

Talc is a magnesium silicate mineral with chemical formula written as $3MgO{\cdot}4SiO_2H_2O$ which corresponds to 4.8% H_2O, 31.7% MgO, and 63.5% SiO_2. It is chemically inert to acids and alkalis and can withstand temperatures up to 1300 °C. In pulverized form it is whiter in appearance. Talc is valued for its extreme softness, smoothness, high lubricating and hiding power and ability to absorb oil and grease. Talc is, therefore, used by organized sector of industries because of its valuable properties. Pulverized talc has wide industrial applications in cosmetics as body and face powder; filler in rubber, textile, plastic, asbestos products, polishes and soaps; as a loading agent for paper of all kinds; used in pharmaceuticals as a carrier of insecticidal and pesticidal dusts.

Since, talc products are marketed in a multitude of grades which have physical or functional characteristics especially suited for particular applications and products, so occupational and consumer exposures to talc are complex. Talc miners have shown higher rates of lung cancer and other respiratory illnesses from exposure to industrial grade talc, which contains dangerous silica and asbestos (Hollinger, 1990; National Toxicology Program, 1993). The common household hazard posed by talc is inhalation of baby powder by infants (Hollinger, 1990). Talc particles have been found to be translocated after intrapleural administration in rats (Werebe and Pazetti, 1999). Talc particles are able to move through the human reproductive system and become imbedded in the lining of the ovary. Researchers have found talc particles in ovarian tumors and have found that women with ovarian cancer have used talcum powder in their genital area more frequently than healthy women (Henderson et al., 1971; Harlow et al., 1992; Harlow and Hartge, 1995). Numerous studies have shown a strong link between frequent use of talc in the female genital area and ovarian cancer (Heller et al., 1996; Chang and Risch, 1997; Cook et al., 1997; Cramer et al., 1999; Mills et al., 2004; Wild, 2006). In an epidemiologic study aimed to analyze the interactions between talc use and genes involved in detoxification pathway, (viz; glutathione S-transferase M1 (GSTM1), glutathione S-transferase T1 (GSTT1), and N-acetyltransferase 2 (NAT2), suggest that women with certain genetic variants may have a higher risk of

* Corresponding author. Address: Fibre Toxicology Division, Indian Institute of Toxicology Research, P.O. Box No. 80, Mahatma Gandhi Marg, Lucknow 226 001, UP, India. Tel.: +91 522 2620207/2227586; fax: +91 522 2628227.
E-mail addresses: iqbal@iitr.res.in, ahmadi@sify.com (I. Ahmad).

0887-2333/$ - see front matter © 2010 Elsevier Ltd. All rights reserved.
doi:10.1016/j.tiv.2010.03.002

ovarian cancer associated with genital use of talc (Gates et al., 2008).

Nanopowder of talc is a recent introduction and is used for improving quality of many industrial products. Nanopowder of talc is being used in plastics for higher strength and stiffness, better thermal and creep resistance; in papers for higher opacity, better gloss and printing quality; in cosmetics and paints for better gloss, smoother surface, resistance to water and cracking, etc. Owing to their unique nano-size, nanoparticles are provided with many special physicochemical properties, and thereby may yield extraordinary hazards for human health (Donaldson et al., 2002; Kipen and Laskin, 2005; Holsapple et al., 2005; Nel et al., 2006; Borm et al., 2006). Since, talc with a multitude of physical and functional characteristics is used for particular applications, so occupational and consumer exposures to talc are likely to vary accordingly. Risk of occupational and environmental exposure to nanoparticles of talc has obviously increased.

Since, physical and functional characteristics of talc and other minerals depend, in part, from one geographical region/source to other, therefore, the first objective of the present study was to evaluate cytotoxicity of talc nanoparticles from the two sources-indigenous nanotalc (Indian origin) and commercial nanotalc (American origin) using human bronchoalveolar carcinoma-derived cells (A_{549}). Indigenous micro-scale talc particle was used for comparative size-dependent toxicity with the two types of nanotalc. The second objective was to study the mechanism of cytotoxicity induced by talc nano- and micro-particles. In the present study, different types of talc particles were dispersed in the cell culture medium at varying concentrations and then exposed to cells. Cytotoxicity was measured by determining cell viability using MTT assay and live-dead staining method. To elucidate the possible mechanisms of cytotoxicity, biomarkers for cytotoxicity and oxidative stress, namely lactate dehydrogenase (LDH) leakage in cell culture medium, reactive oxygen species (ROS) generation, intracellular reduced glutathione (GSH) level, and malondialdehyde (MDA) as an indicator of lipid peroxidation and membrane damage, were measured. Antioxidant, ascorbic acid, was used to delineate further the potential mechanism of oxidative stress and as a potential preventive measure. In the toxicity of minerals, the iron content has been a key factor, acting through Fenton reaction and the Haber–Weiss cycle. Some metals like Fe, Pb, and Cr was measured in the talc from two sources. A role of differential amount of iron present in indigenous and commercial talc, in the perspective of cytotoxicity and oxidative stress has, therefore, also been established.

2. Materials and methods

2.1. Nanoparticles

Indigenous cosmetic grade talc was collected from Udaipur, Rajasthan, India and prepared into micro- and nanoparticles. As a standard reference, Nanopowder of talc (i.e. commercial nanotalc) was purchased from (M.K. Impex Canada, Catalpa Road, Mississauga, Canada). As per the information provided by the supplier, the powder size was 70–120 nm and the country of origin was USA. For indigenous nanotalc a stone of talc was crushed into fine particles and fed into a ball mill (PM 100, Retsch, Germany) and grinded for 5 days at an alternative cycles of grinding (10 min) and halt (30 min) at 350 rpm using a mixture of different sizes of balls. The sizes of nanoparticles were measured by transmission electron microscopy (TEM) and found to be 80–130 nm. Indian talc particles (i.e. indigenous micro talc) 50–65 μm served as negative control for a comparative study on nanotoxicity of indigenous and commercial varieties of nanotalc.

2.2. Chemicals

Fetal bovine serum, Penicillin–streptomycin, DMEM F-12 medium, HBSS was purchased from Invitrogen Co. (Carlsbad, CA, USA). MTT [3-(4,5-dimethylthiazol-2-yl)-2,5 diphenyltetrazolium bromide], NADH, Pyruvic acid, L-ascorbic acid, glutathione reduced (GSH), o-phthalaldehyde (OPT), 2′,7′-dichlorofluorescin diacetate (DCFH-DA), 1,1,3,3-tetraethoxypropane (TEP), 2-thiobarbituric acid (TBA), sodium dodecyl sulphate (SDS), Na_2HPO_4, NaH_2PO_4, were obtained from Sigma–Aldrich. Ultrapure DI-water was prepared using a Milli-Q system (Millipore, Bedford, MA, USA). All other chemicals used were of reagent grade.

2.3. Estimation of heavy metals in indigenous and commercial talc

Talc samples were digested in digesting mixture (HNO_3 and perchloric acid in a ratio of 4:1) for 24 h on hot plate in a fume hood. The digested samples were dissolved in 1% HNO_3 and filtered. The filtrate was used for metal analysis by atomic absorption spectroscopy (AAS). Before analysis, AAS was calibrated every time by running at least three standard concentration (1, 3 and 5 mg/L) of each metal. Values have been expressed as% metal content in talc samples.

2.4. Measurement of hydrodynamic size of nanotalc

These particles were suspended in complete cell culture media, ultrasonicated at 30 W for 2 min (Sonics Vibra Cell, India) and a dynamic light scattering (DLS – Malvern Instruments USA) performed for particle size distribution in culture media.

2.5. Cell culture and treatment with talc particles

The A_{549} cell line has been established in permanent culture from a human lung adenocarcinoma (Lieber et al., 1976). *In vitro*, these cells are largely differentiated as alveolar epithelial cells, type II (Croute et al., 1990). The A_{549} cells were obtained from National Centre For Cell Science (NCCS), Pune, India. Cells were maintained in DMEM F-12 medium supplemented with 10% fetal bovine serum, 100 U/ml penicillin, and 100 μg/ml streptomycin, and grown at 37 °C in a humidified, 5% CO_2 incubator. For the determination of GSH, MDA, and LDH levels, A_{549} cells were plated into 75-cm^2 flasks at a density of 2.0×10^6 cells per flask in 12 ml culture medium and allowed to attach for 24 h. Then, the freshly dispersed talc nanoparticles suspensions in cell culture medium were prepared and diluted to appropriate concentrations (50, 100, and 200 μg/ml) and immediately applied to the cells in 15 ml culture medium. Cells not exposed to particles served as controls in each experiment. The selection of the 50–200 μg/ml dosage range of talc nanoparticles was based on a preliminary dose–response study (data not shown). A dosage level lower than 50 μg/ml did not result cytotoxicity significantly. The 48 h exposure time was chosen for investigation; the responses at 24-h exposure were not as pronounced as that at 48 h. Therefore, all the data presented here is that of 48 h exposure. Throughout the studies presented in this paper, we utilized a particle dose of 20 μg/cm^2 = 100 μg/ml.

2.6. Cell viability assay

Cytotoxicity was measured by determining cell viability using MTT assay and live-dead staining method.

2.6.1. MTT assay

Cell proliferation/viability was assessed by the MTT assay as first described by Mossman (1983) and later modified by Hansen et al. (1989). This assay is based on the ability of viable cells, but

not of dead cells, to reduce soluble, yellow 3-(4,5-dimethyl thiazol-2-yl)-2,5-diphenyl tetrazolium bromide (MTT) into insoluble, blue formazon product. Briefly, around 10,000 A_{549} cells per well were plated in 96-well microtiter plates in a 100 μl of medium. The next day, the medium was changed and the cells were treated with talc nanoparticles at 50-, 100-, and 200 μg/ml for 48 h. After the exposure time completed, the medium was aspirated off and 100 μl MTT laden media (0.5 mg MTT/ml of media without phenol red and serum, filtered through 0.22 μm filter) added and incubated for 2 h. The reaction was stopped and formazan crystal thus formed was solubilised by mixing an equal volume of stop mix solution containing 20% SDS in 50% *N*,*N*-dimethylformamide and left overnight on a shaker. To minimize the interference in absorbance caused by previously dosed talc particles (at concentrations like 50–200 μg/ml obviously resulting in turbidity!), the plates were centrifuged at 3000 rpm for 5 min to settle down the particles and a clear 100 μl supernatant was transferred to other fresh wells of microtiter plate and then absorbance at 570 nm was taken by a microplate reader (Omega Fluostar). Following noncellular background (blank consisting of yellow MTT- and stop mix-solutions) subtraction, all data were normalized to the MTT conversion activity of media-treated control cells. This value corresponds to 0% decrease in MTT conversion activity and represents 100% cell viability.

2.6.2. Live-dead staining (trypan blue exclusion) assay

In addition to the MTT assay, the cell viability was also determined by the trypan blue exclusion method. The percentage of non-stained live cells was evaluated using a haemocytometer. A total of 200 cells were counted for each measurement.

2.7. LDH leakage

The activity of cytoplasmic LDH released into the culture media was determined with the method described elsewhere (Wroblewski and LaDue, 1955; Welder et al., 1991). A 100-μl sample from the centrifuged culture media was collected after the cells were treated for 48 h. The LDH activity was assayed in 3.0 ml of reaction mixture with 100 μl of pyruvic acid (2.5 mg/ml phosphate buffer) and 100 μl of NADH (2.5 mg/ml phosphate buffer) and the rest of the volume adjusted with phosphate buffer (0.1 M, pH 7.4). The rate of NADH oxidation was determined by following the decrease in absorbance at 340 nm for 3 min at 30 s interval at 25 °C using a spectrophotometer (Thermo-Spectronic). The amount of LDH released is represented as LDH activity (IU/L) in culture media.

2.8. Intracellular ROS measurement

The generation of intracellular ROS was measured using 2′,7′-dichlorofluorescin diacetate (DCFH-DA) probe (Wang and Joseph, 1999). DCFH-DA passively enters the cell where it is broken down into cell impermeable, non-fluorescent reduced dichlorofluorescin (DCFH) and diacetate by cellular esterases. Now DCFH becomes oxidized with intracellular ROS to form the highly fluorescent compound dichlorofluorescin (DCF) that may be cell permeable. Briefly, 10 mM DCFH-DA stock solution made in dimethyl sulfoxide (DMSO) was diluted in culture medium without serum or other additive to yield a 100 μM working solution. After 48 h of exposure to talc nanoparticles, the cells in the 12-well plate were washed twice with HBSS and then incubated in 1 ml working solution of DCFH-DA at 37 °C for 30 min. The cells were lysed in alkaline solution and centrifuged at 3000 rpm. A 200 μl supernatant was transferred to black 96-well plate and fluorescence was then read at 480-nm excitation and 520-nm emission using a microplate reader (Omega Fluostar). The intensity of untreated control well was assumed to be 100% and data is represented in percent of control.

2.9. Determination of intracellular GSH

The cellular content of GSH was quantified by the fluorometric assay of Hissin and Hilf (1976). After exposure, cells were lysed in 20 mM Tris (pH 7.0) by repeated cycles of freeze–thaw and centrifuged at 10,000 rpm for 10 min at 4 °C. The supernatant was transferred to another tube and protein content was measured. For the determination of intracellular GSH, protein in this supernatant was precipitated at 1% perchloric acid and again centrifuged at 10,000 rpm for 5 min at 4 °C. Now 20 μl sample was mixed with 160 μl of 0.1 M phosphate-5 mM EDTA buffer, pH 8.3 and 20 μl *o*-phthalaldehyde (OPT, 1 mg/ml in methanol) in a black 96-well plate. After 2 h incubation at room temperature in the dark, fluorescence was measured at an emission wavelength of 460 nm and an excitation wavelength of 355 nm, along with similarly prepared standards of GSH in 1% perchloric acid. Results are expressed as nmol GSH/mg of cellular protein.

2.10. Determination of thiobarbituric acid-reactive substances (TBARS)

LPO was assessed by the TBARS assay, which detects mainly malondialdehyde (MDA), an end product of the peroxidation of polyunsaturated fatty acids and related esters. TBARS was measured by slight modification of the method of Ohkawa et al. (1979). Subconfluent cells were scraped in 75-cm^2 flasks, washed two times by isotonic trace element-free Tris–HCl buffer (400 mM, pH 7.3). A 200-μl aliquot of cell suspension was subsequently mixed with 800 μl of LPO assay cocktail containing (0.4% (w/v) thiobarbituric acid, 0.5% (w/v) SDS, 5% (v/v) acetic acid, pH 3.5 and incubated for 60 min at 95 °C. The sample was cooled using tap water and centrifuged at 5000 rpm for 5 min. The absorbance of the supernatants was read at 532 nm against a standard curve prepared using the MDA standard (10 mM 1,1,3,3-tetramethoxypropane in 20 mM Tris–HCl, pH 7.4). Results were calculated as nmol of MDA/mg of cellular protein.

2.11. Addition of L-ascorbic acid

To test the potential antioxidant effects afforded by ascorbic acid, 1.5 mM was applied to cell culture 30 min before exposure with particles. A dosage of 200 μg/ml of the two varieties of talc was then exposed for 48 h and MDA level was measured as illustrated above.

2.12. Estimation of protein

The total protein concentration was measured by the Bradford method (Bradford, 1976) using a ready to use Bradford reagent (Sigma–Aldrich, USA) and bovine serum albumin as the standard.

2.13. Statistics

Data were expressed as the mean ± SD from three independent experiments. One-way ANOVA and Dunnett's Multiple Comparison Test was applied using Graph Pad prism (Version 5.0) software for significance testing, using a p value $\leqslant 0.05$.

3. Results

3.1. Iron contamination in talc samples

Indigenous and commercial talc samples were analyzed for contamination of heavy metals (Fe, Pb, and Cr). The results are given in Table 1. Indigenous talc contained almost 2.3 times higher iron level in comparison to commercial talc. Pb was not in detectable

Table 1
Metal contamination in talc samples.

Name of metal	% Metal content	
	Indigenous talc	Commercial talc
Fe	0.19	0.08
Cr	Not detectable	0.0046
Pd	Not detectable	Not detectable

limit in both the samples. However Cr was present in trace amount in commercial nanotalc.

3.2. Hydrodynamic size of talc nanoparticles in culture media

The size measured by a dynamic light scattering method was the particles hydrodynamic size, which indicates the extent of aggregation of particles in suspension. The measurements have been given in Table 2. Results show that aggregation occurred and the aggregation was not uniform.

3.3. The concentration-, size-, and origin-dependent cytotoxicity of talc particles

The A_{549} cells were exposed with indigenous microtalc (50–65 μm) particles, indigenous talc nanoparticles (80–130 nm) and commercial talc nanoparticles (70–120 nm) for 48-h exposure, and the cell viability was assessed by MTT assay. Cell viability decreased as a function of concentration, size and geographical origin of particles. Cell viability decreased to 93.0%, 91.6%, and 83.6% for indigenous microtalc and 81.6%, 67.0%, and 47.30% for indigenous nanotalc and 88.3%, 77.6%, and 64.0% for commercial nanotalc particles when exposed at 50-, 100-, and 200 μg/ml, respectively (Fig. 1). Fig. 2 shows the results on cell viability obtained by trypan blue exclusion test for similar experiment. Cell viability decreased to about 93.0%, 90.6%, and 83.6% for indigenous microtalc and 83.6%, 73.6%, and 57.30% for indigenous nanotalc and 88.6%, 78.6%, and 69.6% for commercial nanotalc particles exposed at 50-, 100-, and 200 μg/ml, respectively. The IC_{50}s evaluated by MTT and trypan blue assay is given in Table 3.

3.4. Cell membrane damage

LDH release, a marker of cell membrane damage, was measured at 50, 100, and 200 μg/ml for the 48-h exposure (Fig. 3). Following exposure to talc particles at concentrations mentioned above, the LDH activity in the culture media is increased in a concentration-dependent manner and found to 18.1%, 32.9%, and 61.3%, respectively for indigenous microtalc and 99.2%, 193.6%, and 275.6%, respectively for indigenous nanotalc and 46.2%, 103.7%, and 178.7%, respectively for commercial nanotalc. The indigenous nanotalc induced a significantly higher ($p < 0.05$) cell membrane damage when compared with its micro-scale size and commercial nanotalc for a particular concentration. For instance, 50-, 100-, and 200 μg/ml exposure of indigenous nanotalc induced 1.4-, 1.44-, and 1.3-fold higher membrane damage when compared with the same concentrations of commercial nanotalc induced membrane damage. Similarly indigenous nanotalc induced membrane damage was 1.6-, 2.2-, and 2.3 times higher than that of indigenous microtalc.

Table 2
Actual and hydrodynamic sizes of Indigenous and Commercial nanotalc in culture media.

Type of nanoparticles	Actual size (nm)	Hydrodynamic size (nm)
Commercial nanotalc	70–120	800 ± 100
Indigenous nanotalc	80–130	750 ± 120

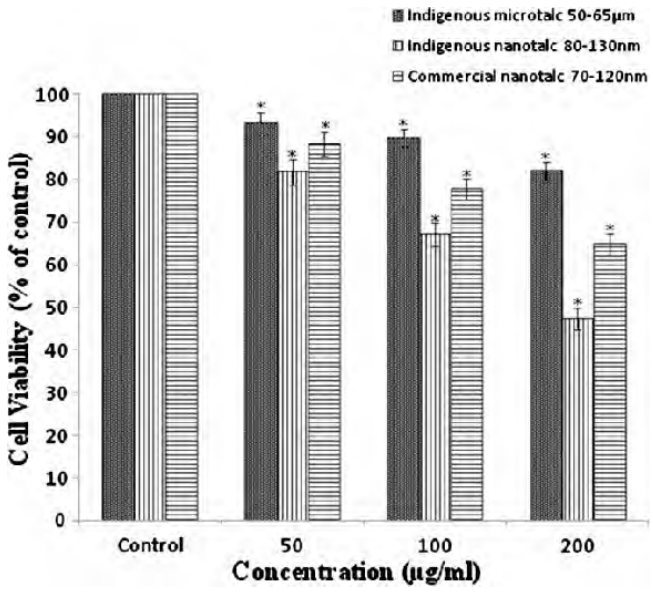

Fig. 1. Viability of A_{549} cells after 48-h exposure to indigenous microtalc, indigenous nanotalc and commercial nanotalc particles evaluated by MTT assay at indicated concentrations. Values are mean ± SD from three independent experiments. Triplicates of each treatment group were used in each independent experiment. *Denotes a significant difference from the control ($p < 0.05$).

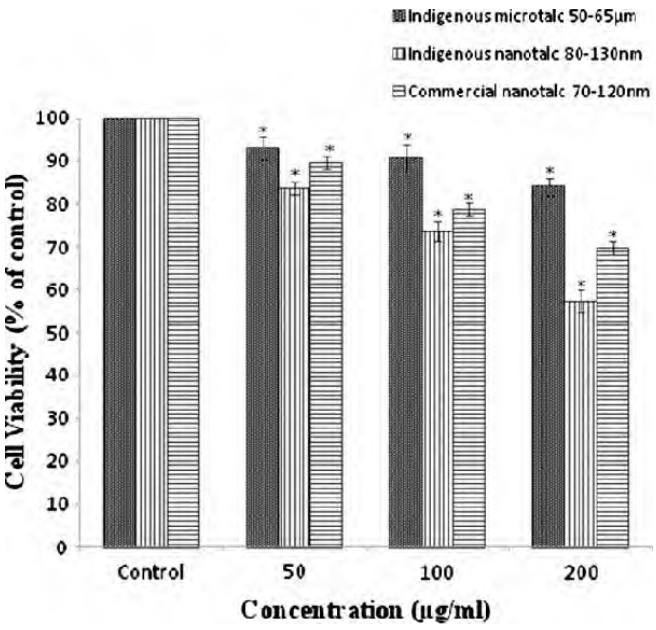

Fig. 2. Viability of A_{549} cells after 48-h exposure to indigenous microtalc, indigenous nanotalc and commercial nanotalc particles evaluated by trypan blue assay at indicated concentrations. Values are mean ± SD from three independent experiments. Triplicates of each treatment group were used in each independent experiment. *Denotes a significant difference from the control ($p < 0.05$).

3.5. ROS generation

The ability of talc micro- and nanoparticles to induce intracellular oxidant production in A_{549} cells was assessed by measuring DCF fluorescence as a reporter of ROS generation. DCF fluorescence intensity significantly ($p < 0.05$) increased after 48 h exposure to all examined micro and nanoparticles at concentrations of 50-,

Table 3
IC_{50} values of different talc particles measured by MTT and trypan blue.

Types of talc nanoparticles	IC_{50} by MTT assay (μg/ml)	IC_{50} by trypan blue assay (μg/ml)
Indigenous microtalc (50–65 μm)	600	630
Indigenous nanotalc (80–130 nm)	190	255
Commercial nanotalc (70–120 nm)	277.5	325

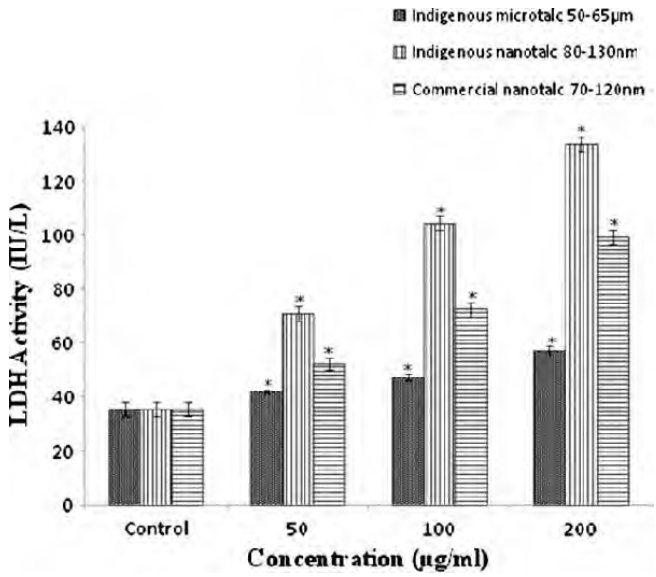

Fig. 3. The LDH activities in the cell culture medium after 48-h exposure to indigenous microtalc, indigenous nanotalc and commercial nanotalc particles at indicated concentrations. Values are mean ± SD from three independent experiments. *Denotes a significant difference from the control ($p < 0.05$).

100-, and 200 μg/ml, and evaluated to be 136%, 155%, and 175%, respectively for indigenous microtalc and 150%, 203%, and 265%, respectively for indigenous nanotalc and 136%, 175%, and 205%, respectively for commercial nanotalc (Fig. 4). The highest fluorescence obtained was that for indigenous nanotalc at 200 μg/ml.

3.6. Cellular GSH level and LPO induced by talc nanoparticles

Following exposure to talc particles at concentrations 50, 100, and 200 μg/ml for 48 h, the intracellular GSH level exhibited a concentration-dependent decrease (Fig. 5). The GSH levels were reduced by 3%, 11.56%, and 18.8% for indigenous microtalc and 14.2%, 18.8%, and 25.4% for indigenous nanotalc and 6.6%, 11.5%, and 20.8%, respectively for commercial nanotalc.

In order to elucidate the lipid peroxidation induced by talc particles, the MDA concentration was measured. Each type of nanoparticles elevated the intracellular MDA concentration which was dependent on dosage and source of talc particle origins (Fig. 6). The MDA levels were elevated by 1.3-fold, 1.4-fold, and 1.9-fold, respectively for indigenous microtalc, and 1.6-fold, 2.3-fold, and 3.1-fold, respectively for indigenous nanotalc and 1.4-fold, 1.7-fold, and 2.1-fold, respectively for commercial nanotalc, compared to the control untreated groups.

3.7. Inhibitory effect afforded by ascorbic acid on LPO induced by talc nanoparticles

In an additional set of studies, L-ascorbic acid was added to the cells during exposure to micro- and nanotalc, each group exposed at 200 μg/ml, as a test to determine if the oxidative damage to A_{549} cells could be prevented. Results show that L-ascorbic acid effectively prevented the generation of MDA level induced by talc particles (Fig. 7). MDA level was reduced up to control level for indigenous microtalc in the presence of ascorbic acid. When indigenous nanotalc induced MDA was 3.1-fold, in the presence of ascorbic acid it was reduced and found to be 2.1-fold of control. When commercial nanotalc induced MDA was 2.1-fold, in the presence of ascorbic acid it was 1.3-fold of control.

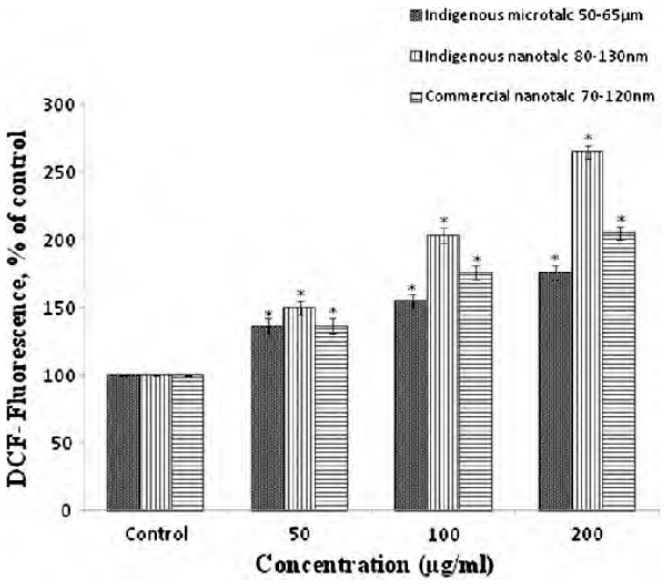

Fig. 4. DCF-fluorescence intensity after 48-h exposure to indigenous microtalc, indigenous nanotalc and commercial nanotalc particles at indicated concentrations. Values are mean ± SD from three independent experiments. *Denotes a significant difference from the control ($p < 0.05$).

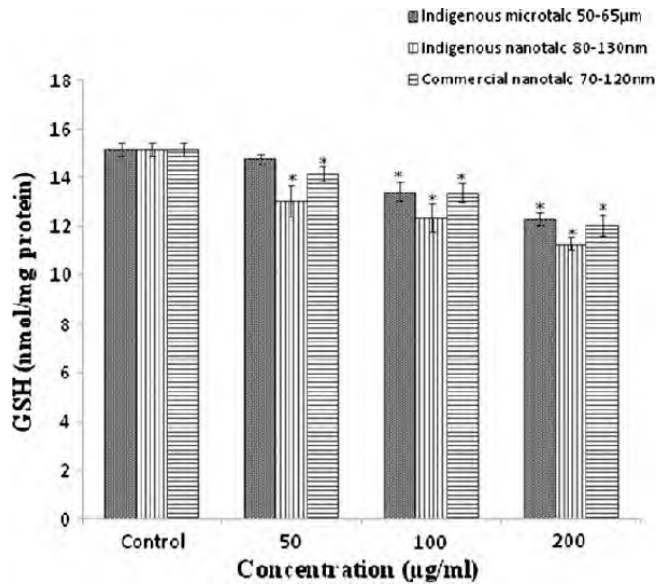

Fig. 5. Cellular GSH levels of A_{549} cells after 48-h exposure to indigenous microtalc, indigenous nanotalc and commercial nanotalc particles at indicated concentrations. Values are mean ± SD from three independent experiments. *Denotes a significant difference from the control ($p < 0.05$).

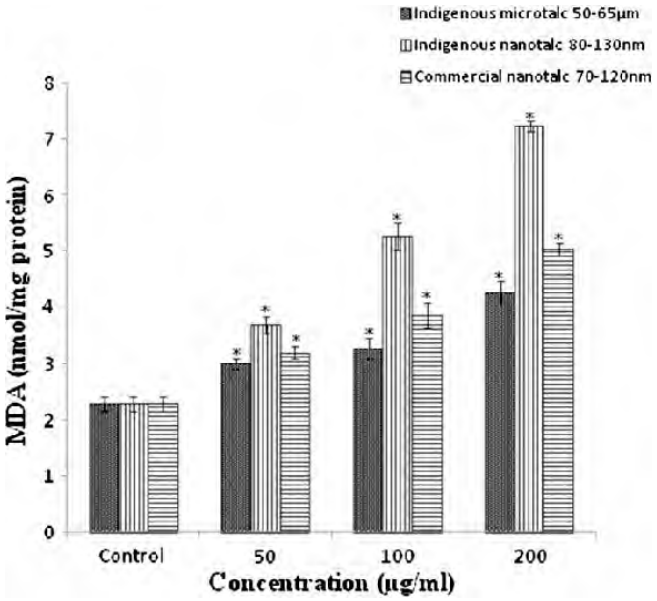

Fig. 6. Cellular MDA levels of A_{549} cells after 48-h exposure to indigenous microtalc, indigenous nanotalc and commercial nanotalc particles at indicated concentrations. Values are mean ± SD from three independent experiments. *Denotes a significant difference from the control ($p < 0.05$).

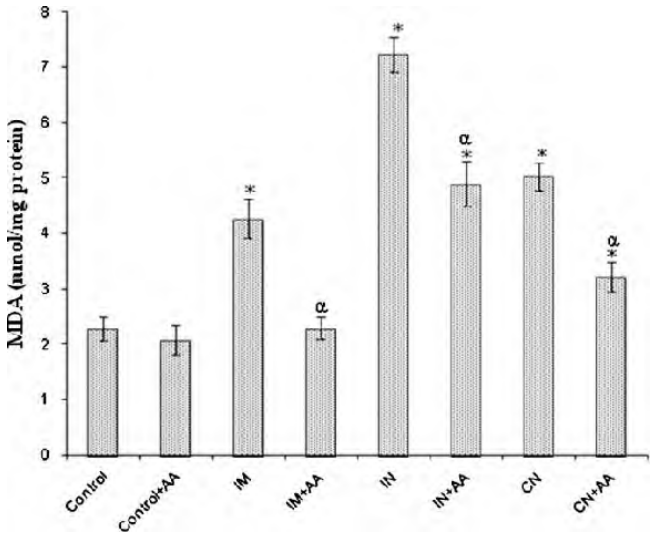

Fig. 7. Showing the inhibitory effect of ascorbic acid on cellular MDA levels of A_{549} cells under indicated conditions of 48-h exposure. #AA (1.5 mM L-ascorbic acid); IM (200 μg/ml indigenous microtalc); IN (200 μg/ml indigenous nanotalc); CN (200 μg/ml commercial nanotalc) Values are mean ± SD from three independent experiments. *Denotes a significant difference from the control ($p < 0.05$). α indicates the significant inhibitory effect of ascorbic acid (AA) on lipid peroxidation versus either, IM, IN or CN.

4. Discussion

At present, an *in vitro* toxicological study of talc nanoparticles is lacking. In this study, the cytotoxicity of two types of talc nanoparticles was investigated in cultured human bronchoalveolar carcinoma-derived cells (A_{549}). This cell line has been widely used in *in vitro* cytotoxicity studies (Huang et al., 2004; Bakand et al., 2006). Present study showed that the two types of talc nanoparticles caused significant reduction in cell viability as a function of concentration and their iron content. The talc nanoparticles from two sources induced the enhanced generation of ROS and MDA production. Consequently, redundant free radicals would interact with biomolecules including proteins, enzymes, membrane lipids and even DNA which could be oxidized, modified, destructured and ultimately dysfunctioned (Marnett, 2000; Hensley and Floyd, 2002).

Oxidative stress has been suggested to play an important role in the mechanism of toxicity of a number of compounds whether by production of free radicals or by depleting cellular antioxidant capacity. Cellular integrity is affected by oxidative stress when the production of ROS overwhelms antioxidant defense mechanism (Halliwell et al., 1992; Chen and Yu, 1994). ROS are oxygen-containing molecules, such as hydrogen peroxide (H_2O_2), superoxide anion ($O_2^{\cdot-}$), and hydroxyl radical ($HO^{\cdot}$), that have a greater chemical activity than molecular oxygen. ROS are generated in many inflammatory conditions in the lung and have been associated with cell injury and apoptosis (Anderson et al., 1994; Meyer et al., 1993). Many other studies have shown that nanoparticles may produce toxicity by generating ROS. Recently, Buz'Zard and Lau (2007) have reported enhanced ROS generation in human ovarian cell culture and have found an increased cell proliferation and neoplastic transformation of human ovarian stromal and epithelial cells exposed with talc. In the present study too, talc micro and nanoparticles induced significantly higher ROS generation compared with untreated A_{549} cells when using the fluorescent dichlorofluorescin probe. Moreover, indigenous nanotalc resulted higher ROS generation than commercial nanotalc.

GSH is the most abundant nonproteinous tripeptide containing a sulfhydryl group in virtually all cells, and it plays a significant role in many biological processes. It also constitutes the first line of the cellular defense mechanism against oxidative injury and is the major intracellular redox buffer in ubiquitous cell types (Meister, 1989). GSH acts as a cosubstrate in the GSH peroxidase-catalyzed reduction of hydrogen peroxide or lipid peroxides (Forman et al., 1997) leading to its depletion. Previous studies demonstrated that ROS generation following GSH depletion caused mitochondrial damage (Martensson et al., 1989; Meister, 1995), which has been implicated in apoptosis (Green and Reed, 1998). There was a significant depletion of GSH between the control and the treated groups except for indigenous microtalc at 50 μg/ml. In terms of GSH depletion, indigenous nanotalc was found to be the most toxic.

In the toxicity mechanism of minerals, the iron content has been a key factor. Iron-dependent ROS generation from fibers results in the generation of hydroxyl radicals through the Fenton reaction and the Haber–Weiss cycle. Iron-dependent LPO could be important, since this process requires redox cycling of iron and does not necessarily require H_2O_2 or ROS (Halliwell and Gutteridge, 1990). Indeed, iron has a key role in both the initiation and propagation of LPO, leading to the generation of peroxyl and alkoxyl radicals as well as lipid peroxides (Halliwell and Gutteridge, 1990). It has been known for several years that the surface iron (II) or leachable iron (II) on mineral surfaces reduces molecular oxygen to superoxide anion, which then dismutates to hydrogen peroxide. In the presence of asbestos or silica, hydrogen peroxide and superoxide react via a Fenton-like reaction driven by iron to form the potent hydroxyl radical *in vitro* leading to cellular LPO (Mossman et al., 1996). Since, LPO is a sensitive parameter for toxic effects of various environmental pollutants with oxidative properties (Krug and Culig, 1991; Beck-Speier et al., 2001; Oberdorster, 2004; Sayes et al., 2005); the authors suspected that the relatively high iron content in both the nanotalc may play a key role to yield higher ROS and in turn caused higher LPO. There are other nanomaterials, such as C_{60}, which mediates cytotoxicity primarily through lipid peroxidation (Sayes et al., 2005; Isakovic et al., 2006) whereas carboxyfullerenes (made by certain surface modifications of C_{60}) have been shown to impart cytoprotective activity by eliminating reactive oxygen species (ROS) and antago-

nizing the effects of the oxidative stress-dependent cytotoxicity (Dugan et al., 1997, 2001; Bogdanovic et al., 2004; Isakovic et al., 2006). Recently Scarfì et al. (2009) has reported that plasma membrane contact with quartz, a kind of silica, is sufficient to trigger membrane LPO, TNF-α release and cell death in mouse macrophage cell line RAW 264.7. The authors hypothesize that contact of particles with cell membranes initiate ROS generation and LPO in a ratio of amount of iron present in talc nanoparticles.

For a given mass compared with larger particles, the ratio of surface to total atoms or molecules increases exponentially with decreasing particle size. Particle size is thereby an essential determinant of the fraction of reactive groups on particle surface (Oberdorster et al., 2005; Nel et al., 2006). For example, several studies found that ultrafine particles of titania are more toxic than its larger counterparts having the same chemical composition (Donaldson et al., 1998; Gilmour et al., 1997; Oberdorster et al., 1992, 1995; Oberdorster, 1996, 2000). Similarly, surface area-dependent induction of oxidative stress and consequently, proinflammatory effects have been found to correlate in case of polystyrene particles by Brown et al. (2001) and Lin et al. (2006) have reported higher toxicity of the two sizes (15 and 46 nm) of silica nanoparticles than micro silica (5 μm) on A_{549} cells. Here two sizes (15 and 46 nm) of silica nanoparticles induced no significant differences in the toxicity and similar was the case in a study done by Sayes et al. (2006), where smaller nanoparticles of titania had effects comparable to larger nanoparticles of titania but showed a phase-dependent differential toxicity where anatase titania (photoactive phase), able to generate ROS more strongly, was 100 times more toxic than an equivalent sample of rutile titania. In the present study, both nanoparticles would have been resulted differential surface iron activity per given mass resulting in differential toxicity. When indigenous nanotalc induced toxicity is compared with indigenous microtalc, size-dependent factor becomes apparent because all the compositional factors are constant. But when commercial nanotalc (having larger surface area but lower iron content) induced toxicity is compared with indigenous microtalc, the results show a complex function of size and impurities. Since, micro talc size is very large (50–65 μm), than commercial nanotalc (70–120 nm), perhaps size becomes the primary determinant of toxicity, resulting in higher toxicity of commercial nanotalc than indigenous micro talc.

Another pathway of free radical generation by asbestos, silica or particulates like these (e.g. talc particles) occurs via an oxidative burst when fibers and particles are phagocytised by AMs or other cell types, including alveolar epithelial cells and fibroblasts (Churg, 1996). Phagocytic cells can endocytose small particles, whereas bigger crystals and fibers are subject to so called "frustrated phagocytosis". Experimental studies suggest that in *in vivo* conditions "frustrated phagocytosis" appears to have a dramatic influence on the sustained generation of ROS (Hansen and Mossman, 1987; Vallyathan et al., 1992). Repeated "frustrated phagocytosis" would be expected to attract more phagocytes, resulting in chronic enhanced generation of ROS, which in turn contribute to inflammasome activation, resulting in the secretion of IL-1β leading to the initiation of pulmonary fibrosis (Dostert et al., 2008; Cassel et al., 2008). Since, talc and asbestos are physically and chemically similar, found together in nature and being particulate structure like silica and asbestos, talc particles may also generate ROS through activation of NADPH oxidase by frustrated phagocytosis, leading to the initiation of so called talcosis particularly in occupationally exposed workers.

Antioxidants, such as α-tocopherol, uric acid and L-ascorbic acid, typically prevent cellular damages caused by oxygen radicals by acting as ROS scavengers (Packer et al., 1979; Burton and Ingold, 1981). Ascorbic acid (or vitamin C) acts as a potent water soluble antioxidant in biological fluids (Frei et al., 1989, 1990) by scavenging physiologically relevant ROS and reactive nitrogen species (RNS) (Halliwell, 1996). However, it should be noted that antioxidative potential of ascorbic acid has not been validated in certain conditions (Bowry et al., 1992; Poulsen et al., 1998; Levine et al., 1998). Ascorbic acid contributes significantly to cellular antioxidation as a water soluble chain-breaking radical scavenger (Asard, 2008) and to the recycling of plasma membrane α-tocopherol (vitamin E) via the reduction of the α-tocopheroxyl radical (Aguirre and May, 2008). The latter activity may assist ascorbic acid to protect against LPO in membranes (May et al., 1998). We, therefore, tested the LPO preventive potential of antioxidant L-ascorbic acid, on nanotalc and microtalc challenged A_{549} cells. Results show that 1.5 mM L-ascorbic acid effectively, but not completely, inhibited MDA level induced by talc nanoparticles. Determining the optimum concentration of ascorbic acid that might completely suppress LPO without causing any side-effect is a matter of concern (Halliwell, 1999) and the evaluation of interrelationship between LPO and chelating effect of iron present on the surface of talc particles by deferoxamine mesylate on LPO is under investigation. Oxidative stress is known to elicit varying effects on the activity of antioxidant enzymes. The three primary scavenger enzymes involved in detoxifying ROS in mammalian systems are catalase, superoxide dismutase and glutathione peroxidase (MatÉs et al., 1999). For example the activity of GPx can provide important clue about the consumption rate of GSH in enzymatic detoxification of ROS. The activity of antioxidant enzymes can therefore provide further insight in understanding the mechanism of toxicity caused by talc particles and is currently under investigation.

5. Conclusion

We have presented a preliminary data on the toxicity response elicited by the two types of talc nanoparticles, depending on their different geological origin. Since, talc with a multitude of physical and functional characteristics due to different geological context and deposits, is used for particular applications, so occupational and consumer exposures to talc and its toxic effects are likely to vary accordingly, which is obvious in this study. The cytotoxicity seems to be due to primarily through induction of LPO, as a potential mechanism of toxicity discussed above. Addition of 1.5 mM of L-ascorbic acid, a ROS scavenger, significantly, though not completely, reduced LPO. Data clearly suggest that exposure of talc, particularly nanopowder, should be protected in humans at risk of occupational as well as domestic exposure.

Acknowledgments

One of the authors (MJA) gratefully acknowledges the financial support provided by University Grants Commission (UGC), Govt. of India and CSIR networked project (NWP-17). The authors thank Dr. Alok Dhawan (*In Vitro* Toxicology Division, IITR, Lucknow, India) for providing DLS measurements. The IITR Communication no. of this article is 2782.

References

Aguirre, R., May, J.M., 2008. Inflammation in the vascular bed: importance of vitamin C. Pharmacology and Therapeutics 119, 96–103.

Anderson, M.T., Staal, F.J., Gitler, C., Herzenberg, L.A., 1994. Separation of oxidant-initiated and redox-regulated steps in the NF-κB signal transduction pathway. Proceedings of the National Academy of Sciences USA 91, 11527–11531.

Asard, H., 2008. Ascorbate. In: Banerjee, R. (Ed.), Redox Biochemistry. A John Wiley and Sons Inc., Hoboken, pp. 22–27.

Bakand, S., Winder, C., Khalil, C., Hayes, A., 2006. A novel in vitro exposure technique for toxicity testing of selected volatile organic compounds. Journal of Environmental Monitoring 8, 100–105.

Beck-Speier, I., Dayal, N., Karg, E., Maier, K.L., Roth, C., Ziesenis, A., Heyder, J., 2001. Agglomerates of ultrafine particles of elemental carbon and TiO_2 induce generation of lipid mediators in alveolar macrophages. Environmental Health Perspective 109, 613–618.

Bogdanovic, G., Kojic, V., Dordevic, A., Canadanovic-Brunet, J., Vojinovic-Miloradov, M., Baltic, V.V., 2004. Modulating activity of fullerol C-60 $(OH)_{(22)}$ on doxorubicin-induced cytotoxicity. Toxicology in Vitro 18, 629–637.

Borm, P.J., Robbins, D., Haubold, S., Kuhlbusch, T., Fissan, H., Donaldson, K., Schins, R., Stone, V., Kreyling, W., Lademann, J., 2006. The potential risks of nanomaterials: a review carried out for ECETOC. Particle and Fibre Toxicology 3, 11.

Bowry, V.W., Ingold, K.U., Stocker, R., 1992. Vitamin-E in human low density-lipoprotein—when and how this antioxidant becomes a prooxidant. Biochemical Journal 4, 288–341.

Bradford, M.M., 1976. A rapid and sensitive method for the quantitation of microgram quantities of protein utilizing the principle of protein-dye binding. Analytical Biochemistry 72, 248–254.

Brown, D.M., Wilson, M.R., MacNee, W., Stone, V., Donaldson, K., 2001. Size-dependent proinflammatory effects of ultrafine polystyrene particles: a role for surface area and oxidative stress in the enhanced activity of ultrafines. Toxicology and Applied Pharmacology 175, 191–199.

Burton, G.W., Ingold, K.U., 1981. Autoxidation of biological molecules. 1. The antioxidant activity of vitamin-E and related chain-breaking phenolic antioxidants in vitro. Journal of the American Chemical Society 103, 6472–6477.

Buz'Zard, A.R., Lau, B.H., 2007. Pycnogenol reduces talc-induced neoplastic transformation in human ovarian cell cultures. Phytotherapy Research 21, 579–586.

Cassel, S.L., Eisenbarth, S.C., Iyer, S.S., Sadler, J.J., Colegio, O.R., Tephly, L.A., Carter, A.B., Rothman, P.B., Flavell, R.A., Sutterwala, F.S., 2008. The Nalp3 inflammasome is essential for the development of silicosis. Proceedings of the National Academy of Sciences USA 105, 9035–9040.

Chang, S., Risch, H.A., 1997. Perineal talc exposure and risk of ovarian carcinoma. Cancer 79, 2396–2401.

Chen, J.J., Yu, B.P., 1994. Alteration in mitochondrial membrane fluidity by lipid peroxidation products. Free Radical Biology and Medicine 17, 411–418.

Churg, A., 1996. The uptake of mineral particles by pulmonary epithelial cells. American Journal of Respiratory and Critical Care Medicine 154, 1124–1140.

Cook, L.S., Kamb, M.L., Weiss, N.S., 1997. Perineal powder exposure and the risk of ovarian cancer. American Journal of Epidemiology 145, 459–465.

Cramer, D.W., Liberman, R.E., Titus-Ernstoff, L., Welch, W.R., Greenberg, E.R., Baron, J.A., Harlow, B.L., 1999. Genital talc exposure and risk of ovarian cancer. International Journal of Cancer 81, 351–356.

Croute, F., Gaubin, Y., Prevost, M.C., Beaupain, R., Pianezzi, B., Soleihavoup, J.P., 1990. Effects of hypergravity on lung carcinoma cells maintained in continuous organotypic culture. Aviation, Space, and Environmental Medicine, 1002–1006.

Donaldson, K., Li, X.Y., MacNee, W., 1998. Ultrafine (nanometre) particle mediated lung injury. Journal of Aerosol Science 29, 553–560.

Donaldson, K., Brown, D., Clouter, A., Duffin, R., MacNee, W., Renwick, L., Tran, L., Stone, V., 2002. The pulmonary toxicology of ultrafine particles. Journal of Aerosol Medicine 15, 213–220.

Dostert, C., Pétrilli, V., Bruggen, R.V., Steele, C., Mossman, B.T., Tschopp, J., 2008. Innate immune activation through Nalp3 inflammasome sensing of asbestos and silica. Science 320, 674–677.

Dugan, L.L., Lovett, E.G., Quick, K.L., Lotharius, J., Lin, T.T., O'Malley, K.L., 2001. Fullerene-based antioxidants and neurodegenerative disorders. Parkinsonism and Related Disorders 7, 243–246.

Dugan, L.L., Turetsky, D.M., Du, C., Lobner, D., Wheeler, M., Almli, C.R., Clifton, K.F., Shen, C.K.F., Luh, T.Y., Choi, D.W., Lin, T.S., 1997. Carboxyfullerenes as neuroprotective agents. Proceedings of the National Academy of Sciences USA 94, 9434–9439.

Forman, H.J., Liu, R., Tian, L., 1997. Glutathione cycling in oxidative stress. In: Clerch, L.B., Massaro, D.J. (Eds.), Oxygen, Gene Expression, and Cellular Function: Lung Biology in Health and Disease, vol. 105. Marcel Dekker, New York, pp. 99–112.

Frei, B., England, L., Ames, B.N., 1989. Ascorbate is an outstanding antioxidant in human blood plasma. Proceedings of the National Academy of Sciences USA 86, 6377–6381.

Frei, B., Stocker, R., England, L., Ames, B.N., 1990. Ascorbate: the most effective antioxidant in human blood plasma. Advances in Experimental Medicine and Biology 264, 155–163.

Gates, M.A., Tworoger, S.S., Terry, K.L., Titus-Ernstoff, L., Rosner, B., Vivo, I.D., Cramer, D.W., Hankinson, S.E., 2008. Talc use, variants of the *GSTM1*, *GSTT1*, and *NAT2* genes, and risk of epithelial ovarian cancer. Cancer Epidemiology, Biomarkers and Prevention 17, 2436–2444.

Gilmour, P., Brown, D.M., Beswick, P.H., Benton, E., MacNee, W., Donaldson, K., 1997. Surface free radical activity of PM10 and ultrafine titanium dioxide: A unifying factor in their toxicity? The Annals of Occupational Hygiene 41 (Suppl. 1), 32–38.

Green, D.G., Reed, J.C., 1998. Mitochondria and apoptosis. Science 281, 1309–1312.

Halliwell, B., Gutteridge, J.M., 1990. Role of free radicals and catalytic metal ions in human disease: an overview. Methods in Enzymology 186, 1–85.

Halliwell, B., 1996. Vitamin C: antioxidant or pro-oxidant in vivo? Free Radical Research 25, 439–454.

Halliwell, B., 1999. Establishing the significance and optimal intake of dietary antioxidants: the biomarker concept. Nutrition Reviews 57, 104–113.

Halliwell, B., Gutteridge, J.M., Cross, C.E., 1992. Free radicals, antioxidants, and human disease: where are we now? The Journal of Laboratory and Clinical Medicine 119, 598–620.

Hansen, K., Mossman, B.T., 1987. Generation of superoxide (O^{2-}) from alveolar macrophages exposed to asbestiform and non-asbestiform particles. Cancer Research 47, 1681–1686.

Hansen, M.B., Nielsen, S.E., Berg, K., 1989. Re-examination and further development of a precise and rapid dye method for measuring cell growth/kill. Journal of Immunological Methods 119, 203–210.

Harlow, B.L., Cramer, D.W., Bell, D.A., Welch, W.R., 1992. Perineal exposure to talc and ovarian cancer risk. Obstetrics and Gynecology 80, 19–26.

Harlow, B.L., Hartge, P.A., 1995. A review of perineal talc exposure and risk of ovarian cancer. Regulatory Toxicology and Pharmacology 21, 254–260.

Heller, D.S., Westhoff, C., Gordon, R.E., Katz, N., 1996. The relationship between perineal cosmetic talc usage and ovarian talc particle burden. American Journal of Obstetrics and Gynecology 174, 1507–1510.

Henderson, W.J., Joslin, C.A., Turnbull, A.C., Griffiths, K., 1971. Talc and carcinoma of the ovary and cervix. The Journal of Obstetrics and Gynaecology of the British Commonwealth 78, 266–272.

Hensley, K., Floyd, R.A., 2002. Reactive oxygen species and protein oxidation in aging: a look back, a look ahead. Archives of Biochemistry and Biophysics 397, 377–383.

Hissin, P.J., Hilf, R., 1976. A fluorometric method for determination of oxidized and reduced glutathione in tissues. Analytical Biochemistry 74, 214–226.

Hollinger, M.A., 1990. Pulmonary toxicity of inhaled and intravenous talc. Toxicology Letters 52, 121–127.

Holsapple, M.P., Farland, W.H., Landry, T.D., Monteiro-Riviere, N.A., Carter, J.M., Walker, N.J., Thomas, K.V., 2005. Research strategies for safety evaluation of nanomaterials, part II: toxicological and safety evaluation of nanomaterials, current challenges and data needs. Toxicological Sciences 88, 12–17.

Huang, M., Khor, E., Lim, L.Y., 2004. Uptake and cytotoxicity of chitosan molecules and nanoparticles: effects of molecular weight and degree of deacetylation. Pharmaceutical Research 21, 344–353.

Isakovic, A., Markovic, Z., Todorovic-Markovic, B., Nikolic, N., Vranjes-Djuric, S., Mirkovic, M., Dramicanin, M., Harhaji, L., Raicevic, N., Nikolic, Z., Trajkovic, V., 2006. Distinct cytotoxic mechanisms of pristine versus hydroxylated fullerene. Toxicological Sciences 91, 173–183.

Kipen, H.M., Laskin, D.L., 2005. Smaller is not always better: nanotechnology yields nanotoxicology. American Journal of Physiology-Lung Cellular and Molecular Physiology 289, L696–L697.

Krug, H.F., Culig, H., 1991. Directed shift of fatty-acids from phospholipids to triacylglycerols in HL-60 cells induced by nanomolar concentrations of triethyl lead chloride – involvement of a pertussis toxin-sensitive pathway. Molecular Pharmacology 39, 511–516.

Levine, M.A., Daruwala, R.C., Park, J.B., Rumsey, S.C., Wang, Y., 1998. Does vitamin C have a pro-oxidant effect? Nature (London) 395, 231.

Lieber, M., Smith, B., Szakal, A., Nelson-Rees, W., Todoro, G., 1976. A continuous tumor cell line from a human lung carcinoma with properties of type II alveolar epithelial cells. International Journal of Cancer 17, 62–70.

Lin, W., Huang, Y.W., Zhou, X.D., Ma, Y., 2006. In vitro toxicity of silica nanoparticles in human lung cancer cells. Toxicology and Applied Pharmacology 217, 252–259.

Marnett, L.J., 2000. Oxyradicals and DNA damage. Carcinogenesis 21, 361–370.

Martensson, J., Jain, A., Frayer, W., Meister, A., 1989. Glutathione metabolism in the lung: inhibition of its synthesis leads to lamellar body and mitochondrial defects. Proceedings of the National Academy of Sciences USA 86, 5296–5300.

MatÉs, J.M., Pérez-Gómez, C., DeCastro, I.N., 1999. Antioxidant enzymes and human diseases. Clinical Biochemistry 32, 595–603.

May, J.M., Qu, Z.-C., Mendiratta, S., 1998. Protection and recycling of α-tocopherol in human erythrocytes by intracellular ascorbic acid. Archives of Biochemistry and Biophysics 349, 281–289.

Meister, A., 1989. Molecular properties and clinical applications. In: Glutathione Centennial. Academic Press, New York.

Meister, A., 1995. Mitochondrial changes associated with glutathione deficiency. Biochemica et Biophysica Acta 1271, 35–42.

Meyer, M., Schreck, R., Baeuerle, P.A., 1993. H_2O_2 and antioxidants have opposite effects on activation of NF-κB and AP-1 in intact cells: AP-1 as secondary antioxidant-responsive factor. The EMBO Journal 12, 2005–2015.

Mills, P.K., Riordan, D.G., Cress, R.D., Young, H.A., 2004. Perineal talc exposure and epithelial ovarian cancer risk in the Central Valley of California. International Journal of Cancer 112, 458–464.

Mossman, T., 1983. Rapid colorimetric assay for cellular growth and survival: application to proliferation and cytotoxicity assays. Journal of Immunological Methods 65, 55–63.

Mossman, B.T., Kamp, D.W., Weitzman, S.A., 1996. Mechanisms of carcinogenesis and clinical features of asbestos-associated cancers. Cancer Investigation 14, 466–480.

National Toxicology Program, 1993. NTP Toxicology and Carcinogenesis Studies of Talc (Non-asbestiform) in Rats and Mice (Inhalation Studies), vol. 421, pp. 1–287.

Nel, A., Xia, T., Madler, L., Li, N., 2006. Toxic potential of materials at the nanolevel. Science 311, 622–627.

Oberdorster, G., Ferin, J., Gelein, R., Soderholm, S., Finkelstein, J., 1992. Role of alveolar macrophage in lung injury: studies with ultrafine particles. Environmental Health Perspective 97, 193–199.

Oberdorster, G., Gelein, R., Ferin, J., Weiss, B., 1995. Association of particulate air pollution and acute mortality: involvement of ultrafine particles? Inhalation Toxicology 7, 111–124.

Oberdorster, G., 1996. Significance of particle parameters in the evaluation of exposure–dose–response relationships of inhaled particles. Inhalation Toxicology 8, 73–89.

Oberdorster, G., 2000. Toxicology of ultrafine particles: in vivo studies. Philosophical Transactions of the Royal Society 358, 2719–2740.

Oberdorster, E., 2004. Manufactured nanomaterials (fullerenes, C-60) induce oxidative stress in the brain of juvenile largemouth bass. Environmental Health Perspective 112, 1058–1062.

Oberdorster, G., Oberdorster, E., Oberdorster, J., 2005. Nanotoxicology: an emerging discipline evolving from studies of ultrafine particles. Environmental Health Perspective 113, 823–839.

Ohkawa, H., Ohisi, N., Yagi, Y., 1979. Assay for lipid peroxides in animal tissues by thiobarbituric acid reaction. Analytical Biochemistry 95, 351–358.

Packer, J.E., Slater, T.F., Willson, R.L., 1979. Direct observation of a free radical interaction between vitamin E and vitamin C. Nature (London) 278, 737–738.

Poulsen, H.E., Weimann, A., Salonen, J.T., Nyyssonen, K., Loft, S., Cadet, J., Douki, T., Ravanat, J., 1998. Does vitamin C have a pro-oxidant effect? Nature (London) 395, 231–232.

Sayes, C.M., Gobin, A.M., Ausman, K.D., Mendez, J., West, J.L., Colvin, V.L., 2005. Nano-C (60) cytotoxicity is due to lipid peroxidation. Biomaterials 26, 7587–7595.

Sayes, C.M., Wahi, R., Kurian, P.A., Liu, Y., West, J.L., Ausman, K.D., Warheit, D.B., Colvin, V.L., 2006. Correlating nanoscale titania structure with toxicity: a cytotoxicity and inflammatory response study with human dermal fibroblasts and human lung epithelial cells. Toxicological Sciences 92, 174–185.

Scarfi, S., Magnone, M., Ferraris, C., Pozzolini, M., Benvenuto, F., Benatti, U., Giovine, M., 2009. Ascorbic acid pre-treated quartz stimulates TNF-α release in RAW 264.7 murine macrophages through ROS production and membrane lipid peroxidation. Respiratory Research 10, 25.

Vallyathan, V., Mega, J.F., Shi, X., Dalal, N.S., 1992. Enhanced generation of free radicals from phagocytes induced by mineral dusts. American Journal of Respiratory Cell and Molecular Biology 6, 404–413.

Wang, H., Joseph, J.A., 1999. Quantifying cellular oxidative stress by dichlorofluorescin assay using microplate reader. Free Radical Biology and Medicine 27, 612–616.

Welder, A.A., Grant, R., Bradlaw, J., Acosta, D., 1991. A primary culture system of adult rat heart cells for the study of toxicologic agent. In Vitro Cellular and Developmental Biology 27A, 921–926.

Wild, P., 2006. Lung cancer risk and talc not containing asbestiform fibres: a review of the epidemiological evidence. Occupational and Environmental Medicine 63, 4–9.

Werebe, E.C., Pazetti, R., 1999. Systemic distribution of talc after intrapleural administration in rats. Chest 115, 190–193.

Wroblewski, F., LaDue, J.S., 1955. Lactate dehydrogenase activity in blood. Proceedings of the Society for Experimental Biology and Medicine 90, 210–213.

Exhibit 97

Original Article

Reproductive Sciences
1-10

DOI: 10.1177/1933719119831773
journals.sagepub.com/home/rsx
SAGE

Molecular Basis Supporting the Association of Talcum Powder Use With Increased Risk of Ovarian Cancer

Nicole M. Fletcher, PhD[1], Amy K. Harper, MD[2], Ira Memaj, BS[1], Rong Fan, MS[1], Robert T. Morris, MD[2], and Ghassan M. Saed, PhD[1,2]

Abstract

Genital use of talcum powder and its associated risk of ovarian cancer is an important controversial topic. Epithelial ovarian cancer (EOC) cells are known to manifest a persistent prooxidant state. Here we demonstrated that talc induces significant changes in key redox enzymes and enhances the prooxidant state in normal and EOC cells. Using real-time reverse transcription polymerase chain reaction and enzyme-linked immunosorbent assay, levels of CA-125, caspase-3, nitrate/nitrite, and selected key redox enzymes, including myeloperoxidase (MPO), inducible nitric oxide synthase (iNOS), superoxide dismutase (SOD), catalase (CAT), glutathione peroxidase (GPX), and glutathione reductase (GSR), were determined. TaqMan genotype analysis utilizing the QuantStudio 12K Flex was used to assess single-nucleotide polymorphisms in genes corresponding to target enzymes. Cell proliferation was determined by MTT proliferation assay. In all talc-treated cells, there was a significant dose-dependent increase in prooxidant iNOS, nitrate/nitrite, and MPO with a concomitant decrease in antioxidants CAT, SOD, GSR, and GPX ($P < .05$). Remarkably, talc exposure induced specific point mutations that are known to alter the activity in some of these key enzymes. Talc exposure also resulted in a significant increase in inflammation as determined by increased tumor marker CA-125 ($P < .05$). More importantly, talc exposure significantly induced cell proliferation and decreased apoptosis in cancer cells and to a greater degree in normal cells ($P < .05$). These findings are the first to confirm the cellular effect of talc and provide a molecular mechanism to previous reports linking genital use to increased ovarian cancer risk.

Keywords

talc, epithelial ovarian cancer, oxidative stress, single-nucleotide polymorphism, cell proliferation

Introduction

Ovarian cancer is the most lethal gynecologic malignancy and ranks fifth in cancer deaths among women diagnosed with cancer.[1] Epithelial ovarian cancer (EOC) has long been considered a heterogeneous disease with respect to histopathology, molecular biology, and clinical outcome.[1,2] Although surgical techniques and treatments have advanced over the years, the prognosis of EOC remains poor, with a 5-year survival rate of 50% in advanced stage.[2] This is largely due to the lack of early warning symptoms and screening methods and the development of chemoresistance.[1,2] Moreover, ovarian cancer is known to be associated with germline mutations in the *BRCA1* or *BRCA2* genes, but with a rate of only 20 % to 40%, suggesting the presence of other unknown mutations in other predisposition genes.[3] Additional genetic variations including single-nucleotide polymorphisms (SNPs) have been hypothesized to act as low to moderate penetrant alleles that contribute to ovarian cancer risk.[3,4]

The pathophysiology of EOC is not fully understood but has been strongly associated with inflammation and the resultant oxidative stress.[5] We have previously characterized EOC cells to manifest a persistent prooxidant state as evident by the upregulation of key oxidants and downregulation of key antioxidants, which is further enhanced in chemoresistant EOC cells.[6] The expression of key prooxidant/inflammatory enzymes such as inducible nitric oxide synthase (iNOS), nicotinamide adenine dinucleotide phosphate (NAD(P)H) oxidase, and myeloperoxidase (MPO), as well as an increase in nitric oxide (NO) levels, was increased in EOC tissues and cells.[6] Additionally, we have shown that EOC cells manifest lower apoptosis, which

[1] Department of Obstetrics and Gynecology, Wayne State University School of Medicine, Detroit, MI, USA
[2] Department of Gynecologic Oncology, Karmanos Cancer Institute, Detroit, MI, USA

Corresponding Author:
Ghassan M. Saed, Departments of Obstetrics and Gynecology and Oncology, Karmanos Cancer Institute, Wayne State University School of Medicine, Detroit, MI 48201, USA.
Email: gsaed@med.wayne.edu

was markedly induced by inhibiting iNOS, indicating a strong link between apoptosis and NO/iNOS pathways in these cells.[6]

The cellular redox balance is maintained by key antioxidants including catalase (CAT), superoxide dismutase (SOD), or by glutathione peroxidase (GPX) coupled with glutathione reductase (GSR).[5] Other important scavengers include thioredoxin coupled with thioredoxin reductase, and glutaredoxin, which utilizes glutathione (GSH) as a substrate.[7] We have previously reported that a genotype switch in key antioxidants is a potential mechanism leading to the acquisition of chemoresistance in EOC cells.[7] We have studied the effects of genetic polymorphisms in key redox genes on the acquisition of the oncogenic phenotype in EOC cells, including genes that control the levels of cellular reactive oxygen species and oxidative damage and SNPs for genes involved in carcinogen metabolism (detoxification and/or activation), antioxidants, and DNA repair pathways.[4,6] Several function-altering SNPs have been identified in key antioxidants, including CAT, GPX, GSR, and SOD.[4]

Several studies have suggested the possible association between genital use of talcum powder and risk of EOC.[7-12] Association between the use of cosmetic talc in genital hygiene and ovarian cancer was first described in 1982 by Cramer et al, and many subsequent studies supported this finding.[7-12] Talc and asbestos are both silicate minerals; the carcinogenic effects of asbestos have been extensively studied and documented in the medical literature.[7-12] Asbestos fibers in the lung initiate an inflammatory and scarring process, and it has been proposed that ground talc, as a foreign body, might initiate a similar inflammatory response.[7] The objective of this study was to determine the effects of talcum powder on the expression of key redox enzymes, CA-125 levels, and cell proliferation and apoptosis in normal and EOC cells.

Material and Methods

Cell Lines

Ovarian cancer cells SKOV-3 (ATCC), A2780 (Sigma Aldrich, St Louis, Missouri), and TOV112D (a kind gift from Gen Sheng Wu at Wayne State University, Detroit, Michigan) and normal cells human macrophages (EL-1; ATCC, Manassas, Virginia), human primary normal ovarian epithelial cells (Cell Biologics, Chicago, Illinois), human ovarian epithelial cells (HOSEpiC; ScienCell Research Laboratories, Inc, Carlsbad, California), and immortalized human fallopian tube secretory epithelial cells (FT33; Applied Biological Materials, Richmond, British Columbia, Canada) were used. All cells were grown in media and conditions following manufacturer's protocol. EL-1 cells were grown in IMDM media (ATCC) supplemented with 0.1 mM hypoxanthine and 0.1 mM thymidine solution (H-T, ATCC) and 0.05 mM β-mercaptoethanol. SKOV-3 EOC cells were grown in HyClone McCoy's 5A medium (Fisher Scientific, Waltham, Massachusetts), A2780 EOC cells were grown in HyClone RPMI-1640 (Fisher Scientific), and both TOV112D EOC cells were grown in MCDB105 (Cell Applications, San Diego, California) and Medium 199 (Fisher Scientific; 1:1). All media were supplemented with fetal bovine serum (Innovative Research, Novi, Michigan) and penicillin/streptomycin (Fisher Scientific), per their manufacturer specifications. Human primary normal ovarian epithelial cells were grown in complete human epithelial cell medium (Cell Biologics).

Treatment of Cells

Talcum baby powder (Johnson & Johnson, New Brunswick, NJ, #30027477, Lot#13717RA) was dissolved in dimethyl sulfoxide (DMSO; Sigma Aldrich) at a concentration of 500 mg in 10 mL and was filtered with a 0.2 µm syringe filter (Corning). Sterile DMSO was used as a control for all treatments. Cells were seeded in 100-mm cell culture dishes (3×10^6) and were treated 24 hours later with 5, 20, or 100 µg/mL of talc for 72 hours. Cell pellets were collected for RNA, DNA, and protein extraction. Cell culture media were collected for CA-125 analysis by enzyme-linked immunosorbent assay (ELISA).

Real-Time Reverse Transcription Polymerase Chain Reaction

Total RNA was extracted from all cells using the RNeasy mini kit (Qiagen, Valencia, California). Measurement of the amount of RNA in each sample was performed using a Nanodrop spectrophotometer (Thermo Fisher Scientific, Waltham, Massachusetts). A 20 µL complementary DNA reaction volume containing 0.5 µg RNA was prepared using the SuperScript VILO Master Mix Kit (Life Technologies, Carlsbad, California). Optimal oligonucleotide primer pairs were selected for each target using Beacon designer (Premier Biosoft, Inc; Table 1). Quantitative reverse transcription polymerase chain reaction (RT-PCR) was performed using the EXPRESS SYBR GreenER qPCR supermix kit (Life Technologies) and the Cepheid 1.2f detection system (Sunnyvale, CA) previously described.[6] Standards with known concentrations and lengths were designed specifically for β-*actin* (79 bp), *CAT* (105 bp), *NOS2* (89 bp), *GSR* (103 bp), *GPX1* (100 bp), *MPO* (79 bp), and *SOD3* (84 bp), allowing for construction of a standard curve using a 10-fold dilution series.[6] All samples were normalized to β-*actin*. A final melting curve analysis was performed to demonstrate specificity of the PCR product.

Protein Detection

Cell pellets were lysed utilizing cell lysis buffer (20 mM Tris–HCl [pH 7.5], 150 mM NaCl, 1 mM Na_2EDTA, 1 mM EGTA, 1% Triton, 2.5 sodium pyrophosphate, 1 mM β-glycerophosphate, 1 mM Na_3VO_4, 1 µg/mL leupeptin) containing a cocktail of protease inhibitors. Samples were centrifuged at 13 000 rpm for 10 minutes at 4°C. Total protein concentration of cell lysates from control and talc-treated cells was measured with the Pierce BCA protein assay kit (Thermo Scientific, Rockford, Illinois).

Table 1. Real-Time RT-PCR Oligionucleotide Primers.

Accession Number	Gene	Sense (5′-3′)	Antisense (3′-5′)	Amplicon (bp)	Annealing Time (seconds) and Temperature (°C)
NM_001101	β-*actin*	ATGACTTAGTTGCGTTACAC	AATAAAGCCATGCCAATCTC	79	10, 64
NM_001752	*CAT*	GGTTGAACAGATAGCCTTC	CGGTGAGTGTCAGGATAG	105	10, 63
NM_003102	*SOD3*	GTGTTCCTGCCTGCTCCT	TCCGCCGAGTCAGAGTTG	84	60, 64
NM_000637	*GSR*	TCACCAAGTCCCATATAGAAATC	TGTGGCGATCAGGATGTG	116	10, 63
NM_000581	*GPX1*	GGACTACACCCAGATGAAC	GAGCCCTTGCGAGGTGTAG	91	10, 66
NM_000625	*NOS2*	GAGGACCACATCTACCAAGGAGGAG	CCAGGCAGGCGGAATAGG	89	30, 59
NM_000250	*MPO*	CACTTGTATCCTCTGGTTCTTCAT	TCTATATGCTTCTCACGCCTAGTA	79	60, 63

Abbreviation: RT-PCR, reverse transcription polymerase chain reaction.

Detection of Protein/Activity by ELISA

The following ELISA kits were used (Cayman Chemical, Ann Arbor, Michigan): CAT, SOD, GSR, GPX, and MPO. Nitrite (NO_2^-)/nitrate (NO_3^-) were determined spectrophotometrically by Griess assay as previously reported.[6] CA-125 protein levels were measured in cell media by ELISA (Ray Biotech, Norcross, Georgia).

TaqMan SNP Genotyping Assay

DNA was isolated utilizing the EZ1 DNA tissue kit (Qiagen) for EOC cells. The TaqMan SNP genotyping assay set (Applied Biosystems, Carlsbad, California; NCBI dbSNP genome build 37, MAF source 1000 genomes) was used to genotype the SNPs (Table 1). The Applied Genomics Technology Center (AGTC, Wayne State University) performed these assays. Analysis was done utilizing the QuantStudio 12 K Flex real-time PCR system (Applied Biosystems).

Cell Proliferation and Apoptosis

Cell proliferation was assessed with the TACS MTT cell proliferation assay (Trevigen, Gaithersburg, Maryland) after treatment with talc (100 μg/mL) for 24 hours. The Caspase-3 Colorimetric Activity Assay Kit (Chemicon, Temecula, California) was used to determine levels of caspase-3 activity after treatment of normal and EOC cells with various doses of talc as previously described.[6] Equal concentrations of cell lysate were used. The assay is based on spectrophotometric detection of the chromophore p-nitroaniline (pNA) after cleavage from the labeled substrate DEVD-pNA. The free pNA can be quantified using a spectrophotometer or a microtiter plate reader at 405 nm. Comparison of the absorbance of pNA from an apoptotic sample with its control allows determination of the percentage increase in caspase-3 activity.

Statistical Analysis

Normality was examined using the Kolmogorov-Smirnov test and by visual inspection of quantile–quantile plots. Because most of the data were not normally distributed, differences in distributions were examined using the Kruskal-Wallis test. Generalized linear models were fit to examine pairwise differences in estimated least squares mean expression values by exposure to 0, 5, 20, or 100 μg/mL of talc. We used the Tukey-Kramer adjustment for multiple comparisons, and the regression models were fit using log2 transformed analyte expression values after adding a numeric constant "1" to meet model assumptions while avoiding negative transformed values. P values below .05 are statistically significant.

Results

Talc Treatment Decreased the Expression of Antioxidant Enzymes SOD and CAT in Normal and EOC Cells

Real-time RT-PCR and ELISA assays were utilized to determine the CAT and SOD messenger RNA (mRNA) and protein levels in cells before and after 72 hours talc treatment, respectively (Figure 1). The CAT (Figure 1A and C) and SOD (Figure 1B and D) mRNA and protein levels were significantly decreased in a dose-dependent manner in talc-treated cells compared to controls ($P < .05$).

Talc Treatment Increased the Expression of Prooxidants iNOS, NO_2^-/NO_3^-, and MPO in Normal and EOC Cells

Real-time RT-PCR and NO_2^-/NO_3^- assays were utilized to determine the iNOS mRNA and NO levels in cells before and after 72 hours talc treatment, respectively (Figure 2). The iNOS mRNA and NO levels were significantly increased in a dose-dependent manner in talc-treated cells as compared to their controls (Figure 2A and C, $P < .05$). As expected, there was no detectable MPO in normal ovarian and fallopian tube cells, and thus, talc treatment did not have any effect. However, MPO mRNA and protein levels were significantly increased in a dose-dependent manner in talc-treated ovarian cancer cells and macrophages compared to controls (Figure 2B and D, $P < .05$).

Talc Treatment Decreased the Expression of Antioxidant Enzymes, GPX and GSR, in Normal and EOC Cells

Real-time RT-PCR and ELISA assays were utilized to determine the GPX and GSR mRNA and protein levels in cells before and

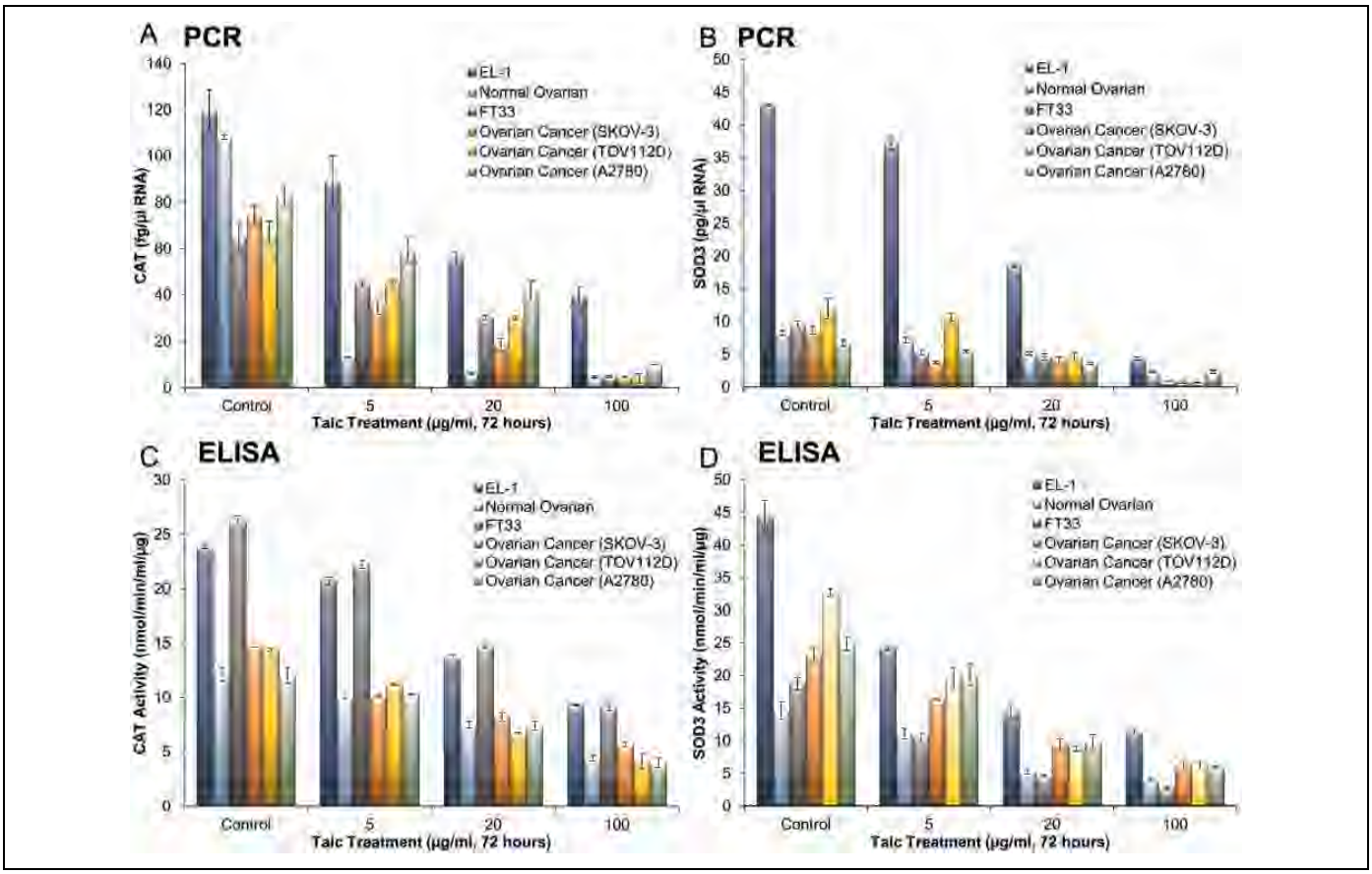

Figure 1. Decreased expression and activity of key antioxidant enzymes, CAT and SOD3. The mRNA (real-time RT-PCR) and protein/activity levels (ELISA) of CAT (A and C) and SOD3 (B and D) were determined in macrophages (EL-1), human primary ovarian epithelial cells (normal ovarian), fallopian tube (FT33), and ovarian cancer (SKOV-3, TOV112D, and A2780) cell lines before and after treatment with various doses of talc over 72 hours. Experiments were performed in triplicate. Expression is depicted as the mean, with error bars representing standard deviation. All changes in response to talc treatment were significant ($P < .05$) in all cells and in all doses as compared to controls. CAT indicates catalase; SOD3, superoxide dismutase 3; mRNA, messenger RNA; RT-PCR, reverse transcription polymerase chain reaction; ELISA, enzyme-linked immunosorbent assay.

after 72 hours of talc treatment, respectively (Figure 3). The GPX (Figure 3A and C) and GSR (Figure 3B and D) mRNA and protein levels were significantly decreased in a dose-dependent manner in talc-treated cells compared to controls ($P < .05$).

Talc Exposure Induced Known Genotype Switches in Key Oxidant and Antioxidant Enzymes

Talc treatment was associated with a genotype switch in *NOS2* from the common C/C genotype in untreated cells to T/T, the SNP genotype, in talc-treated cells, except in A2780 and TOV112D (Table 2). Additionally, the observed decrease in CAT expression and activity was associated with a genotype switch from common C/C genotype in CAT in untreated cells to C/T, the SNP genotype, in TOV112D and all normal talc-treated cells. However, there was no detectable genotype switch in CAT in A2780, SKOV3, and TOV112D (Table 2). Remarkably, there was no observed genotype switch in the selected SNP for SOD3 and GSR in all talc-treated cells. All cells, except for HOSEpiC cells, manifest the SNP genotype of *GPX1* (C/T). Intriguingly, talc treatment reversed this SNP genotype to the normal genotype (Table 2).

Talc Treatment Increased CA-125 Levels in Normal and EOC Cells

CA-125 ELISA assay was performed in protein isolated from cell media before and after talc treatment. CA-125 levels were significantly increased in a dose-dependent manner in all cells (Figure 4, $P < .05$). There was no detectable CA-125 protein in macrophages.

Talc Treatment Increased Cell Proliferation and Decreased Apoptosis

MTT cell proliferation assay was used to determine cell viability, and caspase-3 activity assay was utilized to determine apoptosis of all cell lines after 24 hours of talc treatment (Figure 5). Cell proliferation was significantly increased from the baseline in all talc-treated cells ($P < .05$), but to a greater degree in normal

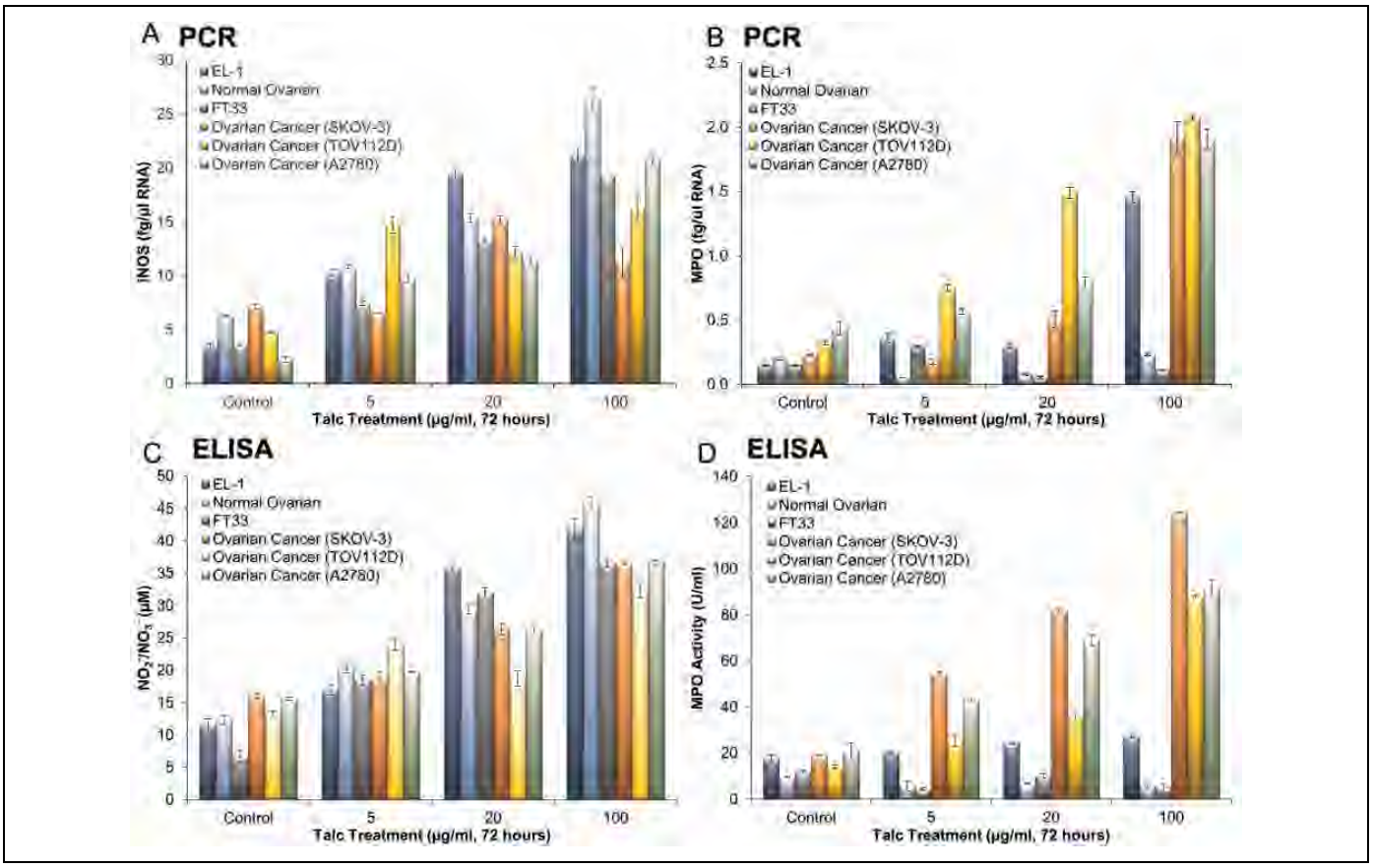

Figure 2. Increased expression and activity of key prooxidants, iNOS, NO_2^-/NO_3^-, and MPO. The mRNA (real-time RT-PCR) and protein/activity levels (ELISA) of iNOS (A and C) and MPO (B and D) were determined in macrophages (EL-1), human primary ovarian epithelial cells (normal ovarian), fallopian tube (FT33), and ovarian cancer (SKOV-3, TOV112D, and A2780) cell lines before and after treatment with various doses of talc over 72 hours. As expected, there was no detectable MPO in normal ovarian and fallopian tube cells, and thus, talc treatment did not have any effect. Experiments were performed in triplicate. Expression is depicted as the mean, with error bars representing standard deviation. All changes in response to talc treatment were significant ($P < .05$) in iNOS and MPO-positive cells and in all doses as compared to controls. iNOS indicates inducible nitric oxide synthase; MPO, myeloperoxidase; mRNA, messenger RNA; RT-PCR, reverse transcription polymerase chain reaction; ELISA, enzyme-linked immunosorbent assay.

as compared to cancer cells. As anticipated, caspase-3 was significantly reduced in cancer as compared to normal cells. Talc treatment resulted in decreased caspase-3 activity in all cells as compared to controls (Figure 6, $P < .05$), indicating a decrease in apoptosis.

Discussion

The claim that regular use of talcum powder for hygiene purpose is associated with an increased risk of ovarian cancer is based on several reports confirming the presence of talc particles in the ovaries and other parts of the female reproductive tract as well as in lymphatic vessels and tissues of the pelvis.[7-12] The ability of talc particles to migrate through the genital tract to the distal fallopian tube and ovaries is well accepted.[10] To date, the exact mechanism is not fully understood, though several studies have pointed toward the peristaltic pump feature of the uterus and fallopian tubes, which is known to enhance transport of sperm into the oviduct ipsilateral to the ovary bearing the dominant follicle.[8-12]

There are reports supporting the epidemiologic association of talc use and risk of ovarian cancer.[11,12] Recent studies have shown that risks for EOC from genital talc use vary by histologic subtype, menopausal status at diagnosis, hormone therapy use, weight, and smoking. These observations suggest that estrogen and/or prolactin may play a role via macrophage activity and inflammatory response to talc. There has been debate as to the significance of the epidemiologic studies based on the fact that the reported epidemiologic risk of talc use and risk of ovarian cancer, although consistent, are relatively modest (30%-40%), and there is inconsistent increase in risk with duration of use. This observation is due, in part, to the challenges in quantifying exposure as well as the failure of epidemiological studies to obtain necessary information about the frequency and duration of usage.[11-13]

In this study, we have shown beyond doubt that talc alters key redox and inflammatory markers, enhances cell proliferation, and inhibits apoptosis, which are hallmarks of ovarian cancer. More importantly, this effect is also manifested by talc in normal cells, including surface ovarian epithelium,

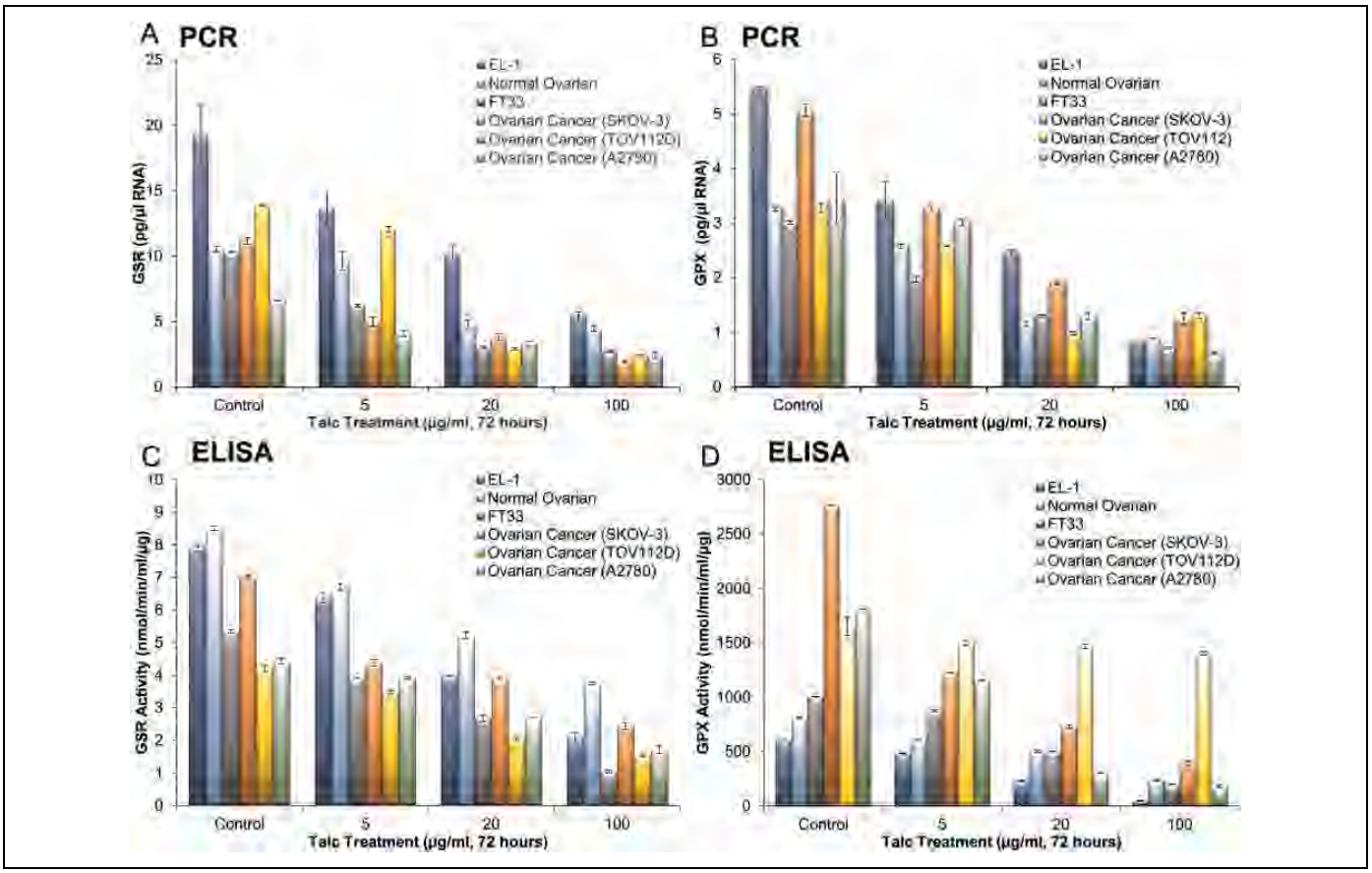

Figure 3. Decreased expression and activity of key antioxidant enzymes, GSR and GPX. The mRNA (real-time RT-PCR) and protein/activity levels (ELISA) of GSR (A and C) and GPX (B and D) were determined in macrophages (EL-1), human primary ovarian epithelial cells (normal ovarian), fallopian tube (FT33), and ovarian cancer (SKOV-3, TOV112D, and A2780) cell lines before and after treatment with various doses of talc over 72 hours. Experiments were performed in triplicate. Expression is depicted as the mean, with error bars representing standard deviation. All changes in response to talc treatment were significant ($P < .05$) in all cells and in all doses as compared to controls. GSR indicates glutathione reductase; GPX, glutathione peroxidase; mRNA, messenger RNA; RT-PCR, reverse transcription polymerase chain reaction; ELISA, enzyme-linked immunosorbent assay.

fallopian tube, and macrophages. Oxidative stress has been implicated in the pathogenesis of ovarian cancer, specifically by increased expression of several key prooxidant enzymes such as iNOS, MPO, and NAD(P)H oxidase in EOC tissues and cells as compared to normal cells indicating an enhanced redox state, as we have recently demonstrated (Figure 7).[6] This redox state is further enhanced in chemoresistant EOC cells as evident by a further increase in iNOS and NO_2^-/NO_3^- and a decrease in GSR levels, suggesting a shift toward a prooxidant state.[6] Antioxidant enzymes, key regulators of cellular redox balance, are differentially expressed in various cancers, including ovarian.[6,14] Specifically, GPX expression is reduced in prostate, bladder, kidney, and estrogen receptor negative breast cancer cell lines, though GPX is increased in other cancerous tissues from breast.[14] Glutathione reductase levels, on the other hand, are elevated in lung cancer, although differentially expressed in breast and kidney cancer.[5,15] Similarly, CAT was decreased in breast, bladder, and lung cancer while increased in brain cancer.[16-18] Superoxide dismutase is expressed in lung, colorectal, gastric ovarian, and breast cancer, while decreased activity and expression have been reported in colorectal carcinomas and pancreatic cancer cells.[18-21] Collectively, this differential expression of antioxidants demonstrates the unique and complex redox microenvironment in cancer. Glutathione reductase is a flavoprotein that catalyzes the NADPH-dependent reduction of oxidized glutathione (GSSG) to GSH. This enzyme is essential for the GSH redox cycle that maintains adequate levels of reduced cellular GSH. A high GSH to GSSG ratio is essential for protection against oxidative stress (Figure 5). Treatment with talc significantly reduced GSR in normal and cancer cells, altering the redox balance (Figure 3A and C). Likewise, GPX is an enzyme that detoxifies reactive electrophilic intermediates and thus plays an important role in protecting cells from cytotoxic and carcinogenic agents. Overexpression of GPX is triggered by exogenous chemical agents and reactive oxygen species and is thus thought to represent an adaptive response to stress.[15] Indeed, treatment of normal and cancer cells with talc significantly reduced GPX, which compromised the overall cell response to stress (Figure 3B and D).

Table 2. SNP Characteristics (A) and SNP Genotyping of Key Redox Enzymes in Untreated and Talc-Treated (100 μg/mL) Human Primary Ovarian Epithelial Cells (Normal Ovarian), Human Ovarian Surface Epithelial Cells (HOSEpiC), Fallopian Tube (FT33), and Ovarian Cancer (A2780, SKOV-3, TOV112D) Cell Lines (B).

	Gene (rs Number)				
	CAT (rs769217)	*NOS*$_2$ (rs2297518)	*GSR* (rs8190955)	*GPX1* (rs3448)	*SOD3* (rs2536512)
A					
MAF	0.123	0.173	0.191	0.176	0.476
SNP	C-262T	C2087T	G201T	C-1040T	A377T
Chromosome location	11p13	17q11.2	8p12	3q21.31	4p15.2
Amino acid switch	Isoleucine to Threonine	Serine to Leucine	Unknown	Unknown	Alanine to threonine
Effect on activity	Decrease	Increase	Unknown	Unknown	Decrease
B					
A2780: Control	C/C	C/C	G/G	C/T	A/A
A2780: Talc	C/C	C/C	G/G	C/C	A/A
SKOV-3: Control	C/C	C/C	G/G	C/T	A/A
SKOV-3: Talc	C/C	T/T	G/G	C/C	A/A
TOV112D: Control	C/C	C/C	G/G	C/T	A/A
TOV112D: Talc	C/T	C/C	G/G	C/C	A/A
HOSEpiC: Control	C/C	C/C	G/G	C/T	A/A
HOSEpiC: Talc	C/T	T/T	G/G	C/T	A/A
FT33: Control	C/C	C/C	G/G	C/T	A/A
FT33: Talc	C/T	T/T	G/G	C/C	A/A
Normal ovarian: Control	C/C	C/C	G/G	C/T	A/A
Normal ovarian: Talc	C/T	T/T	G/G	C/C	A/A

Abbreviation: SNP, single-nucleotide polymorphism.

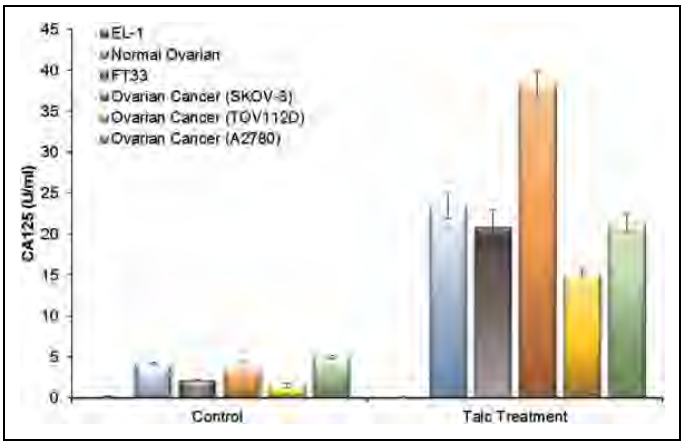

Figure 4. Increased CA-125 levels in response to talc treatment. The level of ovarian cancer biomarker CA-125 was determined by ELISA before and after 72 hours of talc treatment (100 μg/mL) in macrophages (EL-1), human primary ovarian epithelial cells (normal ovarian), fallopian tube (FT33), and ovarian cancer (SKOV-3, TOV112D, and A2780) cells. Experiments were performed in triplicate. Expression is depicted as the mean, with error bars representing standard deviation. All changes in response to talc treatment were significant ($P < .05$) in all cells as compared to controls. ELISA indicates enzyme-linked immunosorbent assay.

We have previously reported that EOC cells manifest increased cell proliferations and decreased apoptosis.[6] In this study, we have shown that talc enhances cell proliferation and induces an inhibition in apoptosis in EOC cells, but more importantly in normal cells, suggesting talc is a stimulus to the development of the oncogenic phenotype. We also previously reported a cross talk between iNOS and MPO in ovarian cancer, which contributed to the lower apoptosis observed in ovarian cancer cells.[6,22] Myeloperoxidase, an abundant hemoprotein, previously known to be present solely in neutrophils and monocytes, is a key oxidant enzyme that utilizes NO produced by iNOS as a 1-electron substrate generating NO^+, a labile nitrosylating species.[6,23,24] We were the first to report that MPO was expressed by EOC cells and tissues and that silencing MPO gene expression utilizing MPO-specific siRNA induced apoptosis in EOC cells through a mechanism that involved the S-nitrosylation of caspase-3 by MPO.[22] Additionally, we have compelling evidence that MPO serves as a source of free iron under oxidative stress, where both NO^+ and superoxide are elevated.[6] Iron reacts with hydrogen peroxide (H_2O_2) and catalyzes the generation of highly reactive hydroxy radical ($HO^•$), thereby increasing oxidative stress, which in turn increases free iron concentrations by the Fenton and Haber-Weiss reaction.[6,24] We have previously highlighted the potential benefits of the combination of serum MPO and free iron as biomarkers for early detection and prognosis of ovarian cancer.[25] Collectively, we now have substantial evidence demonstrating that altered oxidative stress may play a role in maintaining the oncogenic phenotype of EOC cells. Treatment of normal or ovarian cancer cells with talc resulted in a significant increase in MPO and iNOS, supporting the role of talc in the enhancement of a prooxidant state that is a major cause in the development and maintenance of the oncogenic phenotype (Figure 2).

Furthermore, CA-125, which exists as a membrane-bound and secreted protein in EOC cells, has been established as a

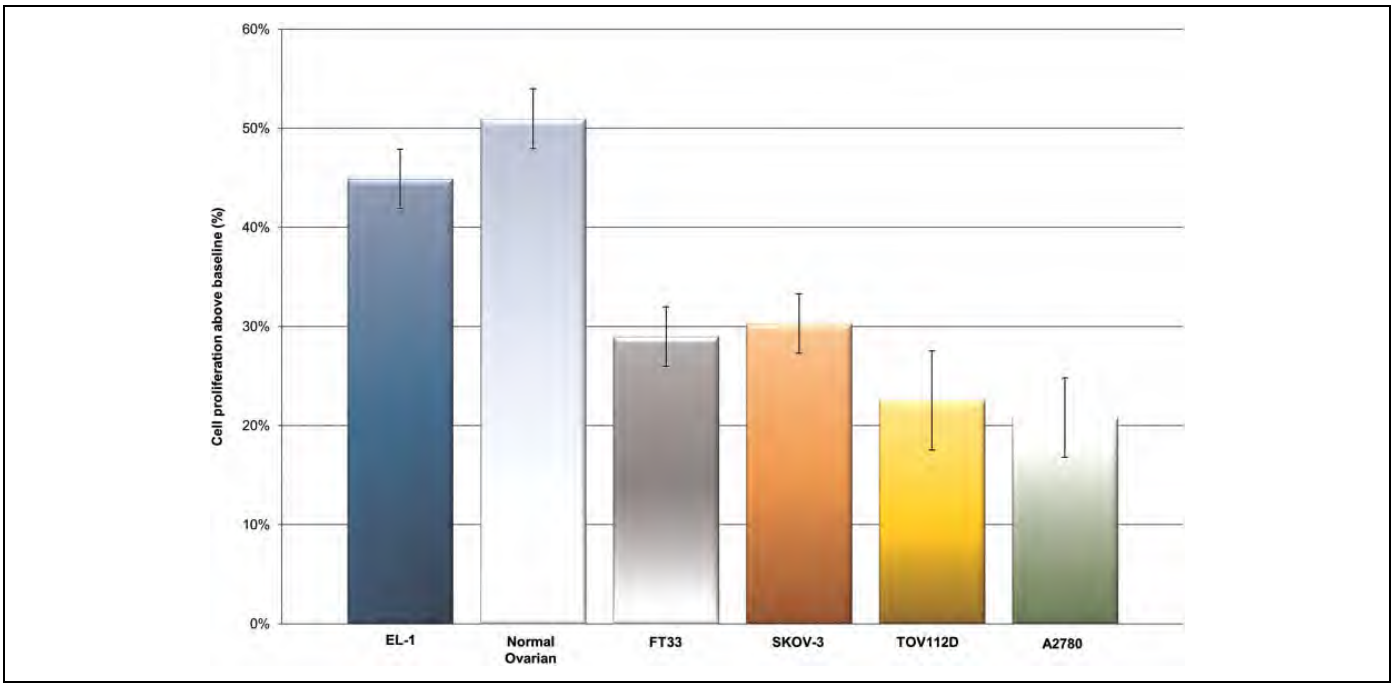

Figure 5. Increased cell proliferation in response to talc treatment. Cell proliferation was determined by MTT cell proliferation assay after 24 hours of talc treatment (100 μg/mL) in macrophages (EL-1), human primary ovarian epithelial cells (normal ovarian), fallopian tube (FT33), and ovarian cancer (SKOV-3, TOV112D, and A2780) cells. Experiments were performed in triplicate. Cell proliferation is depicted as the mean, with error bars representing standard deviation. All changes in response to talc treatment were significant ($P < .05$) in all cells as compared to controls.

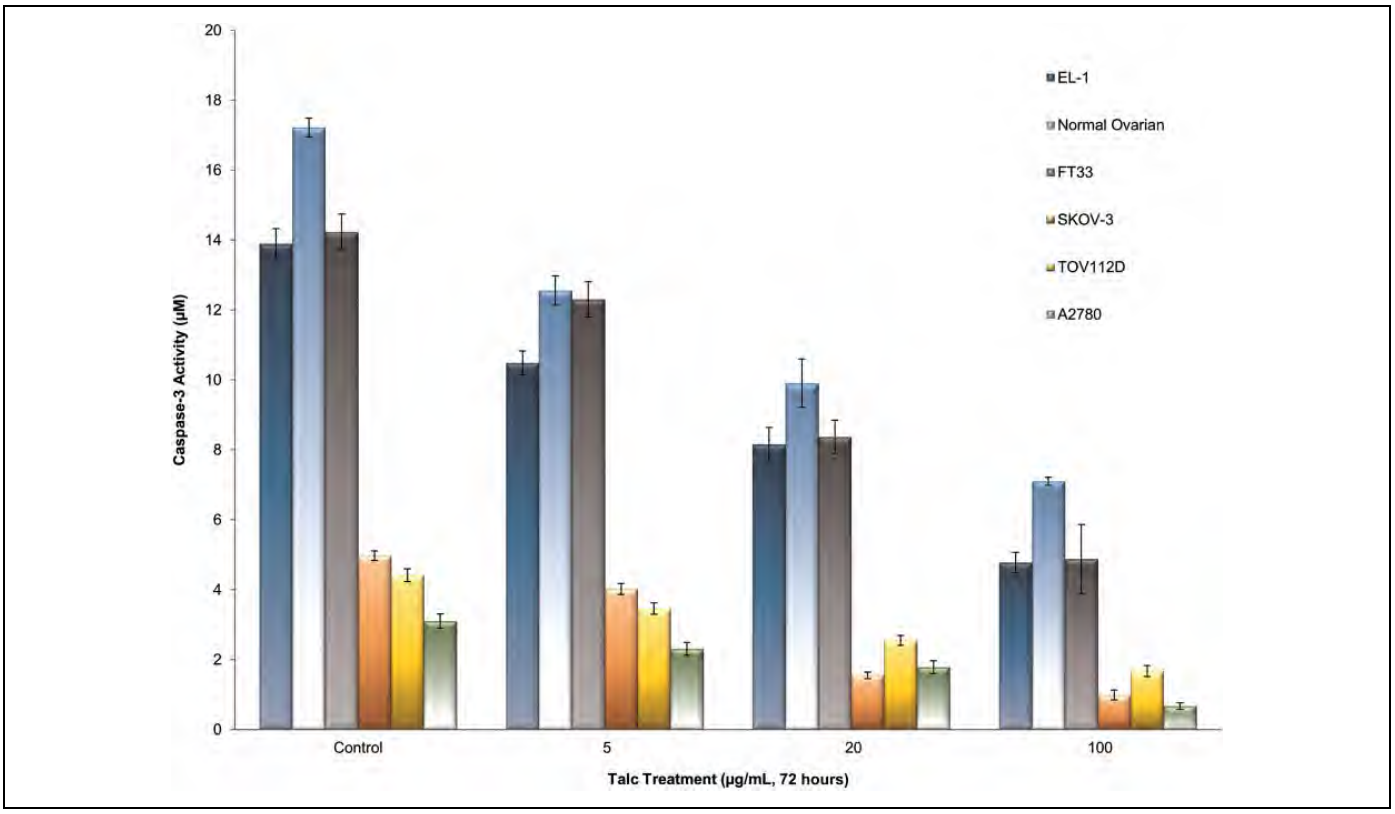

Figure 6. Decreased apoptosis in response to talc treatment. Caspase-3 activity was used to measure the degree of apoptosis in all cells. Caspase-3 activity assay was utilized to determine caspase-3 activity in macrophages (EL-1), human primary ovarian epithelial cells (normal ovarian), fallopian tube (FT33), and ovarian cancer (SKOV-3, TOV112D, and A2780) cell lines before and after treatment with various doses of talc over 72 hours. Experiments were performed in triplicate. Expression is depicted as the mean, with error bars representing standard error. All changes in response to talc treatment were significant ($P < .05$) in all cells and in all doses as compared to controls.

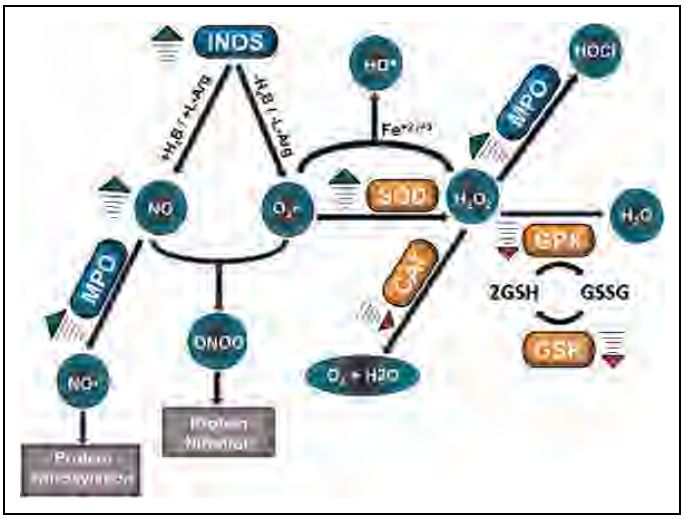

Figure 7. Epithelial ovarian cancer (EOC) cells have been reported to manifest a persistent prooxidant state as evident by the upregulation (green arrows) of key oxidants iNOS, NO, NO^+, $ONOO^-$, OH^-, O_2^+, and MPO (blue) and downregulation (red arrows) of key antioxidants SOD, CAT, GPX, and GSR (orange). This redox state was also shown to be further enhanced in chemoresistant EOC cells. In this study, talcum powder altered the redox state, as indicated by the arrows, of both normal and EOC cells to create an enhanced prooxidant state. iNOS indicates inducible nitric oxide synthase; MPO, myeloperoxidase; SOD, superoxide dismutase; CAT, catalase; GPX, glutathione peroxidase; GSR, glutathione reductase.

biomarker for disease progression and response to treatment.[2] CA-125 expression was significantly increased from nearly undetectable levels in controls to values approaching clinical significance (35 U/mL in postmenopausal women[26]) in talc-treated cells (Figure 4, $P < .05$) without the physiologic effects on the tumor microenvironment one would expect to be present in the human body, thus highlighting the implications of the prooxidant states caused by talc alone.

To elucidate the mechanism by which talc alters the redox balance to favor a prooxidant state not only in ovarian cancer cells, but more importantly in normal cells, we have examined selected known gene mutations corresponding to SNPs known to be associated with altered enzymatic activity and increased cancer risk.[6,27] Our results show that the *CAT* SNP (rs769217) resulting in decreased enzymatic activity was induced in all normal cell lines tested and in TOV112D EOC lines, but was not detected in A2780 or SKOV-3 cell lines (Table 2). Nevertheless, our results confirm a decrease in CAT expression and enzymatic activity in all talc-treated cells (Figure 1), indicating the existence of other *CAT* SNPs. The *SOD3* (rs2536512) and *GSR* (rs8190955) SNP genotypes were not detected in any cell line, yet SOD3 and GSR activity and expression were decreased in all talc-treated cells, again suggesting the presence of other SNPs. Our results have also shown that all cells, except for HOSEpiC cells, manifest the SNP genotype of *GPX1* (C/T) before talc treatment. Intriguingly, talc treatment reversed this SNP genotype to the normal genotype (Table 2). Consistent with this finding, we have previously reported that acquisition of chemoresistance by ovarian cancer cells is associated with a switch from the *GPX1* SNP genotype to the normal *GPX1* genotype.[6] It is not understood why a *GPX1* SNP genotype predominates in untreated normal and ovarian cancer cells. Our results showed that talc treatment was associated with a genotype switch from common C/C genotype in *NOS2* in untreated cells to T/T, the SNP genotype, in talc-treated cells, except in A2780 and TOV112D (Table 2). Nevertheless, our results confirm an increase in iNOS expression and enzymatic activity in all talc-treated cells (Figure 2), again suggesting the existence of other *NOS2* SNPs. Collectively, these findings support the notion that talc treatment induced gene point mutations that happen to correspond to SNPs in locations with functional effects, thus altering overall redox balance for the initiation and development of ovarian cancer. Future studies examining such SNPs are important to fully elucidate a genotype switch mechanism induced by talc exposure.

In summary, this is the first study to clearly demonstrate that talc induces inflammation and alters the redox balance favoring a prooxidant state in normal and EOC cells. We have shown a dose-dependent significant increase in key prooxidants, iNOS, NO_2^-/NO_3^-, and MPO, and a concomitant decrease in key antioxidant enzymes, CAT, SOD, GPX, and GSR, in all talc-treated cells (both normal and ovarian cancer) compared to their controls. Additionally, there was a significant increase in CA-125 levels in all the talc-treated cells compared to their controls, except in macrophages. The mechanism by which talc alters the cellular redox and inflammatory balance involves the induction of specific mutations in key oxidant and antioxidant enzymes that correlate with alterations in their activities. The fact that these mutations happen to correspond to known SNPs of these enzymes indicate a genetic predisposition to developing ovarian cancer with genital talcum powder use.

Authors' Note

Ghassan M. Saed is also affiliated with Department of Gynecologic Oncology, Karmanos Cancer Institute, Detroit, MI, USA.

Acknowledgment

Special thanks to Imaan Singh for her technical contributions in acquiring the data and in development of graphics.

Declaration of Conflicting Interests

The author(s) declared the following potential conflicts of interest with respect to the research, authorship, and/or publication of this article: Dr. Saed has served as a paid consultant and expert witness in the talcum powder litigation.

Funding

The author(s) received no financial support for the research, authorship, and/or publication of this article.

References

1. Berek JS, Bertelsen K, du Bois A, et al. Epithelial ovarian cancer (advanced stage): consensus conference (1998) [in French]. *Gynecol Obstet Fertil*. 2000;28(7-8):576-583.

2. Jelovac D, Armstrong DK. Recent progress in the diagnosis and treatment of ovarian cancer. *CA Cancer J Clin*. 2011;61(3):183-203.
3. Prat J, Ribe A, Gallardo A. Hereditary ovarian cancer. *Hum Pathol*. 2005;36(8):861-870.
4. Ramus SJ, Vierkant RA, Johnatty SE, et al. Consortium analysis of 7 candidate SNPs for ovarian cancer. *Int J Cancer*. 2008; 123(2):380-388.
5. Reuter S, Gupta SC, Chaturvedi MM, Aggarwal BB. Oxidative stress, inflammation, and cancer: how are they linked? *Free Radic Biol Med*. 2010;49(11):1603-1616.
6. Fletcher NM, Belotte J, Saed MG, et al. Specific point mutations in key redox enzymes are associated with chemoresistance in epithelial ovarian cancer. *Free Radic Biol Med*. 2016;102:122-132.
7. Cramer DW, Welch WR, Scully RE. Wojciechowski CA. Ovarian cancer and talc: a case-control study. *Cancer*. 1982;50:372-376.
8. Cramer DW, Liberman RF, Titus-Ernstoff L, et al. Genital talc exposure and risk of ovarian cancer. *Int J Cancer*. 1999;81: 351-356.
9. Ness RB, Grisso JA, Cottreau C, et al. Factors related to inflammation of the ovarian epithelium and risk of ovarian cancer. *Epidemiology*. 2000;11:111-117.
10. Henderson WJ, Joslin CA, Turnbull AC, Griffiths K. Talc and carcinoma of the ovary and cervix. *J Obstet Gynaecol Br Commonw*. 1971;78:266-272.
11. Terry KL, Karageorgi S, Shvetsov YB, et al. Genital powder use and risk of ovarian cancer: a pooled analysis of 8,525 cases and 9,859 controls. *Cancer Prev Res (Phila)*. 2013;6(8):811-821.
12. Penninkilampi R, Eslick GD. Perineal talc use and ovarian cancer: a systematic review and meta-analysis. *Epidemiology*. 2018; 29(1):41-49.
13. Reid BM, Permuth JB, Sellers TA. Epidemiology of ovarian cancer: a review. *Cancer Biol Med*. 2017;14(1):9-32.
14. Brigelius-Flohe R, Kipp A. Glutathione peroxidases in different stages of carcinogenesis. *Biochim Biophys Acta*. 2009;1790(11): 1555-1568.
15. Sun Y. Free radicals, antioxidant enzymes, and carcinogenesis. *Free Radic Biol Med*. 1990;8(6):583-599.
16. Popov B, Gadjeva V, Valkanov P, Popova S, Tolekova A. Lipid peroxidation, superoxide dismutase and catalase activities in brain tumor tissues. *Arch Physiol Biochem*. 2003;111(5):455-459.
17. Ray G, Batra S, Shukla NK, et al. Lipid peroxidation, free radical production and antioxidant status in breast cancer. *Breast Cancer Res Treat*. 2000;59(2):163-170.
18. Chung-man Ho J, Zheng S, Comhair SA, Farver C, Erzurum SC. Differential expression of manganese superoxide dismutase and catalase in lung cancer. *Cancer Res*. 2001;61(23):8578-8585.
19. Radenkovic S, Milosevic Z, Konjevic G, et al. Lactate dehydrogenase, catalase, and superoxide dismutase in tumor tissue of breast cancer patients in respect to mammographic findings. *Cell Biochem Biophys*. 2013;66(2):287-295.
20. Hu Y, Rosen DG, Zhou Y, et al. Mitochondrial manganese-superoxide dismutase expression in ovarian cancer: role in cell proliferation and response to oxidative stress. *J Biol Chem*. 2005; 280(47):39485-39492.
21. Svensk AM, Soini Y, Paakko P, Hiravikoski P, Kinnula VL. Differential expression of superoxide dismutases in lung cancer. *Am J Clin Pathol*. 2004;122(3):395-404.
22. Saed GM, Ali-Fehmi R, Jiang ZL, et al. Myeloperoxidase serves as a redox switch that regulates apoptosis in epithelial ovarian cancer. *Gynecol Oncol*. 2010;116(2):276-281.
23. Galijasevic S, Saed GM, Hazen SL, Abu-Soud HM. Myeloperoxidase metabolizes thiocyanate in a reaction driven by nitric oxide. *Biochemistry*. 2006;45(4):1255-1262.
24. Galijasevic S, Maitra D, Lu T, Sliskovic I, Abdulhamid I, Abu-Soud HM. Myeloperoxidase interaction with peroxynitrite: chloride deficiency and heme depletion. *Free Radic Biol Med*. 2009; 47(4):431-439.
25. Fletcher NM, Jiang Z, Ali-Fehmi R, et al. Myeloperoxidase and free iron levels: potential biomarkers for early detection and prognosis of ovarian cancer. *Cancer Biomark*. 2011;10(6):267-275.
26. Scholler N, Urban N. CA125 in ovarian cancer. *Biomark Med*. 2007;1(4):513-523.
27. Belotte J, Fletcher NM, Saed MG, et al. A single nucleotide polymorphism in catalase is strongly associated with ovarian cancer survival. *PLoS One*. 2015;10(8):e0135739.

Exhibit 98

Review

Inflammation and cancer: back to Virchow?

Fran Balkwill, Alberto Mantovani

The response of the body to a cancer is not a unique mechanism but has many parallels with inflammation and wound healing. This article reviews the links between cancer and inflammation and discusses the implications of these links for cancer prevention and treatment. We suggest that the inflammatory cells and cytokines found in tumours are more likely to contribute to tumour growth, progression, and immunosuppression than they are to mount an effective host anti-tumour response. Moreover cancer susceptibility and severity may be associated with functional polymorphisms of inflammatory cytokine genes, and deletion or inhibition of inflammatory cytokines inhibits development of experimental cancer. If genetic damage is the "match that lights the fire" of cancer, some types of inflammation may provide the "fuel that feeds the flames". Over the past ten years information about the cytokine and chemokine network has led to development of a range of cytokine/chemokine antagonists targeted at inflammatory and allergic diseases. The first of these to enter the clinic, tumour necrosis factor antagonists, have shown encouraging efficacy. In this article we have provided a rationale for the use of cytokine and chemokine blockade, and further investigation of non-steroidal anti-inflammatory drugs, in the chemoprevention and treatment of malignant diseases.

It was in 1863 that Rudolf Virchow noted leucocytes in neoplastic tissues and made a connection between inflammation and cancer. He suggested that the "lymphoreticular infiltrate" reflected the origin of cancer at sites of chronic inflammation. Over the past ten years our understanding of the inflammatory microenvironment of malignant tissues has supported Virchow's hypothesis, and the links between cancer and inflammation are starting to have implications for prevention and treatment.

Panel 1 lists some cancers where the inflammatory process is a cofactor in carcinogenesis. About 15% of the global cancer burden is attributable to infectious agents,[1] and inflammation is a major component of these chronic infections. Moreover, increased risk of malignancy is associated with the chronic inflammation caused by chemical and physical agents,[2] and autoimmune and inflammatory reactions of uncertain aetiology.[3]

Inflammatory cells in tumour microenvironment

The inflammatory microenvironment of tumours is characterised by the presence of host leucocytes both in the supporting stroma and in tumour areas.[4] Tumour-infiltrating lymphocytes may contribute to cancer growth and spread, and to the immunosuppression associated with malignant disease.

Macrophages

Tumour-associated macrophages (TAM) are a major component of the infiltrate of most, if not all, tumours.[5] TAM derive from circulating monocytic precursors, and are directed into the tumour by chemoattractant cytokines called chemokines. Many tumour cells also produce cytokines called colony-stimulating factors that prolong survival of TAM. When appropriately activated, TAM can kill tumour cells or elicit tissue destructive reactions centred on the vascular endothelium. However, TAM also produce growth and angiogenic factors as well as protease enzymes which degrade the extracellular matrix. Hence, TAM can stimulate tumour-cell proliferation, promote angiogenesis, and favour invasion and metastasis.[6] Direct evidence for the importance of protease production by TAM, neutrophils, and mast cells during experimental carcinogenesis has recently been reported.[7] This dual potential of TAM is expressed in the "macrophage balance" hypothesis.[5]

Dendritic cells

Dendritic cells have a crucial role in both the activation of antigen-specific immunity and the maintenance of tolerance, providing a link between innate and adaptive immunity. Tumour-associated dendritic cells (TADC) usually have an immature phenotype with defective ability to stimulate T cells.[8] In breast cancer, immature TADC are interspersed in the tumour mass, whereas mature dendritic cells are confined to the peritumoral area.[8] In papillary thyroid carcinoma TADC are also immature but they tend to localise at the invasive edge of the tumour.[8] This distribution of TADC is clearly different from that of TAM, which are evenly scattered in tumour tissue. The immaturity of TADC may reflect lack of effective

Panel 1: **Some associations between inflammation and cancer risk**

Malignancy	Inflammatory stimulus/condition
Bladder	Schistosomiasis
Cervical	Papillomavirus
Ovarian	Pelvic inflammatory disease/talc/tissue remodelling
Gastric	*H pylori* induced gastritis
MALT lymphoma	*H pylori*
Oesophageal	Barrett's metaplasia
Colorectal	Inflammatory bowel disease
Hepatocellular	Hepatitis virus (B and C)
Bronchial	Silica, asbestos, cigarette smoke
Mesothelioma	Asbestos
Kaposi's sarcoma	Human herpesvirus type 8

Lancet 2001; **357:** 539–45

ICRF Translational Oncology Laboratory, St Bartholomew's and Royal London School of Medicine and Dentistry, Charterhouse Square, London EC1M 6BQ, UK (Prof F Balkwill PhD); **and Department of Immunology and Cell Biology, Istituto di Ricerche Farmacologiche Mario Negri, and Institute of General Pathology, Milan State University, Milan, Italy** (Prof A Mantovani MD)
(e-mail: f.balkwill@icrf.icnet.uk; mantovani@marionegri.it)

maturation signals, prompt migration of mature cells to lymph nodes, or the presence of maturation inhibitors. TADC are likely to be poor inducers of effective responses to tumour antigens.

Lymphocytes

Natural killer cells are rare in the tumour microenvironment.[4] The predominant T-cell population has a "memory" phenotype. The cytokine repertoire of these tumour-infiltrating T cells (TIL) has not been studied systematically but in some tumours (eg, Kaposi's sarcoma, Hodgkin's disease, bronchial carcinoma, and cervical carcinoma) they produce mainly interleukins (IL) 4 and 5 and not interferon-γ.[9] IL 4 and 5 are cytokines associated with the T-helper type 2 (Th2) cells whereas interferon-γ is associated with Th1 responses. Polarised Th2 responses are generally ineffective against tumours and viruses. Signalling via the T-cell receptor is also defective in TIL.[10]

Tumours: wounds that do not heal

Besides inflammatory cells, tumour stroma consists of new blood vessels, connective tissue, and a fibrin-gel matrix. In his 1986 review Dvorak showed how wound healing and tumour stroma formation share many important properties ("Tumors: wounds that do not heal"[11]). Wound healing is usually self-limiting whereas tumours secrete a vascular permeability factor, vascular endothelial growth factor (VEGF), that can lead to persistent extravasation of fibrin and fibronectin and continuous generation of extracellar matrix. Platelets in wounds are a critical source of cytokines, especially transforming growth factor β (TGF-β) and VEGF. Platelet release of such factors may also be important in tumour angiogenesis.[12] In addition, malignant cells themselves secrete proinflammatory cytokines.[13]

Proinflammatory cytokines

The cytokine network of several common tumours is rich in inflammatory cytokines, growth factors, and chemokines but generally lacks cytokines involved in specific and sustained immune responses.[13] There is now evidence that inflammatory cytokines and chemokines, which can be produced by the tumour cells and/or tumour-associated leucocytes and platelets, may contribute directly to malignant progression. Many cytokines and chemokines are inducible by hypoxia, which is a major physiological difference between tumour and normal tissue.[14] Examples are tumour necrosis factor (TNF), IL 1 and 6, and chemokines.

Tumour necrosis factor

TNF is a major mediator of inflammation, with actions directed towards both tissue destruction and recovery. While inducing death of diseased cells at the site of inflammation, TNF stimulates fibroblast growth. It can destroy blood vessels but also induce angiogenic factors.[15] Likewise, in malignant disease, high-dose local TNF selectively destroys tumour blood vessels,[16] but when chronically produced this cytokine may act as an endogenous tumour promoter, contributing to the tissue remodelling and stromal development necessary for tumour growth and spread.

TNF can be detected in malignant and/or stromal cells in human ovarian, breast, prostate, bladder, and colorectal cancer, lymphomas, and leukaemias, often in association with ILs 1 and 6 and macrophage colony stimulating factor.[13,17] In epithelial ovarian cancer, TNF mRNA is found in epithelial tumour islands, where there is a positive correlation with tumour grade.[17] The p55 TNF receptor is found on tumour and stromal cells and the p75 receptor localises to the leucocyte infiltrate in ovarian cancer, suggesting possibilities for both paracrine and autocrine action.[17] TNF is also implicated in the induction of a chemokine called monocyte chemotactic protein-1, which can regulate the macrophage and lymphocyte infiltrate,[4] and of matrix metalloprotease-9, in the ovarian tumour microenvironment. In breast cancer, infiltrating macrophages are a major source of TNF, which may regulate thymidine phosphorylase, a key angiogenic enzyme in the tumour epithelium.[18] In prostate cancer, tumour cell TNF production correlates with loss of androgen responsiveness. In non-Hodgkin lymphoma, myelogenous leukaemia, and chronic lymphocytic leukaemia, high

Glossary: **Specialised leucocytes, cytokines, chemokines**

—	Abbreviation	Group	New human nomenclature
Specialised leucocytes			
Natural killer cells	NK	..	..
Tumour-associated dendritic cells	TADC	..	..
Tumour-associated macrophages	TAM	..	..
Tumour-infiltrating leucocytes	TIL	..	..
Cytokines			
Interferon-γ	IFN-γ	Proinflammatory/Th1	..
Interleukins 1, 6	IL-1, -6	Proinflammatory	..
Interleukins 4, 5, 10	IL-4, -5, -10	Immune regulatory/Th2	..
Macrophage colony-stimulating factor	M-CSF	Growth factor	..
Migration inhibitory factor	MIF	Proinflammatory	..
Transforming growth factor β	TGFβ	Growth factor	..
Tumour necrosis factor	TNF	Proinflammatory	..
Vascular endothelial growth factor	VEGF	Angiogenic/vascular permeability	..
Chemokines			
Eotaxin	..	CC	CCL11
B cell attracting chemokine	BCA-1	CXC	CXCL13
Gro-α/mgsa-α	gro-α	CXC	CXCL1
Interleukin-8	IL-8	CXC	CXCL8
IP-10	IP-10	CXC	CXCL10
Macrophage derived chemokine	MDC	CC	CCL22
Monocyte chemotactic protein-1	MCP-1	CC	CCL2
Thymus and activation regulated chemokine	TARC	CC	CCL17
Viral macrophage inhibitory protein	vMIP	CC	..

circulating levels of TNF and its soluble receptors are associated with poor prognosis.[19]

There is also evidence for pro-cancer actions of TNF in animal models.[20–22] For example, treatment of ascitic ovarian cancer xenografts with TNF promotes adhesion of free-floating tumour cells to the peritoneum and solid tumour formation,[20] and overexpression of TNF confers invasive properties on some tumour cell lines.[21]

Direct evidence for the involvement of TNF in malignancy comes from the observation that mice lacking the gene for TNF are resistant to skin carcinogenesis.[23] TNF may be involved in the early stages of skin tumour promotion in normal mice, being transiently but extensively induced in keratinocytes after application of tumour promoter.[23] Pentoxifylline (an inhibitor of inflammatory cytokine production) inhibits papilloma development in skin carcinogenesis models,[24] and intraperitoneal injection of TNF enhances papilloma development and vascularisation of tumours.

Interleukins 1 and 6

In mouse models of metastasis, treatment with an IL-1 receptor antagonist (which inhibits the action of IL-1) significantly decreased tumour development, suggesting that local production of this cytokine aids development of metastases. Moreover, mice deficient in IL-1β were resistant to the development of experimental metastases.[25]

In human multiple myeloma the malignant cells home to the bone marrow where they stimulate stromal cells to secrete the inflammatory cytokines IL-1, IL-6, and TNF. The cytokines stimulate myeloma cell growth and promote resistance to therapy.[26] Intraperitoneal injection of mineral oil in mice induces chronic inflammation followed by myeloma. IL-6-deficient mice resist these changes, showing defective recruitment of macrophages to the peritoneum and a reduced incidence of myeloma.

Panel 2: **Actions of cytokines and chemokines which may facilitate cancer growth, invasion and metastasis**

DNA damage via reactive oxygen
Inhibition of DNA repair via reactive oxygen
Functional inactivation of tumour suppressor genes
Autocrine/paracrine growth and survival factors for malignant cells
Induction of vascular permeability and extravasation of fibrin/fibronectin
Tissue remodelling via induction/activation of matrix metalloproteinases
Control of tumour-cell migration, direct and indirect
Control of leucocyte infiltrate
Modulation of cell:cell adhesion molecules
Subversion of host immune responses
Stimulation of angiogenesis and angiogenic factor production
Resistance to cytotoxic drugs
Loss of androgen responsiveness

Chemokines

Inflammatory cytokines are major inducers of a family of chemoattractant cytokines called chemokines that play a central role in leucocyte recruitment to sites of inflammation. Most tumours produce chemokines of the two major groups α (or CXC) and β (or CC).[5,27,28] Typically CXC chemokines are active on neutrophils and lymphocytes whereas CC chemokines act on several leucocyte subsets including monocytes, eosinophils, dendritic cells, lymphocytes, and natural killer cells but not neutrophils. Evidence from murine models and human tumours suggests that CC

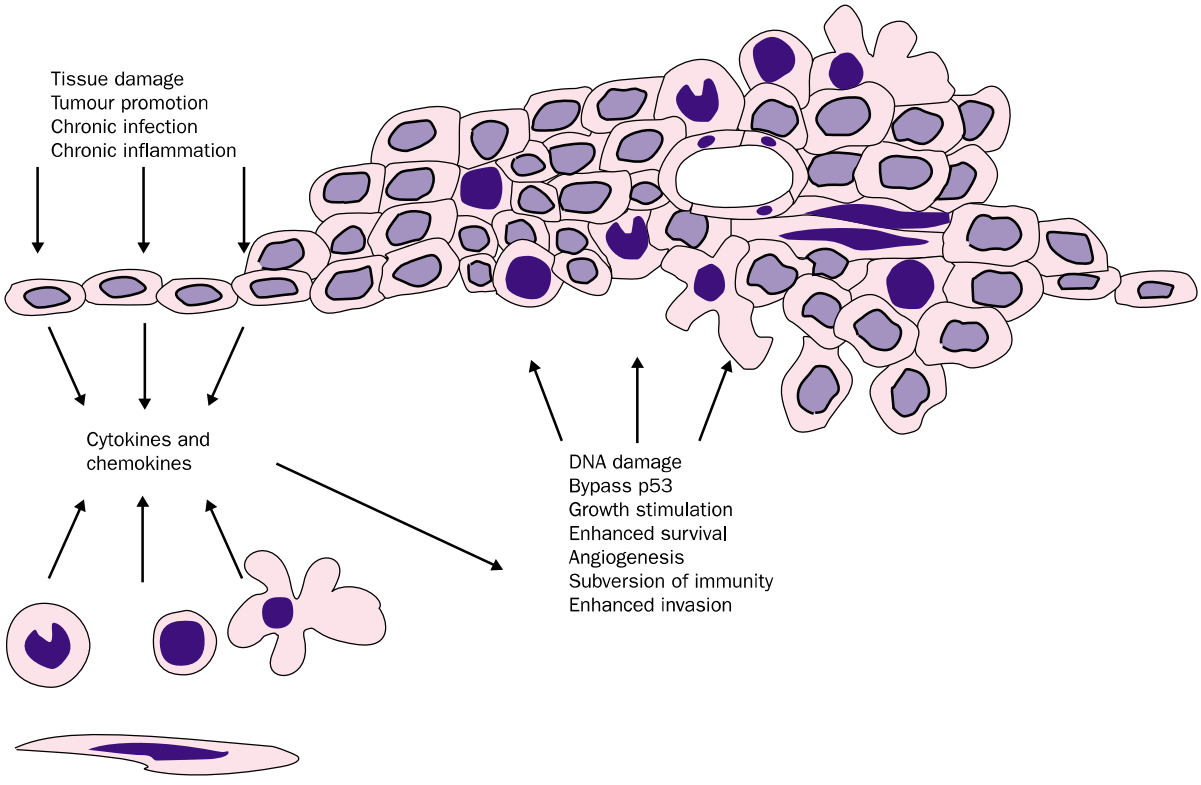

Figure 1: **Chronic inflammation, tissue damage, and chronic infection may stimulate cytokines and chemokines that contribute to development of malignant disease**

chemokines are major determinants of macrophage and lymphocyte infiltration in melanoma, carcinoma of the ovary, breast, and cervix, and in sarcomas and gliomas.[5,27,28] In Hodgkin's disease the malignant Reed-Sternberg cells express two chemokines, the macrophage-derived chemokine and thymus and activation-regulated chemokine,[9,29] that attract Th2 lymphocytes. Production of the chemokine eotaxin by stromal cells correlates with eosinophil infiltration in Hodgkin's lymphoma. Eosinophils are frequently present in tumours such as colorectal cancer.

Human and murine tumours also frequently secrete CXC chemokines such as interleukin-8. These chemokines are potent neutrophil attractants yet neutrophils are rare in tumours.[4] However, both IL-8 and a related chemokine called "gro" induce proliferation and migration of melanoma cells. When the *gro* gene was overexpressed in a non-malignant melanocyte cell line, the cells could form tumours in mice.[30] This effect probably involved both direct growth stimulation and promotion of an inflammatory response. Inflammation and wound healing have indeed been implicated in the initial steps of melanocyte oncogenesis.[31] IL-8 production is also associated with the tumorigenic and metastatic potential of pancreatic cancer cells and this chemokine is strongly inducible by hypoxia.

Helicobacter pylori induced gastritis is associated with gastric carcinoma and mucosa-associated lymphoid tissue B-cell lymphoma. BCA-1 is one of the chemokines induced by *H pylori*,[32] and it is thought that BCA-1 attracts B-cells to the mucosa where they become targets for the carcinogenic process that occurs during inflammation.

Receptors for chemokines (CCR and CXRC) are expressed both by infiltrating leucocytes and by cancer cells. The leucocytes may lose receptor expression once they are exposed to inflammatory cytokines in the tumour microenvironment, as shown for CCR2 on TAM in ovarian cancer.[33] Downregulation of CCR2 is likely to act as a signal for the retention of macrophages at the tumour site. Melanoma cells express the CXC receptors CXCR 1 and 2, and the ligand for these receptors (IL-8) will stimulate migration and proliferation of these tumour cells.[30] An ovarian cancer cell line also expressed a functional form of CXCR2.[34] These observations raise the interesting possibility that tumour cells may use chemokine gradients to spread around the body.[35]

Mechanisms of action of inflammatory cytokines in tumour microenvironment

An inflammatory cytokine network may influence survival, growth, mutation, proliferation, differentiation, and movement of both tumour and stromal cells. Moreover, these cytokines can regulate communication between tumour and stromal cells, and tumour interactions with the extracellular matrix. We will now look in more detail at the mechanisms by which cytokines and chemokines might act to promote tumours (panel 2, figure 1).

DNA damage

TNF is a transforming agent for carcinogen-treated fibroblasts. Two weeks of exposure to the cytokine in vitro is sufficient to render cells capable of tumour formation in nude mice.[36] The molecular basis may involve induction of reactive oxygen. Reactive oxygen in the form of NO is often generated by inflammatory cytokine induction of NO synthase.[37] NO can directly oxidise DNA, resulting in mutagenic changes, and may damage some DNA repair proteins.[37] Furthermore, inducible NO synthase has been detected in gynaecological carcinomas. Inflammatory cytokines may also affect genome integrity via inhibition of cytochrome p450 or glutathione S-transferase isoenzymes.

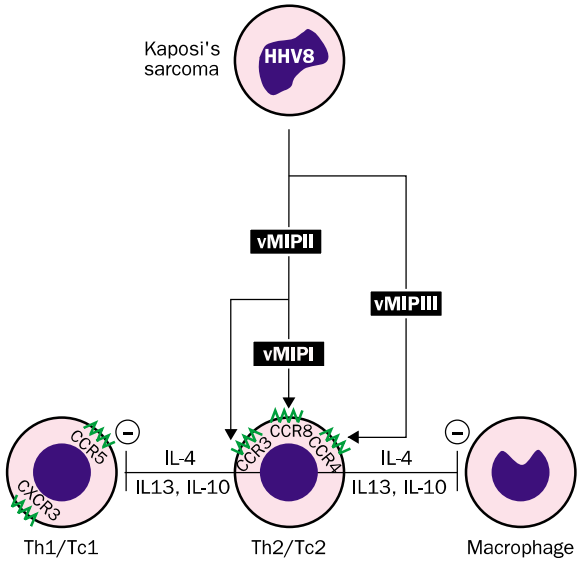

Figure 2: **Kaposi's sarcoma virus human herpesvirus 8 encodes three chemokines that recognise receptors preferentially expressed on polarised Th2 cells**
These cells are ineffective antiviral and antitumour effectors and produce cytokines which block differentiation of Th1 cells and activation of macrophages.

Bypassing p53

Another link between inflammatory cytokines and DNA damage comes from recent studies of the regulation of the tumour-suppressor protein p53. In tumours, p53 is often functionally inactivated even though the p53 gene remains intact. A search for negative regulators of p53 activity highlighted an inflammatory cytokine known as migration inhibitory factor.[38] Treatment of cells with this factor overcame p53 activity. It is not clear whether other cytokines can also inactivate p53 but chronic bypass of p53 function could enhance the proliferation of initiated cells, extend lifespan, and create a deficient response to genetic damage.[38] Migration is also strongly induced by hypoxia.[14]

Actions as growth and survival factors

Cytokines and chemokines have the potential to stimulate tumour-cell proliferation and survival and some of them may also act as autocrine growth and survival factors for malignant cells. IL-6 is a growth factor for haematological malignancies;[26] IL-1 has growth stimulating activity for gastric carcinoma that may be related to genetic predisposition[39] and for myeloid leukaemias; and growth of melanomas is promoted by IL-8 and related chemokines.[30]

Angiogenesis

Angiogenesis is important in the evolution of both cancer and inflammatory diseases that may predispose to cancer.[40] Once a tumour is established it may attain further characteristics, via mutations or hypoxia, which stimulate new blood vessels.

The inflammatory cell infiltrate, particularly TAM, may contribute to tumour angiogenesis, and there are many reports of associations between macrophage infiltration, vascularity, and prognosis.[41] Moreover TNF, IL-1, and IL-6 can stimulate production of angiogenic factors such as VEGF. Inflammatory macrophages also produce TGF-β1 that is itself angiogenic and induces production of VEGF.

Chemokines also have a role. Some CXC chemokines (eg, IL-8) are proangiogenic whereas others such as IP-10 have antiangiogenic activity.[42] Chemokines have direct

Panel 3: Links between cancer and inflammation suggested by experimental and clinical observations

Many inflammatory conditions predispose to cancer
Functional polymorphisms of cytokine genes associated with cancer susceptibility and severity
Distinct populations of inflammatory cells detected in many cancers
Inflammatory cytokines detected in many cancers; associated with poor prognosis, may be upregulated by local hypoxia
Chemokines detected in many cancers, associated with inflammatory infiltrate and cell motility
Deletion of cytokines and chemokines protects against carcinogens, experimental metastases and lymphoproliferative syndrome
Inflammatory cytokines implicated in action of non-genotoxic liver carcinogens
The inflammatory cytokine TNF is directly transforming in vitro

actions on microvascular endothelial cells. In addition, CC chemokines may inhibit or stimulate angiogenesis indirectly, via their influence on TAM. In many tumours (eg, non-small-cell lung cancer and pancreatic carcinoma) it is the balance between proangiogenic and antiangiogenic cytokines and chemokines, rather than absolute amounts, that regulates tumour angiogenesis.

Invasion and metastasis

Cytokines and chemokines affect various stages in the process of metastasis. TNF and CC chemokines can induce production of proteases important for invasion in both tumour cells and macrophages. Indeed, monocytes infiltrating the tumour tissue may provide cancer cells with a ready-made path for invasion (the "countercurrent invasion theory").[43] In one skin tumour model, paracrine matrix metalloproteinase-9 production by inflammatory cells was implicated in epithelial hyperproliferation, angiogenesis and increased malignant potential, and skin tumour development was reduced in mice genetically "knocked out" for this protein. Chimaeric mice expressing this metalloproteinase only in cells of bone marrow origin developed skin tumours at the same rate as control mice, highlighting the importance of stromal inflammatory cells in epithelial carcinogenesis. TNF and IL-1 augment expression of adhesion molecules on endothelial cells.[2–5] IL-18 derived from the endothelium may be the ultimate mediator of one tumour cytokine-induced adhesion molecule.[26] Certain tumour cells have receptors for adhesion molecules and use these molecular tools, typical of migrating leucocytes, to seed at distant anatomical sites.[44] Furthermore, chemokine agonists induce migration or proliferation of some tumour cells.[30] Receptors that are essential for lymphocyte and dendritic cell homing to lymph nodes,[8] could play a role in lymphatic dissemination of certain carcinomas. Direct evidence for chemokines guiding the secondary localisation of cancer has been obtained in one mouse model.[35] Mice deficient in Fas ligand develop a fatal lymphoproliferative syndrome. This phenotype is largely abolished when mice are crossed with mice unable to make TNF. One explanation may be that TNF induces chemokines that promote trafficking of the cells and accumulation of lymph nodes.[45]

Thus, tumour cells use the same molecular tools (adhesion molecules, cytokines, chemokines, chemokine receptors) and pathways as leucocytes do to spread to distant anatomical sites during inflammation.

Subversion of immunity

The prevalence of Th2 cells is common to tumours suggesting that this polarisation may be a general strategy to subvert immune responses against tumours. Inflammatory reactions are diverse, reflecting the variety of properties that can be acquired by macrophages.[46] At one extreme, interferon-activated (or type I) macrophages produce high levels of proinflammatory cytokines and Th1-attracting chemokines. At the other, activated (type II) macrophages produce high levels of antagonist to IL-1 receptor and the Th2-attracting macrophage-derived chemokine. In the murine and human tumours studied, TAM are skewed to the type II phenotype. TAM spontaneously release large amounts of IL-10 to TGFβ[47] both of which are immunosuppressive. Some chemokines induce IL-10 in macrophages and the monocyte chemotactic protein-1 polarises immunity in the Th2 direction.[48] Thus chronic exposure to high chemokine concentrations in the tumour microenvironment may set in motion a vicious cycle leading to skewing towards a type II inflammatory response.[47]

Some viruses encode chemokines and their inhibitors and receptors. Of particular interest is human herpesvirus type 8, which is involved in the pathogenesis of Kaposi's sarcoma. The virus genome codes for three chemokines[49] which are selective attractants of polarised Th2 cells. The virus-encoded chemokines might subvert immunity by activating type 2 responses and diverting effective Th1 defence mechanisms (figure 2).[49,50]

Interfering with chemotherapy

Another similarity between inflammation and cancer is raised plasma concentrations of acute-phase proteins (such as C-reactive protein and α_1-acid glycoprotein). The latter binds with high affinity to, and blocks activity of, the experimental cancer drug STI571[51] which normally has activity against chronic myelogenous leukaemia in mice. If acute-phase proteins do bind to and inactivate anticancer drugs there would be obvious implications for therapy.

Local inflammaton and systemic anti-inflammation: a paradox

In terms of inflammatory reactions, neoplastic disorders constitute a paradox. Tumours produce inflammatory cytokines and chemokines and are infiltrated by leucocytes. However, neoplastic disorders are associated with a defective capacity to mount inflammatory reactions at sites other than the tumour, and circulating monocytes from cancer patients are defective in their capacity to respond to chemoattractants.[52]

Various factors originating in the tumour microenvironment may contribute to the systemic anti-inflammation associated with cancer. Chemokines leaking into the systemic circulation are likely to desensitise circulating leucocytes;[53] increased concentrations of TNF receptors and the type II decoy IL-1 receptor may buffer inflammatory cytokines; and tumours also produce anti-inflammatory cytokines.[47] Thus a defective capacity to mount a systemic inflammatory response in cancer patients could coexist with continuous leucocyte recruitment at the tumour site.

Inflammatory cytokines as cancer-modifier genes

Cytokine genes are highly polymorphic and since polymorphisms are frequently in regions of DNA that regulate transcription or posttranscriptional events, they may be functionally significant. Four studies of such polymorphisms and cancer susceptibility and severity suggest that some cytokines may be cancer-modifier genes.

Systemic release of TNF and lymphotoxin contributes to the severity of non-Hodgkin lymphoma.[19] In a study of 273 lymphoma patients, the TNF-308 polymorphism was associated with high plasma levels of the cytokine at presentation of disease.[54]

Associations have also been found between genotype changes in the promoter regions of TNF and prostate cancer. The relative risk of incidence for prostate cancer was 14-fold higher in men with the TNF-308 polymorphism and the relative incidence for prostate cancer was 17 times higher in patients with genotype *GA* at 488 region of TNF.[55]

Patients with extensive corpus gastritis, hypochlorhydria, and gastric atrophy as a result of *H pylori* infection have the greatest risk of gastric malignancy. IL-1β is upregulated during *H pylori* infection, is important in the inflammatory response of the gastric mucosa, and is a potent inhibitor of gastric acid secretion. A decreased flow of gastric secretions may increase damage by allowing accumulation of bacterial toxins and inflammatory mediators. IL-1 gene cluster polymorphisms, thought to enhance IL-1β production, confer an increased risk of chronic hypochlorhydria in response to *H pylori* and of gastric cancer.[39] Pancreatic cancer patients homozygous for allele 2 of the IL-1β gene had significantly shorter survival (144 *vs* 256 days), higher IL-1β production and higher C-reactive levels than other patients or controls.[56]

Implications for prevention and treatment

TNF blockade

Two TNF antagonists (etanercept, Enbrel [Immunex]) and infliximab, Remicade [Centocor]) have been licensed for clinical trial in the treatment of rheumatoid arthritis and Crohn's disease, with over 70 000 patients now treated.[57] There is clinical evidence for five actions of the anti-TNF antibody in rheumatoid arthritis joint tissue—namely, inhibition of cytokine/chemokine production, reduced angiogenesis, prevention of leucocyte infiltration, inhibition of matrix metalloproteases, and improvement of bone-marrow function—and all these actions would be useful in a biological therapy for cancer.

Apart from the data on TNF and cancer growth and spread, some experiments suggest a role for TNF in the development of cancer cachexia,[58] and this might be another benefit of TNF antagonist therapy. Thalidomide inhibits the processing of mRNA for TNF (and VEGF), and continuous low-dose thalidomide has shown activity in patients with advanced myeloma.[59] Several clinical studies are underway using etanercept to assess the role of anti-TNF therapy as a single agent or in combination with other therapies in malignancy. The role of etanercept in ameliorating the adverse effects of other cancer therapies is also being evaluated. There are also ongoing and planned clinical trials with infliximab. As with other "biological" approaches to cancer treatment, anti-TNF therapy may be optimal in an adjuvant setting with minimal disease. Careful recording of the incidence of malignant disease in patients receiving TNF antagonists for inflammatory disease could give some indication of the potential of these agents in the chemoprevention of cancer.

Chemokine antagonism

The chemokine system is part of the strategy used by tumours to recruit pro-tumour inflammatory responses and to seed at distinct anatomical sites. Chemokine receptors belong to a family of receptors (7 transmembrane G-protein coupled receptors) which is already a target of pharmacological interest. Tumours driven by chemokines and those where chemokines are implicated in metastasis (eg, seeding to lymph nodes) may be an appropriate target for chemokine antagonists now under development.[30,35] This approach is supported by data from mouse experiments.[60]

IL-6 antagonism

IL-6 is a major growth factor for myeloma cells.[26] In advanced disease there is an excess of IL-6 production and raised serum concentrations are associated with plasmablastic proliferative activity and short survival. When a mouse monoclonal antibody to IL-6 was given to ten patients with myeloma there was evidence of a biological effect, with decreased C-reactive protein, lower IL-6 production, and resolution of low-grade fever in six patients. However, host response to the murine antibody complicated this study.[61]

Nonsteroidal anti-inflammatory agents

People who have taken non-steroidal anti-inflammatory drugs (NSAIDs), are at reduced risk of colon cancer.[62,63] This may also be true for cancers of the oesophagus, stomach, and rectum, and in rodents experimental bladder, breast, and colon cancer is reduced when NSAIDs are administered concurrently with carcinogens.[64] NSAIDs inhibit cyclooxygenase enzymes and angiogenesis. Cyclooxygenase-2 is induced by cytokines and expressed in both inflammatory disease and cancer. When the cyclooxygenase-2 inhibitor celecoxib was tested on familial adenomatous polyposis patients in a double-blind placebo-controlled study[65] six months of twice daily treatment with 400 mg led to a significant reduction in the colorectal polyp burden.

We thank Adrian Harris, Fionula Brennan, Yuti Chernajovsky, Maurizio D'Incalci, Silvio Garattini, Giovanna Mantovani, Davide Lauri, and Gianni Tognoni for useful discussion.

FB is supported by the Imperial Cancer Research Fund, Queen Mary College, University of London, and by a visiting scientist award from the CNR, Italy. AM is supported by AIRC, MURST, and CNR, Italy.

References

1 Parkin DM, Pisani P, Muñoz N, Ferlay J. In: Newton R, Beral V, Weiss RA, eds. Infections and human cancer. Cold Spring Harbor, NY: Cold Spring Harbor Laboratory Press, 1999.
2 Gulumian M. The role of oxidative stress in diseases caused by mineral dusts and fibres: current status and future of prophylaxis and treatment. *Mol Cell Biochem* 1999; **196:** 69–77.
3 Ekbom A, Helmick C, Zack M, Adami H-O. Ulcerative colitis and colorectal cancer. *N Engl J Med* 1990; **323:** 1228–33.
4 Negus RPK, Stamp GWQ, Hadley J, Balkwill FR. Quantitative assessment of the leucocyte infiltrate in ovarian cancer and its relationship to the expression of C-C chemokines. *Am J Pathol* 1997; **150:** 1723–34.
5 Mantovani A, Bottazzi B, Colotta F, Sozzani S, Ruco L. The origin and function of tumor-associated macrophages. *Immunol Today* 1992; **13:** 265–70.
6 Mantovani A, Bussolino F, Dejana E. Cytokine regulation of endothelial cell function. *FASEB J* 1992; **6:** 2591–99.
7 Coussens LM, Tinkle CL, Hanahan D, Werb Z. MMP-9 supplied by bone marrow-derived cells contributes to skin carcinogenesis. *Cell* 2000; **103:** 481–90.
8 Allavena P, Sica A,Vecchi A, Locati M, Sozzani S, Mantovani A. The chemokine receptor switch paradigm and dendritic cell migration: its significance in tumor tissues. *Immunol Rev* 2000; **177:** 141–49.
9 van den Berg A, Visser L, Poppema S. High expression of the CC chemokine TARC in Reed-Sternberg cells: a possible explanation for the characteristic T-cell infiltrate in Hodgkin's lymphoma. *Am J Pathol* 1999; **154:** 1685–91.
10 Mizoguchi H, O'Shea JJ, Longo DL, Loeffler CM, McVicar DW, Ochoa AC. Alterations in signal transduction molecules in T lymphocytes from tumor-bearing mice. *Science* 1992; **258:** 1795–98.
11 Dvorak HF. Tumors: wounds that do not heal. *N Engl J Med* 1986; **315:** 1650–59.
12 Pinedo HM, Verheul HMW, D'Amato RJ, Folkman J. Involvement of platelets in tumour angiogenesis? *Lancet* 1998; **352:** 1775–77.
13 Burke F, Relf M, Negus R, Balkwill F. A cytokine profile of normal and malignant ovary. *Cytokine* 1996; **8:** 578–85.
14 Koong AC, Denko NC, Hudson KM, et al. Candidate genes for hypoxic tumor phenotype. *Cancer Res* 2000; **60:** 883–87.
15 Kollias G, Douni E, Kassiotis G, Kontoyiannis D. On the role of

tumor necrosis factor and receptors in models of multiorgan failure, rheumatoid arthritis, multiple sclerosis and inflammatory bowel disease. *Immunol Rev* 1999; **169:** 175–94.

16 Lejeune FJ, Ruegg C, Lienard D. Clinical applications of TNF-a in cancer. *Curr Opin Immunol* 1998; **10:** 573–80.

17 Naylor MS, Stamp GWH, Foulkes WD, Eccles D, Balkwill FR. Tumor necrosis factor and its receptors in human ovarian cancer. *J Clin Invest* 1993; **91:** 2194–206.

18 Leek RD, Landers R, Fox SB, Ng F, Harris AL, Lewis CE. Association of tumour necrosis factor alpha and its receptors with thymidine phosphorylase expression in invasive breast carcinoma. *Br J Cancer* 1998; **77:** 2246–51.

19 Warzocha K, Salles G, Bienvenu J, et al. Tumor necrosis factor ligand-receptor system can predict treatment outcome in lymphoma patients. *J Clin Oncol* 1997; **15:** 499–508.

20 Malik STA, Griffin DB, Fiers W, Balkwill FR. Paradoxical, effects of tumour necrosids factor in experimental ovarian cancer. *Int J Cancer* 1989; **44:** 918–25.

21 Malik STA, Naylor S, East N, Oliff A, Balkwill FR. Cells secreting tumour necrosis factor show enhanced metastasis in nude mice. *Eur J Cancer* 1990; **26:** 1031–34.

22 Roberts RA, Kimber I. Cytokines in non-genotoxic hepatocarcinogenesis. *Carcinogenesis* 1999; **20:** 1397–401.

23 Moore R, Owens D, Stamp G, et al. Tumour necrosis factor-a deficient mice are resistant to skin carcinogenesis. *Nat Med* 1999; **5:** 828–31.

24 Robertson FM, Ross MS, Tober KL, Long BW, Oberyszyn TM. Inhibition of pro-inflammatory cytokine gene expression and papilloma growth during murine multistage carcinogenesis by pentoxifylline. *Carcinogenesis* 1996; **17:** 1719–28.

25 Vidal-Vanaclocha F, Fantuzzi G, Mendoza L, et al. IL-18 regulates IL-1b-dependent hepatic melanoma metastasis via vascular cell adhesion molecule-1. *PNAS* 2000; **97:** 734–39.

26 Tricot G. New insights into role of microenvironment in multiple myeloma. *Lancet* 2000; **355:** 248–50.

27 Negus RPM, Stamp GWH, Relf MG, et al. The detection and localization of monocyte chemoattractant protein-1 (MCP-1) in human ovarian cancer. *J Clin Invest* 1995; **95:** 2391–96.

28 Luboshits G, Shina S, Kaplan O, et al. Elevated expression of the CC chemokine regulated on activation, normal T cell expressed and secreted (RANTES) in advanced breast carcinoma. *Cancer Res* 1999; **59:** 4681–87.

29 Cossman J, Annunziata CM, Barash S, et al. Reed-Sternberg cell genome expression supports a B-cell lineage. *Blood* 1999; **94:** 411–16.

30 Hanghnegahdar H, Du J, Wang Z, et al. The tumorigenic and angiogenic effects of MGSSA/GRO proteins in melanoma. *J Leukoc Biol* 2000; **67:** 53–62.

31 Medrano EE, Farooqui JZ, Boissy RE, Boissy YL, Akadiri B, Nordlund JJ. Chronic growth stimulation of human adult melanocytes by inflammatory mediators in vitro: implications for nevus formation and initial steps in melanocyte oncogenesis. *Proc Natl Acad Sci* 1993; **90:** 1790–94.

32 Mazzucchelli L, Blaser A, Kappeler A, et al. BCA-1 is highly expressed in *Helicobacter pylori*-induced mucosa-associated lymphoid tissue and gastric lymphoma. *J Clin Invest* 1999; **104:** R49–R54.

33 Sica A, Saccani A, Bottazzi B, et al. Defective expression of the monocyte chemotactic protein-1 receptor CCR2 in macrophages associated with human ovarian carcinoma. *J Immunol* 2000; **164:** 733–38.

34 Venkatakrishnan G, Salgia E, Groopman JE. Chemokine receptors CXCR-1/2 activate mitogen activated protein kinase via the epidermal growth factor receptor in ovarian cancer cells. *J Biol Chem* 2000; **275:** 6868–75.

35 Wang JM, Chertov O, Proost P, et al. Purification and identification of chemokines potenetially involved in kidney-specific metastasis by a murine lymphoma variant: induction of migration and NFkB activation. *Int J Cancer* 1998; **75:** 900–07.

36 Komori A, Yatsunami M, Suganuma S, et al. Tumor necrosis factor acts as a tumor promoter in BALB/3T3 cell transformation. *Cancer Res* 1993; **53:** 1982–85.

37 Jaiswal M, LaRusso NF, Burgart LJ, Gores GJ. Inflammatory cytokines induce DNA damage and inhibit DNA repair in cholangiocarcinoma cells by a nitric oxide-dependent mechanism. *Cancer Res* 2000; **60:** 184–90.

38 Hudson JD, Shoaibi MA, Maestro R, Carnero A, Hannon GJ, Beach DH. A proinflammatory cytokine inhibits p53 tumor suppressor activity. *J Exp Med* 1999; **190:** 1375–82.

39 El-Omar EM, Carrington M, Chow WH, et al. Interleukin-1 polymorphisms associated with increased risk of gastric cancer. *Nature* 2000; **404:** 398–402.

40 O'Byrne KJ, Dalgleish AG, Browning MJ, Steward WP, Harris AL. The relationship between angiogenesis and the immune response in carcinogenesis and the progression of malignant disease. *Eur J Cancer* 2000; **36:** 151–69.

41 Leek RD, Landers RJ, Harris AL, Lewis CE. Necrosis correlates with high vascular density and focal macrophage infiltration in invasive carcinoma of the breast. *Br J Cancer* 1999; **79:** 991–95.

42 Keane MP, Strieter RM. In Mantovani A, ed. Chemokines: chemical immunology: vol 72. Basel: Karger, 1999: 86–101.

43 Opdenakker G, Van Damme J. Chemotactic factors, passive invasion and metastasis of cancer cells. *Immunol Today* 1992; **13:** 463–64.

44 Martin Padura I, Mortarini R, Lauri D, et al. Heterogeneity in human melanoma cell adhesion to cytokine activated endothelia cells correlates with VLA-4 expression. *Cancer Res* 1991; **51:** 2239–41.

45 Korner H. Cretney E, Wilhelm P, Kelly JM, Rollinghoff M, Smyth SJD, Smyth MJ. Tumor necrosis factor sustains the generalized lymphoproliferative disorder (gld) phenotype. *J Exp Med* 2000; **191:** 89–96.

46 Goerdt S, Orfanos CE. Other function, other genes: alternative activation of antigen-presenting cells. *Immunity* 1999; **10:** 137–42.

47 Sica A, Saccani A, Bottazi B, et al. Autocrine production of IL-10 mediates defective IL-12 production and NF-κB activation of tumor-associated macrophages. *J Immunol* 2000; **164:** 762–67.

48 Gu L, Tseng R, Horner RM, Tam C, Loda M, Rollins BJ. Control of TH2 polarization by the chemokine monocyte chemoattractant protein-1. *Nature* 2000; **404:** 407–11.

49 Sozzani S, Luini W, Bianchi G, et al. The viral chemokine macrophage inflammatory protein-II is a selective Th2 chemoattractant. *Blood* 1998; **92:** 4036–39.

50 Endres MJ, Garlisi CJ, Xiao H, Shan L, Hendrick JA. The Kaposi's sarcoma-related herpes virus (KSHV)-encoded chemokine vMIP-1 is a specific agonist for the CC receptor (CCR)8. *J Exp Med* 1999; **189:** 1993–98.

51 Gambacorti-Passerini C, Barni R, LeCoutre P, et al. Role of alpha 1 acidic glycoprotein in the in vivo resistance of human BCR-ABL (+) leukemic cells to the abl inhibitor STI571. *JNCI* 2000; **92:** 1641–50.

52 Snyderman R, Cianciolo GJ. Immunosuppressive activity in the retroviral envelope protein P15E and its possible relationship to neoplasia. *Immunol Today* 1984; **5:** 240–44.

53 Rutledge BJ, Rayburn H, Rosenberg R, et al. High level monocyte chemoattractant protein-1 expression in transgenic mice increases their susceptibility to intracellular pathogens. *J Immunol* 1995; **155:** 4838–43.

54 Warzocha K, Ribeiro P, Bienvenu J, et al. Genetic polymorphisms in the tumor necrosis factor locus influence non-Hodgkin's lymphoma outcome. *Blood* 1998; **91:** 3574–81.

55 Oh BR, Sasaki M, Perinchery G, et al. Frequent genotype changes at −308 and 488 regions of the tumor necrosis factor-alpha (TNF-alpha) gene in patients with prostate cancer. *J Urol* 2000; **163:** 1584–87.

56 Barber MD, Powell JJ, Lynch SF, Fearon KCH, Ross JA. A polymorphism of the interleukin-1β gene influences survival in pancreatic cancer. *Br J Cancer* 2000; **83:** 1443–47.

57 Maini RN, Taylor PC. Anti-cytokine therapy for rheumatoid arthritis. *Annu Rev Med* 2000; **51:** 207–29.

58 Tisdale MJ. Biology of cachexia. *JNCI* 1997; **89:** 1763–73.

59 Singhal S, Mehta J, Desikan R, et al. Antitumor activity of thalidomide in refractory multiple myeloma. *N Engl J Med* 1999; **341:** 1565–71.

60 Peng L, Shu S, Krauss J. Monocyte chemoattractant protein inhibits the generation of tumor-reactive T cells. *Cancer Res* 1997; **57:** 4849–54.

61 Bataille R, Barlogie B, Lu ZY, et al. Biologic effects of anti-interleukin-6 murine monoclonal antibody in advanced multiple myeloma. *Blood* 1995; **86:** 685–91.

62 Thun MJ, Namboodiri MM, Calle EE, Flanders WD, Heath CW Jr. Aspirin use and risk of fatal cancer. *Cancer Res* 1993; **53:** 1322–27.

63 Langman MJ, Cheng KK, Gilman EA, Lancashire RJ. Effect of anti-inflammatory drugs on overall risk of common cancer: case-control study in general practice research database. *BMJ* 2000; **320:** 1642–46.

64 Reddy BS, Rao CV, Seibert K. Evaluation of cyclooxygenase-2 inhibitor for potential chemopreventive properties in colon carcinogenesis. *Cancer Res* 1996; **56:** 4566–69.

65 Steinbach G, Lynch PM, Phillips RKS, et al. The effect of celecoxib a cyclooxygenase-2 inhibitor, in familial adenomatous polyposis. *N Engl J Med* 2000; **342:** 1946–52.

Further reading available on http://www.icnet/labs/balkwill/virchow.html
http://www.marionegri.it/virchow

Exhibit 99

Cell

Leading Edge
Review

Hallmarks of Cancer: The Next Generation

Douglas Hanahan[1,2,*] and Robert A. Weinberg[3,*]
[1]The Swiss Institute for Experimental Cancer Research (ISREC), School of Life Sciences, EPFL, Lausanne CH-1015, Switzerland
[2]The Department of Biochemistry & Biophysics, UCSF, San Francisco, CA 94158, USA
[3]Whitehead Institute for Biomedical Research, Ludwig/MIT Center for Molecular Oncology, and MIT Department of Biology, Cambridge, MA 02142, USA
*Correspondence: dh@epfl.ch (D.H.), weinberg@wi.mit.edu (R.A.W.)
DOI 10.1016/j.cell.2011.02.013

The hallmarks of cancer comprise six biological capabilities acquired during the multistep development of human tumors. The hallmarks constitute an organizing principle for rationalizing the complexities of neoplastic disease. They include sustaining proliferative signaling, evading growth suppressors, resisting cell death, enabling replicative immortality, inducing angiogenesis, and activating invasion and metastasis. Underlying these hallmarks are genome instability, which generates the genetic diversity that expedites their acquisition, and inflammation, which fosters multiple hallmark functions. Conceptual progress in the last decade has added two emerging hallmarks of potential generality to this list—reprogramming of energy metabolism and evading immune destruction. In addition to cancer cells, tumors exhibit another dimension of complexity: they contain a repertoire of recruited, ostensibly normal cells that contribute to the acquisition of hallmark traits by creating the "tumor microenvironment." Recognition of the widespread applicability of these concepts will increasingly affect the development of new means to treat human cancer.

INTRODUCTION

We have proposed that six hallmarks of cancer together constitute an organizing principle that provides a logical framework for understanding the remarkable diversity of neoplastic diseases (Hanahan and Weinberg, 2000). Implicit in our discussion was the notion that as normal cells evolve progressively to a neoplastic state, they acquire a succession of these hallmark capabilities, and that the multistep process of human tumor pathogenesis could be rationalized by the need of incipient cancer cells to acquire the traits that enable them to become tumorigenic and ultimately malignant.

We noted as an ancillary proposition that tumors are more than insular masses of proliferating cancer cells. Instead, they are complex tissues composed of multiple distinct cell types that participate in heterotypic interactions with one another. We depicted the recruited normal cells, which form tumor-associated stroma, as active participants in tumorigenesis rather than passive bystanders; as such, these stromal cells contribute to the development and expression of certain hallmark capabilities. During the ensuing decade this notion has been solidified and extended, revealing that the biology of tumors can no longer be understood simply by enumerating the traits of the cancer cells but instead must encompass the contributions of the "tumor microenvironment" to tumorigenesis.

In the course of remarkable progress in cancer research subsequent to this publication, new observations have served both to clarify and to modify the original formulation of the hallmark capabilities. In addition, yet other observations have raised questions and highlighted mechanistic concepts that were not integral to our original elaboration of the hallmark traits. Motivated by these developments, we now revisit the original hallmarks, consider new ones that might be included in this roster, and expand upon the functional roles and contributions made by recruited stromal cells to tumor biology.

HALLMARK CAPABILITIES—CONCEPTUAL PROGRESS

The six hallmarks of cancer—distinctive and complementary capabilities that enable tumor growth and metastatic dissemination—continue to provide a solid foundation for understanding the biology of cancer (Figure 1; see the Supplemental Information for downloadable versions of the figures for presentations). In the first section of this Review, we summarize the essence of each hallmark as described in the original presentation in 2000, followed by selected illustrations (demarcated by subheadings in italics) of the conceptual progress made over the past decade in understanding their mechanistic underpinnings. In subsequent sections we address new developments that broaden the scope of the conceptualization, describing in turn two enabling characteristics crucial to the acquisition of the six hallmark capabilities, two new emerging hallmark capabilities, the constitution and signaling interactions of the tumor microenvironment crucial to cancer phenotypes, and we finally discuss the new frontier of therapeutic application of these concepts.

Sustaining Proliferative Signaling

Arguably the most fundamental trait of cancer cells involves their ability to sustain chronic proliferation. Normal tissues carefully control the production and release of growth-promoting signals that instruct entry into and progression through the cell growth-and-division cycle, thereby ensuring a homeostasis of cell

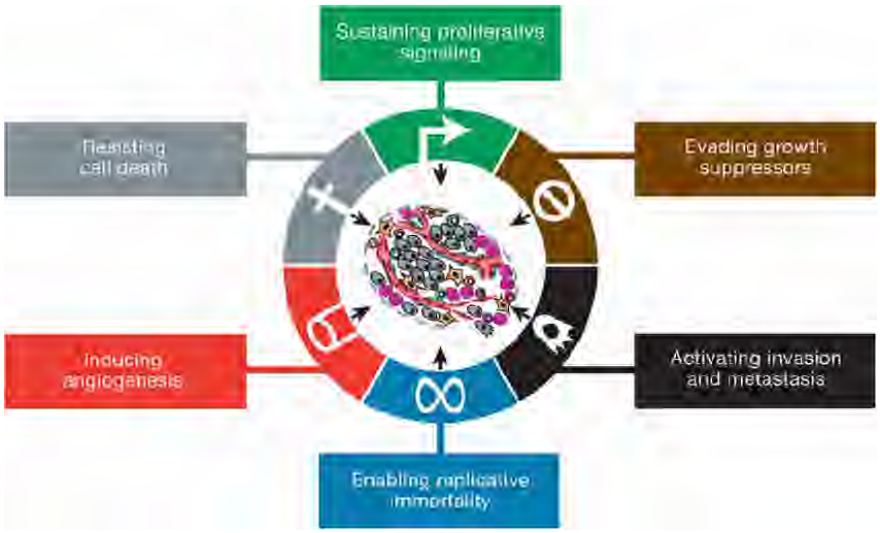

Figure 1. The Hallmarks of Cancer
This illustration encompasses the six hallmark capabilities originally proposed in our 2000 perspective. The past decade has witnessed remarkable progress toward understanding the mechanistic underpinnings of each hallmark.

number and thus maintenance of normal tissue architecture and function. Cancer cells, by deregulating these signals, become masters of their own destinies. The enabling signals are conveyed in large part by growth factors that bind cell-surface receptors, typically containing intracellular tyrosine kinase domains. The latter proceed to emit signals via branched intracellular signaling pathways that regulate progression through the cell cycle as well as cell growth (that is, increases in cell size); often these signals influence yet other cell-biological properties, such as cell survival and energy metabolism.

Remarkably, the precise identities and sources of the proliferative signals operating within normal tissues were poorly understood a decade ago and in general remain so. Moreover, we still know relatively little about the mechanisms controlling the release of these mitogenic signals. In part, the understanding of these mechanisms is complicated by the fact that the growth factor signals controlling cell number and position within tissues are thought to be transmitted in a temporally and spatially regulated fashion from one cell to its neighbors; such paracrine signaling is difficult to access experimentally. In addition, the bioavailability of growth factors is regulated by sequestration in the pericellular space and extracellular matrix, and by the actions of a complex network of proteases, sulfatases, and possibly other enzymes that liberate and activate them, apparently in a highly specific and localized fashion.

The mitogenic signaling in cancer cells is, in contrast, better understood (Lemmon and Schlessinger, 2010; Witsch et al., 2010; Hynes and MacDonald, 2009; Perona, 2006). Cancer cells can acquire the capability to sustain proliferative signaling in a number of alternative ways: They may produce growth factor ligands themselves, to which they can respond via the expression of cognate receptors, resulting in autocrine proliferative stimulation. Alternatively, cancer cells may send signals to stimulate normal cells within the supporting tumor-associated stroma, which reciprocate by supplying the cancer cells with various growth factors (Cheng et al., 2008; Bhowmick et al., 2004). Receptor signaling can also be deregulated by elevating the levels of receptor proteins displayed at the cancer cell surface, rendering such cells hyperresponsive to otherwise-limiting amounts of growth factor ligand; the same outcome can result from structural alterations in the receptor molecules that facilitate ligand-independent firing.

Growth factor independence may also derive from the constitutive activation of components of signaling pathways operating downstream of these receptors, obviating the need to stimulate these pathways by ligand-mediated receptor activation. Given that a number of distinct downstream signaling pathways radiate from a ligand-stimulated receptor, the activation of one or another of these downstream pathways, for example, the one responding to the Ras signal transducer, may only recapitulate a subset of the regulatory instructions transmitted by an activated receptor.

Somatic Mutations Activate Additional Downstream Pathways

High-throughput DNA sequencing analyses of cancer cell genomes have revealed somatic mutations in certain human tumors that predict constitutive activation of signaling circuits usually triggered by activated growth factor receptors. Thus, we now know that ~40% of human melanomas contain activating mutations affecting the structure of the B-Raf protein, resulting in constitutive signaling through the Raf to mitogen-activated protein (MAP)-kinase pathway (Davies and Samuels 2010). Similarly, mutations in the catalytic subunit of phosphoinositide 3-kinase (PI3-kinase) isoforms are being detected in an array of tumor types, which serve to hyperactivate the PI3-kinase signaling circuitry, including its key Akt/PKB signal transducer (Jiang and Liu, 2009; Yuan and Cantley, 2008). The advantages to tumor cells of activating upstream (receptor) versus downstream (transducer) signaling remain obscure, as does the functional impact of crosstalk between the multiple pathways radiating from growth factor receptors.

Disruptions of Negative-Feedback Mechanisms that Attenuate Proliferative Signaling

Recent results have highlighted the importance of negative-feedback loops that normally operate to dampen various types of signaling and thereby ensure homeostatic regulation of the flux of signals coursing through the intracellular circuitry (Wertz and Dixit, 2010; Cabrita and Christofori, 2008; Amit et al., 2007; Mosesson et al., 2008). Defects in these feedback mechanisms are capable of enhancing proliferative signaling. The prototype of this type of regulation involves the Ras oncoprotein: the oncogenic effects of Ras do not result from a hyperactivation of its signaling powers; instead, the oncogenic mutations affecting *ras* genes compromise Ras GTPase activity, which

operates as an intrinsic negative-feedback mechanism that normally ensures that active signal transmission is transitory.

Analogous negative-feedback mechanisms operate at multiple nodes within the proliferative signaling circuitry. A prominent example involves the PTEN phosphatase, which counteracts PI3-kinase by degrading its product, phosphatidylinositol (3,4,5) trisphosphate (PIP_3). Loss-of-function mutations in PTEN amplify PI3K signaling and promote tumorigenesis in a variety of experimental models of cancer; in human tumors, PTEN expression is often lost by promoter methylation (Jiang and Liu, 2009; Yuan and Cantley, 2008).

Yet another example involves the mTOR kinase, a coordinator of cell growth and metabolism that lies both upstream and downstream of the PI3K pathway. In the circuitry of some cancer cells, mTOR activation results, via negative feedback, in the inhibition of PI3K signaling. Thus, when mTOR is pharmacologically inhibited in such cancer cells (such as by the drug rapamycin), the associated loss of negative feedback results in increased activity of PI3K and its effector Akt/PKB, thereby blunting the antiproliferative effects of mTOR inhibition (Sudarsanam and Johnson, 2010; O'Reilly et al., 2006). It is likely that compromised negative-feedback loops in this and other signaling pathways will prove to be widespread among human cancer cells and serve as an important means by which these cells can achieve proliferative independence. Moreover, disruption of such self-attenuating signaling may contribute to the development of adaptive resistance toward drugs targeting mitogenic signaling.

Excessive Proliferative Signaling Can Trigger Cell Senescence

Early studies of oncogene action encouraged the notion that ever-increasing expression of such genes and the signals manifested in their protein products would result in correspondingly increased cancer cell proliferation and thus tumor growth. More recent research has undermined this notion, in that excessively elevated signaling by oncoproteins such as RAS, MYC, and RAF can provoke counteracting responses from cells, specifically induction of cell senescence and/or apoptosis (Collado and Serrano, 2010; Evan and d'Adda di Fagagna, 2009; Lowe et al., 2004). For example, cultured cells expressing high levels of the Ras oncoprotein may enter into the nonproliferative but viable state called senescence; in contrast, cells expressing lower levels of this protein may avoid senescence and proliferate.

Cells with morphological features of senescence, including enlarged cytoplasm, the absence of proliferation markers, and expression of the senescence-induced β-galactosidase enzyme, are abundant in the tissues of mice engineered to overexpress certain oncogenes (Collado and Serrano, 2010; Evan and d'Adda di Fagagna, 2009) and are prevalent in some cases of human melanoma (Mooi and Peeper, 2006). These ostensibly paradoxical responses seem to reflect intrinsic cellular defense mechanisms designed to eliminate cells experiencing excessive levels of certain types of signaling. Accordingly, the relative intensity of oncogenic signaling in cancer cells may represent compromises between maximal mitogenic stimulation and avoidance of these antiproliferative defenses. Alternatively, some cancer cells may adapt to high levels of oncogenic signaling by disabling their senescence- or apoptosis-inducing circuitry.

Evading Growth Suppressors

In addition to the hallmark capability of inducing and sustaining positively acting growth-stimulatory signals, cancer cells must also circumvent powerful programs that negatively regulate cell proliferation; many of these programs depend on the actions of tumor suppressor genes. Dozens of tumor suppressors that operate in various ways to limit cell growth and proliferation have been discovered through their characteristic inactivation in one or another form of animal or human cancer; many of these genes have been validated as bona fide tumor suppressors through gain- or loss-of-function experiments in mice. The two prototypical tumor suppressors encode the RB (retinoblastoma-associated) and TP53 proteins; they operate as central control nodes within two key complementary cellular regulatory circuits that govern the decisions of cells to proliferate or, alternatively, activate senescence and apoptotic programs.

The RB protein integrates signals from diverse extracellular and intracellular sources and, in response, decides whether or not a cell should proceed through its growth-and-division cycle (Burkhart and Sage, 2008; Deshpande et al., 2005; Sherr and McCormick, 2002). Cancer cells with defects in RB pathway function are thus missing the services of a critical gatekeeper of cell-cycle progression whose absence permits persistent cell proliferation. Whereas RB transduces growth-inhibitory signals that originate largely outside of the cell, TP53 receives inputs from stress and abnormality sensors that function within the cell's intracellular operating systems: if the degree of damage to the genome is excessive, or if the levels of nucleotide pools, growth-promoting signals, glucose, or oxygenation are suboptimal, TP53 can call a halt to further cell-cycle progression until these conditions have been normalized. Alternatively, in the face of alarm signals indicating overwhelming or irreparable damage to such cellular subsystems, TP53 can trigger apoptosis. Notably, the various effects of activated TP53 are complex and highly context dependent, varying by cell type as well as by the severity and persistence of conditions of cell stress and genomic damage.

Although the two canonical suppressors of proliferation—TP53 and RB—have preeminent importance in regulating cell proliferation, various lines of evidence indicate that each operates as part of a larger network that is wired for functional redundancy. For example, chimeric mice populated throughout their bodies with individual cells lacking a functional *Rb* gene are surprisingly free of proliferative abnormalities, despite the expectation that loss of RB function would allow continuous firing of the cell division cycle in these cells and their lineal descendants; some of the resulting clusters of *Rb* null cells should, by all rights, progress to neoplasia. Instead, the *Rb* null cells in such chimeric mice have been found to participate in relatively normal tissue morphogenesis throughout the body; the only neoplasia observed was in the development of pituitary tumors late in life (Lipinski and Jacks, 1999). Similarly, *TP53* null mice develop normally, show largely proper cell and tissue homeostasis, and again develop abnormalities later in life, in the form of leukemias and sarcomas (Ghebranious and Donehower, 1998). Both examples must reflect the operations of redundantly acting mechanisms that serve to constrain inappropriate replication of cells lacking these key proliferation suppressors.

Mechanisms of Contact Inhibition and Its Evasion

Four decades of research have demonstrated that the cell-to-cell contacts formed by dense populations of normal cells propagated in two-dimensional culture operate to suppress further cell proliferation, yielding confluent cell monolayers. Importantly, such "contact inhibition" is abolished in various types of cancer cells in culture, suggesting that contact inhibition is an in vitro surrogate of a mechanism that operates in vivo to ensure normal tissue homeostasis, one that is abrogated during the course of tumorigenesis. Until recently, the mechanistic basis for this mode of growth control remained obscure. Now, however, mechanisms of contact inhibition are beginning to emerge.

One mechanism involves the product of the *NF2* gene, long implicated as a tumor suppressor because its loss triggers a form of human neurofibromatosis. Merlin, the cytoplasmic *NF2* gene product, orchestrates contact inhibition via coupling cell-surface adhesion molecules (e.g., E-cadherin) to transmembrane receptor tyrosine kinases (e.g., the EGF receptor). In so doing, Merlin strengthens the adhesivity of cadherin-mediated cell-to-cell attachments. Additionally, by sequestering growth factor receptors, Merlin limits their ability to efficiently emit mitogenic signals (Curto et al., 2007; Okada et al., 2005).

A second mechanism of contact inhibition involves the LKB1 epithelial polarity protein, which organizes epithelial structure and helps maintain tissue integrity. LKB1 can, for example, overrule the mitogenic effects of the powerful Myc oncogene when the latter is upregulated in organized, quiescent epithelial structures; in contrast, when LKB1 expression is suppressed, epithelial integrity is destabilized, and epithelial cells become susceptible to Myc-induced transformation (Partanen et al., 2009; Hezel and Bardeesy, 2008). *LKB1* has also been identified as a tumor suppressor gene that is lost in certain human malignancies (Shaw, 2009), possibly reflecting its normal function as a suppressor of inappropriate proliferation. It remains to be seen how frequently these two mechanisms of contact-mediated growth suppression are compromised in human cancers; no doubt yet other contact-induced proliferative barriers are yet to be discovered. Clearly mechanisms like these that enable cells to construct and maintain architecturally complex tissues represent important means of suppressing and counterbalancing inappropriate proliferative signals.

Corruption of the TGF-β Pathway Promotes Malignancy

TGF-β is best known for its antiproliferative effects, and evasion by cancer cells of these effects is now appreciated to be far more elaborate than simple shutdown of its signaling circuitry (Ikushima and Miyazono, 2010; Massagué, 2008; Bierie and Moses, 2006). In many late-stage tumors, TGF-β signaling is redirected away from suppressing cell proliferation and is found instead to activate a cellular program, termed the epithelial-to-mesenchymal transition (EMT), that confers on cancer cells traits associated with high-grade malignancy, as discussed in further detail below.

Resisting Cell Death

The concept that programmed cell death by apoptosis serves as a natural barrier to cancer development has been established by compelling functional studies conducted over the last two decades (Adams and Cory, 2007; Lowe et al., 2004: Evan and Littlewood, 1998). Elucidation of the signaling circuitry governing the apoptotic program has revealed how apoptosis is triggered in response to various physiologic stresses that cancer cells experience during the course of tumorigenesis or as a result of anticancer therapy. Notable among the apoptosis-inducing stresses are signaling imbalances resulting from elevated levels of oncogene signaling, as mentioned earlier, and DNA damage associated with hyperproliferation. Yet other research has revealed how apoptosis is attenuated in those tumors that succeed in progressing to states of high-grade malignancy and resistance to therapy (Adams and Cory, 2007; Lowe et al., 2004).

The apoptotic machinery is composed of both upstream regulators and downstream effector components (Adams and Cory, 2007). The regulators, in turn, are divided into two major circuits, one receiving and processing extracellular death-inducing signals (the extrinsic apoptotic program, involving for example the Fas ligand/Fas receptor), and the other sensing and integrating a variety of signals of intracellular origin (the intrinsic program). Each culminates in activation of a normally latent protease (caspases 8 and 9, respectively), which proceeds to initiate a cascade of proteolysis involving effector caspases responsible for the execution phase of apoptosis, in which the cell is progressively disassembled and then consumed, both by its neighbors and by professional phagocytic cells. Currently, the intrinsic apoptotic program is more widely implicated as a barrier to cancer pathogenesis.

The "apoptotic trigger" that conveys signals between the regulators and effectors is controlled by counterbalancing pro- and antiapoptotic members of the Bcl-2 family of regulatory proteins (Adams and Cory, 2007). The archetype, Bcl-2, along with its closest relatives (Bcl-x_L, Bcl-w, Mcl-1, A1) are inhibitors of apoptosis, acting in large part by binding to and thereby suppressing two proapoptotic triggering proteins (Bax and Bak); the latter are embedded in the mitochondrial outer membrane. When relieved of inhibition by their antiapoptotic relatives, Bax and Bak disrupt the integrity of the outer mitochondrial membrane, causing the release of proapoptotic signaling proteins, the most important of which is cytochrome *c*. The released cytochrome *c* activates, in turn, a cascade of caspases that act via their proteolytic activities to induce the multiple cellular changes associated with the apoptotic program. Bax and Bak share protein-protein interaction domains, termed BH3 motifs, with the antiapoptotic Bcl-2-like proteins that mediate their various physical interactions. The activities of a subfamily of related proteins, each of which contains a single such BH3 motif, are coupled to a variety of sensors of cellular abnormality; these "BH3-only" proteins act either by interfering with antiapoptotic Bcl-2 proteins or by directly stimulating the proapoptotic members of this family (Adams and Cory, 2007; Willis and Adams, 2005).

Although the cellular conditions that trigger apoptosis remain to be fully enumerated, several abnormality sensors that play key roles in tumor development have been identified (Adams and Cory, 2007; Lowe et al., 2004). Most notable is a DNA-damage sensor that functions via the TP53 tumor suppressor (Junttila and Evan, 2009); TP53 induces apoptosis by upregulating expression of the Noxa and Puma BH3-only proteins, doing so in response to substantial levels of DNA breaks and other chromosomal abnormalities. Alternatively, insufficient survival

factor signaling (for instance inadequate levels of interleukin-3 in lymphocytes or of insulin-like growth factor 1/2 [Igf1/2] in epithelial cells) can elicit apoptosis through a BH3-only protein called Bim. Yet another condition leading to cell death involves hyperactive signaling by certain oncoproteins, such as Myc, which triggers apoptosis (in part via Bim and other BH3-only proteins) unless counterbalanced by antiapoptotic factors (Junttila and Evan, 2009; Lowe et al., 2004).

Tumor cells evolve a variety of strategies to limit or circumvent apoptosis. Most common is the loss of TP53 tumor suppressor function, which eliminates this critical damage sensor from the apoptosis-inducing circuitry. Alternatively, tumors may achieve similar ends by increasing expression of antiapoptotic regulators (Bcl-2, Bcl-x_L) or of survival signals (Igf1/2), by downregulating proapoptotic factors (Bax, Bim, Puma), or by short-circuiting the extrinsic ligand-induced death pathway. The multiplicity of apoptosis-avoiding mechanisms presumably reflects the diversity of apoptosis-inducing signals that cancer cell populations encounter during their evolution to the malignant state.

The structure of the apoptotic machinery and program, and the strategies used by cancer cells to evade its actions, were widely appreciated by the beginning of the last decade. The most notable conceptual advances since then have involved other forms of cell death that broaden the scope of "programmed cell death" as a barrier to cancer.

Autophagy Mediates Both Tumor Cell Survival and Death

Autophagy represents an important cell-physiologic response that, like apoptosis, normally operates at low, basal levels in cells but can be strongly induced in certain states of cellular stress, the most obvious of which is nutrient deficiency (Levine and Kroemer, 2008; Mizushima, 2007). The autophagic program enables cells to break down cellular organelles, such as ribosomes and mitochondria, allowing the resulting catabolites to be recycled and thus used for biosynthesis and energy metabolism. As part of this program, intracellular vesicles termed autophagosomes envelope intracellular organelles and then fuse with lysosomes wherein degradation occurs. In this fashion, low-molecular-weight metabolites are generated that support survival in the stressed, nutrient-limited environments experienced by many cancer cells.

Like apoptosis, the autophagy machinery has both regulatory and effector components (Levine and Kroemer, 2008; Mizushima, 2007). Among the latter are proteins that mediate autophagosome formation and delivery to lysosomes. Of note, recent research has revealed intersections between the regulatory circuits governing autophagy, apoptosis, and cellular homeostasis. For example, the signaling pathway involving the PI3-kinase, AKT, and mTOR kinases, which is stimulated by survival signals to block apoptosis, similarly inhibits autophagy; when survival signals are insufficient, the PI3K signaling pathway is downregulated, with the result that autophagy and/or apoptosis may be induced (Levine and Kroemer, 2008; Sinha and Levine, 2008; Mathew et al., 2007).

Another interconnection between these two programs resides in the Beclin-1 protein, which has been shown by genetic studies to be necessary for induction of autophagy (Levine and Kroemer, 2008; Sinha and Levine, 2008; Mizushima, 2007). Beclin-1 is a member of the BH3-only subfamily of apoptotic regulatory proteins, and its BH3 domain allows it to bind the Bcl-2/Bcl-x_L proteins. Stress-sensor-coupled BH3 proteins can displace Beclin-1 from its association with Bcl-2/Bcl-x_L, enabling the liberated Beclin-1 to trigger autophagy, much as they can release proapoptotic Bax and Bak to trigger apoptosis. Hence, stress-transducing BH3 proteins (e.g., Bid, Bad, Puma, et al.) can induce apoptosis and/or autophagy depending on the physiologic state of the cell.

Mice bearing inactivated alleles of the *Beclin-1* gene or of certain other components of the autophagy machinery exhibit increased susceptibility to cancer (White and DiPaola, 2009: Levine and Kroemer, 2008). These results suggest that induction of autophagy can serve as a barrier to tumorigenesis that may operate independently of or in concert with apoptosis. Accordingly, autophagy appears to represent yet another barrier that needs to be circumvented during tumor development (White and DiPaola, 2009).

Perhaps paradoxically, nutrient starvation, radiotherapy, and certain cytotoxic drugs can induce elevated levels of autophagy that are apparently cytoprotective for cancer cells, impairing rather than accentuating the killing actions of these stress-inducing situations (White and DiPaola, 2009; Apel et al., 2009; Amaravadi and Thompson, 2007; Mathew et al., 2007). Moreover, severely stressed cancer cells have been shown to shrink via autophagy to a state of reversible dormancy (White and DiPaola, 2009; Lu et al., 2008). This survival response may enable the persistence and eventual regrowth of some late-stage tumors following treatment with potent anticancer agents. Thus, in analogy to TGF-β signaling, which can be tumor suppressing at early stages of tumorigenesis and tumor promoting later on, autophagy seems to have conflicting effects on tumor cells and thus tumor progression (Apel et al., 2009; White and DiPaola, 2009). An important agenda for future research will involve clarifying the genetic and cell-physiologic conditions that dictate when and how autophagy enables cancer cells to survive or causes them to die.

Necrosis Has Proinflammatory and Tumor-Promoting Potential

In contrast to apoptosis, in which a dying cell contracts into an almost-invisible corpse that is soon consumed by neighbors, necrotic cells become bloated and explode, releasing their contents into the local tissue microenvironment. Although necrosis has historically been viewed much like organismic death, as a form of system-wide exhaustion and breakdown, the conceptual landscape is changing: cell death by necrosis is clearly under genetic control in some circumstances, rather than being a random and undirected process (Galluzzi and Kroemer, 2008; Zong and Thompson, 2006).

Perhaps more important, necrotic cell death releases proinflammatory signals into the surrounding tissue microenvironment, in contrast to apoptosis and autophagy, which do not. As a consequence, necrotic cells can recruit inflammatory cells of the immune system (Grivennikov et al., 2010; White et al., 2010; Galluzzi and Kroemer, 2008), whose dedicated function is to survey the extent of tissue damage and remove associated necrotic debris. In the context of neoplasia, however, multiple lines of evidence indicate that immune inflammatory cells can be actively tumor promoting, given that such cells are capable

of fostering angiogenesis, cancer cell proliferation, and invasiveness (see below). Additionally, necrotic cells can release bioactive regulatory factors, such as IL-1α, which can directly stimulate neighboring viable cells to proliferate, with the potential, once again, to facilitate neoplastic progression (Grivennikov et al., 2010). Consequently, necrotic cell death, while seemingly beneficial in counterbalancing cancer-associated hyperproliferation, may ultimately do more damage than good. Accordingly, incipient neoplasias and potentially invasive and metastatic tumors may gain an advantage by tolerating some degree of necrotic cell death, doing so in order to recruit tumor-promoting inflammatory cells that bring growth-stimulating factors to the surviving cells within these growths.

Enabling Replicative Immortality

By 2000, it was widely accepted that cancer cells require unlimited replicative potential in order to generate macroscopic tumors. This capability stands in marked contrast to the behavior of the cells in most normal cell lineages in the body, which are able to pass through only a limited number of successive cell growth-and-division cycles. This limitation has been associated with two distinct barriers to proliferation: senescence, a typically irreversible entrance into a nonproliferative but viable state, and crisis, which involves cell death. Accordingly, when cells are propagated in culture, repeated cycles of cell division lead first to induction of senescence and then, for those cells that succeed in circumventing this barrier, to a crisis phase, in which the great majority of cells in the population die. On rare occasion, cells emerge from a population in crisis and exhibit unlimited replicative potential. This transition has been termed immortalization, a trait that most established cell lines possess by virtue of their ability to proliferate in culture without evidence of either senescence or crisis.

Multiple lines of evidence indicate that telomeres protecting the ends of chromosomes are centrally involved in the capability for unlimited proliferation (Blasco, 2005; Shay and Wright, 2000). The telomeres, composed of multiple tandem hexanucleotide repeats, shorten progressively in nonimmortalized cells propagated in culture, eventually losing the ability to protect the ends of chromosomal DNAs from end-to-end fusions; such fusions generate unstable dicentric chromosomes whose resolution results in a scrambling of karyotype that threatens cell viability. Accordingly, the length of telomeric DNA in a cell dictates how many successive cell generations its progeny can pass through before telomeres are largely eroded and have consequently lost their protective functions, triggering entrance into crisis.

Telomerase, the specialized DNA polymerase that adds telomere repeat segments to the ends of telomeric DNA, is almost absent in nonimmortalized cells but expressed at functionally significant levels in the vast majority (~90%) of spontaneously immortalized cells, including human cancer cells. By extending telomeric DNA, telomerase is able to counter the progressive telomere erosion that would otherwise occur in its absence. The presence of telomerase activity, either in spontaneously immortalized cells or in the context of cells engineered to express the enzyme, is correlated with a resistance to induction of both senescence and crisis/apoptosis; conversely, suppression of telomerase activity leads to telomere shortening and to activation of one or the other of these proliferative barriers.

The two barriers to proliferation—senescence and crisis/apoptosis—have been rationalized as crucial anticancer defenses that are hard-wired into our cells, being deployed to impede the outgrowth of clones of preneoplastic and frankly neoplastic cells. According to this thinking, most incipient neoplasias exhaust their endowment of replicative doublings and are stopped in their tracks by one or the other of these barriers. The eventual immortalization of rare variant cells that proceed to form tumors has been attributed to their ability to maintain telomeric DNA at lengths sufficient to avoid triggering senescence or apoptosis, achieved most commonly by upregulating expression of telomerase or, less frequently, via an alternative recombination-based telomere maintenance mechanism. Hence, telomere shortening has come to be viewed as a clocking device that determines the limited replicative potential of normal cells and thus one that must be overcome by cancer cells.

Reassessing Replicative Senescence

Whereas telomere maintenance has been increasingly substantiated as a condition critical to the neoplastic state, the concept of replication-induced senescence as a general barrier requires refinement and reformulation. (Differences in telomere structure and function in mouse versus human cells have also complicated investigation of the roles of telomeres and telomerase in replicative senescence.) Recent experiments have revealed that the induction of senescence in certain cultured cells can be delayed and possibly eliminated by the use of improved cell culture conditions, suggesting that recently explanted primary cells may be able to proliferate unimpeded in culture up the point of crisis and the associated induction of apoptosis triggered by critically shortened telomeres (Ince et al., 2007; Passos et al., 2007; Zhang et al., 2004; Sherr and DePinho, 2000). In contrast, experiments in mice engineered to lack telomerase indicate that the consequently shortened telomeres can shunt premalignant cells into a senescent state that contributes (along with apoptosis) to attenuated tumorigenesis in mice genetically destined to develop particular forms of cancer (Artandi and DePinho, 2010). Such telomerase null mice with highly eroded telomeres exhibit multiorgan dysfunction and abnormalities that include evidence for both senescence and apoptosis, perhaps analogous to the senescence and apoptosis observed in cell culture (Artandi and DePinho, 2010; Feldser and Greider, 2007).

Of note, and as discussed earlier, a morphologically similar form of cell senescence induced by excessive or unbalanced oncogene signaling is now well documented as a protective mechanism against neoplasia; the possible interconnections of this form of senescence with telomerase and telomeres remain to be ascertained. Thus, cell senescence is emerging conceptually as a protective barrier to neoplastic expansion that can be triggered by various proliferation-associated abnormalities, including high levels of oncogenic signaling and, apparently, subcritical shortening of telomeres.

Delayed Activation of Telomerase May Both Limit and Foster Neoplastic Progression

There is now evidence that clones of incipient cancer cells often experience telomere loss-induced crisis relatively early during

the course of multistep tumor progression due to their inability to express significant levels of telomerase. Thus, extensively eroded telomeres have been documented in premalignant growths through the use of fluorescence in situ hybridization (FISH), which has also revealed the end-to-end chromosomal fusions that signal telomere failure and crisis (Kawai et al., 2007; Hansel et al., 2006). These results also suggest that such cells have passed through a substantial number of successive telomere-shortening cell divisions during their evolution from fully normal cells-of-origin. Accordingly, the development of some human neoplasias may be aborted by telomere-induced crisis long before they succeed in becoming macroscopic, frankly neoplastic growths.

In contrast, the absence of TP53-mediated surveillance of genomic integrity may permit other incipient neoplasias to survive initial telomere erosion and attendant chromosomal breakage-fusion-bridge (BFB) cycles. The genomic alterations resulting from these BFB cycles, including deletions and amplifications of chromosomal segments, evidently serve to increase the mutability of the genome, thereby accelerating the acquisition of mutant oncogenes and tumor suppressor genes. The realization that impaired telomere function can actually foster tumor progression has come from the study of mutant mice that lack both p53 and telomerase function (Artandi and DePinho, 2010, 2000). The proposition that these two defects can cooperatively enhance human tumorigenesis has not yet been directly documented.

Circumstantial support for the importance of transient telomere deficiency in facilitating malignant progression has come, in addition, from comparative analyses of premalignant and malignant lesions in the human breast (Raynaud et al., 2010; Chin et al., 2004). The premalignant lesions did not express significant levels of telomerase and were marked by telomere shortening and nonclonal chromosomal aberrations. In contrast, overt carcinomas exhibited telomerase expression concordantly with the reconstruction of longer telomeres and the fixation (via clonal outgrowth) of the aberrant karyotypes that would seem to have been acquired after telomere failure but before the acquisition of telomerase activity. When portrayed in this way, the delayed acquisition of telomerase function serves to generate tumor-promoting mutations, whereas its subsequent activation stabilizes the mutant genome and confers the unlimited replicative capacity that cancer cells require in order to generate clinically apparent tumors.

New Functions of Telomerase

Telomerase was discovered because of its ability to elongate and maintain telomeric DNA, and almost all telomerase research has been posited on the notion that its functions are confined to this crucial function. However, in recent years it has become apparent that telomerase exerts functions that are relevant to cell proliferation but unrelated to telomere maintenance. The noncanonical roles of telomerase, and in particular its protein subunit TERT, have been revealed by functional studies in mice and cultured cells; in some cases novel functions have been demonstrated in conditions where the telomerase enzymatic activity has been eliminated (Cong and Shay, 2008). Among the growing list of telomere-independent functions of TERT/telomerase is the ability of TERT to amplify signaling by the Wnt pathway, by serving as a cofactor of the β-catenin/LEF transcription factor complex (Park et al., 2009). Other ascribed telomere-independent effects include demonstrable enhancement of cell proliferation and/or resistance to apoptosis (Kang et al., 2004), involvement in DNA-damage repair (Masutomi et al., 2005), and RNA-dependent RNA polymerase function (Maida et al., 2009). Consistent with these broader roles, TERT can be found associated with chromatin at multiple sites along the chromosomes, not just at the telomeres (Park et al., 2009; Masutomi et al., 2005). Hence, telomere maintenance is proving to be the most prominent of a diverse series of functions to which TERT contributes. The contributions of these additional functions of telomerase to tumorigenesis remain to be fully elucidated.

Inducing Angiogenesis

Like normal tissues, tumors require sustenance in the form of nutrients and oxygen as well as an ability to evacuate metabolic wastes and carbon dioxide. The tumor-associated neovasculature, generated by the process of angiogenesis, addresses these needs. During embryogenesis, the development of the vasculature involves the birth of new endothelial cells and their assembly into tubes (vasculogenesis) in addition to the sprouting (angiogenesis) of new vessels from existing ones. Following this morphogenesis, the normal vasculature becomes largely quiescent. In the adult, as part of physiologic processes such as wound healing and female reproductive cycling, angiogenesis is turned on, but only transiently. In contrast, during tumor progression, an "angiogenic switch" is almost always activated and remains on, causing normally quiescent vasculature to continually sprout new vessels that help sustain expanding neoplastic growths (Hanahan and Folkman, 1996).

A compelling body of evidence indicates that the angiogenic switch is governed by countervailing factors that either induce or oppose angiogenesis (Baeriswyl and Christofori, 2009; Bergers and Benjamin, 2003). Some of these angiogenic regulators are signaling proteins that bind to stimulatory or inhibitory cell-surface receptors displayed by vascular endothelial cells. The well-known prototypes of angiogenesis inducers and inhibitors are vascular endothelial growth factor-A (VEGF-A) and thrombospondin-1 (TSP-1), respectively.

The VEGF-A gene encodes ligands that are involved in orchestrating new blood vessel growth during embryonic and postnatal development, and then in homeostatic survival of endothelial cells, as well as in physiological and pathological situations in the adult. VEGF signaling via three receptor tyrosine kinases (VEGFR-1–3) is regulated at multiple levels, reflecting this complexity of purpose. Thus, VEGF gene expression can by upregulated both by hypoxia and by oncogene signaling (Ferrara, 2009; Mac Gabhann and Popel, 2008; Carmeliet, 2005). Additionally, VEGF ligands can be sequestered in the extracellular matrix in latent forms that are subject to release and activation by extracellular matrix-degrading proteases (e.g., MMP-9; Kessenbrock et al., 2010). In addition, other proangiogenic signals, such as members of the fibroblast growth factor (FGF) family, have been implicated in sustaining tumor angiogenesis when their expression is chronically upregulated (Baeriswyl and Christofori, 2009). TSP-1, a key counterbalance in the

angiogenic switch, also binds transmembrane receptors displayed by endothelial cells and thereby evokes suppressive signals that can counteract proangiogenic stimuli (Kazerounian et al., 2008).

The blood vessels produced within tumors by chronically activated angiogenesis and an unbalanced mix of proangiogenic signals are typically aberrant: tumor neovasculature is marked by precocious capillary sprouting, convoluted and excessive vessel branching, distorted and enlarged vessels, erratic blood flow, microhemorrhaging, leakiness, and abnormal levels of endothelial cell proliferation and apoptosis (Nagy et al., 2010; Baluk et al., 2005).

Angiogenesis is induced surprisingly early during the multistage development of invasive cancers both in animal models and in humans. Histological analyses of premalignant, noninvasive lesions, including dysplasias and in situ carcinomas arising in a variety of organs, have revealed the early tripping of the angiogenic switch (Raica et al., 2009; Hanahan and Folkman, 1996). Historically, angiogenesis was envisioned to be important only when rapidly growing macroscopic tumors had formed, but more recent data indicate that angiogenesis also contributes to the microscopic premalignant phase of neoplastic progression, further cementing its status as an integral hallmark of cancer.

The past decade has witnessed an astonishing outpouring of research on angiogenesis. Amid this wealth of new knowledge, we highlight several advances of particular relevance to tumor physiology.

Gradations of the Angiogenic Switch

Once angiogenesis has been activated, tumors exhibit diverse patterns of neovascularization. Some tumors, including such highly aggressive types as pancreatic ductal adenocarcinomas, are hypovascularized and replete with stromal "deserts" that are largely avascular and indeed may even be actively antiangiogenic (Olive et al., 2009). Many other tumors, including human renal and pancreatic neuroendocrine carcinomas, are highly angiogenic and consequently densely vascularized (Zee et al., 2010; Turner et al., 2003).

Collectively, such observations suggest an initial tripping of the angiogenic switch during tumor development that is followed by a variable intensity of ongoing neovascularization, the latter being controlled by a complex biological rheostat that involves both the cancer cells and the associated stromal microenvironment (Baeriswyl and Christofori, 2009; Bergers and Benjamin, 2003). Of note, the switching mechanism can vary in its form, even though the net result is a common inductive signal (e.g., VEGF). In some tumors, dominant oncogenes operating within tumor cells, such as *Ras* and *Myc*, can upregulate expression of angiogenic factors, whereas in others, such inductive signals are produced indirectly by immune inflammatory cells, as discussed below. The direct induction of angiogenesis by oncogenes that also drive proliferative signaling illustrates the important principle that distinct hallmark capabilities can be coregulated by the same transforming agents.

Endogenous Angiogenesis Inhibitors Present Natural Barriers to Tumor Angiogenesis

Research in the 1990s revealed that TSP-1 as well as fragments of plasmin (angiostatin) and type 18 collagen (endostatin) can act as endogenous inhibitors of angiogenesis (Ribatti, 2009; Kazerounian, et al., 2008; Folkman, 2006, 2002; Nyberg et al., 2005). The last decade has seen reports of another dozen such agents (Ribatti, 2009; Folkman, 2006; Nyberg et al., 2005). Most are proteins, and many are derived by proteolytic cleavage of structural proteins that are not themselves angiogenic regulators. A number of these endogenous inhibitors of angiogenesis can be detected in the circulation of normal mice and humans. The genes encoding several endogenous angiogenesis inhibitors have been deleted from the mouse germline without untoward physiological effects; the growth of autochthonous and implanted tumors, however, is enhanced as a consequence (Ribatti, 2009; Nyberg et al., 2005). By contrast, if the circulating levels of an endogenous inhibitor are genetically increased (e.g., via overexpression in transgenic mice or in xenotransplanted tumors), tumor growth is impaired (Ribatti, 2009; Nyberg et al., 2005); interestingly, wound healing and fat deposition are impaired or accelerated by elevated or ablated expression of such genes (Cao, 2010; Seppinen et al., 2008). The data suggest that such endogenous angiogenesis inhibitors serve under normal circumstances as physiologic regulators that modulate transitory angiogenesis during tissue remodeling and wound healing; they may also act as intrinsic barriers to induction and/or persistence of angiogenesis by incipient neoplasias.

Pericytes Are Important Components of the Tumor Neovasculature

Pericytes have long been known as supporting cells that are closely apposed to the outer surfaces of the endothelial tubes in normal tissue vasculature, where they provide important mechanical and physiologic support to the endothelial cells. Tumor-associated vasculature, in contrast, was portrayed as lacking appreciable coverage by these auxiliary cells. However, careful microscopic studies conducted in recent years have revealed that pericytes are associated, albeit loosely, with the neovasculature of most if not all tumors (Raza et al., 2010; Bergers and Song, 2005). More importantly, mechanistic studies discussed below have revealed that pericyte coverage is important for the maintenance of a functional tumor neovasculature.

A Variety of Bone Marrow-Derived Cells Contribute to Tumor Angiogenesis

It is now clear that a repertoire of cell types originating in the bone marrow play crucial roles in pathological angiogenesis (Qian and Pollard, 2010; Zumsteg and Christofori, 2009; Murdoch et al., 2008; De Palma et al., 2007). These include cells of the innate immune system—notably macrophages, neutrophils, mast cells, and myeloid progenitors—that infiltrate premalignant lesions and progressed tumors and assemble at the margins of such lesions; the peri-tumoral inflammatory cells help to trip the angiogenic switch in previously quiescent tissue and to sustain ongoing angiogenesis associated with tumor growth, in addition to facilitating local invasion, as noted below. In addition, they can help protect the vasculature from the effects of drugs targeting endothelial cell signaling (Ferrara, 2010). Additionally, several types of bone marrow-derived "vascular progenitor cells" have been observed in certain cases to have migrated into neoplastic lesions and become intercalated into the neovasculature as pericytes or endothelial cells (Patenaude et al., 2010; Kovacic and Boehm, 2009; Lamagna and Bergers, 2006).

Activating Invasion and Metastasis

In 2000, the mechanisms underlying invasion and metastasis were largely an enigma. It was clear that as carcinomas arising from epithelial tissues progressed to higher pathological grades of malignancy, reflected in local invasion and distant metastasis, the associated cancer cells typically developed alterations in their shape as well as in their attachment to other cells and to the extracellular matrix (ECM). The best characterized alteration involved the loss by carcinoma cells of E-cadherin, a key cell-to-cell adhesion molecule. By forming adherens junctions with adjacent epithelial cells, E-cadherin helps to assemble epithelial cell sheets and maintain the quiescence of the cells within these sheets. Increased expression of E-cadherin was well established as an antagonist of invasion and metastasis, whereas reduction of its expression was known to potentiate these phenotypes. The frequently observed downregulation and occasional mutational inactivation of E-cadherin in human carcinomas provided strong support for its role as a key suppressor of this hallmark capability (Berx and van Roy, 2009; Cavallaro and Christofori, 2004).

Additionally, expression of genes encoding other cell-to-cell and cell-to-ECM adhesion molecules is demonstrably altered in some highly aggressive carcinomas, with those favoring cytostasis typically being downregulated. Conversely, adhesion molecules normally associated with the cell migrations that occur during embryogenesis and inflammation are often upregulated. For example, N-cadherin, which is normally expressed in migrating neurons and mesenchymal cells during organogenesis, is upregulated in many invasive carcinoma cells. Beyond the gain and loss of such cell-cell/matrix attachment proteins, the master regulators of invasion and metastasis were largely unknown or, when suspected, lacking in functional validation (Cavallaro and Christofori, 2004).

The multistep process of invasion and metastasis has been schematized as a sequence of discrete steps, often termed the invasion-metastasis cascade (Talmadge and Fidler, 2010; Fidler, 2003). This depiction envisions a succession of cell-biologic changes, beginning with local invasion, then intravasation by cancer cells into nearby blood and lymphatic vessels, transit of cancer cells through the lymphatic and hematogenous systems, followed by escape of cancer cells from the lumina of such vessels into the parenchyma of distant tissues (extravasation), the formation of small nodules of cancer cells (micrometastases), and finally the growth of micrometastatic lesions into macroscopic tumors, this last step being termed "colonization."

Research into the capability for invasion and metastasis has accelerated dramatically over the past decade as powerful new research tools and refined experimental models have become available, and as critical regulatory genes were identified. While still an emerging field replete with major unanswered questions, significant progress has been made in delineating important features of this complex hallmark capability. An admittedly incomplete representation of these advances is highlighted below.

The EMT Program Broadly Regulates Invasion and Metastasis

A developmental regulatory program, referred to as the "epithelial-mesenchymal transition" (EMT), has become prominently implicated as a means by which transformed epithelial cells can acquire the abilities to invade, to resist apoptosis, and to disseminate (Klymkowsky and Savagner, 2009; Polyak and Weinberg, 2009; Thiery et al., 2009; Yilmaz and Christofori, 2009; Barrallo-Gimeno and Nieto, 2005). By co-opting a process involved in various steps of embryonic morphogenesis and wound healing, carcinoma cells can concomitantly acquire multiple attributes that enable invasion and metastasis. This multifaceted EMT program can be activated transiently or stably, and to differing degrees, by carcinoma cells during the course of invasion and metastasis.

A set of pleiotropically acting transcriptional factors, including Snail, Slug, Twist, and Zeb1/2, orchestrate the EMT and related migratory processes during embryogenesis; most were initially identified by developmental genetics. These transcriptional regulators are expressed in various combinations in a number of malignant tumor types and have been shown in experimental models of carcinoma formation to be causally important for programming invasion; some have been found to elicit metastasis when ectopically overexpressed (Micalizzi et al., 2010; Taube et al., 2010; Schmalhofer et al., 2009; Yang and Weinberg, 2008). Included among the cell-biological traits evoked by such transcription factors are loss of adherens junctions and associated conversion from a polygonal/epithelial to a spindly/fibroblastic morphology, expression of matrix-degrading enzymes, increased motility, and heightened resistance to apoptosis—all traits implicated in the processes of invasion and metastasis. Several of these transcription factors can directly repress E-cadherin gene expression, thereby depriving neoplastic epithelial cells of this key suppressor of motility and invasiveness (Peinado et al., 2004).

The available evidence suggests that these transcription factors regulate one another as well as overlapping sets of target genes. No rules have yet been established to describe their interactions and the conditions that govern their expression. Evidence from developmental genetics indicates that contextual signals received from neighboring cells in the embryo are involved in triggering expression of these transcription factors in those cells destined to pass through an EMT (Micalizzi et al., 2010); in an analogous fashion, increasing evidence suggests that heterotypic interactions of cancer cells with adjacent tumor-associated stromal cells can induce expression of the malignant cell phenotypes that are known to be choreographed by one or more of these transcriptional regulators (Karnoub and Weinberg, 2006–2007; Brabletz et al., 2001). Moreover, cancer cells at the invasive margins of certain carcinomas can be seen to have undergone an EMT, suggesting that these cancer cells are subject to microenvironmental stimuli distinct from those received by cancer cells located in the cores of these lesions (Hlubek et al., 2007).

Although the evidence is still incomplete, it would appear that EMT-inducing transcription factors are able to orchestrate most steps of the invasion-metastasis cascade save the final step of colonization. We still know rather little about the various manifestations and temporal stability of the mesenchymal state produced by an EMT. Although expression of EMT-inducing transcription factors has been observed in certain nonepithelial tumor types, such as sarcomas and neuroectodermal tumors, their roles in programming malignant traits in these tumors are

presently poorly documented. Additionally, it remains to be determined whether invasive carcinoma cells necessarily acquire their capability through activation of parts of the EMT program, or whether alternative regulatory programs can also enable this capability.

Heterotypic Contributions of Stromal Cells to Invasion and Metastasis

It is increasingly apparent that crosstalk between cancer cells and cells of the neoplastic stroma is involved in the acquired capability for invasive growth and metastasis (Egeblad et al., 2010; Qian and Pollard, 2010; Joyce and Pollard, 2009; Kalluri and Zeisberg, 2006). Such signaling may impinge on carcinoma cells and act to alter their hallmark capabilities as suggested above. For example, mesenchymal stem cells (MSCs) present in the tumor stroma have been found to secrete CCL5/RANTES in response to signals released by cancer cells; CCL5 then acts reciprocally on the cancer cells to stimulate invasive behavior (Karnoub et al., 2007).

Macrophages at the tumor periphery can foster local invasion by supplying matrix-degrading enzymes such as metalloproteinases and cysteine cathepsin proteases (Kessenbrock et al., 2010; Joyce and Pollard, 2009; Palermo and Joyce, 2008; Mohamed and Sloane, 2006); in one model system, the invasion-promoting macrophages are activated by IL-4 produced by the cancer cells (Gocheva et al., 2010). And in an experimental model of metastatic breast cancer, tumor-associated macrophages (TAMs) supply epidermal growth factor (EGF) to breast cancer cells, while the cancer cells reciprocally stimulate the macrophages with CSF-1; their concerted interactions facilitate intravasation into the circulatory system and metastatic dissemination of the cancer cells (Qian and Pollard, 2010; Wyckoff et al., 2007).

Observations like these indicate that the phenotypes of high-grade malignancy do not arise in a strictly cell-autonomous manner, and that their manifestation cannot be understood solely through analyses of tumor cell genomes. One important implication, still untested, is that the ability to negotiate most of the steps of the invasion-metastasis cascade may be acquired in certain tumors without the requirement that the associated cancer cells undergo additional mutations beyond those that were needed for primary tumor formation.

Plasticity in the Invasive Growth Program

The role of contextual signals in inducing an invasive growth capability (often via an EMT) implies the possibility of reversibility, in that cancer cells that have disseminated from a primary tumor to a more distant tissue site may no longer benefit from the activated stroma and invasion/EMT-inducing signals that they experienced while residing in the primary tumor; in the absence of ongoing exposure to these signals, carcinoma cells may revert in their new homes to a noninvasive state. Thus, carcinoma cells that have undergone an EMT during initial invasion and metastatic dissemination may pass through the reverse process, termed the mesenchymal-epithelial transition (MET). This plasticity may result in the formation of new tumor colonies of carcinoma cells exhibiting a histopathology similar to those of carcinoma cells in the primary tumor that never underwent an EMT (Hugo et al., 2007). Moreover, the notion that cancer cells routinely pass through a complete EMT program is likely to be simplistic; instead, in many cases, cancer cells may enter into an EMT program only partially, thereby acquiring new mesenchymal traits while continuing to express residual epithelial traits.

Distinct Forms of Invasion May Underlie Different Cancer Types

The EMT program regulates a particular type of invasiveness that has been termed "mesenchymal." In addition, two other distinct modes of invasion have been identified and implicated in cancer cell invasion (Friedl and Wolf, 2008, 2010). "Collective invasion" involves nodules of cancer cells advancing en masse into adjacent tissues and is characteristic of, for example, squamous cell carcinomas; interestingly, such cancers are rarely metastatic, suggesting that this form of invasion lacks certain functional attributes that facilitate metastasis. Less clear is the prevalence of an "amoeboid" form of invasion (Madsen and Sahai, 2010; Sabeh et al., 2009), in which individual cancer cells show morphological plasticity, enabling them to slither through existing interstices in the extracellular matrix rather than clearing a path for themselves, as occurs in both the mesenchymal and collective forms of invasion. It is presently unresolved whether cancer cells participating in the collective and amoeboid forms of invasion employ components of the EMT program, or whether entirely different cell-biological programs are responsible for choreographing these alternative invasion programs.

Another emerging concept, noted above, involves the facilitation of cancer cell invasion by inflammatory cells that assemble at the boundaries of tumors, producing the extracellular matrix-degrading enzymes and other factors that enable invasive growth (Kessenbrock et al., 2010; Qian and Pollard, 2010; Joyce and Pollard, 2009); these functions may obviate the need of cancer cells to produce these proteins through activation of EMT programs. Thus, cancer cells may secrete the chemoattractants that recruit the proinvasive inflammatory cells rather than producing the matrix-degrading enzymes themselves.

The Daunting Complexity of Metastatic Colonization

Metastasis can be broken down into two major phases: the physical dissemination of cancer cells from the primary tumor to distant tissues, and the adaptation of these cells to foreign tissue microenvironments that results in successful colonization, i.e., the growth of micrometastases into macroscopic tumors. The multiple steps of dissemination would seem to be in the purview of the EMT and similarly acting migratory programs. Colonization, however, is not strictly coupled with physical dissemination, as evidenced by the presence in many patients of myriad micrometastases that have successfully disseminated but never progress to macroscopic metastatic tumors (Talmadge and Fidler, 2010; McGowan et al., 2009; Aguirre-Ghiso, 2007; Townson and Chambers, 2006; Fidler, 2003).

In some types of cancer, the primary tumor may release systemic suppressor factors that render such micrometastases dormant, as revealed clinically by explosive metastatic growth soon after resection of the primary growth (Demicheli et al., 2008; Folkman, 2002). In others, however, such as breast cancer and melanoma, macroscopic metastases may erupt decades after a primary tumor has been surgically removed or pharmacologically destroyed; these metastatic tumor growths evidently

reflect dormant micrometastases that have solved, after much trial and error, the complex problem of tissue colonization (Barkan, et al., 2010; Aguirre-Ghiso, 2007; Townson and Chambers, 2006).

One can infer from such natural histories that micrometastases may lack other hallmark capabilities necessary for vigorous growth, such as the ability to activate angiogenesis; indeed the inability of certain experimentally generated dormant micrometastases to form macroscopic tumors has been ascribed to their failure to activate tumor angiogenesis (Naumov et al., 2008; Aguirre-Ghiso, 2007). Additionally, recent experiments have shown that nutrient starvation can induce intense autophagy that causes cancer cells to shrink and adopt a state of reversible dormancy; such cells may exit this state and resume active growth and proliferation when changes in tissue microenvironment, such as access to more nutrients, permit (Kenific et al., 2010; Lu et al., 2008). Other mechanisms of micrometastatic dormancy may involve anti-growth signals embedded in normal tissue extracellular matrix (Barkan et al., 2010) and tumor-suppressing actions of the immune system (Teng et al., 2008; Aguirre-Ghiso, 2007).

Most disseminated cancer cells are likely to be poorly adapted, at least initially, to the microenvironment of the tissue in which they have landed. Accordingly, each type of disseminated cancer cell may need to develop its own set of ad hoc solutions to the problem of thriving in the microenvironment of one or another foreign tissue (Gupta et al., 2005). These adaptations might require hundreds of distinct colonization programs, each dictated by the type of disseminating cancer cell and the nature of the tissue microenvironment in which colonization is proceeding. As further discussed below, however, certain tissue microenviroments may be preordained to be intrinsically hospitable to disseminated cancer cells (Peinado et al., 2011; Talmadge and Fidler, 2010).

Metastatic dissemination has long been depicted as the last step in multistep primary tumor progression, and indeed for many tumors that is likely the case, as illustrated by recent genome sequencing studies that present genetic evidence for clonal evolution of pancreatic ductal adenocarcinoma to metastasis (Campbell et al., 2010; Luebeck, 2010; Yachida et al., 2010). On the other hand, evidence has recently emerged indicating that cells can disseminate remarkably early, dispersing from ostensibly noninvasive premalignant lesions in both mice and humans (Coghlin and Murray, 2010; Klein, 2009). Additionally, micrometastases can be spawned from primary tumors that are not obviously invasive but possess a neovasculature lacking in lumenal integrity (Gerhardt and Semb, 2008). Although cancer cells can clearly disseminate from such pre-neoplastic lesions and seed the bone marrow and other tissues, their capability to colonize these sites and develop into pathologically significant macrometastases remains unproven. At present, we view this early metastatic dissemination as a demonstrable phenomenon in mice and humans whose clinical significance is yet to be established.

Beyond the timing of their dissemination, it also remains unclear when and where cancer cells develop the ability to colonize foreign tissues as macroscopic tumors. This capability may arise during primary tumor formation as a result of a tumor's particular developmental path prior to any dissemination, such that primary tumor cells entering the circulation are fortuitously endowed with the ability to colonize certain distant tissue sites (Talmadge and Fidler, 2010). Alternatively, the ability to colonize specific tissues may only develop in response to the selective pressure on already disseminated cancer cells to adapt to growth in foreign tissue microenvironments.

Having developed such tissue-specific colonizing ability, the cells in metastatic colonies may proceed to disseminate further, not only to new sites in the body but also back to the primary tumors in which their ancestors arose. Accordingly, tissue-specific colonization programs that are evident among cells within a primary tumor may originate not from classical tumor progression occurring within the primary lesion but instead from emigrants that have returned home (Kim et al., 2009). Such reseeding is consistent with the aforementioned studies of human pancreatic cancer metastasis (Campbell et al., 2010; Luebeck, 2010; Yachida et al., 2010). Stated differently, the phenotypes and underlying gene expression programs of the populations of cancer cells (and of the cancer stem cells discussed below) within primary tumors may be significantly modified by reverse migration of their distant metastatic progeny.

Implicit in this self-seeding process is another notion: the supportive stroma that arises in a primary tumor and contributes to its acquisition of malignant traits may intrinsically provide a hospitable site for reseeding and colonization by circulating cancer cells emanating from metastatic lesions.

Clarifying the regulatory programs that enable metastatic colonization represents an important agenda for future research. Substantial progress is being made, for example, in defining sets of genes ("metastatic signatures") that correlate with and appear to facilitate the establishment of macroscopic metastases in specific tissues (Coghlin and Murray, 2010; Bos et al., 2009; Olson et al., 2009; Nguyen et al., 2009; Gupta et al., 2005). The challenge is considerable, given the apparent multitude of distinct colonization programs cited above. Moreover, colonization is unlikely to depend exclusively on cell-autonomous processes. Instead, it almost certainly requires the establishment of a permissive tumor microenvironment composed of critical stromal support cells. For these reasons, the process of colonization is likely to encompass a large number of cell-biological programs that are, in aggregate, considerably more complex and diverse than the preceding steps of metastatic dissemination.

Programming of Hallmark Capabilities by Intracellular Circuitry

In 2000, we presented a metaphor, in which the numerous signaling molecules affecting cancer cells operate as nodes and branches of elaborate integrated circuits that are reprogrammed derivatives of the circuits operating in normal cells. The ensuing decade has both solidified the original depiction of these circuits and expanded the catalog of signals and the interconnections of their signaling pathways. It is difficult if not impossible to graphically portray this circuit comprehensively and coherently, as was already the case in 2000.

We now suggest a portrayal of this circuitry that is aligned with individual hallmarks of cancer. Thus, the intracellular integrated

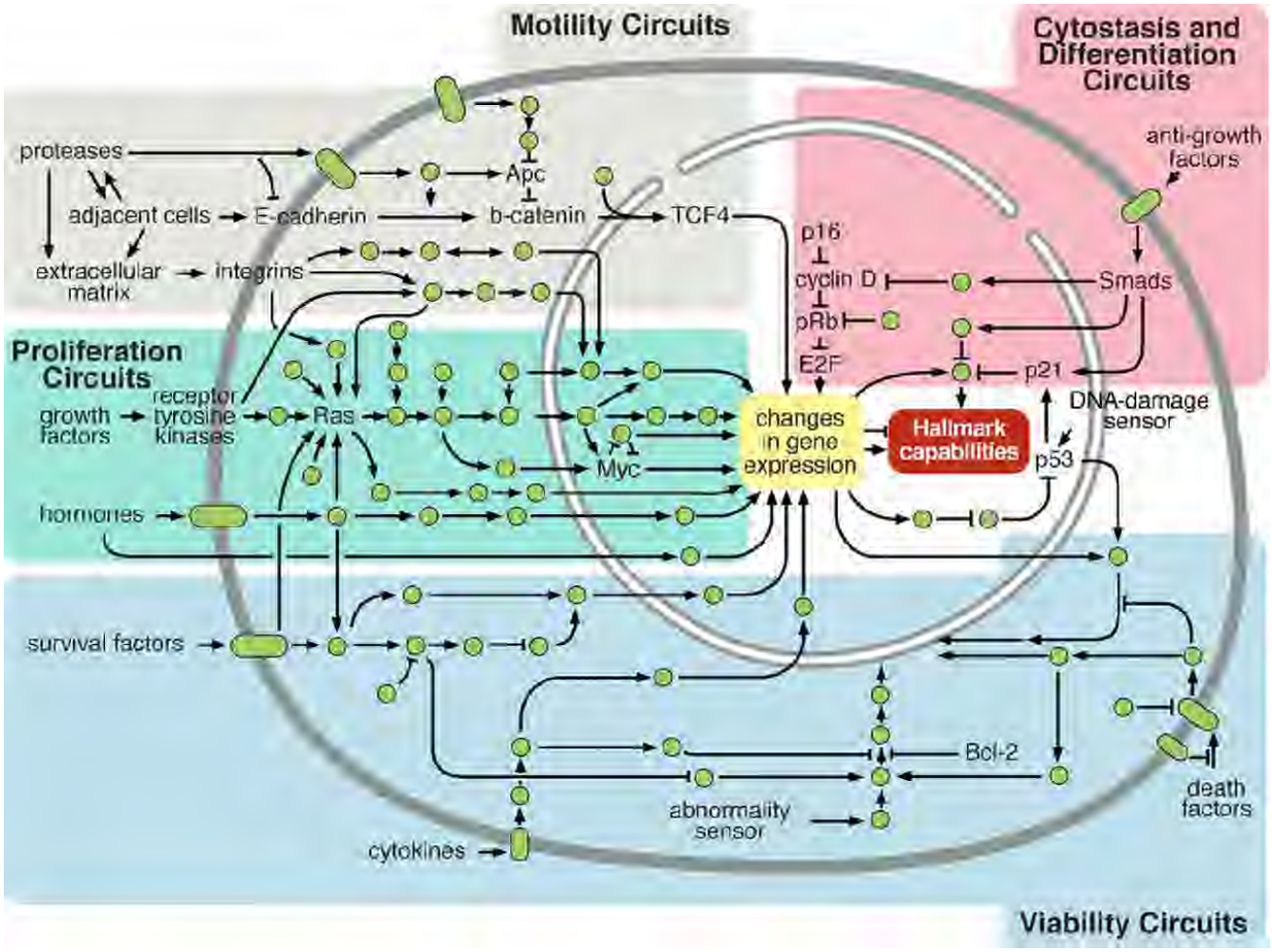

Figure 2. Intracellular Signaling Networks Regulate the Operations of the Cancer Cell
An elaborate integrated circuit operates within normal cells and is reprogrammed to regulate hallmark capabilities within cancer cells. Separate subcircuits, depicted here in differently colored fields, are specialized to orchestrate the various capabilities. At one level, this depiction is simplistic, as there is considerable crosstalk between such subcircuits. In addition, because each cancer cell is exposed to a complex mixture of signals from its microenvironment, each of these subcircuits is connected with signals originating from other cells in the tumor microenvironment, as outlined in Figure 5.

circuit can be segmented into distinct subcircuits, each of which is specialized to support a discrete cell-biological property in normal cells and is reprogrammed in order to implement a hallmark capability in cancer cells (Figure 2). Only a subset of hallmark capabilities are addressed in this figure, either because their underlying control circuits remain poorly understood or because they overlap extensively with those portrayed here.

An additional dimension of complexity involves considerable interconnections and thus crosstalk between the individual subcircuits. For example, certain oncogenic events can affect multiple capabilities, as illustrated by the diverse effects that prominent oncogenes, such as mutant *RAS* and upregulated *MYC*, have on multiple hallmark capabilities (e.g., proliferative signaling, energy metabolism, angiogenesis, invasion, and survival). We anticipate that future renditions of this integrated circuit will encompass subcircuits and associated hallmark capabilities that are still not addressed here.

ENABLING CHARACTERISTICS AND EMERGING HALLMARKS

We have defined the hallmarks of cancer as acquired functional capabilities that allow cancer cells to survive, proliferate, and disseminate; these functions are acquired in different tumor types via distinct mechanisms and at various times during the course of multistep tumorigenesis. Their acquisition is made possible by two *enabling characteristics*. Most prominent is the development of genomic instability in cancer cells, which generates random mutations including chromosomal rearrangements; among these are the rare genetic changes that can orchestrate hallmark capabilities. A second enabling characteristic involves the inflammatory state of premalignant and frankly malignant lesions that is driven by cells of the immune system, some of which serve to promote tumor progression through various means.

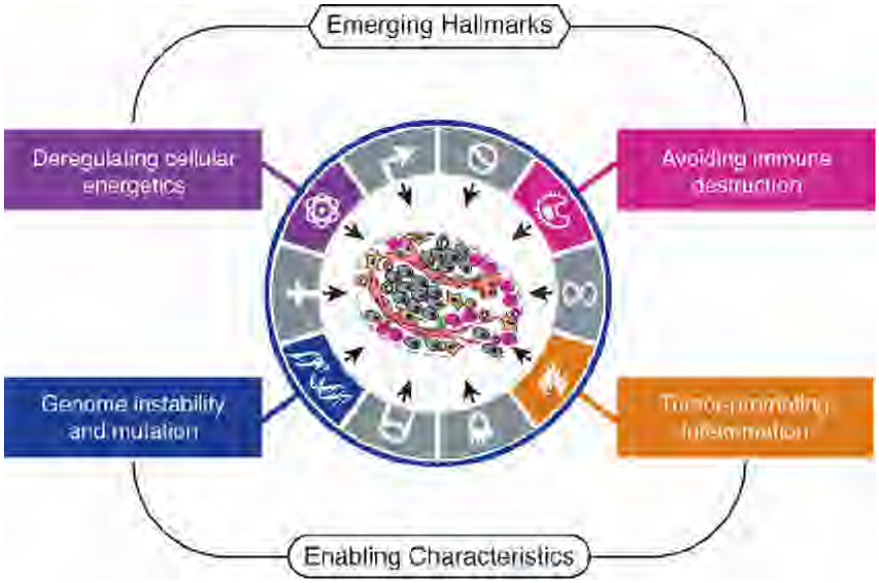

Figure 3. Emerging Hallmarks and Enabling Characteristics

An increasing body of research suggests that two additional hallmarks of cancer are involved in the pathogenesis of some and perhaps all cancers. One involves the capability to modify, or reprogram, cellular metabolism in order to most effectively support neoplastic proliferation. The second allows cancer cells to evade immunological destruction, in particular by T and B lymphocytes, macrophages, and natural killer cells. Because neither capability is yet generalized and fully validated, they are labeled as emerging hallmarks. Additionally, two consequential characteristics of neoplasia facilitate acquisition of both core and emerging hallmarks. Genomic instability and thus mutability endow cancer cells with genetic alterations that drive tumor progression. Inflammation by innate immune cells designed to fight infections and heal wounds can instead result in their inadvertent support of multiple hallmark capabilities, thereby manifesting the now widely appreciated tumor-promoting consequences of inflammatory responses.

Yet other distinct attributes of cancer cells have been proposed to be functionally important for the development of cancer and might therefore be added to the list of core hallmarks (Negrini et al., 2010; Luo et al., 2009; Colotta et al., 2009). Two such attributes are particularly compelling. The first involves major reprogramming of cellular energy metabolism in order to support continuous cell growth and proliferation, replacing the metabolic program that operates in most normal tissues and fuels the physiological operations of the associated cells. The second involves active evasion by cancer cells from attack and elimination by immune cells; this capability highlights the dichotomous roles of an immune system that both antagonizes and enhances tumor development and progression. Both of these capabilities may well prove to facilitate the development and progression of many forms of human cancer and therefore can be considered to be emerging hallmarks of cancer. These enabling characteristics and *emerging hallmarks,* depicted in Figure 3, are discussed individually below.

An Enabling Characteristic: Genome Instability and Mutation

Acquisition of the multiple hallmarks enumerated above depends in large part on a succession of alterations in the genomes of neoplastic cells. Simply depicted, certain mutant genotypes confer selective advantage on subclones of cells, enabling their outgrowth and eventual dominance in a local tissue environment. Accordingly, multistep tumor progression can be portrayed as a succession of clonal expansions, each of which is triggered by the chance acquisition of an enabling mutant genotype. Because heritable phenotypes, e.g., inactivation of tumor suppressor genes, can also be acquired through epigenetic mechanisms such as DNA methylation and histone modifications (Berdasco and Esteller, 2010; Esteller, 2007; Jones and Baylin, 2007), some clonal expansions may well be triggered by nonmutational changes affecting the regulation of gene expression.

The extraordinary ability of genome maintenance systems to detect and resolve defects in the DNA ensures that rates of spontaneous mutation are usually very low during each cell generation. In the course of acquiring the roster of mutant genes needed to orchestrate tumorigenesis, cancer cells often increase the rates of mutation (Negrini et al., 2010; Salk et al., 2010). This mutability is achieved through increased sensitivity to mutagenic agents, through a breakdown in one or several components of the genomic maintenance machinery, or both. In addition, the accumulation of mutations can be accelerated by compromising the surveillance systems that normally monitor genomic integrity and force genetically damaged cells into either senescence or apoptosis (Jackson and Bartek, 2009; Kastan, 2008; Sigal and Rotter, 2000). The role of TP53 is central here, leading to its being called the "guardian of the genome" (Lane, 1992).

A diverse array of defects affecting various components of the DNA-maintenance machinery—often referred to as the "caretakers" of the genome (Kinzler and Vogelstein, 1997)—have been documented. The catalog of defects in these caretaker genes includes those whose products are involved in (1) detecting DNA damage and activating the repair machinery, (2) directly repairing damaged DNA, and (3) inactivating or intercepting mutagenic molecules before they have damaged the DNA (Negrini et al., 2010; Ciccia and Elledge, 2010; Jackson and Bartek, 2009; Kastan, 2008; Harper and Elledge, 2007; Friedberg et al., 2006). From a genetic perspective, these caretaker genes behave much like tumor suppressor genes, in that their functions can be lost during the course of tumor progression, with such losses being achieved either through inactivating mutations or via epigenetic repression. Mutant copies of many of these caretaker genes have been introduced into the mouse germline and result, predictably, in increased cancer incidence, supporting their potential involvement in human cancer development (Barnes and Lindahl, 2004).

In the decade since we first enumerated the cancer hallmarks, another major source of tumor-associated genomic instability has been uncovered: as described earlier, the loss of telomeric DNA in many tumors generates karyotypic instability and associated amplification and deletion of chromosomal segments (Artandi and DePinho, 2010). When viewed in this light, telomerase is more than an enabler of the hallmark capability for unlimited replicative potential and must also be added to the list of critical caretakers responsible for maintaining genome integrity.

Advances in the molecular-genetic analysis of cancer cell genomes have provided the most compelling demonstrations of function-altering mutations and of ongoing genomic instability during tumor progression. One type of analysis—comparative genomic hybridization (CGH)—documents the gains and losses of gene copy number across the cell genome; in many tumors, the pervasive genomic aberrations revealed by CGH provide clear evidence for loss of control of genome integrity. Importantly, the recurrence of specific aberrations (both amplifications and deletions) at particular sites in the genome indicates that such sites are likely to harbor genes whose alteration favors neoplastic progression (Korkola and Gray, 2010).

More recently, with the advent of efficient and economical DNA-sequencing technologies, higher-resolution analyses have become possible. Early studies are revealing distinctive patterns of DNA mutations in different tumor types (see http://cancergenome.nih.gov/). In the not-too-distant future, the sequencing of entire cancer cell genomes promises to clarify the prevalence of ostensibly random mutations scattered across cancer cell genomes. Thus, recurring genetic alterations may point to a causal role of particular mutations in tumor pathogenesis.

Although the specifics of genome alteration vary dramatically between different tumor types, the large number of genome maintenance and repair defects that have already been documented in human tumors, together with abundant evidence of widespread destabilization of gene copy number and nucleotide sequence, persuade us that instability of the genome is inherent to the great majority of human cancer cells. This leads, in turn, to the conclusion that the defects in genome maintenance and repair are selectively advantageous and therefore instrumental for tumor progression, if only because they accelerate the rate at which evolving premalignant cells can accumulate favorable genotypes. As such, genome instability is clearly an enabling characteristic that is causally associated with the acquisition of hallmark capabilities.

An Enabling Characteristic: Tumor-Promoting Inflammation

Pathologists have long recognized that some tumors are densely infiltrated by cells of both the innate and adaptive arms of the immune system and thereby mirror inflammatory conditions arising in non-neoplastic tissues (Dvorak, 1986). With the advent of better markers for accurately identifying the distinct cell types of the immune system, it is now clear that virtually every neoplastic lesion contains immune cells present at densities ranging from subtle infiltrations detectable only with cell type-specific antibodies to gross inflammations that are apparent even by standard histochemical staining techniques (Pagès et al., 2010). Historically, such immune responses were largely thought to reflect an attempt by the immune system to eradicate tumors, and indeed, there is increasing evidence for antitumoral responses to many tumor types with an attendant pressure on the tumor to evade immune destruction, as discussed below.

By 2000, there were already clues that the tumor-associated inflammatory response had the unanticipated, paradoxical effect of enhancing tumorigenesis and progression, in effect helping incipient neoplasias to acquire hallmark capabilities. In the ensuing decade, research on the intersections between inflammation and cancer pathogenesis has blossomed, producing abundant and compelling demonstrations of the functionally important tumor-promoting effects that immune cells—largely of the innate immune system—have on neoplastic progression (DeNardo et al., 2010; Grivennikov et al., 2010; Qian and Pollard, 2010; Colotta et al., 2009). Inflammation can contribute to multiple hallmark capabilities by supplying bioactive molecules to the tumor microenvironment, including growth factors that sustain proliferative signaling, survival factors that limit cell death, proangiogenic factors, extracellular matrix-modifying enzymes that facilitate angiogenesis, invasion, and metastasis, and inductive signals that lead to activation of EMT and other hallmark-facilitating programs (DeNardo et al., 2010; Grivennikov et al., 2010; Qian and Pollard, 2010; Karnoub and Weinberg, 2006–2007).

Importantly, inflammation is in some cases evident at the earliest stages of neoplastic progression and is demonstrably capable of fostering the development of incipient neoplasias into full-blown cancers (Qian and Pollard, 2010; de Visser et al., 2006). Additionally, inflammatory cells can release chemicals, notably reactive oxygen species, that are actively mutagenic for nearby cancer cells, accelerating their genetic evolution toward states of heightened malignancy (Grivennikov et al., 2010). As such, inflammation can be considered an enabling characteristic for its contributions to the acquisition of core hallmark capabilities. The cells responsible for this enabling characteristic are described in the section below on the tumor microenvironment.

An Emerging Hallmark: Reprogramming Energy Metabolism

The chronic and often uncontrolled cell proliferation that represents the essence of neoplastic disease involves not only deregulated control of cell proliferation but also corresponding adjustments of energy metabolism in order to fuel cell growth and division. Under aerobic conditions, normal cells process glucose, first to pyruvate via glycolysis in the cytosol and thereafter to carbon dioxide in the mitochondria; under anaerobic conditions, glycolysis is favored and relatively little pyruvate is dispatched to the oxygen-consuming mitochondria. Otto Warburg first observed an anomalous characteristic of cancer cell energy metabolism (Warburg, 1930, 1956a, 1956b): even in the presence of oxygen, cancer cells can reprogram their glucose metabolism, and thus their energy production, by limiting their energy metabolism largely to glycolysis, leading to a state that has been termed "aerobic glycolysis."

The existence of this metabolic switch in cancer cells has been substantiated in the ensuing decades. Such reprogramming of

energy metabolism is seemingly counterintuitive, in that cancer cells must compensate for the ~18-fold lower efficiency of ATP production afforded by glycolysis relative to mitochondrial oxidative phosphorylation. They do so in part by upregulating glucose transporters, notably GLUT1, which substantially increases glucose import into the cytoplasm (Jones and Thompson, 2009; DeBerardinis et al., 2008; Hsu and Sabatini, 2008). Indeed, markedly increased uptake and utilization of glucose have been documented in many human tumor types, most readily by noninvasively visualizing glucose uptake using positron emission tomography (PET) with a radiolabeled analog of glucose (^{18}F-fluorodeoxyglucose, FDG) as a reporter.

Glycolytic fueling has been shown to be associated with activated oncogenes (e.g., *RAS*, *MYC*) and mutant tumor suppressors (e.g., *TP53*) (DeBerardinis et al., 2008; Jones and Thompson, 2009), whose alterations in tumor cells have been selected primarily for their benefits in conferring the hallmark capabilities of cell proliferation, avoidance of cytostatic controls, and attenuation of apoptosis. This reliance on glycolysis can be further accentuated under the hypoxic conditions that operate within many tumors: the hypoxia response system acts pleiotropically to upregulate glucose transporters and multiple enzymes of the glycolytic pathway (Semenza, 2010a; Jones and Thompson, 2009; DeBerardinis et al., 2008). Thus, both the Ras oncoprotein and hypoxia can independently increase the levels of the HIF1α and HIF2α transcription factors, which in turn upregulate glycolysis (Semenza, 2010a, 2010b; Kroemer and Pouyssegur, 2008).

A functional rationale for the glycolytic switch in cancer cells has been elusive, given the relatively poor efficiency of generating ATP by glycolysis relative to mitochondrial oxidative phosphorylation. According to one long-forgotten (Potter, 1958) and recently revived and refined hypothesis (Vander Heiden et al., 2009), increased glycolysis allows the diversion of glycolytic intermediates into various biosynthetic pathways, including those generating nucleosides and amino acids; this facilitates, in turn, the biosynthesis of the macromolecules and organelles required for assembling new cells. Moreover, Warburg-like metabolism seems to be present in many rapidly dividing embryonic tissues, once again suggesting a role in supporting the large-scale biosynthetic programs that are required for active cell proliferation.

Interestingly, some tumors have been found to contain two subpopulations of cancer cells that differ in their energy-generating pathways. One subpopulation consists of glucose-dependent ("Warburg-effect") cells that secrete lactate, whereas cells of the second subpopulation preferentially import and utilize the lactate produced by their neighbors as their main energy source, employing part of the citric acid cycle to do so (Kennedy and Dewhirst, 2010; Feron, 2009; Semenza, 2008). These two populations evidently function symbiotically: the hypoxic cancer cells depend on glucose for fuel and secrete lactate as waste, which is imported and preferentially used as fuel by their better-oxygenated brethren. Although this provocative mode of intratumoral symbiosis has yet to be generalized, the cooperation between lactate-secreting and lactate-utilizing cells to fuel tumor growth is in fact not an invention of tumors but rather again reflects cooption of a normal physiological mechanism, in this case one operating in muscle (Kennedy and Dewhirst, 2010; Feron, 2009; Semenza, 2008). Additionally, it is becoming apparent that oxygenation, ranging from normoxia to hypoxia, is not necessarily static in tumors but instead fluctuates temporally and regionally (Hardee et al., 2009), likely as a result of the instability and chaotic organization of the tumor-associated neovasculature.

Altered energy metabolism is proving to be as widespread in cancer cells as many of the other cancer-associated traits that have been accepted as hallmarks of cancer. This realization raises the question of whether deregulating cellular energy metabolism is therefore a core hallmark capability of cancer cells that is as fundamental as the six well-established core hallmarks. In fact, the redirection of energy metabolism is largely orchestrated by proteins that are involved in one way or another in programming the core hallmarks of cancer. When viewed in this way, aerobic glycolysis is simply another phenotype that is programmed by proliferation-inducing oncogenes.

Interestingly, activating (gain-of-function) mutations in the isocitrate dehydrogenase 1/2 (IDH) enzymes have been reported in glioma and other human tumors (Yen et al., 2010). Although these mutations may prove to have been clonally selected for their ability to alter energy metabolism, there is confounding data associating their activity with elevated oxidation and stability of the HIF-1 transcription factors (Reitman and Yan, 2010), which could in turn affect genome stability and angiogenesis/invasion, respectively, thus blurring the lines of phenotypic demarcation. Currently, therefore, the designation of reprogrammed energy metabolism as an emerging hallmark seems most appropriate, to highlight both its evident importance as well as the unresolved issues surrounding its functional independence from the core hallmarks.

An Emerging Hallmark: Evading Immune Destruction

A second, still-unresolved issue surrounding tumor formation involves the role that the immune system plays in resisting or eradicating formation and progression of incipient neoplasias, late-stage tumors, and micrometastases. The long-standing theory of immune surveillance proposes that cells and tissues are constantly monitored by an ever-alert immune system, and that such immune surveillance is responsible for recognizing and eliminating the vast majority of incipient cancer cells and thus nascent tumors. According to this logic, solid tumors that do appear have somehow managed to avoid detection by the various arms of the immune system or have been able to limit the extent of immunological killing, thereby evading eradication.

The role of defective immunological monitoring of tumors would seem to be validated by the striking increases of certain cancers in immunocompromised individuals (Vajdic and van Leeuwen, 2009). However, the great majority of these are virus-induced cancers, suggesting that much of the control of this class of cancers normally depends on reducing viral burden in infected individuals, in part through eliminating virus-infected cells. These observations, therefore, seem to shed little light on the possible role of the immune system in limiting formation of the >80% of tumors of nonviral etiology. In recent years, however, an increasing body of evidence, both from genetically engineered mice and from clinical epidemiology, suggests that

the immune system operates as a significant barrier to tumor formation and progression, at least in some forms of non-virus-induced cancer.

When mice genetically engineered to be deficient for various components of the immune system were assessed for the development of carcinogen-induced tumors, it was observed that tumors arose more frequently and/or grew more rapidly in the immunodeficient mice relative to immunocompetent controls. In particular, deficiencies in the development or function of $CD8^+$ cytotoxic T lymphocytes (CTLs), $CD4^+$ T_h1 helper T cells, or natural killer (NK) cells each led to demonstrable increases in tumor incidence; moreover, mice with combined immunodeficiencies in both T cells and NK cells were even more susceptible to cancer development. The results indicated that, at least in certain experimental models, both the innate and adaptive cellular arms of the immune system are able to contribute significantly to immune surveillance and thus tumor eradication (Teng et al., 2008; Kim et al., 2007).

In addition, transplantation experiments have shown that cancer cells that originally arose in immunodeficient mice are often inefficient at initiating secondary tumors in syngeneic immunocompetent hosts, whereas cancer cells from tumors arising in immunocompetent mice are equally efficient at initiating transplanted tumors in both types of hosts (Teng et al., 2008; Kim et al., 2007). Such behavior has been interpreted as follows: Highly immunogenic cancer cell clones are routinely eliminated in immunocompetent hosts—a process that has been referred to as "immunoediting"—leaving behind only weakly immunogenic variants to grow and generate solid tumors; such weakly immunogenic cells can thereafter colonize both immunodeficient and immunocompetent hosts. Conversely, when arising in immunodeficient hosts, the immunogenic cancer cells are not selectively depleted and can, instead, prosper along with their weakly immunogenic counterparts. When cells from such nonedited tumors are serially transplanted into syngeneic recipients, the immunogenic cancer cells are rejected when they confront, for the first time, the competent immune systems of their secondary hosts (Smyth et al., 2006). (Unanswered in these particular experiments is the question of whether the chemical carcinogens used to induce such tumors are prone to generate cancer cells that are especially immunogenic.)

Clinical epidemiology also increasingly supports the existence of antitumoral immune responses in some forms of human cancer (Bindea et al., 2010; Ferrone and Dranoff, 2010; Nelson, 2008). For example, patients with colon and ovarian tumors that are heavily infiltrated with CTLs and NK cells have a better prognosis than those that lack such abundant killer lymphocytes (Pagès et al., 2010; Nelson, 2008); the case for other cancers is suggestive but less compelling and is the subject of ongoing investigation. Additionally, some immunosuppressed organ transplant recipients have been observed to develop donor-derived cancers, suggesting that in the ostensibly tumor-free donors, the cancer cells were held in check, in a dormant state, by a fully functional immune system (Strauss and Thomas, 2010).

Still, the epidemiology of chronically immunosuppressed patients does not indicate significantly increased incidences of the major forms of nonviral human cancer, as noted above. This might be taken as an argument against the importance of immune surveillance as an effective barrier to tumorigenesis and tumor progression. We note, however, that HIV and pharmacologically immunosuppressed patients are predominantly immunodeficient in the T and B cell compartments and thus do not present with the multicomponent immunological deficiencies that have been produced in the genetically engineered mutant mice lacking both NK cells and CTLs; this leaves open the possibility that such patients still have residual capability for an immunological defense against cancer that is mounted by NK and other innate immune cells.

In truth, the above discussions of cancer immunology simplify tumor-host immunological interactions, as highly immunogenic cancer cells may well evade immune destruction by disabling components of the immune system that have been dispatched to eliminate them. For example, cancer cells may paralyze infiltrating CTLs and NK cells, by secreting TGF-β or other immunosuppressive factors (Yang et al., 2010; Shields et al., 2010). More subtle mechanisms operate through the recruitment of inflammatory cells that are actively immunosuppressive, including regulatory T cells (Tregs) and myeloid-derived suppressor cells (MDSCs). Both can suppress the actions of cytotoxic lymphocytes (Mougiakakos et al., 2010; Ostrand-Rosenberg and Sinha, 2009).

In light of these considerations and the still-rudimentary demonstrations of antitumor immunity as a significant barrier to tumor formation and progression in humans, we present immunoevasion as another emerging hallmark, whose generality as a core hallmark capability remains to be firmly established.

THE TUMOR MICROENVIRONMENT

Over the past decade, tumors have increasingly been recognized as organs whose complexity approaches and may even exceed that of normal healthy tissues. When viewed from this perspective, the biology of a tumor can only be understood by studying the individual specialized cell types within it (Figure 4, upper) as well as the "tumor microenvironment" that they construct during the course of multistep tumorigenesis (Figure 4, lower). This depiction contrasts starkly with the earlier, reductionist view of a tumor as nothing more than a collection of relatively homogeneous cancer cells, whose entire biology could be understood by elucidating the cell-autonomous properties of these cells. We enumerate here a set of cell types known to contribute in important ways to the biology of many tumors and discuss the regulatory signaling that controls their individual and collective functions. Most of these observations stem from the study of carcinomas, in which the neoplastic epithelial cells constitute a compartment (the parenchyma) that is clearly distinct from the mesenchymal cells forming the tumor-associated stroma.

Cancer Cells and Cancer Stem Cells

Cancer cells are the foundation of the disease; they initiate tumors and drive tumor progression forward, carrying the oncogenic and tumor suppressor mutations that define cancer as a genetic disease. Traditionally, the cancer cells within tumors

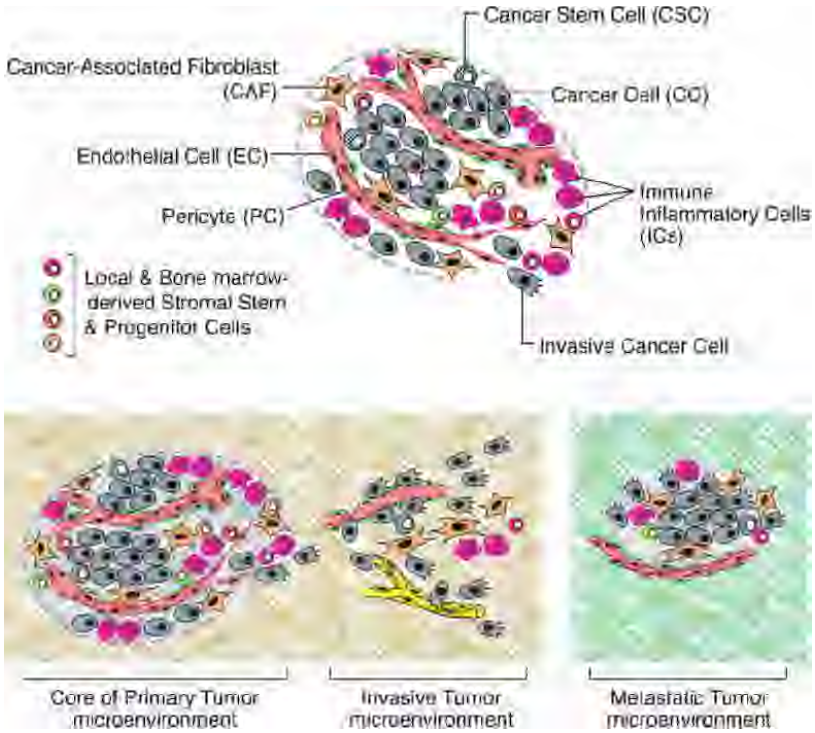

Figure 4. The Cells of the Tumor Microenvironment

(Upper) An assemblage of distinct cell types constitutes most solid tumors. Both the parenchyma and stroma of tumors contain distinct cell types and subtypes that collectively enable tumor growth and progression. Notably, the immune inflammatory cells present in tumors can include both tumor-promoting as well as tumor-killing subclasses.

(Lower) The distinctive microenvironments of tumors. The multiple stromal cell types create a succession of tumor microenvironments that change as tumors invade normal tissue and thereafter seed and colonize distant tissues. The abundance, histologic organization, and phenotypic characteristics of the stromal cell types, as well as of the extracellular matrix (hatched background), evolve during progression, thereby enabling primary, invasive, and then metastatic growth. The surrounding normal cells of the primary and metastatic sites, shown only schematically, likely also affect the character of the various neoplastic microenvironments. (Not shown are the premalignant stages in tumorigenesis, which also have distinctive microenvironments that are created by the abundance and characteristics of the assembled cells.)

have been portrayed as reasonably homogeneous cell populations until relatively late in the course of tumor progression, when hyperproliferation combined with increased genetic instability spawn distinct clonal subpopulations. Reflecting such clonal heterogeneity, many human tumors are histopathologically diverse, containing regions demarcated by various degrees of differentiation, proliferation, vascularity, inflammation, and/or invasiveness. In recent years, however, evidence has accumulated pointing to the existence of a new dimension of intratumor heterogeneity and a hitherto-unappreciated subclass of neoplastic cells within tumors, termed cancer stem cells (CSCs).

Although the evidence is still fragmentary, CSCs may prove to be a common constituent of many if not most tumors, albeit being present with widely varying abundance. CSCs are defined operationally through their ability to efficiently seed new tumors upon inoculation into recipient host mice (Cho and Clarke, 2008; Lobo et al., 2007). This functional definition is often complemented by including the expression in CSCs of markers that are also expressed by the normal stem cells in the tissue-of-origin (Al-Hajj et al., 2003).

CSCs were initially implicated in the pathogenesis of hematopoietic malignancies (Reya et al., 2001; Bonnet and Dick, 1997) and then years later were identified in solid tumors, in particular breast carcinomas and neuroectodermal tumors (Gilbertson and Rich, 2007; Al-Hajj et al., 2003). Fractionation of cancer cells on the basis of displayed cell-surface markers has yielded subpopulations of neoplastic cells with a greatly enhanced ability, relative to the corresponding majority populations, to seed new tumors upon implantation in immunodeficient mice. These often-rare tumor-initiating cells proved to share transcriptional profiles with certain normal tissue stem cell populations, motivating their designation as stem-like.

The origins of CSCs within a solid tumor have not been clarified and indeed may well vary from one tumor type to another. In some tumors, normal tissue stem cells may serve as the cells-of-origin that undergo oncogenic transformation to yield CSCs; in others, partially differentiated transit-amplifying cells, also termed progenitor cells, may suffer the initial oncogenic transformation thereafter assuming more stem-like character. Once primary tumors have formed, the CSCs, like their normal counterparts, may self-renew as well as spawn more differentiated derivatives; in the case of neoplastic CSCs, these descendant cells form the great bulk of many tumors. It remains to be established whether multiple distinct classes of increasingly neoplastic stem cells form during inception and subsequent multistep progression of tumors, ultimately yielding the CSCs that have been described in fully developed cancers.

Recent research has interrelated the acquisition of CSC traits with the EMT transdifferentiation program discussed above (Singh and Settleman, 2010; Mani et al., 2008; Morel et al., 2008). Induction of this program in certain model systems can induce many of the defining features of stem cells, including self-renewal ability and the antigenic phenotypes associated with both normal and cancer stem cells. This concordance suggests that the EMT program not only may enable cancer cells to physically disseminate from primary tumors but also can confer on such cells the self-renewal capability that is crucial to their subsequent clonal expansion at sites of dissemination (Brabletz et al., 2005). If generalized, this connection raises an important corollary hypothesis: the heterotypic signals that trigger an EMT, such as those released by an activated, inflammatory stroma, may also be important in creating and maintaining CSCs.

An increasing number of human tumors are reported to contain subpopulations with the properties of CSCs, as defined operationally through their efficient tumor-initiating capabilities upon xenotransplantation into mice. Nevertheless, the importance of CSCs as a distinct phenotypic subclass of neoplastic cells remains a matter of debate, as does their oft-cited rarity within tumors (Boiko et al., 2010; Gupta et al., 2009; Quintana et al., 2008). Indeed, it is plausible that the phenotypic plasticity operating within tumors may produce bidirectional interconversion between CSCs and non-CSCs, resulting in dynamic variation in the relative abundance of CSCs. Such plasticity could complicate definitive measurement of their prevalence. Analogous plasticity is already implicated in the EMT program, which can be engaged reversibly (Thiery and Sleeman, 2006).

These complexities notwithstanding, it is evident that this new dimension of tumor heterogeneity holds important implications for successful cancer therapies. Increasing evidence in a variety of tumor types suggests that cells with properties of CSCs are more resistant to various commonly used chemotherapeutic treatments (Singh and Settleman, 2010; Creighton et al., 2009; Buck et al., 2007). Their persistence may help to explain the almost-inevitable disease recurrence following apparently successful debulking of human solid tumors by radiation and various forms of chemotherapy. Indeed, CSCs may well prove to underlie certain forms of tumor dormancy, whereby latent cancer cells persist for years or even decades after surgical resection or radio/chemotherapy, only to suddenly erupt and generate life-threatening disease. Hence, CSCs may represent a double-threat, in that they are more resistant to therapeutic killing and, at the same time, endowed with the ability to regenerate a tumor once therapy has been halted.

This phenotypic plasticity implicit in CSC state may also enable the formation of functionally distinct subpopulations within a tumor that support overall tumor growth in various ways. For example, an EMT can convert epithelial carcinoma cells into mesenchymal, fibroblast-like cancer cells that may well assume the duties of cancer-associated fibroblasts (CAFs) in some tumors. Remarkably, several recent reports have documented the ability of glioblastoma cells (or possibly their associated CSC subpopulations) to transdifferentiate into endothelial-like cells that can substitute for bona fide host-derived endothelial cells in forming a tumor-associated neovasculature (Soda et al., 2011; El Hallani et al., 2010; Ricci-Vitiani et al., 2010; Wang et al., 2010). Observations like these indicate that certain tumors may acquire stromal support by inducing some of their own cancer cells to undergo various types of metamorphosis to produce stromal cell types rather than relying on recruited host cells to provide their functions.

The discovery of CSCs and biological plasticity in tumors indicates that a single, genetically homogeneous population of cells within a tumor may nevertheless be phenotypically heterogeneous due to the presence of cells in distinct states of differentiation. However, an equally important source of phenotypic variability may derive from the genetic heterogeneity within a tumor that accumulates as cancer progression proceeds. Thus, elevated genetic instability operating in later stages of tumor progression may drive rampant genetic diversification that outpaces the process of Darwinian selection, generating genetically distinct subpopulations far more rapidly than they can be eliminated.

Such thinking is increasingly supported by in-depth sequence analysis of tumor cell genomes, which has become practical due to recent major advances in DNA (and RNA) sequencing technology. Thus the sequencing of the genomes of cancer cells microdissected from different sectors of the same tumor (Yachida et al., 2010) has revealed striking intratumoral genetic heterogeneity. Some of this genetic diversity may be reflected in the long-recognized histological heterogeneity within individual human tumors. Alternatively, this genetic diversification may enable functional specialization, producing subpopulations of cancer cells that contribute distinct, complementary capabilities, which then accrue to the common benefit of overall tumor growth as described above.

Endothelial Cells

Much of the cellular heterogeneity within tumors is found in their stromal compartments. Prominent among the stromal constituents are the cells forming the tumor-associated vasculature. Mechanisms of development, differentiation, and homeostasis of endothelial cells composing the arteries, veins, and capillaries were already well understood in 2000. So too was the concept of the "angiogenic switch," which activates quiescent endothelial cells, causing them to enter into a cell-biological program that allows them to construct new blood vessels (see above). Over the last decade, a network of interconnected signaling pathways involving ligands of signal-transducing receptors displayed by endothelial cells (e.g., Notch, Neuropilin, Robo, and Eph-A/B) has been added to the already-prominent VEGF, angiopoietin, and FGF signals. These newly characterized pathways have been functionally implicated in developmental and tumor-associated angiogenesis and illustrate the complex regulation of endothelial cell phenotypes (Pasquale, 2010; Ahmed and Bicknell, 2009; Dejana et al., 2009; Carmeliet and Jain, 2000).

Other avenues of research are revealing distinctive gene expression profiles of tumor-associated endothelial cells and identifying cell-surface markers displayed on the lumenal surfaces of normal versus tumor endothelial cells (Nagy et al., 2010; Ruoslahti et al., 2010; Ruoslahti, 2002). Differences in signaling, in transcriptome profiles, and in vascular "ZIP codes" will likely prove to be important for understanding the conversion of normal endothelial cells into tumor-associated endothelial cells. Such knowledge may lead, in turn, to opportunities to develop novel therapies that exploit these differences in order to selectively target tumor-associated endothelial cells.

Closely related to the endothelial cells of the general circulation are those forming lymphatic vessels (Tammela and Alitalo, 2010). Their role in the tumor-associated stroma, specifically in supporting tumor growth, is poorly understood. Indeed, because of high interstitial pressure within solid tumors, intratumoral lymphatic vessels are typically collapsed and nonfunctional; in contrast, however, there are often functional, actively growing ("lymphangiogenic") lymphatic vessels at the peripheries of tumors and in the adjacent normal tissues that cancer cells

invade. These associated lymphatics likely serve as channels for the seeding of metastases in the draining lymph nodes that are commonly observed in a number of cancer types.

Pericytes

As noted earlier, pericytes represent a specialized mesenchymal cell type (related to smooth muscle cells) with finger-like projections that wrap around the endothelial tubing of blood vessels. In normal tissues, pericytes are known to provide paracrine support signals to the normally quiescent endothelium. For example, Ang-1 secreted by pericytes conveys antiproliferative stabilizing signals that are received by the Tie2 receptors expressed on the surface of endothelial cells; some pericytes also produce low levels of VEGF that serve a trophic function in endothelial homeostasis (Gaengel et al., 2009; Bergers and Song, 2005). Pericytes also collaborate with the endothelial cells to synthesize the vascular basement membrane that anchors both pericytes and endothelial cells and helps vessel walls to withstand the hydrostatic pressure of blood flow.

Genetic and pharmacological perturbation of the recruitment and association of pericytes has demonstrated the functional importance of these cells in supporting the tumor endothelium (Pietras and Ostman, 2010; Gaengel et al., 2009; Bergers and Song, 2005). For example, pharmacological inhibition of signaling through the PDGF receptor expressed by tumor pericytes and bone marrow-derived pericyte progenitors results in reduced pericyte coverage of tumor vessels, which in turn destabilizes vascular integrity and function (Pietras and Ostman, 2010; Raza et al., 2010; Gaengel et al., 2009); interestingly, and in contrast, the pericytes of normal vessels are not prone to such pharmacological disruption, providing another example of the differences in regulation of normal quiescent and tumor vasculature. An intriguing hypothesis, still to be fully substantiated, is that tumors with poor pericyte coverage of their vasculature may be more prone to permit cancer cell intravasation into the circulatory system, enabling subsequent hematogenous dissemination (Raza et al., 2010; Gerhardt and Semb, 2008).

Immune Inflammatory Cells

As also discussed above, infiltrating cells of the immune system are increasingly accepted to be generic constituents of tumors. These inflammatory cells operate in conflicting ways: both tumor-antagonizing and tumor-promoting leukocytes can be found, in various proportions, in most if not all neoplastic lesions. Although the presence of tumor-antagonizing CTLs and NK cells is not surprising, the prevalence of immune cells that functionally enhance hallmark capabilities was largely unanticipated. Evidence began to accumulate in the late 1990s that the infiltration of neoplastic tissues by cells of the immune system serves, perhaps counterintuitively, to promote tumor progression. Such work traced its conceptual roots back to the association of sites of chronic inflammation with tumor formation, and to the observation that tumors could be portrayed as wounds that never heal (Schäfer and Werner, 2008: Dvorak, 1986). In the course of normal wound healing and fighting infections, immune inflammatory cells appear transiently and then disappear, in contrast to their persistence in sites of chronic inflammation, where their presence has been associated with various tissue pathologies, including fibrosis, aberrant angiogenesis, and neoplasia (Grivennikov et al., 2010; Karin et al., 2006).

Over the past decade, the manipulation of genes involved in the determination or effector functions of various immune cell types, together with pharmacological inhibitors of such cells or their functions, has shown them to play diverse and critical roles in fostering tumorigenesis. The roster of tumor-promoting inflammatory cells now includes macrophage subtypes, mast cells, and neutrophils, as well as T and B lymphocytes (Coffelt et al., 2010; DeNardo et al., 2010; Egeblad et al., 2010; Johansson et al., 2008; Murdoch et al., 2008; DePalma et al., 2007). Such studies are yielding a growing list of signaling molecules released by inflammatory cells that serve as effectors of their tumor-promoting actions. These include the tumor growth factor EGF, the angiogenic growth factor VEGF, other proangiogenic factors such as FGF2, chemokines, and cytokines that amplify the inflammatory state; in addition, these cells may produce proangiogenic and/or proinvasive matrix-degrading enzymes, including MMP-9 and other matrix metalloproteinases, cysteine cathepsin proteases, and heparanase (Qian and Pollard, 2010; Murdoch et al., 2008). Consistent with their expression of these diverse effectors, tumor-infiltrating inflammatory cells have been shown to induce and help sustain tumor angiogenesis, to stimulate cancer cell proliferation, to facilitate, via their presence at the margins of tumors, tissue invasion, and to support the metastatic dissemination and seeding of cancer cells (Coffelt et al., 2010; Egeblad et al., 2010; Qian and Pollard, 2010; Mantovani, 2010; Joyce and Pollard, 2009; Mantovani et al., 2008; Murdoch et al., 2008; DePalma et al., 2007).

In addition to fully differentiated immune cells present in tumor stroma, a variety of partially differentiated myeloid progenitors have been identified in tumors (Murdoch et al., 2008). Such cells represent intermediaries between circulating cells of bone marrow origin and the differentiated immune cells typically found in normal and inflamed tissues. Importantly, these progenitors, like their more differentiated derivatives, have demonstrable tumor-promoting activity. Of particular interest, a class of tumor-infiltrating myeloid cells (defined as coexpressing the macrophage marker CD11b and the neutrophil marker Gr1) has been shown to suppress CTL and NK cell activity, having been independently identified as MDSCs (Qian and Pollard, 2010; Ostrand-Rosenberg and Sinha, 2009). This attribute raises the possibility that recruitment of certain myeloid cells may be doubly beneficial for the developing tumor, by directly promoting angiogenesis and tumor progression while at the same time affording a means to evade immune destruction.

The counterintuitive existence of both tumor-promoting and tumor-antagonizing immune cells can be rationalized by invoking the diverse roles of the immune system: On the one hand, the immune system specifically detects and targets infectious agents with the adaptive immune response, which is supported by cells of the innate immune system. On the other, the innate immune system is involved in wound healing and clearing dead cells and cellular debris. These specialized tasks are accomplished by distinct subclasses of inflammatory cells, namely a class of conventional macrophages and neutrophils (engaged in supporting adaptive immunity), and subclasses of ''alternatively activated'' macrophages, neutrophils, and

myeloid progenitors that are engaged in wound healing and tissue housecleaning (Egeblad et al., 2010; Mantovani, 2010; Qian and Pollard, 2010; Johansson et al., 2008). The latter subtypes of immune cells are one of the major sources of the angiogenic, epithelial, and stromal growth factors and matrix-remodeling enzymes that are needed for wound healing, and it is these cells that are recruited and subverted to support neoplastic progression. Similarly, subclasses of B and T lymphocytes may facilitate the recruitment, activation, and persistence of such wound-healing and tumor-promoting macrophages and neutrophils (DeNardo et al., 2010; Egeblad et al., 2010; Biswas and Mantovani, 2010). Of course, other subclasses of B and T lymphocytes and innate immune cell types can mount demonstrable tumor-killing responses. The balance between the conflicting inflammatory responses in tumors is likely to prove instrumental in prognosis and, quite possibly, in therapies designed to redirect these cells toward tumor destruction.

Cancer-Associated Fibroblasts

Fibroblasts are found in various proportions across the spectrum of carcinomas, constituting in many cases the preponderant cell population of the tumor stroma. The term ''cancer-associated fibroblast'' subsumes at least two distinct cell types: (1) cells with similarities to the fibroblasts that create the structural foundation supporting most normal epithelial tissues and (2) myofibroblasts, whose biological roles and properties differ markedly from those of tissue-derived fibroblasts. Myofibroblasts are identifiable by their expression of α-smooth muscle actin (SMA). They are rare in most healthy epithelial tissues, although certain tissues, such as the liver and pancreas, contain appreciable numbers of α-SMA-expressing cells. Myofibroblasts transiently increase in abundance in wounds and are also found in sites of chronic inflammation. Although beneficial to tissue repair, myofibroblasts are problematic in chronic inflammation, contributing to the pathological fibrosis observed in tissues such as lung, kidney, and liver.

Recruited myofibroblasts and reprogrammed variants of normal tissue-derived fibroblastic cells have been demonstrated to enhance tumor phenotypes, notably cancer cell proliferation, angiogenesis, and invasion and metastasis; their tumor-promoting activities have largely been defined by transplantation of cancer-associated fibroblasts admixed with cancer cells into mice, and more recently by genetic and pharmacologic perturbation of their functions in tumor-prone mice (Dirat et al., 2010; Pietras and Ostman, 2010; Räsänen and Vaheri, 2010; Shimoda et al., 2010; Kalluri and Zeisberg, 2006; Bhowmick et al., 2004). Because they secrete a variety of extracellular matrix components, cancer-associated fibroblasts are implicated in the formation of the desmoplastic stroma that characterizes many advanced carcinomas. The full spectrum of functions contributed by both subtypes of cancer-associated fibroblasts to tumor pathogenesis remains to be elucidated.

Stem and Progenitor Cells of the Tumor Stroma

The various stromal cell types that constitute the tumor microenvironment may be recruited from adjacent normal tissue—the most obvious reservoir of such cell types. However, in recent years, the bone marrow has increasingly been implicated as a key source of tumor-associated stromal cells (Bergfeld and DeClerck, 2010; Fang and Salven, 2011; Giaccia and Schipani, 2010; Patenaude et al., 2010; Lamagna and Bergers, 2006). Mesenchymal stem and progenitor cells have been found to transit into tumors from the marrow, where they may differentiate into the various well-characterized stromal cell types. Some of these recent arrivals may also persist in an undifferentiated or partially differentiated state, exhibiting functions that their more differentiated progeny lack.

The bone marrow origins of stromal cell types have been demonstrated using tumor-bearing mice in which the bone marrow cells and thus their disseminated progeny have been selectively labeled with reporters such as green fluorescent protein (GFP). While immune inflammatory cells have been long known to derive from the bone marrow, more recently the progenitors of pericytes and of various subtypes of cancer-associated fibroblasts originating from the bone marrow have been described in various mouse models of cancer (Bergfeld and DeClerck, 2010; Fang and Salven, 2011; Giaccia and Schipani, 2010; Lamagna and Bergers, 2006); the prevalence and functional importance of endothelial progenitors for tumor angiogenesis is currently unresolved (Fang and Salven, 2011; Patenaude et al., 2010). Taken together, these various lines of evidence indicate that tumor-associated stromal cells may be supplied to growing tumors by proliferation of preexisting stromal cells, by differentiation in situ of local stem/progenitor cells originating in the neighboring normal tissue, or via recruitment of bone marrow-derived stem/progenitor cells.

Heterotypic Signaling Orchestrates the Cells of the Tumor Microenvironment

Depictions of the intracellular circuitry governing cancer cell biology (e.g., Figure 2) will need to be complemented by similar diagrams charting the complex interactions between the neoplastic and stromal cells within a tumor and the dynamic extracellular matrix that they collectively erect and remodel (Egeblad et al., 2010; Kessenbrock et al., 2010; Pietras and Ostman, 2010; Polyak et al., 2009). A reasonably complete, graphic depiction of the network of microenvironmental signaling interactions is still far beyond our reach, as the great majority of signaling molecules and pathways remain to be identified. We provide instead a hint of such interactions in Figure 5, upper. These few well-established examples are intended to exemplify a signaling network of remarkable complexity that is of critical importance to tumor pathogenesis.

Another dimension of complexity is not represented in this simple schematic: both neoplastic cells and the stromal cells around them change progressively during the multistep transformation of normal tissues into high-grade malignancies. This histopathological progression must reflect underlying changes in heterotypic signaling between tumor parenchyma and stroma.

Such stepwise progression is likely to depend on back-and-forth reciprocal interactions between the neoplastic cells and the supporting stromal cells, as depicted in Figure 5, lower. Thus, incipient neoplasias begin the interplay by recruiting and activating stromal cell types that assemble into an initial preneoplastic stroma, which in turn responds reciprocally by enhancing

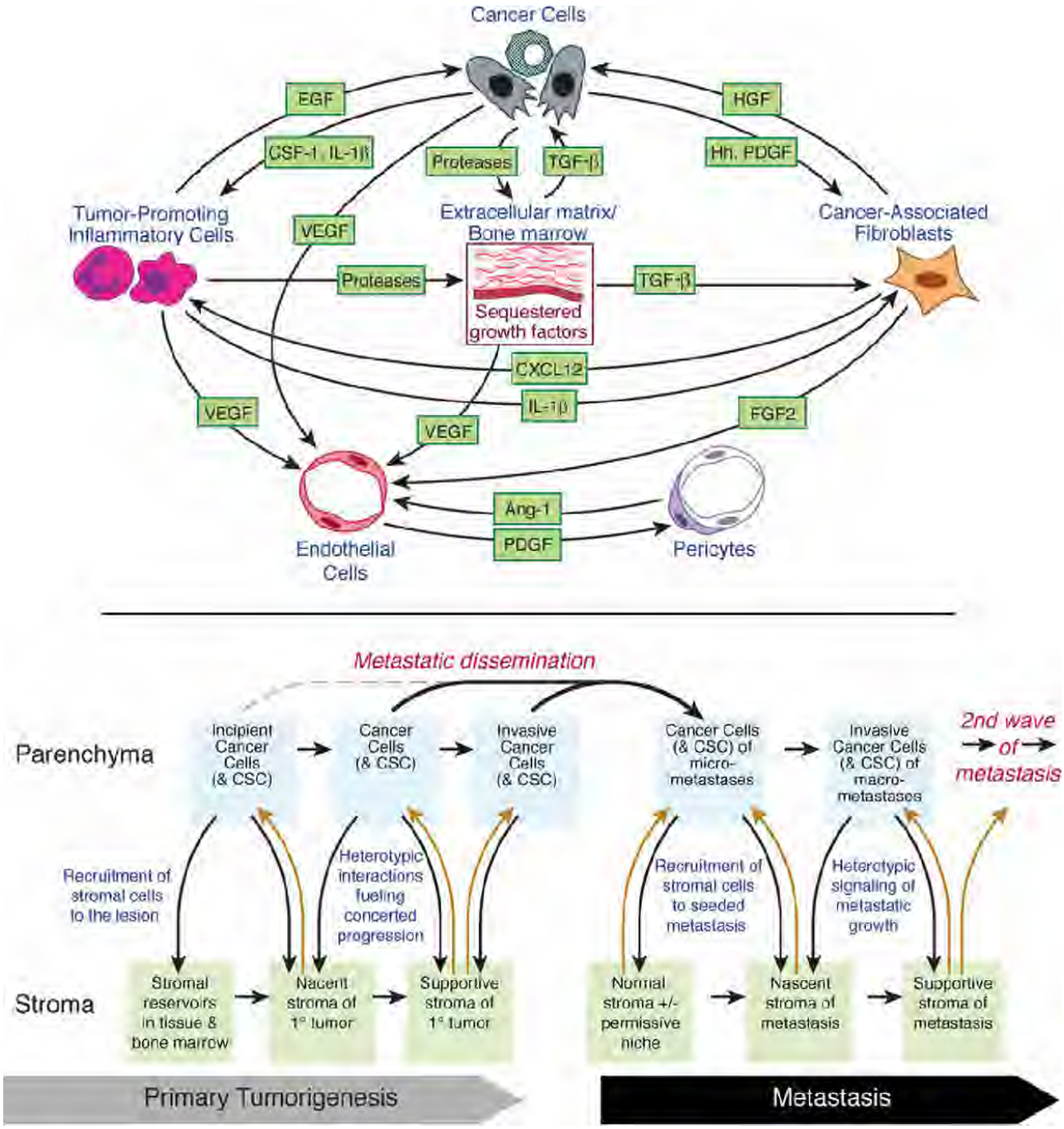

Figure 5. Signaling Interactions in the Tumor Microenvironment during Malignant Progression

(Upper) The assembly and collective contributions of the assorted cell types constituting the tumor microenvironment are orchestrated and maintained by reciprocal heterotypic signaling interactions, of which only a few are illustrated.

(Lower) The intracellular signaling depicted in the upper panel within the tumor microenvironment is not static but instead changes during tumor progression as a result of reciprocal signaling interactions between cancer cells of the parenchyma and stromal cells that convey the increasingly aggressive phenotypes that underlie growth, invasion, and metastatic dissemination. Importantly, the predisposition to spawn metastatic lesions can begin early, being influenced by the differentiation program of the normal cell-of-origin or by initiating oncogenic lesions. Certain organ sites (sometimes referred to as "fertile soil" or "metastatic niches") can be especially permissive for metastatic seeding and colonization by certain types of cancer cells, as a consequence of local properties that are either intrinsic to the normal tissue or induced at a distance by systemic actions of primary tumors. Cancer stem cells may be variably involved in some or all of the different stages of primary tumorigenesis and metastasis.

the neoplastic phenotypes of the nearby cancer cells. The cancer cells, which may further evolve genetically, again feed signals back to the stroma, continuing the reprogramming of normal stromal cells to serve the budding neoplasm; ultimately signals originating in the tumor stroma enable cancer cells to invade normal adjacent tissues and disseminate.

This model of reciprocal heterotypic signaling must be extended to encompass the final stage of multistep tumor progression—metastasis (Figure 5, lower right). The circulating cancer cells that are released from primary tumors leave a microenvironment created by the supportive stroma of such tumors. However, upon landing in a distant organ, these cancer cells encounter a naive, fully normal, tissue microenvironment. Consequently, many of the heterotypic signals that shaped their phenotype while they resided within primary tumors may be absent in sites of dissemination, constituting a barrier to growth of the seeded cancer cells. Thus, the succession of reciprocal cancer cell to stromal cell interactions that defined multistep progression in the primary tumor now must be repeated anew in distant tissues as disseminated cancer cells proceed to colonize their newfound organ sites.

Although this logic applies in some cases of metastasis, in others, as mentioned earlier, certain tissue microenvironments may, for various reasons, already be supportive of freshly seeded cancer cells; such permissive sites have been referred to as "metastatic niches" (Peinado et al., 2011; Coghlin and Murray, 2010). Implicit in this term is the notion that cancer cells seeded in such sites may not need to begin by inducing a supportive stroma because it already preexists, at least in part. Such permissivity may be intrinsic to the tissue site (Talmadge and Fidler, 2010) or preinduced by circulating factors released by the primary tumor (Peinado et al., 2011). The most well-documented components of induced premetastatic niches are tumor-promoting inflammatory cells, although other cell types and the ECM may well prove to play important roles in different metastatic contexts.

The likelihood that signaling interactions between cancer cells and their supporting stroma evolve during the course of multistage tumor development clearly complicates the goal of fully elucidating the mechanisms of cancer pathogenesis. For example, this reality poses challenges to systems biologists seeking to chart the crucial regulatory networks than orchestrate malignant progression. Moreover, it seems likely that understanding these dynamic variations will become crucial to the development of novel therapies designed to successfully target both primary and metastatic tumors.

THERAPEUTIC TARGETING

The introduction of mechanism-based targeted therapies to treat human cancers has been heralded as one of the fruits of three decades of remarkable progress of research into the mechanisms of cancer pathogenesis. We do not attempt here to enumerate the myriad therapies that are under development or have been introduced of late into the clinic. Instead, we consider how the description of hallmark principles is beginning to inform therapeutic development at present and may increasingly do so in the future.

The rapidly growing armamentarium of targeted therapeutics can be categorized according to their respective effects on one or more hallmark capabilities, as illustrated in the examples presented in Figure 6. Indeed, the observed efficacy of these drugs represents, in each case, a validation of a particular capability: if a capability is truly important for the biology of tumors, then its inhibition should impair tumor growth and progression.

We note that most of the hallmark-targeting cancer drugs developed to date have been deliberately directed toward specific molecular targets that are involved in one way or another in enabling particular capabilities. Such specificity of action has been considered a virtue, as it presents inhibitory activity against a target while having, in principle, relatively fewer off-target effects and thus less nonspecific toxicity. In fact, resulting clinical responses have generally been transitory, being followed by almost-inevitable relapses.

One interpretation of this history, supported by growing experimental evidence, is that each of the core hallmark capabilities is regulated by partially redundant signaling pathways. Consequently, a targeted therapeutic agent inhibiting one key pathway in a tumor may not completely shut off a hallmark capability, allowing some cancer cells to survive with residual function until they or their progeny eventually adapt to the selective pressure imposed by the therapy being applied. Such adaptation, which can be accomplished by mutation, epigenetic reprogramming, or remodeling of the stromal microenvironment, can reestablish the functional capability, permitting renewed tumor growth and clinical relapse. Given that the number of parallel signaling pathways supporting a given hallmark must be limited, it may become possible to target all of these supporting pathways therapeutically, thereby preventing the development of adaptive resistance.

In response to therapy, cancer cells may also reduce their dependence on a particular hallmark capability, becoming more dependent on another; this represents a quite different form of acquired drug resistance. This concept is exemplified by recent discoveries of unexpected responses to antiangiogenic therapies. Some have anticipated that effective inhibition of angiogenesis would render tumors dormant and might even lead to their dissolution (Folkman and Kalluri, 2004). Instead, the clinical responses to antiangiogenic therapies have been found to be transitory (Azam et al., 2010; Ebos et al., 2009; Bergers and Hanahan, 2008).

In certain preclinical models, where potent angiogenesis inhibitors succeed in suppressing this hallmark capability, tumors adapt and shift from a dependence upon continuing angiogenesis to heightening the activity of another instead—invasiveness and metastasis (Azam et al., 2010: Ebos et al., 2009; Bergers and Hanahan, 2008). By invading nearby tissues, initially hypoxic cancer cells evidently gain access to normal, preexisting tissue vasculature. Initial clinical validation of this adaptive/evasive resistance is apparent in the increased invasion and local metastasis seen when human glioblastomas are treated with antiangiogenic therapies (Ellis and Reardon, 2009; Norden et al., 2009; Verhoeff et al., 2009). The applicability of this lesson to other human cancers has yet to be established.

Analogous adaptive shifts in dependence on other hallmark traits may also limit efficacy of analogous hallmark-targeting

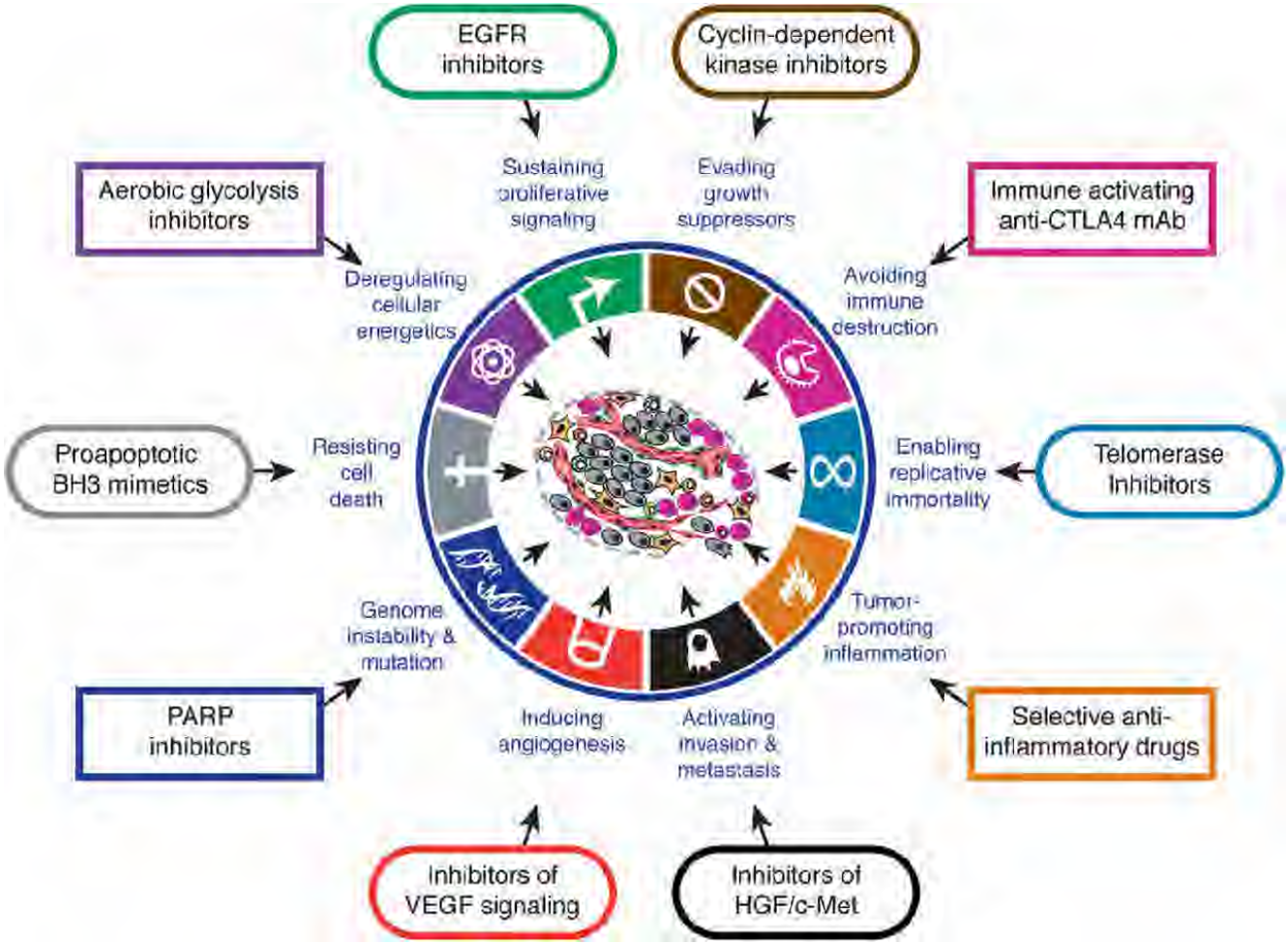

Figure 6. Therapeutic Targeting of the Hallmarks of Cancer

Drugs that interfere with each of the acquired capabilities necessary for tumor growth and progression have been developed and are in clinical trials or in some cases approved for clinical use in treating certain forms of human cancer. Additionally, the investigational drugs are being developed to target each of the enabling characteristics and emerging hallmarks depicted in Figure 3, which also hold promise as cancer therapeutics. The drugs listed are but illustrative examples; there is a deep pipeline of candidate drugs with different molecular targets and modes of action in development for most of these hallmarks.

therapies. For example, the deployment of apoptosis-inducing drugs may induce cancer cells to hyperactivate mitogenic signaling, enabling them to compensate for the initial attrition triggered by such treatments. Such considerations suggest that drug development and the design of treatment protocols will benefit from incorporating the concepts of functionally discrete hallmark capabilities and of the multiple biochemical pathways involved in supporting each of them. Thus, in particular, we can envisage that selective cotargeting of multiple core and emerging hallmark capabilities and enabling characteristics (Figure 6) in mechanism-guided combinations will result in more effective and durable therapies for human cancer.

CONCLUSION AND FUTURE VISION

We have sought here to revisit, refine, and extend the concept of cancer hallmarks, which has provided a useful conceptual framework for understanding the complex biology of cancer. The six acquired capabilities—the hallmarks of cancer—have stood the test of time as being integral components of most forms of cancer. Further refinement of these organizing principles will surely come in the foreseeable future, continuing the remarkable conceptual progress of the last decade.

Looking ahead, we envision significant advances during the coming decade in our understanding of invasion and metastasis. Similarly, the role of aerobic glycolysis in malignant growth will be elucidated, including a resolution of whether this metabolic reprogramming is a discrete capability separable from the core hallmark of chronically sustained proliferation. We remain perplexed as to whether immune surveillance is a barrier that virtually all tumors must circumvent, or only an idiosyncrasy of an especially immunogenic subset of them; this issue too will be resolved in one way or another.

Yet other areas are currently in rapid flux. In recent years, elaborate molecular mechanisms controlling transcription through chromatin modifications have been uncovered, and there are

clues that specific shifts in chromatin configuration occur during the acquisition of certain hallmark capabilities (Berdasco and Esteller, 2010). Functionally significant epigenetic alterations seem likely to be factors not only in the cancer cells but also in the altered cells of the tumor-associated stroma. It is unclear at present whether an elucidation of these epigenetic mechanisms will materially change our overall understanding of the means by which hallmark capabilities are acquired or simply add additional detail to the regulatory circuitry that is already known to govern them.

Similarly, the discovery of hundreds of distinct regulatory microRNAs has already led to profound changes in our understanding of the genetic control mechanisms that operate in health and disease. By now dozens of microRNAs have been implicated in various tumor phenotypes (Garzon et al., 2010), and yet these only scratch the surface of the real complexity, as the functions of hundreds of microRNAs known to be present in our cells and altered in expression in different forms of cancer remain total mysteries. Here again, we are unclear as to whether future progress will cause fundamental shifts in our understanding of the pathogenetic mechanisms of cancer or only add detail to the elaborate regulatory circuits that have already been mapped out.

Finally, the circuit diagrams of heterotypic interactions between the multiple distinct cell types that assemble and collaborate to produce different forms and progressively malignant stages of cancer are currently rudimentary. In another decade, we anticipate that the signaling circuitry describing the intercommunication between these various cells within tumors will be charted in far greater detail and clarity, eclipsing our current knowledge. And, as before (Hanahan and Weinberg, 2000), we continue to foresee cancer research as an increasingly logical science, in which myriad phenotypic complexities are manifestations of a small set of underlying organizing principles.

SUPPLEMENTAL INFORMATION

Supplemental Information includes six figures that are downloadable for presentations and can be found with this article online at doi:10.1016/j.cell.2011.02.013.

ACKNOWLEDGMENTS

We thank Terry Schoop (OFC Graphics, Kensington, CA, USA) for exceptional efforts in preparing the figures. And we thank Gerard Evan (Cambridge, UK), Erwin Wagner (Madrid, ESP), and Zena Werb (San Francisco, USA) for valuable comments and suggestions on the manuscript. D.H. and R.A.W. are American Cancer Society Research Professors. Research in the authors' laboratories has been largely supported by the U.S. National Cancer Institute. Due to space limitations, many primary and historical publications have not been cited, particularly in cases where topical reviews are available.

REFERENCES

Adams, J.M., and Cory, S. (2007). The Bcl-2 apoptotic switch in cancer development and therapy. Oncogene *26*, 1324–1337.

Aguirre-Ghiso, J.A. (2007). Models, mechanisms and clinical evidence for cancer dormancy. Nat. Rev. Cancer *7*, 834–846.

Ahmed, Z., and Bicknell, R. (2009). Angiogenic signalling pathways. Methods Mol. Biol. *467*, 3–24.

Al-Hajj, M., Wicha, M.S., Benito-Hernandez, A., Morrison, S.J., and Clarke, M.F. (2003). Prospective identification of tumorigenic breast cancer cells. Proc. Natl. Acad. Sci. USA *100*, 3983–3988.

Amaravadi, R.K., and Thompson, C.B. (2007). The roles of therapy-induced autophagy and necrosis in cancer treatment. Clin. Cancer Res. *13*, 7271–7279.

Amit, I., Citri, A., Shay, T., Lu, Y., Katz, M., Zhang, F., Tarcic, G., Siwak, D., Lahad, J., Jacob-Hirsch, J., et al. (2007). A module of negative feedback regulators defines growth factor signaling. Nat. Genet. *39*, 503–512.

Apel, A., Zentgraf, H., Büchler, M.W., and Herr, I. (2009). Autophagy-A double-edged sword in oncology. Int. J. Cancer *125*, 991–995.

Artandi, S.E., and DePinho, R.A. (2000). Mice without telomerase: what can they teach us about human cancer? Nat. Med. *6*, 852–855.

Artandi, S.E., and DePinho, R.A. (2010). Telomeres and telomerase in cancer. Carcinogenesis *31*, 9–18.

Azam, F., Mehta, S., and Harris, A.L. (2010). Mechanisms of resistance to antiangiogenesis therapy. Eur. J. Cancer *46*, 1323–1332.

Baeriswyl, V., and Christofori, G. (2009). The angiogenic switch in carcinogenesis. Semin. Cancer Biol. *19*, 329–337.

Baluk, P., Hashizume, H., and McDonald, D.M. (2005). Cellular abnormalities of blood vessels as targets in cancer. Curr. Opin. Genet. Dev. *15*, 102–111.

Barkan, D., Green, J.E., and Chambers, A.F. (2010). Extracellular matrix: a gatekeeper in the transition from dormancy to metastatic growth. Eur. J. Cancer *46*, 1181–1188.

Barnes, D.E., and Lindahl, T. (2004). Repair and genetic consequences of endogenous DNA base damage in mammalian cells. Annu. Rev. Genet. *38*, 445–476.

Barrallo-Gimeno, A., and Nieto, M.A. (2005). The Snail genes as inducers of cell movement and survival: implications in development and cancer. Development *132*, 3151–3161.

Berdasco, M., and Esteller, M. (2010). Aberrant epigenetic landscape in cancer: How cellular identity goes awry. Dev. Cell *19*, 698–711.

Bergers, G., and Benjamin, L.E. (2003). Tumorigenesis and the angiogenic switch. Nat. Rev. Cancer *3*, 401–410.

Bergers, G., and Hanahan, D. (2008). Modes of resistance to anti-angiogenic therapy. Nat. Rev. Cancer *8*, 592–603.

Bergers, G., and Song, S. (2005). The role of pericytes in blood-vessel formation and maintenance. Neuro-oncol. *7*, 452–464.

Bergfeld, S.A., and DeClerck, Y.A. (2010). Bone marrow-derived mesenchymal stem cells and the tumor microenvironment. Cancer Metastasis Rev. *29*, 249–261.

Berx, G., and van Roy, F. (2009). Involvement of members of the cadherin superfamily in cancer. Cold Spring Harb. Perspect. Biol. *1*, a003129.

Bhowmick, N.A., Neilson, E.G., and Moses, H.L. (2004). Stromal fibroblasts in cancer initiation and progression. Nature *432*, 332–337.

Bierie, B., and Moses, H.L. (2006). Tumour microenvironment: TGFbeta: the molecular Jekyll and Hyde of cancer. Nat. Rev. Cancer *6*, 506–520.

Bindea, G., Mlecnik, B., Fridman, W.H., Pagès, F., and Galon, J. (2010). Natural immunity to cancer in humans. Curr. Opin. Immunol. *22*, 215–222.

Biswas, S.K., and Mantovani, A. (2010). Macrophage plasticity and interaction with lymphocyte subsets: cancer as a paradigm. Nat. Immunol. *11*, 889–896.

Blasco, M.A. (2005). Telomeres and human disease: ageing, cancer and beyond. Nat. Rev. Genet. *6*, 611–622.

Boiko, A.D., Razorenova, O.V., van de Rijn, M., Swetter, S.M., Johnson, D.L., Ly, D.P., Butler, P.D., Yang, G.P., Joshua, B., Kaplan, M.J., et al. (2010). Human melanoma-initiating cells express neural crest nerve growth factor receptor CD271. Nature *466*, 133–137.

Bonnet, D., and Dick, J.E. (1997). Human acute myeloid leukemia is organized as a hierarchy that originates from a primitive hematopoietic cell. Nat. Med. *3*, 730–737.

Bos, P.D., Zhang, X.H., Nadal, C., Shu, W., Gomis, R.R., Nguyen, D.X., Minn, A.J., van de Vijver, M.J., Gerald, W.L., Foekens, J.A., and Massagué, J. (2009). Genes that mediate breast cancer metastasis to the brain. Nature *459*, 1005–1009.

Brabletz, T., Jung, A., Reu, S., Porzner, M., Hlubek, F., Kunz-Schughart, L.A., Knuechel, R., and Kirchner, T. (2001). Variable beta-catenin expression in colorectal cancers indicates tumor progression driven by the tumor environment. Proc. Natl. Acad. Sci. USA *98*, 10356–10361.

Brabletz, T., Jung, A., Spaderna, S., Hlubek, F., and Kirchner, T. (2005). Opinion: migrating cancer stem cells - an integrated concept of malignant tumour progression. Nat. Rev. Cancer *5*, 744–749.

Buck, E., Eyzaguirre, A., Barr, S., Thompson, S., Sennello, R., Young, D., Iwata, K.K., Gibson, N.W., Cagnoni, P., and Haley, J.D. (2007). Loss of homotypic cell adhesion by epithelial-mesenchymal transition or mutation limits sensitivity to epidermal growth factor receptor inhibition. Mol. Cancer Ther. *6*, 532–541.

Burkhart, D.L., and Sage, J. (2008). Cellular mechanisms of tumour suppression by the retinoblastoma gene. Nat. Rev. Cancer *8*, 671–682.

Cabrita, M.A., and Christofori, G. (2008). Sprouty proteins, masterminds of receptor tyrosine kinase signaling. Angiogenesis *11*, 53–62.

Campbell, P.J., Yachida, S., Mudie, L.J., Stephens, P.J., Pleasance, E.D., Stebbings, L.A., Morsberger, L.A., Latimer, C., McLaren, S., Lin, M.L., et al. (2010). The patterns and dynamics of genomic instability in metastatic pancreatic cancer. Nature *467*, 1109–1113.

Cao, Y. (2010). Adipose tissue angiogenesis as a therapeutic target for obesity and metabolic diseases. Nat. Rev. Drug Discov. *9*, 107–115.

Carmeliet, P. (2005). VEGF as a key mediator of angiogenesis in cancer. Oncology *69* (*Suppl 3*), 4–10.

Carmeliet, P., and Jain, R.K. (2000). Angiogenesis in cancer and other diseases. Nature *407*, 249–257.

Cavallaro, U., and Christofori, G. (2004). Cell adhesion and signalling by cadherins and Ig-CAMs in cancer. Nat. Rev. Cancer *4*, 118–132.

Cheng, N., Chytil, A., Shyr, Y., Joly, A., and Moses, H.L. (2008). Transforming growth factor-beta signaling-deficient fibroblasts enhance hepatocyte growth factor signaling in mammary carcinoma cells to promote scattering and invasion. Mol. Cancer Res. *6*, 1521–1533.

Chin, K., de Solorzano, C.O., Knowles, D., Jones, A., Chou, W., Rodriguez, E.G., Kuo, W.L., Ljung, B.M., Chew, K., Myambo, K., et al. (2004). In situ analyses of genome instability in breast cancer. Nat. Genet. *36*, 984–988.

Cho, R.W., and Clarke, M.F. (2008). Recent advances in cancer stem cells. Curr. Opin. Genet. Dev. *18*, 1–6.

Ciccia, A., and Elledge, S.J. (2010). The DNA damage response: making it safe to play with knives. Mol. Cell *40*, 179–204.

Coffelt, S.B., Lewis, C.E., Naldini, L., Brown, J.M., Ferrara, N., and De Palma, M. (2010). Elusive identities and overlapping phenotypes of proangiogenic myeloid cells in tumors. Am. J. Pathol. *176*, 1564–1576.

Coghlin, C., and Murray, G.I. (2010). Current and emerging concepts in tumour metastasis. J. Pathol. *222*, 1–15.

Collado, M., and Serrano, M. (2010). Senescence in tumours: evidence from mice and humans. Nat. Rev. Cancer *10*, 51–57.

Colotta, F., Allavena, P., Sica, A., Garlanda, C., and Mantovani, A. (2009). Cancer-related inflammation, the seventh hallmark of cancer: links to genetic instability. Carcinogenesis *30*, 1073–1081.

Cong, Y., and Shay, J.W. (2008). Actions of human telomerase beyond telomeres. Cell Res. *18*, 725–732.

Creighton, C.J., Li, X., Landis, M., Dixon, J.M., Neumeister, V.M., Sjolund, A., Rimm, D.L., Wong, H., Rodriguez, A., Herschkowitz, J.I., et al. (2009). Residual breast cancers after conventional therapy display mesenchymal as well as tumor-initiating features. Proc. Natl. Acad. Sci. USA *106*, 13820–13825.

Curto, M., Cole, B.K., Lallemand, D., Liu, C.H., and McClatchey, A.I. (2007). Contact-dependent inhibition of EGFR signaling by Nf2/Merlin. J. Cell Biol. *177*, 893–903.

Davies, M.A., and Samuels, Y. (2010). Analysis of the genome to personalize therapy for melanoma. Oncogene *29*, 5545–5555.

DeBerardinis, R.J., Lum, J.J., Hatzivassiliou, G., and Thompson, C.B. (2008). The biology of cancer: Metabolic reprogramming fuels cell growth and proliferation. Cell Metab. *7*, 11–20.

Dejana, E., Orsenigo, F., Molendini, C., Baluk, P., and McDonald, D.M. (2009). Organization and signaling of endothelial cell-to-cell junctions in various regions of the blood and lymphatic vascular trees. Cell Tissue Res. *335*, 17–25.

Demicheli, R., Retsky, M.W., Hrushesky, W.J., Baum, M., and Gukas, I.D. (2008). The effects of surgery on tumor growth: a century of investigations. Ann. Oncol. *19*, 1821–1828.

DeNardo, D.G., Andreu, P., and Coussens, L.M. (2010). Interactions between lymphocytes and myeloid cells regulate pro- versus anti-tumor immunity. Cancer Metastasis Rev. *29*, 309–316.

De Palma, M., Murdoch, C., Venneri, M.A., Naldini, L., and Lewis, C.E. (2007). Tie2-expressing monocytes: regulation of tumor angiogenesis and therapeutic implications. Trends Immunol. *28*, 519–524.

Deshpande, A., Sicinski, P., and Hinds, P.W. (2005). Cyclins and cdks in development and cancer: a perspective. Oncogene *24*, 2909–2915.

de Visser, K.E., Eichten, A., and Coussens, L.M. (2006). Paradoxical roles of the immune system during cancer development. Nat. Rev. Cancer *6*, 24–37.

Dirat, B., Bochet, L., Escourrou, G., Valet, P., and Muller, C. (2010). Unraveling the obesity and breast cancer links: a role for cancer-associated adipocytes? Endocr. Dev. *19*, 45–52.

Dvorak, H.F. (1986). Tumors: wounds that do not heal. Similarities between tumor stroma generation and wound healing. N. Engl. J. Med. *315*, 1650–1659.

Ebos, J.M., Lee, C.R., and Kerbel, R.S. (2009). Tumor and host-mediated pathways of resistance and disease progression in response to antiangiogenic therapy. Clin. Cancer Res. *15*, 5020–5025.

Egeblad, M., Nakasone, E.S., and Werb, Z. (2010). Tumors as organs: complex tissues that interface with the entire organism. Dev. Cell *18*, 884–901.

El Hallani, S., Boisselier, B., Peglion, F., Rousseau, A., Colin, C., Idbaih, A., Marie, Y., Mokhtari, K., Thomas, J.L., Eichmann, A., et al. (2010). A new alternative mechanism in glioblastoma vascularization: tubular vasculogenic mimicry. Brain *133*, 973–982.

Ellis, L.M., and Reardon, D.A. (2009). Cancer: The nuances of therapy. Nature *458*, 290–292.

Esteller, M. (2007). Cancer epigenomics: DNA methylomes and histone-modification maps. Nat. Rev. Genet. *8*, 286–298.

Evan, G.I., and d'Adda di Fagagna, F. (2009). Cellular senescence: hot or what? Curr. Opin. Genet. Dev. *19*, 25–31.

Evan, G., and Littlewood, T. (1998). A matter of life and cell death. Science *281*, 1317–1322.

Fang, S., and Salven, P. (2011). Stem cells in tumor angiogenesis. J. Mol. Cell. Cardiol. *50*, 290–295.

Feron, O. (2009). Pyruvate into lactate and back: from the Warburg effect to symbiotic energy fuel exchange in cancer cells. Radiother. Oncol. *92*, 329–333.

Feldser, D.M., and Greider, C.W. (2007). Short telomeres limit tumor progression in vivo by inducing senescence. Cancer Cell *11*, 461–469.

Ferrara, N. (2009). Vascular endothelial growth factor. Arterioscler. Thromb. Vasc. Biol. *29*, 789–791.

Ferrara, N. (2010). Pathways mediating VEGF-independent tumor angiogenesis. Cytokine Growth Factor Rev. *21*, 21–26.

Ferrone, C., and Dranoff, G. (2010). Dual roles for immunity in gastrointestinal cancers. J. Clin. Oncol. *28*, 4045–4051.

Fidler, I.J. (2003). The pathogenesis of cancer metastasis: the 'seed and soil' hypothesis revisited. Nat. Rev. Cancer *3*, 453–458.

Folkman, J. (2002). Role of angiogenesis in tumor growth and metastasis. Semin. Oncol. *29*(6, Suppl 16), 15–18.

Folkman, J. (2006). Angiogenesis. Annu. Rev. Med. *57*, 1–18.

Folkman, J., and Kalluri, R. (2004). Cancer without disease. Nature *427*, 787.

Friedberg, E.C., Aguilera, A., Gellert, M., Hanawalt, P.C., Hays, J.B., Lehmann, A.R., Lindahl, T., Lowndes, N., Sarasin, A., and Wood, R.D. (2006). DNA repair: from molecular mechanism to human disease. DNA Repair (Amst.) *5*, 986–996.

Friedl, P., and Wolf, K. (2008). Tube travel: the role of proteases in individual and collective cancer cell invasion. Cancer Res. *68*, 7247–7249.

Friedl, P., and Wolf, K. (2010). Plasticity of cell migration: a multiscale tuning model. J. Cell Biol. *188*, 11–19.

Gaengel, K., Genové, G., Armulik, A., and Betsholtz, C. (2009). Endothelial-mural cell signaling in vascular development and angiogenesis. Arterioscler. Thromb. Vasc. Biol. *29*, 630–638.

Galluzzi, L., and Kroemer, G. (2008). Necroptosis: a specialized pathway of programmed necrosis. Cell *135*, 1161–1163.

Garzon, R., Marcucci, G., and Croce, C.M. (2010). Targeting microRNAs in cancer: rationale, strategies and challenges. Nat. Rev. Drug Discov. *9*, 775–789.

Gerhardt, H., and Semb, H. (2008). Pericytes: gatekeepers in tumour cell metastasis? J. Mol. Med. *86*, 135–144.

Ghebranious, N., and Donehower, L.A. (1998). Mouse models in tumor suppression. Oncogene *17*, 3385–3400.

Giaccia, A.J., and Schipani, E. (2010). Role of carcinoma-associated fibroblasts and hypoxia in tumor progression. Curr. Top. Microbiol. Immunol. *345*, 31–45.

Gilbertson, R.J., and Rich, J.N. (2007). Making a tumour's bed: glioblastoma stem cells and the vascular niche. Nat. Rev. Cancer *7*, 733–736.

Gocheva, V., Wang, H.W., Gadea, B.B., Shree, T., Hunter, K.E., Garfall, A.L., Berman, T., and Joyce, J.A. (2010). IL-4 induces cathepsin protease activity in tumor-associated macrophages to promote cancer growth and invasion. Genes Dev. *24*, 241–255.

Grivennikov, S.I., Greten, F.R., and Karin, M. (2010). Immunity, inflammation, and cancer. Cell *140*, 883–899.

Gupta, G.P., Minn, A.J., Kang, Y., Siegel, P.M., Serganova, I., Cordón-Cardo, C., Olshen, A.B., Gerald, W.L., and Massagué, J. (2005). Identifying site-specific metastasis genes and functions. Cold Spring Harb. Symp. Quant. Biol. *70*, 149–158.

Gupta, P.B., Chaffer, C.L., and Weinberg, R.A. (2009). Cancer stem cells: mirage or reality? Nat. Med. *15*, 1010–1012.

Hanahan, D., and Folkman, J. (1996). Patterns and emerging mechanisms of the angiogenic switch during tumorigenesis. Cell *86*, 353–364.

Hanahan, D., and Weinberg, R.A. (2000). The hallmarks of cancer. Cell *100*, 57–70.

Hansel, D.E., Meeker, A.K., Hicks, J., De Marzo, A.M., Lillemoe, K.D., Schulick, R., Hruban, R.H., Maitra, A., and Argani, P. (2006). Telomere length variation in biliary tract metaplasia, dysplasia, and carcinoma. Mod. Pathol. *19*, 772–779.

Hardee, M.E., Dewhirst, M.W., Agarwal, N., and Sorg, B.S. (2009). Novel imaging provides new insights into mechanisms of oxygen transport in tumors. Curr. Mol. Med. *9*, 435–441.

Harper, J.W., and Elledge, S.J. (2007). The DNA damage response: Ten years after. Mol. Cell *28*, 739–745.

Hezel, A.F., and Bardeesy, N. (2008). LKB1; linking cell structure and tumor suppression. Oncogene *27*, 6908–6919.

Hlubek, F., Brabletz, T., Budczies, J., Pfeiffer, S., Jung, A., and Kirchner, T. (2007). Heterogeneous expression of Wnt/beta-catenin target genes within colorectal cancer. Int. J. Cancer *121*, 1941–1948.

Hugo, H., Ackland, M.L., Blick, T., Lawrence, M.G., Clements, J.A., Williams, E.D., and Thompson, E.W. (2007). Epithelial—mesenchymal and mesenchymal—epithelial transitions in carcinoma progression. J. Cell. Physiol. *213*, 374–383.

Hsu, P.P., and Sabatini, D.M. (2008). Cancer cell metabolism: Warburg and beyond. Cell *134*, 703–707.

Hynes, N.E., and MacDonald, G. (2009). ErbB receptors and signaling pathways in cancer. Curr. Opin. Cell Biol. *21*, 177–184.

Ikushima, H., and Miyazono, K. (2010). TGFbeta signalling: a complex web in cancer progression. Nat. Rev. Cancer *10*, 415–424.

Ince, T.A., Richardson, A.L., Bell, G.W., Saitoh, M., Godar, S., Karnoub, A.E., Iglehart, J.D., and Weinberg, R.A. (2007). Transformation of different human breast epithelial cell types leads to distinct tumor phenotypes. Cancer Cell *12*, 160–170.

Jackson, S.P., and Bartek, J. (2009). The DNA-damage response in human biology and disease. Nature *461*, 1071–1078.

Jiang, B.H., and Liu, L.Z. (2009). PI3K/PTEN signaling in angiogenesis and tumorigenesis. Adv. Cancer Res. *102*, 19–65.

Johansson, M., Denardo, D.G., and Coussens, L.M. (2008). Polarized immune responses differentially regulate cancer development. Immunol. Rev. *222*, 145–154.

Jones, P.A., and Baylin, S.B. (2007). The epigenomics of cancer. Cell *128*, 683–692.

Jones, R.G., and Thompson, C.B. (2009). Tumor suppressors and cell metabolism: a recipe for cancer growth. Genes Dev. *23*, 537–548.

Joyce, J.A., and Pollard, J.W. (2009). Microenvironmental regulation of metastasis. Nat. Rev. Cancer *9*, 239–252.

Junttila, M.R., and Evan, G.I. (2009). p53—a Jack of all trades but master of none. Nat. Rev. Cancer *9*, 821–829.

Kalluri, R., and Zeisberg, M. (2006). Fibroblasts in cancer. Nat. Rev. Cancer *6*, 392–401.

Kang, H.J., Choi, Y.S., Hong, S.B., Kim, K.W., Woo, R.S., Won, S.J., Kim, E.J., Jeon, H.K., Jo, S.Y., Kim, T.K., et al. (2004). Ectopic expression of the catalytic subunit of telomerase protects against brain injury resulting from ischemia and NMDA-induced neurotoxicity. J. Neurosci. *24*, 1280–1287.

Karin, M., Lawrence, T., and Nizet, V. (2006). Innate immunity gone awry: linking microbial infections to chronic inflammation and cancer. Cell *124*, 823–835.

Karnoub, A.E., and Weinberg, R.A. (2006–2007). Chemokine networks and breast cancer metastasis. Breast Dis. *26*, 75–85.

Karnoub, A.E., Dash, A.B., Vo, A.P., Sullivan, A., Brooks, M.W., Bell, G.W., Richardson, A.L., Polyak, K., Tubo, R., and Weinberg, R.A. (2007). Mesenchymal stem cells within tumour stroma promote breast cancer metastasis. Nature *449*, 557–563.

Kastan, M.B. (2008). DNA damage responses: mechanisms and roles in human disease: 2007 G.H.A. Clowes Memorial Award Lecture. Mol. Cancer Res. *6*, 517–524.

Kawai, T., Hiroi, S., Nakanishi, K., and Meeker, A.K. (2007). Telomere length and telomerase expression in atypical adenomatous hyperplasia and small bronchioloalveolar carcinoma of the lung. Am. J. Clin. Pathol. *127*, 254–262.

Kazerounian, S., Yee, K.O., and Lawler, J. (2008). Thrombospondins in cancer. Cell. Mol. Life Sci. *65*, 700–712.

Kenific, C.M., Thorburn, A., and Debnath, J. (2010). Autophagy and metastasis: another double-edged sword. Curr. Opin. Cell Biol. *22*, 241–245.

Kennedy, K.M., and Dewhirst, M.W. (2010). Tumor metabolism of lactate: the influence and therapeutic potential for MCT and CD147 regulation. Future Oncol. *6*, 127–148.

Kessenbrock, K., Plaks, V., and Werb, Z. (2010). Matrix metalloproteinases: Regulators of the tumor microenvironment. Cell *141*, 52–67.

Kim, M.Y., Oskarsson, T., Acharyya, S., Nguyen, D.X., Zhang, X.H., Norton, L., and Massagué, J. (2009). Tumor self-seeding by circulating cancer cells. Cell *139*, 1315–1326.

Kim, R., Emi, M., and Tanabe, K. (2007). Cancer immunoediting from immune surveillance to immune escape. Immunology *121*, 1–14.

Kinzler, K.W., and Vogelstein, B. (1997). Cancer-susceptibility genes. Gatekeepers and caretakers. Nature *386*, 761–763.

Klein, C.A. (2009). Parallel progression of primary tumours and metastases. Nat. Rev. Cancer *9*, 302–312.

Klymkowsky, M.W., and Savagner, P. (2009). Epithelial-mesenchymal transition: a cancer researcher's conceptual friend and foe. Am. J. Pathol. *174*, 1588–1593.

Korkola, J., and Gray, J.W. (2010). Breast cancer genomes—form and function. Curr. Opin. Genet. Dev. *20*, 4–14.

Kovacic, J.C., and Boehm, M. (2009). Resident vascular progenitor cells: an emerging role for non-terminally differentiated vessel-resident cells in vascular biology. Stem Cell Res. (Amst.) *2*, 2–15.

Kroemer, G., and Pouyssegur, J. (2008). Tumor cell metabolism: Cancer's Achilles' heel. Cancer Cell *13*, 472–482.

Lamagna, C., and Bergers, G. (2006). The bone marrow constitutes a reservoir of pericyte progenitors. J. Leukoc. Biol. *80*, 677–681.

Lane, D.P. (1992). Cancer. p53, guardian of the genome. Nature *358*, 15–16.

Lemmon, M.A., and Schlessinger, J. (2010). Cell signaling by receptor tyrosine kinases. Cell *141*, 1117–1134.

Levine, B., and Kroemer, G. (2008). Autophagy in the pathogenesis of disease. Cell *132*, 27–42.

Lipinski, M.M., and Jacks, T. (1999). The retinoblastoma gene family in differentiation and development. Oncogene *18*, 7873–7882.

Lobo, N.A., Shimono, Y., Qian, D., and Clarke, M.F. (2007). The biology of cancer stem cells. Annu. Rev. Cell Dev. Biol. *23*, 675–699.

Lowe, S.W., Cepero, E., and Evan, G. (2004). Intrinsic tumour suppression. Nature *432*, 307–315.

Luebeck, E.G. (2010). Cancer: Genomic evolution of metastasis. Nature *467*, 1053–1055.

Lu, Z., Luo, R.Z., Lu, Y., Zhang, X., Yu, Q., Khare, S., Kondo, S., Kondo, Y., Yu, Y., Mills, G.B., et al. (2008). The tumor suppressor gene ARHI regulates autophagy and tumor dormancy in human ovarian cancer cells. J. Clin. Invest. *118*, 3917–3929.

Luo, J., Solimini, N.L., and Elledge, S.J. (2009). Principles of cancer therapy: Oncogene and non-oncogene addiction. Cell *136*, 823–837.

Mac Gabhann, F., and Popel, A.S. (2008). Systems biology of vascular endothelial growth factors. Microcirculation *15*, 715–738.

Madsen, C.D., and Sahai, E. (2010). Cancer dissemination—Lessons from leukocytes. Dev. Cell *19*, 13–26.

Maida, Y., Yasukawa, M., Furuuchi, M., Lassmann, T., Possemato, R., Okamoto, N., Kasim, V., Hayashizaki, Y., Hahn, W.C., and Masutomi, K. (2009). An RNA-dependent RNA polymerase formed by TERT and the RMRP RNA. Nature *461*, 230–235.

Mani, S.A., Guo, W., Liao, M.J., Eaton, E.N., Ayyanan, A., Zhou, A.Y., Brooks, M., Reinhard, F., Zhang, C.C., Shipitsin, M., et al. (2008). The epithelial-mesenchymal transition generates cells with properties of stem cells. Cell *133*, 704–715.

Mantovani, A. (2010). Molecular pathways linking inflammation and cancer. Curr. Mol. Med. *10*, 369–373.

Mantovani, A., Allavena, P., Sica, A., and Balkwill, F. (2008). Cancer-related inflammation. Nature *454*, 436–444.

Massagué, J. (2008). TGFβ in cancer. Cell *134*, 215–230.

Masutomi, K., Possemato, R., Wong, J.M., Currier, J.L., Tothova, Z., Manola, J.B., Ganesan, S., Lansdorp, P.M., Collins, K., and Hahn, W.C. (2005). The telomerase reverse transcriptase regulates chromatin state and DNA damage responses. Proc. Natl. Acad. Sci. USA *102*, 8222–8227.

Mathew, R., Karantza-Wadsworth, V., and White, E. (2007). Role of autophagy in cancer. Nat. Rev. Cancer *7*, 961–967.

McGowan, P.M., Kirstein, J.M., and Chambers, A.F. (2009). Micrometastatic disease and metastatic outgrowth: clinical issues and experimental approaches. Future Oncol. *5*, 1083–1098.

Micalizzi, D.S., Farabaugh, S.M., and Ford, H.L. (2010). Epithelial-mesenchymal transition in cancer: parallels between normal development and tumor progression. J. Mammary Gland Biol. Neoplasia *15*, 117–134.

Mizushima, N. (2007). Autophagy: process and function. Genes Dev. *21*, 2861–2873.

Mohamed, M.M., and Sloane, B.F. (2006). Cysteine cathepsins: multifunctional enzymes in cancer. Nat. Rev. Cancer *6*, 764–775.

Mooi, W.J., and Peeper, D.S. (2006). Oncogene-induced cell senescence—halting on the road to cancer. N. Engl. J. Med. *355*, 1037–1046.

Morel, A.-P., Lièvre, M., Thomas, C., Hinkal, G., Ansieau, S., and Puisieux, A. (2008). Generation of breast cancer stem cells through epithelial-mesenchymal transition. PLoS ONE *3*, e2888.

Mosesson, Y., Mills, G.B., and Yarden, Y. (2008). Derailed endocytosis: an emerging feature of cancer. Nat. Rev. Cancer *8*, 835–850.

Mougiakakos, D., Choudhury, A., Lladser, A., Kiessling, R., and Johansson, C.C. (2010). Regulatory T cells in cancer. Adv. Cancer Res. *107*, 57–117.

Murdoch, C., Muthana, M., Coffelt, S.B., and Lewis, C.E. (2008). The role of myeloid cells in the promotion of tumour angiogenesis. Nat. Rev. Cancer *8*, 618–631.

Nagy, J.A., Chang, S.H., Shih, S.C., Dvorak, A.M., and Dvorak, H.F. (2010). Heterogeneity of the tumor vasculature. Semin. Thromb. Hemost. *36*, 321–331.

Naumov, G.N., Folkman, J., Straume, O., and Akslen, L.A. (2008). Tumor-vascular interactions and tumor dormancy. APMIS *116*, 569–585.

Negrini, S., Gorgoulis, V.G., and Halazonetis, T.D. (2010). Genomic instability—an evolving hallmark of cancer. Nat. Rev. Mol. Cell Biol. *11*, 220–228.

Nelson, B.H. (2008). The impact of T-cell immunity on ovarian cancer outcomes. Immunol. Rev. *222*, 101–116.

Nguyen, D.X., Bos, P.D., and Massagué, J. (2009). Metastasis: from dissemination to organ-specific colonization. Nat. Rev. Cancer *9*, 274–284.

Norden, A.D., Drappatz, J., and Wen, P.Y. (2009). Antiangiogenic therapies for high-grade glioma. Nat. Rev. Neurol. *5*, 610–620.

Nyberg, P., Xie, L., and Kalluri, R. (2005). Endogenous inhibitors of angiogenesis. Cancer Res. *65*, 3967–3979.

Okada, T., Lopez-Lago, M., and Giancotti, F.G. (2005). Merlin/NF-2 mediates contact inhibition of growth by suppressing recruitment of Rac to the plasma membrane. J. Cell Biol. *171*, 361–371.

Olive, K.P., Jacobetz, M.A., Davidson, C.J., Gopinathan, A., McIntyre, D., Honess, D., Madhu, B., Goldgraben, M.A., Caldwell, M.E., Allard, D., et al. (2009). Inhibition of Hedgehog signaling enhances delivery of chemotherapy in a mouse model of pancreatic cancer. Science *324*, 1457–1461.

Olson, P., Lu, J., Zhang, H., Shai, A., Chun, M.G., Wang, Y., Libutti, S.K., Nakakura, E.K., Golub, T.R., and Hanahan, D. (2009). MicroRNA dynamics in the stages of tumorigenesis correlate with hallmark capabilities of cancer. Genes Dev. *23*, 2152–2165.

O'Reilly, K.E., Rojo, F., She, Q.B., Solit, D., Mills, G.B., Smith, D., Lane, H., Hofmann, F., Hicklin, D.J., Ludwig, D.L., et al. (2006). mTOR inhibition induces upstream receptor tyrosine kinase signaling and activates Akt. Cancer Res. *66*, 1500–1508.

Ostrand-Rosenberg, S., and Sinha, P. (2009). Myeloid-derived suppressor cells: linking inflammation and cancer. J. Immunol. *182*, 4499–4506.

Pagès, F., Galon, J., Dieu-Nosjean, M.C., Tartour, E., Sautès-Fridman, C., and Fridman, W.H. (2010). Immune infiltration in human tumors: a prognostic factor that should not be ignored. Oncogene *29*, 1093–1102.

Palermo, C., and Joyce, J.A. (2008). Cysteine cathepsin proteases as pharmacological targets in cancer. Trends Pharmacol. Sci. *29*, 22–28.

Park, J.I., Venteicher, A.S., Hong, J.Y., Choi, J., Jun, S., Shkreli, M., Chang, W., Meng, Z., Cheung, P., Ji, H., et al. (2009). Telomerase modulates Wnt signalling by association with target gene chromatin. Nature *460*, 66–72.

Partanen, J.I., Nieminen, A.I., and Klefstrom, J. (2009). 3D view to tumor suppression: Lkb1, polarity and the arrest of oncogenic c-Myc. Cell Cycle *8*, 716–724.

Pasquale, E.B. (2010). Eph receptors and ephrins in cancer: bidirectional signalling and beyond. Nat. Rev. Cancer *10*, 165–180.

Passos, J.F., Saretzki, G., and von Zglinicki, T. (2007). DNA damage in telomeres and mitochondria during cellular senescence: is there a connection? Nucleic Acids Res. *35*, 7505–7513.

Patenaude, A., Parker, J., and Karsan, A. (2010). Involvement of endothelial progenitor cells in tumor vascularization. Microvasc. Res. *79*, 217–223.

Peinado, H., Lavothskin, S., and Lyden, D. (2011). The secreted factors responsible for pre-metastatic niche formation: Old sayings and new thoughts. Semin. Cancer Biol. Published online January 18, 2011. 10.1016/j.semcancer.2011.01.002.

Peinado, H., Marin, F., Cubillo, E., Stark, H.J., Fusenig, N., Nieto, M.A., and Cano, A. (2004). Snail and E47 repressors of E-cadherin induce distinct invasive and angiogenic properties in vivo. J. Cell Sci. *117*, 2827–2839.

Perona, R. (2006). Cell signalling: growth factors and tyrosine kinase receptors. Clin. Transl. Oncol. *8*, 77–82.

Pietras, K., and Ostman, A. (2010). Hallmarks of cancer: interactions with the tumor stroma. Exp. Cell Res. *316*, 1324–1331.

Polyak, K., and Weinberg, R.A. (2009). Transitions between epithelial and mesenchymal states: acquisition of malignant and stem cell traits. Nat. Rev. Cancer *9*, 265–273.

Polyak, K., Haviv, I., and Campbell, I.G. (2009). Co-evolution of tumor cells and their microenvironment. Trends Genet. *25*, 30–38.

Potter, V.R. (1958). The biochemical approach to the cancer problem. Fed. Proc. *17*, 691–697.

Qian, B.Z., and Pollard, J.W. (2010). Macrophage diversity enhances tumor progression and metastasis. Cell *141*, 39–51.

Quintana, E., Shackleton, M., Sabel, M.S., Fullen, D.R., Johnson, T.M., and Morrison, S.J. (2008). Efficient tumour formation by single human melanoma cells. Nature *456*, 593–598.

Raica, M., Cimpean, A.M., and Ribatti, D. (2009). Angiogenesis in pre-malignant conditions. Eur. J. Cancer *45*, 1924–1934.

Räsänen, K., and Vaheri, A. (2010). Activation of fibroblasts in cancer stroma. Exp. Cell Res. *316*, 2713–2722.

Raynaud, C.M., Hernandez, J., Llorca, F.P., Nuciforo, P., Mathieu, M.C., Commo, F., Delaloge, S., Sabatier, L., André, F., and Soria, J.C. (2010). DNA damage repair and telomere length in normal breast, preneoplastic lesions, and invasive cancer. Am. J. Clin. Oncol. *33*, 341–345.

Raza, A., Franklin, M.J., and Dudek, A.Z. (2010). Pericytes and vessel maturation during tumor angiogenesis and metastasis. Am. J. Hematol. *85*, 593–598.

Reitman, Z.J., and Yan, H. (2010). Isocitrate dehydrogenase 1 and 2 mutations in cancer: alterations at a crossroads of cellular metabolism. J. Natl. Cancer Inst. *102*, 932–941.

Reya, T., Morrison, S.J., Clarke, M.F., and Weissman, I.L. (2001). Stem cells, cancer, and cancer stem cells. Nature *414*, 105–111.

Ribatti, D. (2009). Endogenous inhibitors of angiogenesis: a historical review. Leuk. Res. *33*, 638–644.

Ricci-Vitiani, L., Pallini, R., Biffoni, M., Todaro, M., Invernici, G., Cenci, T., Maira, G., Parati, E.A., Stassi, G., Larocca, L.M., and De Maria, R. (2010). Tumour vascularization via endothelial differentiation of glioblastoma stem-like cells. Nature *468*, 824–828.

Ruoslahti, E. (2002). Specialization of tumour vasculature. Nat. Rev. Cancer *2*, 83–90.

Ruoslahti, E., Bhatia, S.N., and Sailor, M.J. (2010). Targeting of drugs and nanoparticles to tumors. J. Cell Biol. *188*, 759–768.

Sabeh, F., Shimizu-Hirota, R., and Weiss, S.J. (2009). Protease-dependent versus -independent cancer cell invasion programs: three-dimensional amoeboid movement revisited. J. Cell Biol. *185*, 11–19.

Salk, J.J., Fox, E.J., and Loeb, L.A. (2010). Mutational heterogeneity in human cancers: origin and consequences. Ann. Rev. Pathol. *5*, 51–75.

Schäfer, M., and Werner, S. (2008). Cancer as an overhealing wound: an old hypothesis revisited. Nat. Rev. Mol. Cell Biol. *9*, 628–638.

Schmalhofer, O., Brabletz, S., and Brabletz, T. (2009). E-cadherin, beta-catenin, and ZEB1 in malignant progression of cancer. Cancer Metastasis Rev. *28*, 151–166.

Semenza, G.L. (2008). Tumor metabolism: cancer cells give and take lactate. J. Clin. Invest. *118*, 3835–3837.

Semenza, G.L. (2010a). HIF-1: upstream and downstream of cancer metabolism. Curr. Opin. Genet. Dev. *20*, 51–56.

Semenza, G.L. (2010b). Defining the role of hypoxia-inducible factor 1 in cancer biology and therapeutics. Oncogene *29*, 625–634.

Seppinen, L., Sormunen, R., Soini, Y., Elamaa, H., Heljasvaara, R., and Pihlajaniemi, T. (2008). Lack of collagen XVIII accelerates cutaneous wound healing, while overexpression of its endostatin domain leads to delayed healing. Matrix Biol. *27*, 535–546.

Shaw, R.J. (2009). Tumor suppression by LKB1: SIK-ness prevents metastasis. Sci. Signal. *2*, pe55.

Shay, J.W., and Wright, W.E. (2000). Hayflick, his limit, and cellular ageing. Nat. Rev. Mol. Cell Biol. *1*, 72–76.

Sherr, C.J., and DePinho, R.A. (2000). Cellular senescence: Mitotic clock or culture shock? Cell *102*, 407–410.

Sherr, C.J., and McCormick, F. (2002). The RB and p53 pathways in cancer. Cancer Cell *2*, 103–112.

Shields, J.D., Kourtis, I.C., Tomei, A.A., Roberts, J.M., and Swartz, M.A. (2010). Induction of lymphoidlike stroma and immune escape by tumors that express the chemokine CCL21. Science *328*, 749–752.

Shimoda, M., Mellody, K.T., and Orimo, A. (2010). Carcinoma-associated fibroblasts are a rate-limiting determinant for tumour progression. Semin. Cell Dev. Biol. *21*, 19–25.

Sigal, A., and Rotter, V. (2000). Oncogenic mutations of the p53 tumor suppressor: the demons of the guardian of the genome. Cancer Res. *60*, 6788–6793.

Singh, A., and Settleman, J. (2010). EMT, cancer stem cells and drug resistance: an emerging axis of evil in the war on cancer. Oncogene *29*, 4741–4751.

Sinha, S., and Levine, B. (2008). The autophagy effector Beclin 1: a novel BH3-only protein. Oncogene *27* (*Suppl 1*), S137–S148.

Smyth, M.J., Dunn, G.P., and Schreiber, R.D. (2006). Cancer immunosurveillance and immunoediting: the roles of immunity in suppressing tumor development and shaping tumor immunogenicity. Adv. Immunol. *90*, 1–50.

Soda, Y., Marumoto, T., Friedmann-Morvinski, D., Soda, M., Liu, F., Michiue, H., Pastorino, S., Yang, M., Hoffman, R.M., Kesari, S., and Verma, I.M. (2011). Feature Article: Transdifferentiation of glioblastoma cells into vascular endothelial cells. Proc. Natl. Acad. Sci. USA. Published online January 24, 2011.

Sudarsanam, S., and Johnson, D.E. (2010). Functional consequences of mTOR inhibition. Curr. Opin. Drug Discov. Devel. *13*, 31–40.

Strauss, D.C., and Thomas, J.M. (2010). Transmission of donor melanoma by organ transplantation. Lancet Oncol. *11*, 790–796.

Talmadge, J.E., and Fidler, I.J. (2010). AACR centennial series: the biology of cancer metastasis: historical perspective. Cancer Res. *70*, 5649–5669.

Tammela, T., and Alitalo, K. (2010). Lymphangiogenesis: Molecular mechanisms and future promise. Cell *140*, 460–476.

Taube, J.H., Herschkowitz, J.I., Komurov, K., Zhou, A.Y., Gupta, S., Yang, J., Hartwell, K., Onder, T.T., Gupta, P.B., Evans, K.W., et al. (2010). Core epithelial-to-mesenchymal transition interactome gene-expression signature is associated with claudin-low and metaplastic breast cancer subtypes. Proc. Natl. Acad. Sci. USA *107*, 15449–15454.

Teng, M.W.L., Swann, J.B., Koebel, C.M., Schreiber, R.D., and Smyth, M.J. (2008). Immune-mediated dormancy: an equilibrium with cancer. J. Leukoc. Biol. *84*, 988–993.

Thiery, J.P., and Sleeman, J.P. (2006). Complex networks orchestrate epithelial-mesenchymal transitions. Nat. Rev. Mol. Cell Biol. *7*, 131–142.

Thiery, J.P., Acloque, H., Huang, R.Y., and Nieto, M.A. (2009). Epithelial-mesenchymal transitions in development and disease. Cell *139*, 871–890.

Townson, J.L., and Chambers, A.F. (2006). Dormancy of solitary metastatic cells. Cell Cycle *5*, 1744–1750.

Turner, H.E., Harris, A.L., Melmed, S., and Wass, J.A. (2003). Angiogenesis in endocrine tumors. Endocr. Rev. *24*, 600–632.

Vajdic, C.M., and van Leeuwen, M.T. (2009). Cancer incidence and risk factors after solid organ transplantation. Int. J. Cancer *125*, 1747–1754.

Vander Heiden, M.G., Cantley, L.C., and Thompson, C.B. (2009). Understanding the Warburg effect: the metabolic requirements of cell proliferation. Science *324*, 1029–1033.

Verhoeff, J.J., van Tellingen, O., Claes, A., Stalpers, L.J., van Linde, M.E., Richel, D.J., Leenders, W.P., and van Furth, W.R. (2009). Concerns about anti-angiogenic treatment in patients with glioblastoma multiforme. BMC Cancer *9*, 444.

Wang, R., Chadalavada, K., Wilshire, J., Kowalik, U., Hovinga, K.E., Geber, A., Fligelman, B., Leversha, M., Brennan, C., and Tabar, V. (2010). Glioblastoma stem-like cells give rise to tumour endothelium. Nature *468*, 829–833.

Warburg, O. (1956a). On the origin of cancer cells. Science *123*, 309–314.

Warburg, O. (1956b). On respiratory impairment in cancer cells. Science *124*, 269–270.

Warburg, O.H. (1930). The Metabolism of Tumours: Investigations from the Kaiser Wilhelm Institute for Biology, Berlin-Dahlem (London, UK: Arnold Constable).

Wertz, I.E., and Dixit, V.M. (2010). Regulation of death receptor signaling by the ubiquitin system. Cell Death Differ. *17*, 14–24.

White, E., Karp, C., Strohecker, A.M., Guo, Y., and Mathew, R. (2010). Role of autophagy in suppression of inflammation and cancer. Curr. Opin. Cell Biol. *22*, 212–217.

White, E., and DiPaola, R.S. (2009). The double-edged sword of autophagy modulation in cancer. Clin. Cancer Res. *15*, 5308–5316.

Willis, S.N., and Adams, J.M. (2005). Life in the balance: how BH3-only proteins induce apoptosis. Curr. Opin. Cell Biol. *17*, 617–625.

Witsch, E., Sela, M., and Yarden, Y. (2010). Roles for growth factors in cancer progression. Physiology (Bethesda) *25*, 85–101.

Wyckoff, J.B., Wang, Y., Lin, E.Y., Li, J.F., Goswami, S., Stanley, E.R., Segall, J.E., Pollard, J.W., and Condeelis, J. (2007). Direct visualization of macrophage-assisted tumor cell intravasation in mammary tumors. Cancer Res. *67*, 2649–2656.

Yachida, S., Jones, S., Bozic, I., Antal, T., Leary, R., Fu, B., Kamiyama, M., Hruban, R.H., Eshleman, J.R., Nowak, M.A., et al. (2010). Distant metastasis occurs late during the genetic evolution of pancreatic cancer. Nature *467*, 1114–1117.

Yang, J., and Weinberg, R.A. (2008). Epithelial-mesenchymal transition: At the crossroads of development and tumor metastasis. Dev. Cell *14*, 818–829.

Yang, L., Pang, Y., and Moses, H.L. (2010). TGF-beta and immune cells: an important regulatory axis in the tumor microenvironment and progression. Trends Immunol. *31*, 220–227.

Yen, K.E., Bittinger, M.A., Su, S.M., and Fantin, V.R. (2010). Cancer-associated IDH mutations: biomarker and therapeutic opportunities. Oncogene *29*, 6409–6417.

Yilmaz, M., and Christofori, G. (2009). EMT, the cytoskeleton, and cancer cell invasion. Cancer Metastasis Rev. *28*, 15–33.

Yuan, T.L., and Cantley, L.C. (2008). PI3K pathway alterations in cancer: variations on a theme. Oncogene *27*, 5497–5510.

Zee, Y.K., O'Connor, J.P., Parker, G.J., Jackson, A., Clamp, A.R., Taylor, M.B., Clarke, N.W., and Jayson, G.C. (2010). Imaging angiogenesis of genitourinary tumors. Nat. Rev. Urol. *7*, 69–82.

Zhang, H., Herbert, B.S., Pan, K.H., Shay, J.W., and Cohen, S.N. (2004). Disparate effects of telomere attrition on gene expression during replicative senescence of human mammary epithelial cells cultured under different conditions. Oncogene *23*, 6193–6198.

Zong, W.X., and Thompson, C.B. (2006). Necrotic death as a cell fate. Genes Dev. *20*, 1–15.

Zumsteg, A., and Christofori, G. (2009). Corrupt policemen: inflammatory cells promote tumor angiogenesis. Curr. Opin. Oncol. *21*, 60–70.

Exhibit 100

Published in final edited form as:
Nature. 2002 December 19; 420(6917): 860–867. doi:10.1038/nature01322.

Inflammation and cancer

Lisa M. Coussens[*,†,§] and **Zena Werb**[‡,§]
Lisa M. Coussens: coussens@cc.ucsf.edu; Zena Werb: zena@itsa.ucsf.edu
[*] Cancer Research Institute, University of California, San Francisco, California 94143 USA
[†] Department of Pathology, University of California, San Francisco, California 94143 USA
[‡] Department of Anatomy, University of California, San Francisco, California 94143 USA
[§] UCSF Comprehensive Cancer Center, University of California, San Francisco, California 94143 USA

Abstract

Recent data have expanded the concept that inflammation is a critical component of tumour progression. Many cancers arise from sites of infection, chronic irritation and inflammation. It is now becoming clear that the tumour microenvironment, which is largely orchestrated by inflammatory cells, is an indispensable participant in the neoplastic process, fostering proliferation, survival and migration. In addition, tumour cells have co-opted some of the signalling molecules of the innate immune system, such as selectins, chemokines and their receptors for invasion, migration and metastasis. These insights are fostering new anti-inflammatory therapeutic approaches to cancer development.

The functional relationship between inflammation and cancer is not new. In 1863, Virchow hypothesized that the origin of cancer was at sites of chronic inflammation, in part based on his hypothesis that some classes of irritants, together with the tissue injury and ensuing inflammation they cause, enhance cell proliferation[1]. Although it is now clear that proliferation of cells alone does not cause cancer, sustained cell proliferation in an environment rich in inflammatory cells, growth factors, activated stroma, and DNA-damage-promoting agents, certainly potentiates and/or promotes neoplastic risk. During tissue injury associated with wounding, cell proliferation is enhanced while the tissue regenerates; proliferation and inflammation subside after the assaulting agent is removed or the repair completed. In contrast, proliferating cells that sustain DNA damage and/or mutagenic assault (for example, initiated cells) continue to proliferate in microenvironments rich in inflammatory cells and growth/survival factors that support their growth. In a sense, tumours act as wounds that fail to heal[2].

Today, the causal relationship between inflammation, innate immunity and cancer is more widely accepted; however, many of the molecular and cellular mechanisms mediating this relationship remain unresolved — these are the focus of this review. Furthermore, tumour cells may usurp key mechanisms by which inflammation interfaces with cancers, to further their colonization of the host. Although the acquired immune response to cancer is intimately related to the inflammatory response, this topic is beyond the scope of this article, but readers are referred to several excellent reviews[3,4].

An overview of inflammation

To understand the role of inflammation in the evolution of cancer, it is important to understand what inflammation is and how it contributes to physiological and pathological processes such as wound healing and infection (Fig. 1). In response to tissue injury, a multifactorial network

of chemical signals initiate and maintain a host response designed to 'heal' the afflicted tissue. This involves activation and directed migration of leukocytes (neutrophils, monocytes and eosinophils) from the venous system to sites of damage (Box 1), and tissue mast cells also have a significant role. For neutrophils, a four-step mechanism is believed to coordinate recruitment of these inflammatory cells to sites of tissue injury and to the provisional extracellular matrix (ECM) that forms a scaffolding upon which fibroblast and endothelial cells proliferate and migrate, thus providing a nidus for reconstitution of the normal microenvironment[5]. These steps involve: activation of members of the selectin family of adhesion molecules (L- P-, and E-selectin) that facilitate rolling along the vascular endothelium; triggering of signals that activate and upregulate leukocyte integrins mediated by cytokines and leukocyte-activating molecules; immobilization of neutrophils on the surface of the vascular endothelium by means of tight adhesion through $\alpha_4\beta_1$ and $\alpha_4\beta_7$ integrins binding to endothelial vascular cell-adhesion molecule-1 (VCAM-1) and MadCAM-1, respectively; and transmigration through the endothelium to sites of injury, presumably facilitated by extracellular proteases, such as matrix metalloproteinases (MMPs).

Box 1

Wound healing as an example of physiological inflammation

Cellular components

Platelet activation and aggregation, in addition to accelerating coagulation, provide a bolus of secreted proteins and α-granule contents to the immediate area, all of which help initiate and accelerate the inflammatory response by the host. Examples of such secreted proteins include arachodonic acid metabolites, heparin, serotonin, thrombin, coagulation factors (factor V), adhesive proteins (fibrinogen and von Willebrand factor), plasma proteins (immunoglobulin-γ and albumin), cell growth factors (platelet-derived growth factor (PDGF), platelet-derived angiogenesis factor, transforming growth factor-α (TGF-α), TGF-β and basic fibroblast growth factor (bFGF)), enzymes (heparanase and factor XIII) and protease inhibitors (plasminogen activator inhibitor-1, α2-macroglobulin and α2-antiplasmin). Following platelet-induced haemostasis and release of TGF-β1 and PDGF, formation of granulation tissue is facilitated by chemotaxis of neutrophils, monocytes, fibroblasts and myofibroblasts, as well as by synthesis of new extracellular matrix (ECM) and neoangiogenesis.

Neutrophil chemotaxis is stimulated by factors such as circulating complement factor 5 (C5a), leukotriene B4, kallikrein, bacterial products (if present) and numerous factors released from platelets at the site (for example, PDGF, TGF-β, platelet-activating factor and platelet factor-4 (PF-4)). Although terminally differentiated with little biosynthetic machinery, neutrophils are capable of considerable production of cytokines/chemokines necessary for effector cell recruitment, activation and response15. These phagocytic cells initiate wound healing by serving as a source of early-response pro-inflammatory cytokines such as tumour necrosis factor-α (TNF-α)68, and interleukin (IL)-1α and IL-1β69. These cytokines mediate leukocyte adherence to the vascular endothelium, thus targeting and restricting leukocytes to areas of repair, and initiate repair by inducing expression of matrix metalloproteinases (MMPs) and keratinocyte growth factor (KGF/FGF-7) by fibroblasts70.

In response to tissue injury, mononuclear phagocytes (that is, macrophage progenitors) migrate from the venous system to the site of tissue injury. They are guided to the site by chemotactic factors, including PF-4, TGF-β, PDGF, chemokines (monocyte chemoattractant protein-1, -2 and -3 (MCP-1/CCL2, MCP-2/CCL8 and MCP-3/CCL7), macrophage inflammatory protein-1α and -1β (MIP-1α/CCL3 and MIP-1β/CCL4), and the cytokines IL-1β and TNF-α. Deployment of monocytes/macrophages to the site of injury

peaks as the number of neutrophils decline. Once present, however, they differentiate into mature macrophages or immature dendritic cells71. After activation, macrophages are the main source of growth factors and cytokines (TGF-β1, PDGF, bFGF, TGF-α, insulin-like growth factor (IGF)-I and -II, TNF-α and IL-1) that modulate tissue repair. Cells in their local microenvironment (for example, endothelial, epithelial, mesenchymal or neuroendocrine cells) are profoundly affected by macrophage products. Macrophages also regulate local tissue remodelling by inducing ECM components, stimulating production of proteolytic enzymes (for example, MMPs and urokinase-type plasminogen activator (uPA)), clearing apoptotic and necrotic cells, and modulating angiogenesis through local production of thrombospondin-1 (refs 72, 73).

Following their activation, mast cells are full of stored and newly synthesized inflammatory mediators. This cell type synthesizes and stores histamine, cytokines and proteases complexed to highly sulphated proteoglycans within granules, and produces lipid mediators and cytokines upon stimulation. Once activated by complement or by binding of antigens to immunoglobulin E (IgE) bound to high-affinity IgE receptors (FcεRI), they degranulate, releasing mediators including heparin, heparanase, histamine, MMPs and serine proteases, and various polypeptide growth factors, including bFGF and vascular endothelial growth factor[74]. These function both in the early initiation phase of inflammation (for example, vascular reaction and exudation), and in the late phase where leukocyte accumulation and wound healing takes place.

Chemotactic cytokines

Chemokines are classified into polypeptide groups identified by the location of cysteine residues near their amino termini (for example, C-C, C-X-C, C and CX_3C). Chemokines represent the largest family of cytokines (~41 human members), forming a complex network for the chemotactic activation of all leukocytes. Chemokine receptors, members of the seven-transmembrane-spanning G-protein-coupled receptors, vary by cell type and degree of cell activation[6]. There is considerable redundancy in chemokine-receptor interaction, as many ligands bind different receptors, or vice versa.

The composition of chemokines produced at sites of tissue wounding not only recruits downstream effector cells (as discussed above), but also dictates the natural evolution of immune reactivity. For example, MCP-1/CCL2, a potent chemotactic protein for monocytes and lymphocytes, simultaneously induces expression of lymphocyte-derived IL-4 in response to antigen challenge while decreasing expression of IL-12 (ref. 75). The net effect of this alteration facilitates a switch from a T_H1-type to a T_H2-type inflammatory response.

Tissue repair

In response to wounding, fibroblasts migrate into the wound bed and initially secrete collagen type III, which is later replaced by collagen type I. Synthesis and deposition of these collagens by fibroblasts is stimulated by factors including TGF-β1, -β2 and -β3, PDGF, IL-1α, -1β and -4, and mast cell tryptase. Once sufficient collagen has been generated, its synthesis is stopped; thus, during wound repair, production as well as the degradation of collagens is under precise spatial and temporal control.

The final phase of the healing process is re-epithelialization and migration of epithelial cells across this amalgam, in a process that requires both dissolution of the fibrin clot and degradation of the underlying dermal collagen. Epithelial cells at the leading edge of the wound express the uPA receptor, which is important for focal activation of uPA, and collagenolytic enzymes of the MMP family. In the absence of the fibrinolytic enzyme plasmin, derived from plasminogen after activation by uPA and tissue-PA, re-epithelialization is dramatically delayed[76].

The pro-inflammatory properties of TGF-β, such as leukocyte recruitment, adhesion and regulation of MMP secretion and activation, are balanced by its ability to also reverse its role, and suppress these events and foster ECM synthesis to mediate tissue repair[8]. As inflammatory cells are activated, their complement of TGF-β receptors change, resulting in differential susceptibility to TGF-β and enhanced sensitivity to suppression by TGF-β[8], a critical event to resolving inflammation.

A family of chemotactic cytokines, named chemokines, which possess a relatively high degree of specificity for chemoattraction of specific leukocyte populations[1,6,7], recruits downstream effector cells and dictates the natural evolution of the inflammatory response. The profile of cytokine/chemokines persisting at an inflammatory site is important in the development of chronic disease. The pro-inflammatory cytokine TNF-α (tumour necrosis factor-α) controls inflammatory cell populations as well as mediating many of the other aspects of the inflammatory process. TGF-β1 is also important, both positively and negatively influencing the processes of inflammation and repair[8]. The key concept is that normal inflammation — for example, inflammation associated with wound healing — is usually self-limiting; however, dysregulation of any of the converging factors can lead to abnormalities and ultimately, pathogenesis — this seems to be the case during neoplastic progression.

Neutrophils (and sometimes eosinophils) are the first recruited effectors of the acute inflammatory response. Monocytes, which differentiate into macrophages in tissues, are next to migrate to the site of tissue injury, guided by chemotactic factors. Once activated, macrophages are the main source of growth factors and cytokines, which profoundly affect endothelial, epithelial and mesenchymal cells in the local microenvironment. Mast cells are also important in acute inflammation owing to their release of stored and newly synthesized inflammatory mediators, such as histamine, cytokines and proteases complexed to highly sulphated proteoglycans, as well as lipid mediators.

Inflammation and neoplastic progression

Peyton Rous was the first to recognize that cancers develop from “subthreshold neoplastic states” caused by viral or chemical carcinogens that induce somatic changes[9,10]. These states, now known as ‘initiation’, involve DNA alterations, are irreversible and can persist in otherwise normal tissue indefinitely until the occurrence of a second type of stimulation (now referred to as ‘promotion’). Promotion can result from exposure of initiated cells to chemical irritants, such as phorbol esters, factors released at the site of wounding, partial organ resection, hormones or chronic irritation and inflammation (Fig. 1). Functionally, many promoters, whether directly or indirectly, induce cell proliferation, recruit inflammatory cells, increase production of reactive oxygen species leading to oxidative DNA damage, and reduce DNA repair. Subversion of cell death and/or repair programmes occurs in chronically inflamed tissues, thus resulting in DNA replication and proliferation of cells that have lost normal growth control. Normal inflammation is self-limiting, because the production of anti-inflammatory cytokines follows the pro-inflammatory cytokines closely (Fig. 2). However, chronic inflammation seems to be due to persistence of the initiating factors or a failure of mechanisms required for resolving the inflammatory response. Why does the inflammatory response to tumours persist?

Inflammatory cell component of tumours

Tumour cells produce various cytokines and chemokines that attract leukocytes. The inflammatory component of a developing neoplasm may include a diverse leukocyte population — for example, neutrophils, dendritic cells, macrophages, eosinophils and mast cells, as well as lymphocytes — all of which are capable of producing an assorted array of

cytokines, cytotoxic mediators including reactive oxygen species, serine and cysteine proteases, MMPs and membrane-perforating agents, and soluble mediators of cell killing, such as TNF-α, interleukins and interferons (IFNs)[11,12].

Monocytes, in the presence of granulocyte–macrophage colony-stimulating factor (GM-CSF) and interleukin (IL)-4, differentiate into immature dendritic cells[13]. Dendritic cells migrate into inflamed peripheral tissue where they capture antigens and, after maturation, migrate to lymph nodes to stimulate T-lymphocyte activation. Soluble factors such as IL-6 and CSF-1, derived from neoplastic cells, push myeloid precursors towards a macrophage-like phenotype14. Interestingly, dendritic cells found in neoplastic infiltrates are frequently immature and defective in T-cell stimulatory capacity.

Tumour-associated macrophages (TAMs) are a significant component of inflammatory infiltrates in neoplastic tissues and are derived from monocytes that are recruited largely by monocyte chemotactic protein (MCP) chemokines. TAMs have a dual role in neoplasms — although they may kill neoplastic cells following activation by IL-2, interferon and IL-12 (refs 15, 16), TAMs produce a number of potent angiogenic and lymphangiogenic growth factors, cytokines and proteases, all of which are mediators that potentiate neoplastic progression17. TAMs and tumour cells also produce IL-10, which effectively blunts the anti-tumour response by cytotoxic T cells. During development of melanoma, activated macrophages produce TGF-β, TNF-α, IL-1α, arachidonate metabolites and extracellular proteases18. In response, melanocytes express IL-8 and vascular endothelial growth factor (VEGF)-A, thereby inducing vascular angiogenesis under paracrine control[18]. Indeed, macrophage infiltration is closely associated with the depth of invasion of primary melanoma due, in part, to macrophage-regulated tumour-associated angiogenesis19.

In addition to altering the local balance of pro-angiogenic factors during melanoma development, during human cervical carcinogenesis, TAMs express VEGF-C and VEGF-D as well as the VEGF receptor-3 (VEGFR-3), all of which are implicated in formation of lymphatic vessels and lymphatic metastases[17]. By placing TAMs at the centre of the recruitment and response to angiogenic and lymphangiogenic stimuli, they may foster the spread of tumours. TAMs also induce VCAM-1 expression on mesothelial cells, a step also believed to be key for tumour cell dissemination into the peritoneum20.

The functional significance of macrophage recruitment to sites of neoplastic growth has been examined by crossing transgenic mice expressing Polyoma virus middle T (PyMT) driven by the mouse mammary tumour virus (MMTV) long terminal repeat, which are prone to development of mammary cancer, with mice containing a null mutation in the CSF-1 gene (*Csf1*^{op})[21]. Whereas the absence of CSF-1 during early neoplastic development is without apparent consequence, development of late-stage invasive carcinoma and pulmonary metastases are significantly attenuated. The key difference between PyMT mice and PyMT/*Csf1*^{op}/*Csf1*^{op} mice is not in the apparent proliferative capacity of neoplastic epithelial cells, but in the failure to recruit mature macrophages into neoplastic tissue in the absence of CSF-1. Targeting CSF-1 expression specifically to mammary epithelium in CSF-1-null/PyMT mice restores macrophage recruitment, primary tumour development and metastatic potential[12]. A similar study showed that subcutaneous growth of Lewis lung cancer cells is impaired in *Csf1*^{op}/*Csf1*^{op} mice22. In this example, however, tumours displayed a decreased mitotic index and pronounced necrosis, apparently resulting from diminished angiogenesis and impaired tumour-stroma formation. These defects were corrected by treatment of tumour-bearing mice with recombinant CSF-1 (ref. 22). Together, these genetic experiments provide a causal link between CSF-1-dependent infiltrating macrophages and the malignant potential of epithelial cells.

Macrophages are not unique among inflammatory cells in potentiation of neoplastic processes. Genetic and functional experiments indicate that neutrophils, mast cells, eosinophils and activated T lymphocytes also contribute to malignancies by releasing extracellular proteases, pro-angiogenic factors and chemokines[11,23–26].

Cancers associated with chronic inflammation

How are inflammatory cells co-opted into the neoplastic process? A plausible hypothesis is that many malignancies arise from areas of infection and inflammation, simply as part of the normal host response. Indeed, there is a growing body of evidence that many malignancies are initiated by infections[11,27–29] (Table 1) — upwards of 15% of malignancies worldwide can be attributed to infections, a global total of 1.2 million cases per year[11]. Persistent infections within the host induce chronic inflammation. Leukocytes and other phagocytic cells induce DNA damage in proliferating cells, through their generation of reactive oxygen and nitrogen species that are produced normally by these cells to fight infection[30]. These species react to form peroxynitrite, a mutagenic agent [30]. Hence, repeated tissue damage and regeneration of tissue, in the presence of highly reactive nitrogen and oxygen species released from inflammatory cells, interacts with DNA in proliferating epithelium resulting in permanent genomic alterations such as point mutations, deletions, or rearrangements. Indeed, p53 mutations are seen at frequencies similar to those in tumours in chronic inflammatory diseases such as rheumatoid arthritis and inflammatory bowel disease[31].

The strongest association of chronic inflammation with malignant diseases is in colon carcinogenesis arising in individuals with inflammatory bowel diseases, for example, chronic ulcerative colitis and Crohn's disease. Hepatitis C infection in the liver predisposes to liver carcinoma, an increased risk of bladder and colon carcinoma is associated with schistosomiasis, whereas chronic *Helicobacter pylori* infection is the world's leading cause of stomach cancer[32]. The Gram-negative bacterium *H. pylori* is established as a definite carcinogen for the development of gastric cancer — the second most common type of cancer globally11،29 — and DNA damage resulting from chronic inflammation is believed the mechanism[32]. Exacerbating DNA damage induced by inflammatory cells is expression of macrophage migration inhibitory factor (MIF) from macrophages and T lymphocytes. MIF is a potent cytokine that overcomes p53 function by suppressing its transcriptional activity[33]. Chronic bypass of p53 regulatory functions in infiltrated tissues can enhance proliferation and extend life span, while also creating an environment with a deficient response to DNA damage, amplifying accumulation of potential oncogenic mutations.

Infectious viral agents, for example, DNA tumour viruses, may also directly transform cells by inserting active oncogenes into the host genome, although other mechanisms also are responsible. While many types of infectious agents are present in animals, only a subset of individuals infected with human papilloma virus, hepatitis B virus (HBV) or Epstein-Barr virus develop virus-associated malignancies. This may reflect immune suppression, the necessity of cofactors necessary for promotion or the fact that a neoplasm can develop only if viral infection has targeted a pluripotent progenitor or stem cell. Such stem cells are typically low in abundance and located in regions of tissues protected from agents that would otherwise harm them[34]. In Rous sarcoma virus infections, inflammation is essential for tumour development and this requirement is mediated by factors such as TGF-β and other cytokines produced by the inflammatory cells35. Epstein-Barr virus also causes sustained proliferation of B lymphocytes, which, when coupled with a secondary mutation, can result in neoplastic progression and malignant conversion to give rise to Burkett's lymphoma.

The molecular mechanism behind the associated risk of hepatocellular carcinoma resulting from HBV and/or hepatitis C virus (HCV) infection is uncertain. Although there is evidence for clonal integration of viral DNA in tumours and surrounding parenchyma cells, there are no

defined transforming sequences found within the viral genomes that can act as viral oncogenes. Moreover, there is no evidence to suggest that viral integration activates either a classical cellular oncogene or inactivates a cellular tumour suppressor gene. HCV core protein interacts with the signal transducer and activator of transcription 3 (STAT3) protein[36], a transcription factor involved in mediating cytokine signalling37. This interaction induces sustained phosphorylation of a critical tyrosine residue, resulting in enhanced proliferation and upregulation of Bcl-x_L and cyclin-D. Thus, chronic viral replication in hepatocytes may alter the local cytokine profile and the apoptotic or proliferative responses in infected cells, with an immune response to the viral proteins resulting in a state of chronic inflammation. Interestingly, a similar pathway involving inflammation, IL-6 and STAT3 is downstream of *H. pylori* in the generation of stomach cancer[38].

The chemokine connection

Chemokines were initially defined functionally as soluble factors regulating directional migration of leukocytes during states of inflammation; however, chemokine biology extends to all cell types, including most human neoplastic cells[6]. Attention first focused on the role of chemokines during malignancy when it was reported that experimental animals without T or natural killer (NK) cell functions, when challenged with a tumour, showed a typical inflammatory infiltrate; this suggested that neoplastic cells either produce chemotactic factors or induce their expression in nearby 'host' cells[39]. It is now appreciated that the chemokine-receptor system can be altered dramatically in neoplastic tissue, particularly at the invasive edges. Moreover, chemokines induce direct effects on stromal and neoplastic cells in addition to their roles in regulating leukocyte recruitment (Fig. 2).

Regulation of tumour growth by chemokines—Some tumour cells not only regulate their chemokine expression to help recruit inflammatory cells, but also use these factors to further the tumour growth and progression. Melanoma is perhaps the best exemplar in which chemokines (for example, GROα/CXCL1, GROβ/CXCL2, GROγ/CXCL3 and IL-8/CXCL8) have been shown to exert autocrine control over neoplastic cell proliferation[40]. Blocking GROα or the CXCR2 receptor attenuates melanoma cell proliferation *in vitro*[41], whereas overexpression of GROα, GROβ or GROγ in a variety of tumour-derived cell lines enhances their colony-forming activity and tumorigenicity in nude mice[42,43]. Other CXCR2 ligands have been identified as having autocrine roles in the growth of pancreatic, head and neck, and non-small-cell lung carcinoma[44,45], whereas in mouse models, ENA-78/CXCL5 variably affects tumour growth, vascularity and apoptosis[46]. Macrophage pro-inflammatory chemokine-3α (MIP-3α/CCL20), a CC chemokine, is overexpressed in pancreatic carcinoma cells and infiltrating macrophages adjacent to tumours; MIP-3α/CCL20 stimulates growth of neoplastic cells while simultaneously enhancing migration of TAMs[47].

Regulation of angiogenesis by chemokines—Activation of angiogenic programmes represents a shift in the balance between pro- and anti-angiogenic factors48. Although angiogenesis is strictly controlled, it is associated with chronic inflammatory diseases, such as psoriasis, rheumatoid arthritis and fibrosis, as well as with tumour growth and metastasis[48]. It is well established that CXC chemokines with the three amino acids (Glu-Leu-Arg/ELR) immediately amino-terminal to the CXC motif (ELR^+) are pro-angiogenic and stimulate endothelial cell chemotaxis, whereas ELR^- CXC chemokines (for example, PF-4/CXCL4, MIG/CXCL9 and IP-10/CXCL10) possess angiostatic activities[44,49]. ELR^+ CXC ligands bind to CXCR2 and to a lesser degree to CXCR1, whereas ELR^- CXC ligands bind to CXCR3, CXCR4 and CXCR5 (ref. 6). Compared to VEGF-A, murine MCP-5/CCL12 exhibits only modest mitogenic properties towards endothelial cells; however, it is a potent chemoattractant. In contrast, stromal-cell-derived factor 1 (SDF-1/CXCL12) induces endothelial expression of VEGF-A; VEGF-A in turn upregulates CXCR4 on endothelial cells7. Although it is not always

clear if the angiostatic and angiogenic effects of chemokines are direct or indirect, it is accepted that the balance between the two regulates neoplastic cell physiology.

Chemokines and metastasis—Malignant cells that possess metastatic capacity have properties endowing them with the ability to invade and survive in ectopic tissue, venous and/or lymphatic environments, as well as ability to reside and proliferate at a distal site (Fig. 3). Much debate exists as to whether malignant cells metastasize to environments favouring their specific growth or whether different organs are endowed with the ability to arrest or attract specific types of malignant cells through chemotactic factors (the so-called homing theory) 48. Studies using a mouse model by Muller and colleagues suggest that the pattern of breast cancer metastases is in part governed by specific interactions between CXCR4 and its ligand SDF-1/CXCL12 (ref. 50). CXCL12 is a rather unique chemokine in that it is the product of resting cells in multiple organs6, and is particularly highly expressed in target organs for breast cancer metastasis50. CXCL12 triggers chemotaxis of malignant mammary carcinoma cells *in vitro*, and the chemotactic activity of extracts of organs targeted by breast cancer cells (bone marrow, liver, lung and lymph nodes) can be neutralized by anti-CXCR4 antibodies. The involvement of CXCR4 in metastasis is not limited to breast cancer, as CXCR4 is expressed in tumour cell lines (for example, prostate carcinomas, B-cell lymphomas, astrogliomas and chronic lymphocytic leukaemias) that also respond to CXCL12 (ref. 51). The broader implications of these observations are that chemokines may be involved in regulating the spectrum of metastases in diverse cancer types.

Tumours commandeer leukocyte adhesion mechanisms

Tumour cells not only take advantage of the trophic factors made by inflammatory cells, but may also use the same adhesion molecules, chemokines and receptors to aid in migration and homing during distant metastatic spread. Evidence suggests that mechanisms used for homing of leukocytes may be appropriated for the dissemination of tumours via the bloodstream and lymphatics. Selectins are adhesion receptors that normally recognize certain vascular mucin-type glycoproteins bearing the carbohydrate structure sialyl-Lewis X and facilitate leukocyte rolling along the blood vessels. Metastatic progression of many epithelial carcinomas correlates with tumour production of mucins containing sialyl-Lewis X. Lung colonization by melanoma cells that express sialyl-Lewis X is significantly reduced in E/P-selectin-deficient mice[52]. P-selectin deficiency attenuates tumour growth and metastasis, and tumours are significantly smaller in mice treated with a receptor antagonist peptide.

These results indicate that receptors expressed in the vasculature are crucial in targeting sialyl-Lewis X-dependent cancer cells[53]. P-selectin facilitates human carcinoma metastasis in immunodeficient mice by mediating early interactions of platelets with blood-borne tumour cells via their cell-surface mucins, a process that can be blocked by heparin[54]. L-selectin on neutrophils, monocytes and/or NK cells also may facilitate metastasis[55]. Metastasis could involve the formation of tumour–platelet–leukocyte emboli that interact with the vasculature of distant organs. In addition, expression of L-selectin on tumour cells can foster metastasis to lymph nodes[56].

Inflammation as an anti-cancer therapeutic opportunity

Perhaps the best evidence for the significance of inflammation during neoplastic progression comes from study of cancer risk among long-term users of aspirin and nonsteroidal anti-inflammatory drugs (NSAIDs). Much data indicates that use of these drugs reduces colon cancer risk by 40–50%, and may be preventative for lung, oesophagus and stomach cancer57,58. The ability of NSAIDs to inhibit cyclo-oxygenases (COX-1 and -2) underlies their mechanism(s) of chemoprevention. COX-2 converts arachidonic acid to prostaglandins, which in turn induces inflammatory reactions in damaged tissues59. Aspirin is non-selective

in its inhibition of platelet function by acetylating and irreversibly inactivating both COX-1 and COX-2. Inactivation prevents platelet synthesis of prostaglandins, endoperoxides and thromboxane A2.

Other NSAIDs, for example, flurbiprofen, may have strong anti-metastatic effects because of their inhibition of platelet aggregation[60]. But NSAIDs may act through mechanisms other than inhibition of COX enzyme activity alone, as some NSAIDs lacking COX-inhibitory function show efficacy in inhibiting colon carcinogenesis[61]. Other mechanisms have been proposed[15], including induction of apoptosis through release of cytochrome C from mitochondria and subsequent activation of caspase-9 and -3, and/or interference with cell-cycle progression, reduction of carcinogen activation and stimulation of immune surveillance.

The pro-inflammatory cytokine TNF-α is also a key downstream mediator in inflammation. Despite the name, TNF-α is important in early events in tumours, regulating a cascade of cytokines, chemokines, adhesions, MMPs and pro-angiogenic activities[1,62]. Thus, TNF-α may be one of the ways in which inflammation acts as a tumour promoter. Blocking antibodies that have significant therapeutic efficacy in other inflammatory diseases[63] may have applications in therapy in cancer.

Tumours are also rich in mucins and other ligands that may include the sialyl-Lewis X epitope recognized by selectins. Because selectins may have a role in metastasis[54,55], targeting the selectin interaction with heparin or antagonists of the receptor may decrease metastasis[54].

MMPs are produced by inflammatory cells and by stromal cells responding to chemokines and cytokines produced by inflammatory cells in tumour microenvironments[25]. Like inflammatory cells, MMPs may both promote tumour progression and attenuate it. Indeed, MMPs may mediate many of the actions of inflammatory cells in neoplasms[64]. MMPs can recruit inflammatory cells by releasing chemoattractants and motogens; they also generate growth-promoting and cytostatic signals. MMPs activate angiogenesis, but also produce fragments of basement-membrane collagens and plasminogen that are angiogenesis inhibitors. They have both apoptotic and anti-apoptotic actions. Thus, the efficacy of MMP inhibitors may be mediated, at least in part, through anti-inflammatory actions[64,65]. Given their diverse actions, it is also not surprising that trials with MMP inhibitors have had mixed results, with efficacy reported mostly during early tumour progression[66].

Inflammatory cells and cancer: friend or foe?

It is now evident that inflammatory cells have powerful effects on tumour development. Early in the neoplastic process, these cells are powerful tumour promoters, producing an attractive environment for tumour growth, facilitating genomic instability and promoting angiogenesis. The inflammatory cells, and the chemokines and cytokines that they produce, influence the whole tumour organ, regulating the growth, migration and differentiation of all cell types in the tumour microenvironment, including neoplastic cells, fibroblasts and endothelial cells. Later in the tumorigenic process, neoplastic cells also divert inflammatory mechanisms such as selectin–ligand interactions, MMP production and chemokine functions to favour neoplastic spread and metastasis. This may be part of an attempt by the tumour to subvert immune cell functions, so favouring tumour development. Yet, the recruitment of inflammatory cells may also be counterproductive for tumour development, and also may represent an attempt by the host to suppress tumour growth.

The pro-tumour actions of inflammatory cells include releasing growth and survival factors, promoting angiogenesis and lymphangiogenesis, stimulating DNA damage, remodelling the ECM to facilitate invasion, coating tumour cells to make available receptors for disseminating cells via lymphatics and capillaries, and evading host defence mechanisms. Although

inflammatory responses should also be anti-tumour, cancer patients are often defective in their inflammatory responses. This may arise by two distinct tumour-mediated mechanisms: a failure to upregulate the anti-inflammatory cytokines, or subversion of the host response resulting from desensitization of receptors owing to high chemokine and cytokine concentrations that then blunt systemic responses. Can we apply these new insights for targeting metastases?

It is clear that anti-inflammatory therapy is efficacious towards early neoplastic progression and malignant conversion. In a fully developed malignancy, there are 'excess' inflammatory cells in the tumour microenvironment. Does the tumour need inflammation to help foster angiogenesis? We must think globally and act locally. One approach is to evaluate whether functional polymorphisms in genes that regulate inflammatory processes (for example, genes encoding MMPs, cytokines, chemokines or selectins) harbour altered risk for developing cancer or are indicators of prognosis. Yet for all the local inflammation in tumours, in many cases the overall innate immunity of the host is blunted. The challenge for the future is to normalize the inflammatory network to regain a normal host response overall: decreasing the high levels of tumour-promoting properties of the infiltrating cells, such as pro-inflammatory cytokines, while increasing their tumour-suppressing properties, such as anti-inflammatory cytokines. In this way, later in tumour progression, we can harness the activities that are anti-tumour while suppressing those that are pro-tumour.

Acknowledgments

Supported by grants from the National Institutes of Health, the American Cancer Society, the V Foundation for Cancer Research, the Edward Mallinckrodt Jr Foundation for Medical Research, and the American Association for Cancer Research.

References

1. Balkwill F, Mantovani A. Inflammation and cancer: back to Virchow? Lancet 2001;357:539–545. [PubMed: 11229684]
2. Dvorak HF. Tumors: wounds that do not heal. Similarities between tumor stroma generation and wound healing. N Engl J Med 1986;315:1650–1659. [PubMed: 3537791]
3. Dranoff G. Tumour immunology: immune recognition and tumor protection. Curr Opin Immunol 2002;14:161–164.
4. Pardoll DM. Spinning molecular immunology into successful immunotherapy. Nature Rev Immunol 2002;2:227–238. [PubMed: 12001994]
5. Chettibi, S.; Ferguson, MWJ. Inflammation: Basic Principles and Clinical Correlates. Gallin, JI.; Snyderman, R., editors. Lipincott, Williams and Wilkinson; Philadelphia: 1999. p. 865-881.
6. Rossi D, Zlotnik A. The biology of chemokines and their receptors. Annu Rev Immunol 2000;18:217–242. [PubMed: 10837058]
7. Homey B, Muller A, Zlotnik A. Chemokines: agents for the immunotherapy of cancer? Nature Rev Immunol 2002;2:175–184. [PubMed: 11913068]
8. Moustakas A, Pardali K, Gaal A, Heldin CH. Mechanisms of TGF-β signaling in regulation of cell growth and differentiation. Immunol Lett 2002;82:85–91. [PubMed: 12008039]
9. Rous P, Kidd J. Conditional neoplasms and subthreshold neoplastic states: a study of the tar tumors of rabbits. J Exp Med 1941;73:365–389. [PubMed: 19871084]
10. Mackenzie IC, Rous P. The experimental disclosure of latent neoplastic changes in tarred skin. J Exp Med 1941;73:391–415. [PubMed: 19871085]
11. Kuper H, Adami HO, Trichopoulos D. Infections as a major preventable cause of human cancer. J Intern Med 2000;248:171–183. [PubMed: 10971784]
12. Wahl LM, Kleinman HK. Tumor-associated macrophages as targets for cancer therapy. J Natl Cancer Inst 1998;90:1583–1584. [PubMed: 9811301]

13. Talmor M, et al. Generation of large numbers of immature and mature dendritic cells from rat bone marrow cultures. Eur J Immunol 1998;28:811–817. [PubMed: 9541575]
14. Allavena P, et al. The chemokine receptor switch paradigm and dendritic cell migration: its significance in tumor tissues. Immunol Rev 2000;177:141–149. [PubMed: 11138772]
15. Brigati C, Noonan DM, Albini A, Benelli R. Tumors and inflammatory infiltrates: friends or foes? Clin Exp Metastasis 2002;19:247–258. [PubMed: 12067205]
16. Tsung K, Dolan JP, Tsung YL, Norton JA. Macrophages as effector cells in interleukin 12-induced T cell-dependent tumor rejection. Cancer Res 2002;62:5069–5075. [PubMed: 12208763]
17. Schoppmann S, et al. Tumor-associated macrophages express lymphatic endothelial growth factors and are related to peritumoral lymphangiogenesis. Am J Pathol 2002;161:947–956. [PubMed: 12213723]
18. Torisu H, et al. Macrophage infiltration correlates with tumor stage and angiogenesis in human malignant melanoma: possible involvement of TNFα and IL-1α. Int J Cancer 2000;85:182–188. [PubMed: 10629075]
19. Ono M, Torisu H, Fukushi J, Nishie A, Kuwano M. Biological implications of macrophage infiltration in human tumor angiogenesis. Cancer Chemother Pharmacol 1999;43:S69–S71. [PubMed: 10357562]
20. Jonjic N, et al. Expression of adhesion molecules and chemotactic cytokines in cultured human mesothelial cells. J Exp Med 1992;176:1165–1174. [PubMed: 1383376]
21. Lin EY, Nguyen AV, Russell RG, Pollard JW. Colony-stimulating factor 1 promotes progression of mammary tumors to malignancy. J Exp Med 2001;193:727–740. [PubMed: 11257139]
22. Nowicki A, et al. Impaired tumor growth in colony-stimulating factor 1 (CSF-1)-deficient, macrophage-deficient op/op mouse: evidence for a role of CSF-1-dependent macrophages in formation of tumor stroma. Int J Cancer 1996;65:112–119. [PubMed: 8543387]
23. DiCarlo E, et al. The intriguing role of polymorphonuclear neutrophils in antitumor reactions. Blood 2001;97:339–345. [PubMed: 11154206]
24. Coussens LM, et al. Inflammatory mast cells up-regulate angiogenesis during squamous epithelial carcinogenesis. Genes Dev 1999;13:1382–1397. [PubMed: 10364156]
25. Coussens LM, Tinkle CL, Hanahan D, Werb Z. MMP-9 supplied by bone marrow-derived cells contributes to skin carcinogenesis. Cell 2000;103:481–490. [PubMed: 11081634]
26. Bergers G, et al. Matrix metalloproteinase-9 triggers the angiogenic switch during carcinogenesis. Nature Cell Biol 2000;2:737–744. [PubMed: 11025665]
27. Blaser MJ, Chyou PH, Nomura A. Age at establishment of *Helicobacter pylori* infection and gastric carcinoma, gastric ulcer, and duodenal ulcer risk. Cancer Res 1995;55:562–565. [PubMed: 7834625]
28. Scholl SM, et al. Anti-colony-stimulating factor-1 antibody staining in primary breast adenocarcinomas correlates with marked inflammatory cell infiltrates and prognosis. J Natl Cancer Inst 1994;86:120–126. [PubMed: 8271294]
29. Shacter E, Weitzman SA. Chronic inflammation and cancer. Oncology 2002;16:217–226. [PubMed: 11866137]
30. Maeda H, Akaike T. Nitric oxide and oxygen radicals in infection, inflammation, and cancer. Biochemistry 1998;63:854–865. [PubMed: 9721338]
31. Yamanishi Y, et al. Regional analysis of p53 mutations in rheumatoid arthritis synovium. Proc Natl Acad Sci USA 2002;99:10025–10030. [PubMed: 12119414]
32. Ernst PB, Gold BD. The disease spectrum of *Helicobacter pylori*: the immunopathogenesis of gastroduodenal ulcer and gastric cancer. Annu Rev Microbiol 2000;54:615–640. [PubMed: 11018139]
33. Hudson JD, et al. A proinflammatory cytokine inhibits p53 tumor suppressor activity. J Exp Med 1999;190:1375–1382. [PubMed: 10562313]
34. Jensen UB, Lowell S, Watt FM. The spatial relationship between stem cells and their progeny in the basal layer of human epidermis: a new view based on whole-mount labeling and lineage analysis. Development 1999;126:2409–2418. [PubMed: 10226000]

35. Martins-Green M, Boudreau N, Bissell MJ. Inflammation is responsible for the development of wound-induced tumors in chickens infected with Rous sarcoma virus. Cancer Res 1994;54:4334–4341. [PubMed: 7519120]

36. Yoshida T, et al. Activation of STAT3 by the hepatitis C virus core protein leads to cellular transformation. J Exp Med 2002;196:641–653. [PubMed: 12208879]

37. Bromberg J, Darnell JE. The role of STATs in transcriptional control and their impact on cellular function. Oncogene 2000;19:2468–2473. [PubMed: 10851045]

38. Tebbutt NC, et al. Reciprocal regulation of gastrointestinal homeostasis by SHP2 and STAT-mediated trefoil gene activation in gp130 mutant mice. Nature Med 2002;8:1089–1097. [PubMed: 12219085]

39. Mantovani A, Muzio M, Garlanda C, Sozzani S, Allavena P. Macrophage control of inflammation: negative pathways of regulation of inflammatory cytokines. Novartis Found Symp 2001;234:120–131. [PubMed: 11199092]

40. Richmond A, Thomas H. Purification of melanoma growth stimulatory activity. J Cell Physiol 1986;129:375–384. [PubMed: 3465735]

41. Norgauer J, Metzner B, Schraufstatter I. Expression and growth-promoting function of the IL-8 receptor β in human melanoma cells. J Immunol 1996;156:1132–1137. [PubMed: 8557989]

42. Balentien E, Mufson BE, Shattuck RL, Derynck R, Richmond A. Effects of MGSA/GRO alpha on melanocyte transformation. Oncogene 1991;6:1115–1124. [PubMed: 1861861]

43. Owen JD, et al. Enhanced tumor-forming capacity for immortalized melanocytes expressing melanoma growth stimulatory activity/growth-regulated cytokine beta and gamma proteins. Int J Cancer 1997;73:94–103. [PubMed: 9334815]

44. Vicari AP, Caux C. Chemokines in cancer. Cytokine Growth Factor Rev 2002;13:143–154. [PubMed: 11900990]

45. Farrow B, Evers BM. Inflammation and the development of pancreatic cancer. Surg Oncol 2002;10:153–169. [PubMed: 12020670]

46. Arenberg DA, et al. Epithelial-neutrophil activating peptide (ENA-78) is an important angiogenic factor in non-small cell lung cancer. J Clin Invest 1998;102:465–472. [PubMed: 9691082]

47. Kleeff J, et al. Detection and localization of Mip-3α/LARC/Exodus, a macrophage proinflammatory chemokine, and its CCR6 receptor in human pancreatic cancer. Int J Cancer 1999;81:650–657. [PubMed: 10225458]

48. Hanahan D, Weinberg RA. The hallmarks of cancer. Cell 2000;100:57–70. [PubMed: 10647931]

49. Strieter RM, et al. The functional role of the ELR motif in CXC chemokine-mediated angiogenesis. J Biol Chem 1995;270:27348–27357. [PubMed: 7592998]

50. Muller A, et al. Involvement of chemokine receptors in breast cancer metastasis. Nature 2001;410:50–56. [PubMed: 11242036]

51. Moore MA. The role of chemoattraction in cancer metastases. BioEssays 2001;23:674–676. [PubMed: 11494314]

52. Kim YJ, Borsig L, Varki NM, Varki A. P-selectin deficiency attenuates tumor growth and metastasis. Proc Natl Acad Sci USA 1998;95:9325–9330. [PubMed: 9689079]

53. Zhang J, et al. Sialyl Lewis X-dependent lung colonization of B16 melanoma cells through a selectin-like endothelial receptor distinct from E- or P-selectin. Cancer Res 2002;62:4194–4198. [PubMed: 12154017]

54. Borsig L, et al. Heparin and cancer revisited: mechanistic connections involving platelets, P-selectin, carcinoma mucins, and tumor metastasis. Proc Natl Acad Sci USA 2001;98:3352–3357. [PubMed: 11248082]

55. Borsig L, Wong R, Hynes RO, Varki NM, Varki A. Synergistic effects of L- and P-selectin in facilitating tumor metastasis can involve non-mucin ligands and implicate leukocytes as enhancers of metastasis. Proc Natl Acad Sci USA 2002;99:2193–2198. [PubMed: 11854515]

56. Qian F, Hanahan D, Weissman IL. L-selectin can facilitate metastasis to lymph nodes in a transgenic mouse model of carcinogenesis. Proc Natl Acad Sci USA 2001;98:3976–3981. [PubMed: 11274419]

57. Baron JA, Sandler RS. Nonsteroidal anti-inflammatory drugs and cancer prevention. Annu Rev Med 2000;51:511–523. [PubMed: 10774479]

58. Garcia-Rodriguez LA, Huerta-Alvarez C. Reduced risk of colorectal cancer among long-term users of aspirin and nonaspirin nonsteroidal antiinflammatory drugs. Epidemiology 2001;12:88–93. [PubMed: 11138826]

59. Williams CS, Mann M, DuBois RN. The role of cyclooxygenases in inflammation, cancer, and development. Oncogene 1999;18:7908–7916. [PubMed: 10630643]

60. Mamytbekova A, Rezabek K, Kacerovska H, Grimova J, Svobodova J. Antimetastatic effect of flurbiprofen and other platelet aggregation inhibitors. Neoplasma 1986;33:417–421. [PubMed: 3762804]

61. Elder DJ, Halton DE, Hague A, Paraskeva C. Induction of apoptotic cell death in human colorectal carcinoma cell lines by a cyclooxygenase-2 (COX-2)-selective nonsteroidal anti-inflammatory drug: independence from COX-2 protein expression. Clin Cancer Res 1997;3:1679–1683. [PubMed: 9815550]

62. Balkwill F. Tumor necrosis factor or tumor promoting factor? Cytokine Growth Factor Rev 2002;13:135–141. [PubMed: 11900989]

63. Shanahan JC, St Clair EW. Tumor necrosis factor-alpha blockade: a novel therapy for rheumatic disease. Clin Immunol 2002;103:231–242. [PubMed: 12173297]

64. Egeblad M, Werb Z. New functions for the matrix metalloproteinases in cancer progression. Nature Rev Cancer 2002;2:161–174. [PubMed: 11990853]

65. Overall CM, Lopez-Otin C. Strategies for MMP inhibition in cancer: innovations for the post-trial era. Nature Rev Cancer 2002;2:657–672. [PubMed: 12209155]

66. Coussens LM, Fingleton B, Matrisian LM. Matrix metalloproteinase inhibitors and cancer: trials and tribulations. Science 2002;295:2387–2392. [PubMed: 11923519]

67. Dalgleish AG, O'Byrne KJ. Chronic immune activation and inflammation in the pathogenesis of AIDS and cancer. Adv Cancer Res 2002;84:231–276. [PubMed: 11883529]

68. Feiken E, Romer J, Eriksen J, Lund LR. Neutrophils express tumor necrosis factor-alpha during mouse skin wound healing. J Invest Dermatol 1995;105:120–123. [PubMed: 7615965]

69. Hubner G, et al. Differential regulation of pro-inflammatory cytokines during wound healing in normal and glucocorticoid-treated mice. Cytokine 1996;8:548–556. [PubMed: 8891436]

70. Chedid M, Rubin JS, Csaky KG, Aaronson SA. Regulation of keratinocyte growth factor gene expression by interleukin 1. J Biol Chem 1994;269:10753–10757. [PubMed: 7511604]

71. Osusky R, Malik P, Ryan SJ. Retinal pigment epithelium cells promote the maturation of monocytes to macrophages in vitro. Ophthalmic Res 1997;29:31–36. [PubMed: 9112264]

72. DiPietro L. Wound healing: the role of the macrophage and other immune cells. Shock 1995;4:233–240. [PubMed: 8564549]

73. Fritsch C, Simon-Assmann P, Kedinger M, Evans GS. Cytokines modulate fibroblast phenotype and epithelial-stroma interactions in rat intestine. Gastroenterology 1997;112:826–838. [PubMed: 9041244]

74. Grutzkau A, et al. Synthesis, storage, and release of vascular endothelial growth factor/vascular permeability factor (VEGF/VPF) by human mast cells: implications for the biological significance of VEGF206. Mol Biol Cell 1998;9:875–884. [PubMed: 9529385]

75. Chensue SW, Ruth JH, Warmington K, Lincoln P, Kunkel SL. In vivo regulation of macrophage IL-12 production during type 1 and type 2 cytokine-mediated granuloma formation. J Immunol 1995;155:3546–3551. [PubMed: 7561051]

76. Romer J, et al. Impaired wound healing in mice with a disrupted plasminogen gene. Nature Med 1996;2:287–292. [PubMed: 8612226]

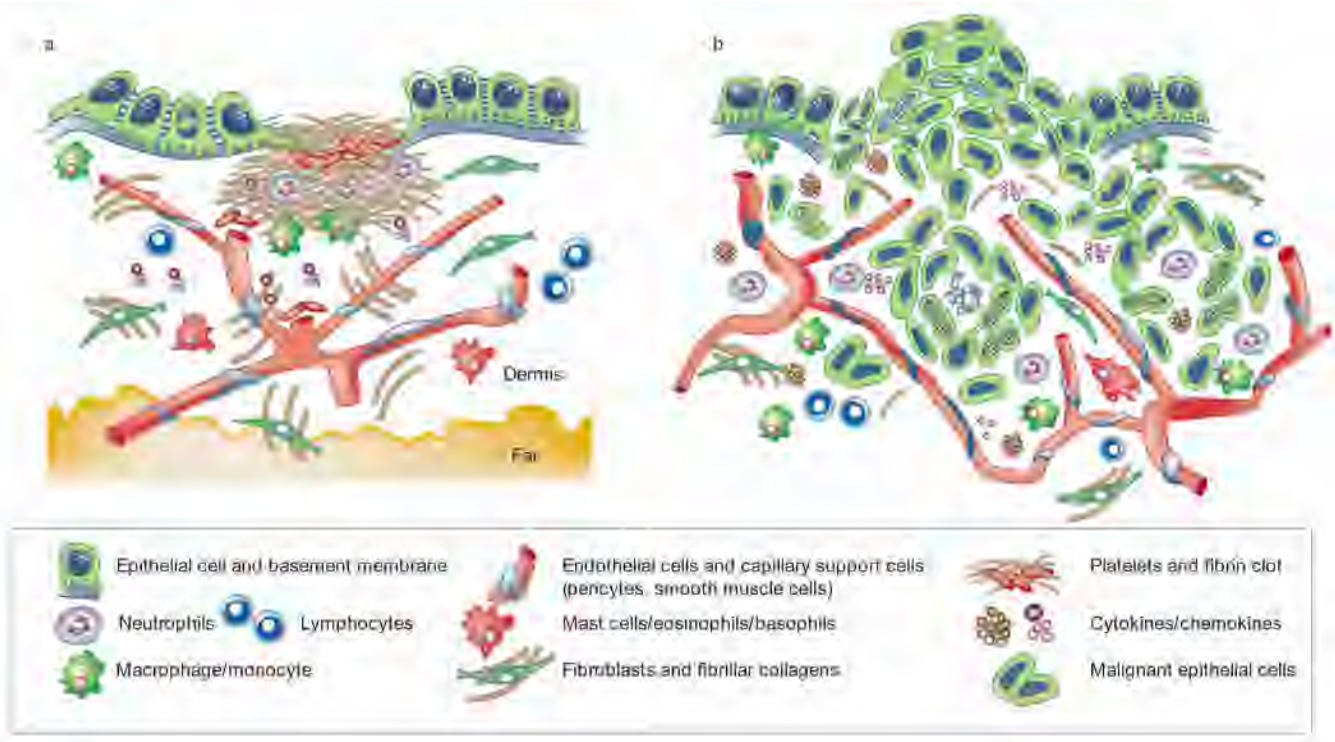

Figure 1.

Wound healing versus invasive tumour growth. **a**, Normal tissues have a highly organized and segregated architecture. Epithelial cells sit atop a basement membrane separated from the vascularized stromal (dermis) compartment. Upon wounding or tissue assault, platelets are activated and form a haemostatic plug where they release vasoactive mediators that regulate vascular permeability, influx of serum fibrinogen, and formation of the fibrin clot. Chemotactic factors such as transforming growth factor-β and platelet-derived growth factor, derived from activated platelets, initiate granulation tissue formation, activation of fibroblasts, and induction and activation of proteolytic enzymes necessary for remodelling of the extracellular matrix (for example, matrix metalloproteinases and urokinase-type plasminogen activator). In combination, granulocytes, monocytes and fibroblasts are recruited, the venous network restored, and re-epithelialization across the wound occurs. Epithelial and stromal cell types engage in a reciprocal signalling dialogue to facilitate healing. Once the wound is healed, the reciprocal signalling subsides. **b**, Invasive carcinomas are less organized. Neoplasia-associated angiogenesis and lymphangiogenesis produces a chaotic vascular organization of blood vessels and lymphatics where neoplastic cells interact with other cell types (mesenchymal, haematopoietic and lymphoid) and a remodelled extracellular matrix. Although the vascular network is not disrupted in the same way during neoplastic progression as it is during wounding, many reciprocal interactions occur in parallel. Neoplastic cells produce an array of cytokines and chemokines that are mitogenic and/or chemoattractants for granulocytes, mast cells, monocytes/macrophages, fibroblasts and endothelial cells. In addition, activated fibroblasts and infiltrating inflammatory cells secrete proteolytic enzymes, cytokines and chemokines, which are mitogenic for neoplastic cells, as well as endothelial cells involved in neoangiogenesis and lymphangiogenesis. These factors potentiate tumour growth, stimulate angiogenesis, induce fibroblast migration and maturation, and enable metastatic spread via engagement with either the venous or lymphatic networks.

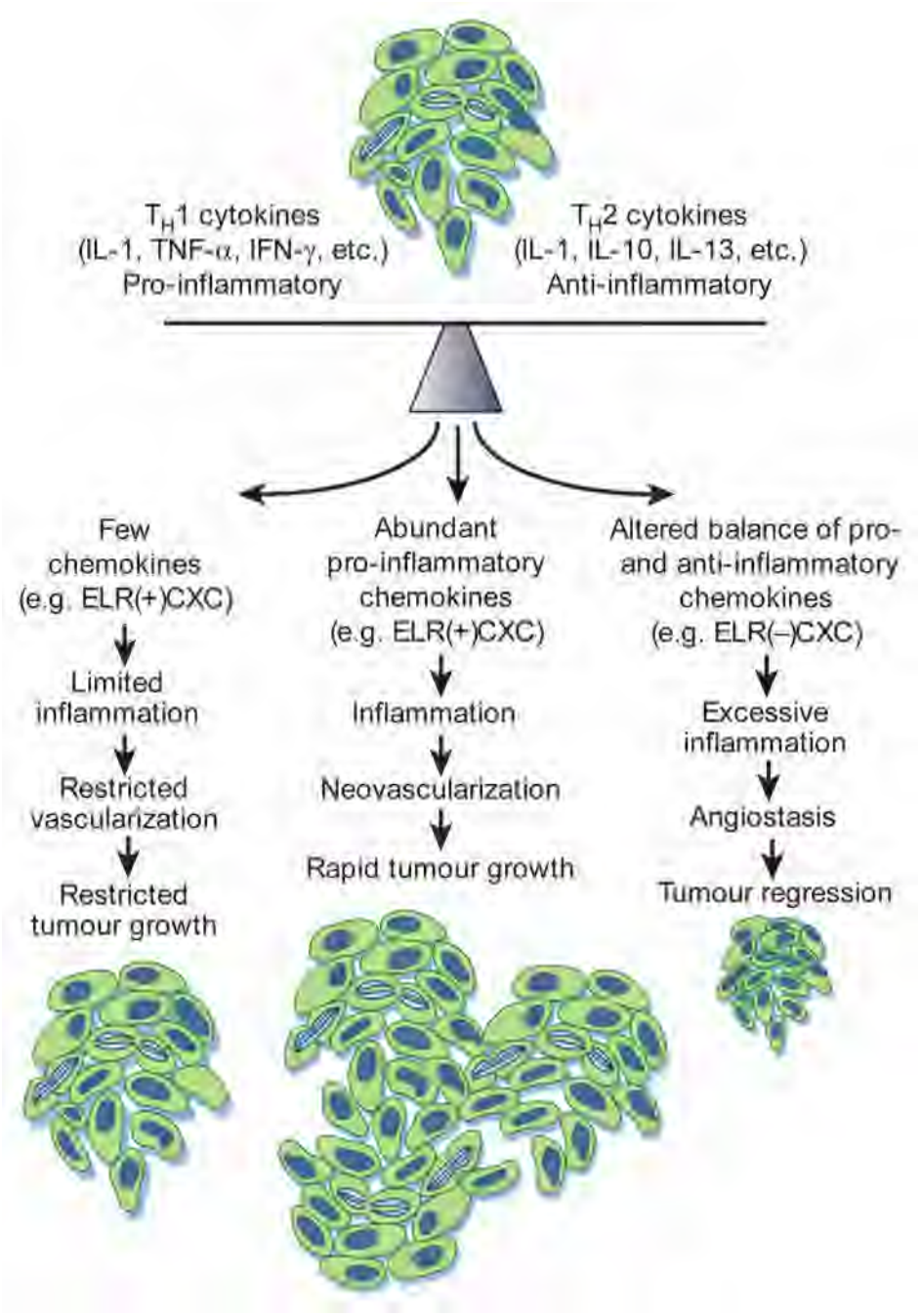

Figure 2.

Cytokine and chemokine balances regulate neoplastic outcome. The balance of cytokines in any given tumour is critical for regulating the type and extent of inflammatory infiltrate that forms. Tumours that produce little or no cytokines or an overabundance of anti-inflammatory cytokines induce limited inflammatory and vascular responses, resulting in constrained tumour growth. In contrast, production of an abundance of pro-inflammatory cytokines can lead to a level of inflammation that potentiates angiogenesis, thus favouring neoplastic growth. Alternatively, high levels of monocytes and/or neutrophil infiltration, in response to an altered balance of pro-versus anti-inflammatory cytokines, can be associated with cytotoxicity,

angiostasis and tumour regression. In tumours, interleukin-10 is generally a product of tumour cells and tumour-associated macrophages.

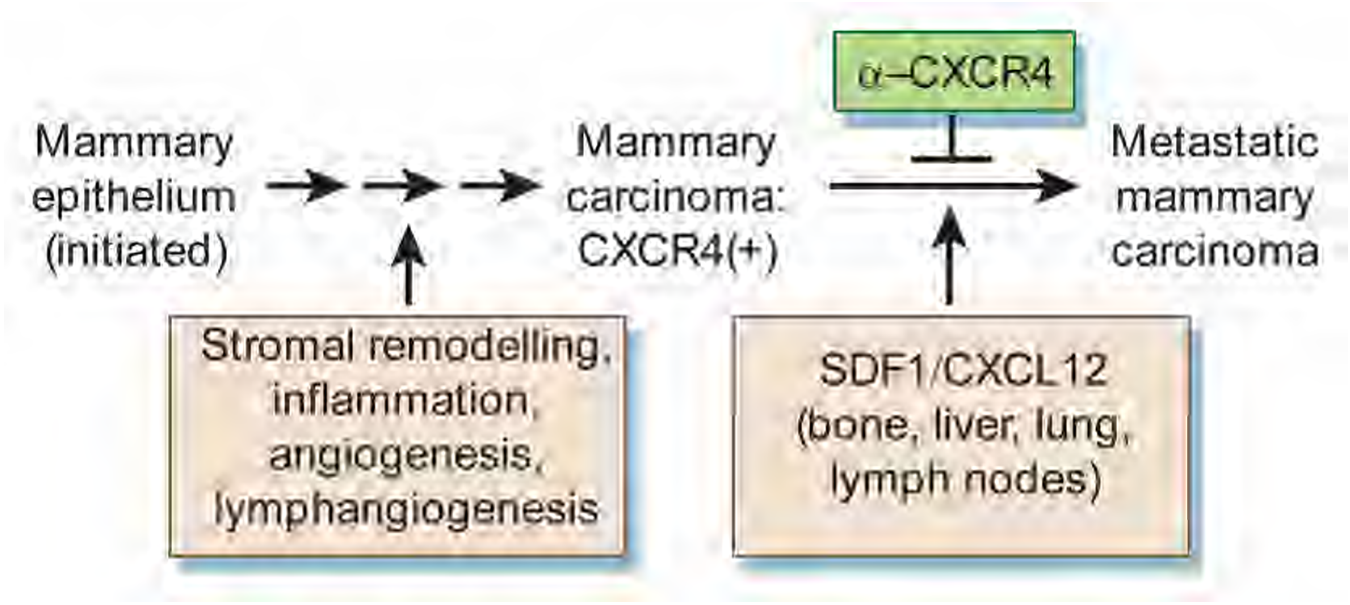

Figure 3.

Cancer metastasis and chemokine signalling. Initiated epithelial cells are promoted by inflammation to undergo neoplastic progression, a process that requires remodelling of the extracellular matrix, recruitment of inflammatory cells, angiogenesis and lymphangiogenesis. Out of this microenvironment, carcinomas arise. These neoplastic cells then turn on expression of chemokine receptors, such as CXCR4. The production of chemokine ligands for these receptors, in sites such as lymph nodes, bone marrow, liver and lung, then facilitates their invasion and migration to secondary sites where malignant cells reside either in a dormant state, or proliferate to form a productive metastatic lesion. Blockade of chemokine receptors, for example, anti-CXCR4 antibodies, attenuates metastatic spread in some experimental systems.

Table 1

Chronic inflammatory conditions associated with neoplasms

Pathologic condition	Associated neoplasm(s)	Aetiologic agent
Asbestosis, silicosis	Mesothelioma, lung carcinoma	Asbestos fibres, silica particles
Bronchitis	Lung carcinoma	Silica, asbestos, smoking (nitrosamines, peroxides)
Cystitis, bladder inflammation	Bladder carcinoma	Chronic indwelling, urinary catheters
Gingivitis, lichen planus	Oral squamous cell carcinoma	
Inflammatory bowel disease, Crohn's disease, chronic ulcerative colitis	Colorectal carcinoma	
Lichen sclerosus	Vulvar squamous cell carcinoma	
Chronic pancreatitis, hereditary pancreatitis	Pancreatic carcinoma	Alcholism, mutation in trypsinogen gene on Ch. 7
Reflux oesophagitis, Barrett's oesophagus	Oesophageal carcinoma	Gastric acids
Sialadenitis	Salivary gland carcinoma	
Sjögren syndrome, Hashimoto's thyroiditis	MALT lymphoma	
Skin inflammation	Melanoma	Ultraviolet light
Cancers associated with infectious agents		
Opisthorchis, *Cholangitis*	Cholangiosarcoma, colon carcnoma	Liver flukes (*Opisthorchis viverrini*), bile acids
Chronic cholecystitis	Gall bladder cancer	Bacteria, gall bladder stones
Gastritis/ulcers	Gastric adenocarcinoma, MALT	*Helicobacter pylori*
Hepatitis	Hepatocellular carcinoma	Hepatitis B and/or C virus
Mononucleosis	B-cell non-Hodgkin's lymphoma, Burkitts lymphoma,	Epstein-Barr Virus
AIDS	Non-Hodgkin's lymphoma, squamous cell carcinomas, Kaposi's sarcoma	Human immunodeficiency virus, human herpesvirus type 8
Osteomyelitis	Skin carcinoma in draining sinuses	Bacterial infection
Pelvic inflammatory disease, chronic cervicitis	Ovarian carcinoma, cervical/anal carcinoma	Gonnorrhoea, chlamydia, human papillomavirus
Chronic cystitis	Bladder, liver, rectal carcinoma, follicular lymphoma of the spleen	Schistosomiasis

Modified from refs 29, 67. MALT, mucosa-associated lymphoid tissue.